UNIVERSITAT DE BARCELONA

Impact of drought periods on carbon processing across surface-hyporheic interfaces in fluvial systems

Impacte dels períodes de sequera sobre el processat de carboni a través de la interfase superficial i zona hiporreica en sistemes fluvials

Astrid Harjung

TESI DOCTORAL

Universitat de Barcelona
Departament de Biologia Evolutiva, Ecologia i Ciències Ambientals
Programa de Doctorat en Ecologia, Ciències Ambientals i Fisiologia Vegetal

Impact of drought periods on carbon processing across surface-hyporheic interfaces in fluvial systems

Impacte dels períodes de sequera sobre el processat de carboni a través de la interfase superficial i zona hiporreica en sistemes fluvials

Memòria presentada per Astrid Harjung per optar al títol de Doctora per la Universitat de Barcelona

Astrid Harjung
Barcelona, febrer de 2018

Vist-i-plau dels directors de la tesi:

Dr. Francesc Sabater Comas
Professor titular
Universitat de Barcelona

Dr. Andrea Butturini
Professor agregat
Universitat de Barcelona

Cover fotos: Fuirosos pool in Summer (by Michael Vieweg)

Dry stream bed Fuirosos

Agraïments

First of all, I want to thank the directors of my thesis, Quico and Andrea, who were navigating me through this adventure (and through the jungle of Fuirosos, DIY superstores in Mataró and different paper jungles) with a lot of experience, patience and motivation, for your support and trust, for sharing your ideas, your knowledge and your passion for science and for your pragmatism, when it was necessary to focus, for teaching me more than I could have ever imagined I would learn about ecology in general and biogeochemistry in particular, about experimental design and DIY inventions in science, and finally almost you have taught me to write short sentences, but ok, to quote one of these wise men: "Aunque no te lo puedes imaginar ahora, hay una vida después del doctorado en que puedes aprender todo esto……". Bueno, perdonad, pero me hacía gracia dedicaros una mega frase en mis agradecimientos. De verdad, me siento muy afortunada que habéis sido mis directores. Quico, ha sigut una gran sort i honor haver tingut la possibilitat d'anar al camp, aprendre i de tenir les converses i les idees d'una persona que té els teus coneixements. Moltes gràcies per compartir la passió per la naturalesa, per motivar sempre i per tota la teva ajuda durant l'arribada a Barcelona i durant la tesis. Andrea, impresiona mucho como haces y vives la ciencia, con toda la integridad y la libertad. Mille grazie por compartir, por mantener el enfoque y sobre todo por tu pragmatismo a la hora de cerrar capítulos y la tesis (y por tu tranquilidad a la hora del susto cuando he pensado que he roto los sensores de fluorescencia, que al final no fue así).

Quiero agradecer a la Mary (me gustaría pintar tu nueva firma de ángel ahora, pero bueno), por todo lo que me has enseñado, en el laboratorio, en el campo y en general. No me puedo imaginar cómo se podría hacer la tesis sin ti. Y claro, sobre todo por enseñarme sitios tan mágicos como Sitges, Girona, Hospitalet y muchos más. Me lo has hecho tan fácil llegar y sentirme en casa en Barcelona!

Bei Kapitel 2 möchte ich meiner Feldpartnerin Tanja danken (tut mir leid, aber das muss jetzt so stehen) „for all the Hot Moments in Fuirosos" (Stammkunden in LaBattloria, Bazarumrundungen, Ballern und maulen, bofen, Ralley fahren) und natürlich die großartige Zusammenarbeit (prost auf zukünfitge Abenteuer/Experimente). Mic, für die tatkräftige Unterstützung im Feld und das schöne Foto vom Umschlag. Christian, für die hilfreichen Kommentare zum Kapitel.

El capítol 3 vaig treballar amb la Núria i l'Anna. Moltes gràcies, Núria per totes les discussions per quadrar els nostres resultats, explicar-me la microbiologia i moltes gràcies Anna per totes las teves idees i per compartir el teu coneixement! He après moltíssim amb vosaltres!

In chapter 4, I was working together with a big group: Jakob, for inviting me to Lunz, for your guidance and organization throughout experiment and your help with writing up a really nice story; danke, für die Motivation (schnell noch DO-sensoren rein) und die vielen wertvollen Ratschläge. Thank you Bet, for your advice throughout this thesis* and for all your indispensable help throughout the experiment! Masumi, für deinen großartigen Einsatz, dein Organisationstalent, das unverzichtbar war bei diesem Projekt, die tollen Fotos und die schöne Zeit in Lunz. Thanks, to our help and advice from Lausanne, Tom, for your valuable input and help with the experimental design and with the manuscript writing and Nicolas for showing us how to process the gas samples and making the Picarro work. Stefan, für seine Hilfe beim Aufbau, seinen Anpacken und sein handwerkliches Geschick. Kyle, for helping us with the experimental set-up and with advice on the sampling strategy. Auch vielen Dank an Gerti, die uns im Labor alles gezeigt und sehr geholfen hat und Josefa für ihre praktischen Tipps und organisatorische Hilfe und allen Mitarbeitern des Wasserclusters, die uns beim Auf-und Abbau und im Labor und bei allem was sonst noch angefallen ist geholfen haben. It was a really good summer!

Another very nice experience was my short stay in Rennes; Ben, for inviting me to participate in the MIMS experiment, I would like to thank all the people that participated, especially Camille (Danke für die gute Zeit!), Elliot (coke for the streams) and Thierry (coffee and croissant, that's field work in Brittany). They can be awake 24h and still smile (ok, Ben can even do that for 48h and still be laughing: Rotkehlchen). Also, thanks to Ben and his colleagues from the Zarnetske Lab, for pre-reviewing Chapter 1. Und Tamara, vielen Dank für die tolle Zeit in Rennes und unseren Roadtrip durch die Bretagne (die Vögel)! Merci beaucoup a tous!

This thesis was performed within a network, giving the chance to work together with a lot of people. I would like to thank the coordinator of the INTERFACES network Stefan for giving us the opportunity to perform our research in such an inspiring network. Gilles and David for their helpful advice and all the other PI's that were advising and helping us throughout this experience. I would like to thank my fellow Interfaces ESR's and ER's Amaia, Ben, Francesco, Jose, Karlie, Kyle, Marta, Mukundh, Myrto, Paul, Tamara, Tanja, Tim and Viktor for the amazing time during the ATCs and other meetings, for all the great discussions and for the fun that science is. Vull donar les gràcies a l'Eugènia i l'Albert, per tot el que ens han ensenyat i aportat i els ànims que ens han donat durant aquests anys.

Ara, tota la tesi ha sigut una súper experiència tant les estades fora com estar a casa, a Barcelona. I que Barcelona sigui com casa és gràcies a la gent del departament d'ecologia que sempre ajuden com poden. I sobre tot, per la benvinguda que donen als altres doctorants que, crec que companys de feina com vosaltres no és fàcil de trobar.

Vull agrair al grup del Manchester (el Bar, no he anat mai a la ciutat, un honor estar en aquest grup): la Mary (sí, la misma Mary Ángeles que al principio y a su chico Oscar), la Bet* (per això l'estrella, perquè recordo encara el primer dia que vaig entrar al departament i em em vas posar ja al grup, m'has ensenyat tot del indexes òptics amb molta paciència i per la makro del fluorímetre!), l'Alba (per estar sempre disposada a ajudar i per compartir una gran boda i per llegir capítol 1), l'Eusebi (pels cafès, les cerveses i pels teus consells durant tota la tesi, i per llegir capítol 1), el Jaime (muchas gracias por estar siempre dispuesto a escuchar o a simplemente tomar cervezas), la Lídia (perquè ets el cor del grup), el Dani (per saber explicar-ho tot), la Patri (por toda la ayuda en Fuirosos y en el laboratorio), l'Esther (per animar-me a aprendre català), el Julio i la Isis. Vull agrair a tots els que m'han portat sempre a tots els eventos. Recordo la tesis de l'Ada (una festa inoblidable!), hablando de fiestas inolvidables, gracias a la Vero (por tu espontaneidad, ofrecer tu ayuda siempre, las conversaciones de la tesis y tu compañerismo), el Tano (no sé de dónde sacas la energía, que sabes todo, festejas más y cocinas increíble y por tu ayuda en la estadística del capítulo 2), Rebeca (la garantía para fiestas inolvidables!) y Luisa, la Marta (Berlín) y totes les aventures: anar a bussejar amb el "fresh" Pol com company (ets una de les persones en les que s'hi pot confiar clarament 100% des del principi, bussejant i amb tot, per totes les excursions i per tota la teva ajuda ara en la recta final amb la tesi, i ja saps que ets un dels més valents que conec), el Eneko que nos ha guiado (por insistir siempre en la happy hour del viernes y por haberme enseñado la costa brava! y aconsejarme con la portada), l'Anna por discutir conmigo los cálculos del metabolismo, por llevarme siempre a esquiar y a buscar bolets y a todas las actividades y Lluís per explicar-me els càlculs del CO2, per fer-me netejar el teu jardí (broma), per les calçotades i les excursions d'escalada, per portar-me al Mulhacén que ha sigut una dels excursions més guais, gracias también al Marc, Núria Catalan, Julio i Pau. I parlant d'Aventura: Aurora, moltíssimes gràcies per totes les esquiades i aventures que hem tingut junts i pels teus consells amb l'estadística per aquesta tesi. Ets tan valenta, aventurera i amiga i et trobo moltíssim de faltar. Em fa molta il·lusió anar amb tu i el Josep una altra vagada a la muntanya o a la platja. I parlant d'escalada: "Salty" Pol (sempre em deixaria assegurar per tu!!! tant en l'escalada com en la vida), gràcies pel teu optimisme i per sempre estar disposat a ajudar en qualsevol cosa, per les tardes d'escalada i cervesa i per la teva ajuda amb el resum i amb l'estadística. Sílvia, ets un pineapple, ets capaç d'aconseguir que tothom se sent-hi a gust quan estàs amb ells, perquè tens un somriure per a tothom, una orella atenta per escoltar i una abraçada quan més ho necessitem. Realment, entre totes les coses bones que m'han passat durant els darrers anys, una de las mes grans ha estat haver-me assegut al teu costat. He gaudit i he rigut molt amb tu, a més del teu suport moral. Myrto, I am so glad that we started together in this Barcelona adventure. You have such a honest and warm personality, that's really amazing, I know I can always count on you (btw. not irrelevant in this context: thank you so much for

correcting parts of this thesis) and I miss the talks, the ouzos and the beers with you (good that there is whatsapp!). Daniel, eres alguien que siempre sigue su camino y que siempre tiene unas palabras para dar ánimos. Gracias, chaparrito! També vull donar les gràcies al Pau, que sempre ajuda amb tot i a la Núria Cid i la Kele pel somriure i donar ànims i al Pablo (locura, te hechamos de menos). Hablando de sonrisas, también la Yaiza (por dar ánimos) y el Hares (a pity that our ways just crossed for such a short time) i l'Aida (que tenim un concert de Dub pendent), el Joan Gomà i el Cesc, la Meritxell, l'Aina i la Sandra (por siempre tener un momento para charlar) y la Núria de Castro, la Neus, el Max (Makro fluorímetre!), la Graciel.la, l'Ignasi, la Marta, i l'Alba. Jen, for visiting us from time to time in the University and for always be ready to help with English and scientific questions. I also want to thank Jose for the fun time during his secondment and for listening 1000 times to my presentation.

También quiero dar las gracias a Fra, por 4 años muy guais de compartir piso y salir por Barcelona y hacer que abandone el Excel por mi bien y ayudarme en Matlab y engancharme a la escalada! Y al Shervin que me ha acogido recién llegando a Barcelona.

Sheela, for your friendship, support and the adventures all around the world (Göttingen, Berlin, Malaysia and finally Barcelona)!

Meiner Masterarbeitsbetreuerin Bettina, ohne deren Ermutigung ich wohl nie ein Doktorat begonnen hätte.

Ich möchte mich bei den Leuten bedanken, die schon seit vielen Jahren immer für mich da sind und direkt und indirekt zum Gelingen dieser Arbeit beigetragen haben: Der Nini, danke für deine Freundschaft, dafür dass ich seit wir uns in der Volkschule kennengelernt haben immer auf dich verlassen kann, für deine unglaubliche Stärke. Meinen Mädls, der Alena, der Hele, der Maria und der Theresa, für alle skypes, die leiwanden Besuche, dafür dass wir für einander da sind, obwohl wir schon so lange weit weg voneinander wohnen, für eure Motivationswhatsapps und Daumen drücken. Dem Pauli (Teile dieser Arbeit korrigiert und Fotos beigesteuert), für alle Telefonate, dass du immer für mich da bist und mich motivierst, für deinen Mut und deine Abenteuerlust, die mich auch mutiger gemacht hat. Dem Matthias (Teile dieser Arbeit verbessert), für die vielen Gespräche auf skype, die leiwanden Reisen, für meinen Raunzereien zuhören und mir dann den Kopf gerade rücken, für deine Spontanität und Unterstützung in allen Lebenslagen. Der Anna, für deine Offenheit, deine Ehrlichkeit, deine Ratschläge, dein Zuhören und bei jeder Gaudi am Start sein. Dem Fabi, dafür dass du es echt schaffst einem einzureden, dass man alles erreichen kann wenn man‘s nur will und immer bei allem dabei (#Motivationstrainer). Der Carmen, fürs sofort ihre Hilfe anbieten beim korrigieren und für die schöne Zeit immer wenn wir uns sehen. Der

Viola, für‘s Daumen drücken, zuhören und deine Besuche und Wiedersehen in Wien und natürlich dem Paul (skypes aus dem Dschungel), der Clara und dem Moritz (Weltreisevorbilder) und dem Vlad (Nachbar!).

Pantelis (irrelevant: contributed a lot correcting the English of this thesis), no worries, I‘ll try not to write in an online freely available text cheesy stuff about you, so to keep it short and encrypted here: For all your support, for listening and advice, for “droning” around and for the great time in terrestrial and aquatic environments.

Und natürlich meiner Familie für all die Unterstützung, immer und überall, meinen Onkeln, Tanten und Cousins. Ganz besonders meinen Großeltern, Anna, Grethe, Heinz (du fehlst) und Martin, dass ihr immer für uns Enkelkinder da seid, für eure Unterstützung und eure Liebe, die uns immer begleitet. Und meinen Brüdern, Andi (und der Kathi, für eure Unterstützung beim Englisch korrigieren und beim feiern in Barcelona) und Chrisi, dass ihr mich immer am Laufenden haltet, dass ich mich immer auf euch verlassen kann und wir uns nicht oft hören müssen um das Gefühl zu haben immer füreinander da zu sein. Und zum Schluss möchte ich mich bei den beiden Menschen bedanken, die immer für mich da sind, bei meinen Eltern, danke, für euer Vertrauen, eure Unterstützung, die schöne gemeinsame Zeit und für so viel mehr, dass ungedruckt bleibt, weil mir die richtigen Worte fehlt, aber ich weiß ihr versteht mich auch so.

Summary

Headwater streams essentially link the terrestrial and the aquatic carbon cycle because they transport terrestrial organic and inorganic carbon downstream towards the oceans. However, most of these inputs are processed during this journey. These processes include down-break of particulate organic matter, transformation and respiration of dissolved organic matter and furthermore, in-stream production of organic matter. In particular, during drought periods the aquatic processes gain importance because terrestrial inputs are diminished. Therefore, carbon cycling in the remaining surface and subsurface flow of the main channel is accelerated and driven by the connectivity of these compartments. As the surface flow ceases carbon processing rates along subsurface flow paths, namely the hyporheic zone, increase.

In the light of climate change, longer drought periods, including in currently humid areas, are expected. Within this context, this thesis aims to understand carbon processing across the surface-hyporheic interface of a Mediterranean intermittent stream during a summer drought. Since dissolved organic matter represents the key energy source of aquatic metabolism that ultimately determine in-stream carbon cycling, we focused on the organic matter quantity and quality. We found increasing retention rates of dissolved organic matter along hyporheic flowpaths as water residence time in this compartment increases with the ceasing of surface flow. The evaluation of optical indices of dissolved organic matter quality revealed that the molecular weight decreased and indices related to biological activity increased. Furthermore, we showed that dissolved organic matter from primary production is rapidly respired in the remaining surface water, while humic-like compounds are processed and respired in the hyporheic zone. The dissolved organic matter processing in the hyporheic zone was paralleled with observations of disproportional high partial pressure of CO_2 in the interstitial pore water. These CO_2 pulses were related to the desiccation of the streambed, as well as dissolved organic matter availability. Our results suggested that the hyporheic zone acts as a humid refuge for microbial activity and that respiration activity immediately restarts when rain events reestablish subsurface flow paths. Associated with this microbial activity, during drought the processing rates of dissolved organic matter, as well as the processing rates of inorganic nutrients were enhanced. Moreover, we explored the effects of a summer drought on subalpine streams by applying different discharge levels in stream-side flumes fed by the water of a subalpine stream. In this experiment, we found high dissolved organic carbon release from in-stream processes in the flumes with the lowest discharges. This dissolved organic carbon release was at the beginning paralleled with a transient increase in gross primary production but continued to rise even when primary production collapsed. While the collapse of primary production might be a consequence

of phosphor limitation, respiration and degradation of dissolved and particulate organic matter in the sediment continued throughout.

In line with our findings from the Mediterranean stream, this mesocosm experiment highlighted the importance of the hyporheic zone and organic matter stored therein for carbon processing during drought periods. In both study sites, the surface water metabolism was ultimately dominated by respiration, and dissolved organic matter quality of the surface water played an important role on processes in the hyporheic zone. Although the investigated study sites were different in many aspects we found surprising similarities in carbon processing with flow reduction. This suggests that findings from Mediterranean streams might be transferable to other climatic regions under global change scenarios.

Resum

Els rius de capçalera connecten essencialment el cicle del carboni terrestre i aquàtic, donat que transporten el carboni orgànic i inorgànic terrestre aigües avall cap als oceans. Tanmateix, la majoria d'aquestes entrades de carboni passen per diferents processos durant aquest viatge. Aquests inclouen: la descomposició de la matèria orgànica particulada, la transformació i la respiració de la matèria orgànica dissolta i, a més, la producció aquàtic de matèria orgànica. Durant els períodes de sequera, els processos aquàtics guanyen importància perquè les aportacions terrestres es redueixen. Per tant, el cicle de carboni a les aigües superficials romanents i a la zona hiporreica s'accelera, a resultes de la connectivitat entre aquests dos compartiments. A mesura que l'aigua de la superfície desapareix, les taxes de processament de carboni al llarg de la zona hiporreica augmenta.

En el escenari actual de canvi climàtic, s'espera un període més llarg de sequera, també en àrees actualment humides. En aquest context, aquesta tesi pretén comprendre el processament del carboni a través de la interfície superficial-hiporreic d'un riu intermitent mediterrani durant una sequera d'estiu. Atès que la matèria orgànica dissolta és la principal font d'energia del metabolisme aquàtic que, en última instància, determina el cicle de carboni aquàtic, aquesta tesis se centra en la quantitat i la qualitat de la matèria orgànica. Hem trobat un augment de la retenció de la matèria orgànica dissolta en medi hiporreic, ja que el temps de residència de l'aigua en aquest compartiment augmenta amb el cessament de aigües superficials. L'avaluació dels índexs òptics de la qualitat de la matèria orgànica dissolta va revelar que el pes molecular es va reduir, i es van incrementar els índexs relacionats amb l'activitat biològica. A més, vam demostrar que la matèria orgànica dissolta de la producció primària es respira ràpidament en l'aigua superficial restant, mentre que els compostos més húmics es processen i es respiren a la zona hiporreica. El processament de matèria orgànica dissolta a la zona hiporreica anava acompanyat per valors de pressió parcial de CO_2 desproporcionadament alts en l'aigua de l' hiporreic. Aquests augments de CO_2 semblaven estar lligats amb la dessecació i la disponibilitat de matèria orgànica dissolta. Els nostres resultats suggereixen que la zona hiporreica actua com un refugi humit per a l'activitat microbiana i que l'activitat de la respiració es reinicia immediatament quan els esdeveniments de pluja restableixen el flux hyporheic. Associada a aquesta activitat microbiana, durant la sequera es van augmentar les taxes de processament de la matèria orgànica dissolta, així com les taxes de processament dels nutrients inorgànics. A més a més, es van explorar els efectes d'una sequera d'estiu en rius de capçalera subalpins aplicant diferents nivells de caudal en mesocosms alimentats per l'aigua d'un riu subalpí. En aquest experiment, vam trobar una elevada alliberació de carboni orgànic dissolt fruit dels processos aquàtics en els mesocosms de

cabals més baixos. Al principi, aquest augment de carboni orgànic dissolt va anar acompanyat per un increment transitori de la producció primària bruta, però va continuar augmentant fins i tot quan la producció primària es va col·lapsar. Aquest fet podria ser una conseqüència de la limitació del fòsfor, però la respiració i la degradació de la matèria orgànica dissolta i particulada en el sediment es varen mantenir al llarg de l'experiment.

En consonància amb els resultats que varem observar en els rius mediterranis, aquest experiment posava de relleu la importància de la zona hiporreica i de la matèria orgànica emmagatzemada en aquesta zona i pel processament del carboni durant els períodes de sequera. En els dos llocs d'estudi, el metabolisme de l'aigua superficial va estar dominat en última instància per la respiració; i la qualitat de la matèria orgànica dissolta de l'aigua superficial va jugar un paper important en els processos de la zona hiporreica. Tot i que els dos llocs d'estudi investigats van ser diferents en molts aspectes, vam trobar similituds sorprenents en el processament del carboni associat a la reducció da cabal. Això suggereix que les troballes en rius del Mediterrani podrien ser transferibles a altres regions climàtiques sota escenaris de canvi global.

Content

II. Results: Chapter 2

III. Results: Chapter 3

List of figures

List of tables

Abbreviations

Abs	Absorbance
ANOVA	Analysis of variance
BIX	Biological index
CAP	Canonical analysis of principal coordinates
CBH	Cellobiohydrolase
CDOM	Colored dissolved organic matter
D	Oxygen deficit
DOC	Dissolved organic carbon
DOM	Dissolved organic matter
E_2:E_3	Absorbance index related to molecular weight
EC	Electrical conductivity
EEM	Excitation-emission-matrix
em	Emission
ER	Ecosystem respiration
ex	Excitation
FI	Fluorescence index
Fl	Fluorescence
GLS	Generalized least squares
GLU	*β*-glucosidase
GPP	Gross primary production
HMW	High molecular weight
HIX	Humification index
HZ	Hyporheic zone
HZ_{dw}	Hyporheic zone further downstream of the bedrock uplift
HZ_{inf}	Hyporheic zone right downstream of the bedrock uplift
HZ_{up}	Hyporheic zone upstream of the bedrock uplift
k	Gas exchange/ aeration coefficient
L	Lateral
L/D ratio	Live-dead ratio
LEU	Leucine-aminopeptidase
LMW	Low molecular weight
NEP	Net ecosystem production
OPD	Oxygen penetration depth
P/R ratio	Production over respiration ratio
PARAFAC	Parallel factor analysis
PCA	Principal component analysis
PDOM	Protein-like dissolved organic matter
PERMANOVA	Permutational analysis of variance
PHOS	Phosphatase
Q	Discharge

RDA	Redundancy analysis
R.U.	Raman Unit
S_R	Spectral slope ratio
$SUVA_{254}$	Specific ultra-violet absorbance at 254 nm
WL	Wavelength
WRT	Water residence time
WT	Water temperature
$\beta:\alpha$	Freshness index
η	Rate of change in %

General Introduction

Nationalpark Gesäuse (top)

Rienz (middle; by Paul Brugner)

Matarranya (bottom)

1 General Introduction

1.1 Global change impacts on freshwater ecosystems

Human activities have severe impacts on fluvial ecosystems, either directly by contamination (Halliday et al. 2015), water abstraction (Palmer et al. 2009) and damming (Ligon et al. 1995; Aristi et al. 2014) or indirectly by contributing to climate change (Solomon et al. 2009; Vörösmarty et al. 2010; Dey and Mishra 2017). In many regions worldwide, climate change poses a threat to freshwater biodiversity and ecosystem processes (Dudgeon et al. 2006) because of the predicted increase in global surface temperature and shifts in precipitation regimes (Pachauri et al. 2014). Specifically, a decrease in long term average precipitation and river discharge, as well as an increase in evaporation rates are expected for most regions worldwide (Bates 2006; Dai et al. 2009; Wu et al. 2017).

Mountainous regions have been shown to be particularly affected by climate change, exhibiting a faster temperature increase than other regions (Schädler and Weingartner 2010). Consequently, more precipitation will fall as rain rather than snow (Barnett et al. 2005) and together with higher rates of evapotranspiration (Viviroli et al. 2011) will result in severe reduction of stream flow during spring and summer (Ficklin et al. 2013; Berghuijs et al. 2014). The changes in flow regime of mountain headwater streams have wide implications, as mountainous regions are estimated to provide more than 30% of the global water runoff from the continents to the oceans (Meybeck et al. 2001) and lower altitude regions are highly dependent on the runoff of mountain headwater streams (Viviroli et al. 2007; García-Ruiz et al. 2011). Headwater streams often experience dry periods with flow interruption causing temporary loss of aquatic habitats and disturbance of solute fluxes (Lake 2003; Ludwig et al. 2009; Ledger et al. 2012). Understanding the implications of hydrological regime change, in particular the occurrence of droughts, on stream ecosystem functioning is important because they ultimately affect several ecological services provided by headwater streams (Hannah et al. 2007; Ulseth et al. 2017).

1.2 Mediterranean intermittent streams

Mediterranean river basins mainly depend on runoff from mountain streams (García-Ruiz et al. 2011) and have by now turned drier with annual precipitation decreases of up to 20% during the 20th century (Hisdal et al. 2001). In future, the Mediterranean river basins are predicted to experience even longer and more severe drought periods

with a more frequent interval (Weiß et al. 2007; Hertig et al. 2013). Consequently, streams in Mediterranean climate regions are highly vulnerable to climate change through an increase of drought periods (Figure 1.1; IPCC 2007; Pachauri et al. 2014), as at the same time rising water demand for agricultural, industrial, urban and touristic development exert additional pressures on the natural flow regime (Gasith and Resh 1999; Skoulikidis et al. 2017a).

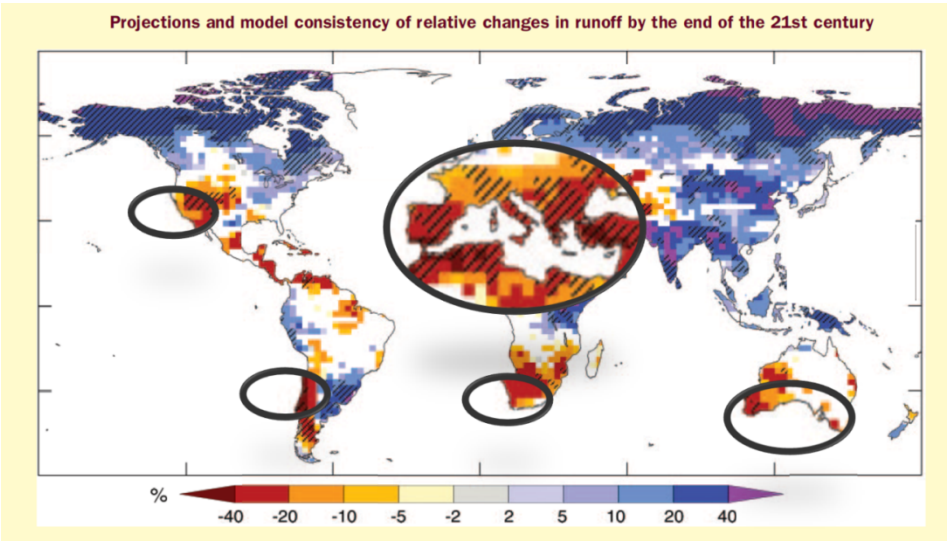

Figure 1.1: Relative changes (between 2080–2099 and present, 1980–1999) of annual surface runoff on the globe, from results of several climate models forced by emissions of scenario A1B. Dashed areas indicate that more than 90% of models agree with the sign of change. The five Mediterranean-climate regions are highlighted. Modified from IPCC (2007).

Water abstractions can convert natural perennial streams into intermittent streams (Datry et al. 2014). Conversely, human activities such as urban and industrial effluents may transform intermittent streams into perennial streams (Hassan and Egozi 2001). In both cases, artificial flow regime alterations are reported to boost the risk of severe ecological changes (Sabater and Tockner 2009; Poff and Zimmerman 2010) that are yet hard to be foreseen because Mediterranean intermittent streams remain among the least studied freshwater ecosystems worldwide (Nikolaidis et al. 2013; Acuña et al. 2014). While perennial streams flow throughout the year, their non-perennial counterparts can cease to surface flow for some time of the year. Depending on this time span non-perennial streams can be classified, either as intermittent with seasonal drought periods of weeks or months or as ephemeral and episodic that are dry most of the year (Mcdonough et al. 2011; Arthington et al. 2014). All these temporary water ways have in common that they were hardly recognized in river management programs and therefore poorly protected on an ecosystem level (Steward et al. 2012) as demonstrated

by abundant cases of misuse including waste disposal, sand and gravel mining or covering by infrastructure (Skoulikidis et al. 2017a). Steward et al. (2012) classified the different connectivity levels of temporary river networks, whereby they differentiated between natural and human-altered temporary river networks. Their review demonstrates the heterogeneity among intermittent streams in different climate regions and furthermore shows the spatial patchiness of environmental conditions induced by natural and man-made morphological elements (pool, riffles, bedrock, gravel bars, dams) that can be found within temporary river networks. Only recently, temporary river networks were targeted by several research disciplines ranging from ecology, biogeochemistry, hydrology and geomorphology to socio-economy and management of these ecosystems (Larned et al. 2010; Leigh et al. 2016).

The growing research on intermittent streams revealed the particularity of these ecosystems, where biogeochemistry is highly modulated by the ceasing of surface flow and the disruption of hydrological connectivity with further impacts on the ecosystem functioning of intermittent streams (Tzoraki et al. 2007; Williams 2007; von Schiller et al. 2011; Gallart et al. 2012; Timoner et al. 2012; Vazquez et al. 2013). For instance, the microbial loop can be affected by low flows and associated low water velocities that increase the thickness of the boundary layer (De Beer et al. 1996; Bishop et al. 1997) and reduce nutrient renewal in biofilms (Hill et al. 2010). Another example is the disconnection with the surrounding watershed, involving that water temperature of the remaining surface flow follows closer the diurnal cycles of air temperature in drying streams (Williams 2007; Robinson et al. 2016) with all ensuing consequences on stream metabolism (Acuña et al. 2008; Yvon-Durocher et al. 2012). By the same token, solute fluxes from the terrestrial compartment are reduced to a minimum (Gasith and Resh 1999; Butturini et al. 2002a; Lake 2003). The disconnection with the terrestrial carbon pool can affect the role of streams as transport ways of terrestrial CO_2 and as biogeochemical reactors of terrestrial organic carbon which change with their hydrological connectivity to the surrounding catchment (Wohl et al. 2012; Hotchkiss et al. 2015; Casas-Ruiz et al. 2017).

1.3 The role of headwater streams in the carbon cycle

Although headwater streams are small and often intermittent, they account for more than 70% of whole stream channel length in the US (Lowe and Likens 2005). A similar estimation can roughly be applied worldwide. Since freshwater ecosystems were estimated to receive about 2.0 to 2.7 Pg of terrestrial carbon per year, headwater streams are an important part of the global carbon cycle, (Cole et al. 2007; Battin et al. 2009; Aufdenkampe et al. 2011). The organic carbon in rivers and streams occurs

mostly in the form of dissolved organic matter. Dissolved organic matter represents a major energy source for microbes, being partly respired to CO_2 and partly incorporated into bacterial biomass, thereby providing carbon to organisms of higher trophic levels (Wetzel 1984; Moody et al. 2013). Only a smaller fraction of approximately 0.3 Pg of terrestrial carbon per year reaches the ocean (Meybeck 1982; Aufdenkampe et al. 2011). Hence, the traditional view on streams and rivers as purely conduits of carbon shifted towards integrating them into global carbon budgets, since not taking them into account leads to the overestimation of the terrestrial carbon sink (Raymond et al. 2013; Butman et al. 2016; Wohl et al. 2017).

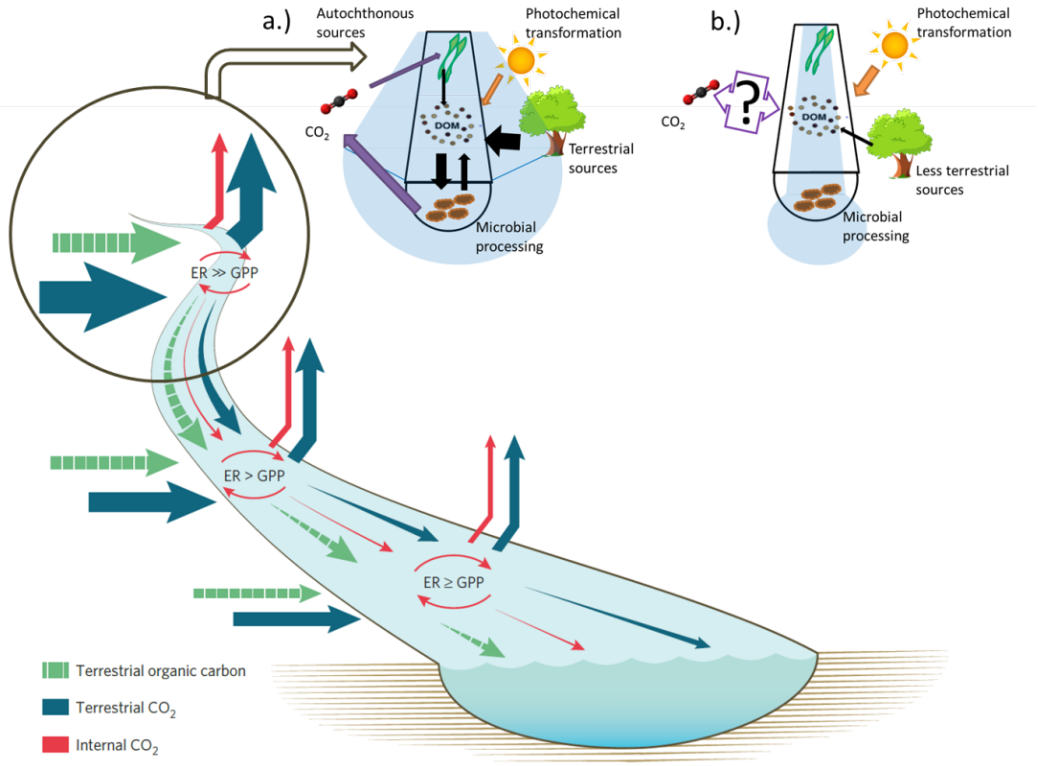

Figure 1.2: Sources and magnitude of net CO_2 emissions along a theoretical stream–river continuum modified from Hotchkiss et al. (2015). Terrestrially derived CO_2 and organic carbon inputs per unit aquatic area decline downstream, decreasing net CO_2 emission rates in rivers compared to streams. Circle represents headwater streams, with a close-up detailing the carbon fluxes in a gaining stream (a) and in a losing stream (b). The question mark represents the uncertainties of carbon fluxes when the stream ceases to flow.

Within this context, headwater streams, apart from covering a substantial portion of the whole fluvial network, are the principal link between the terrestrial-aquatic interface due to their close connection with the surrounding catchment (Lowe and Likens 2005; Wallace and Eggert 2015). Headwater streams were found to process large amounts of the organic matter entering the stream. For instance, Argerich et al. (2016) have shown that a small headwater stream representing only 0.4% of the total area of the watershed, can process and transport similar amounts of carbon per area as estimated on average for rivers. These carbon inputs supply the heterotrophic metabolism of the headwater streams, while high-order rivers have higher rates of in-stream organic carbon production (Figure 1.2; Hotchkiss et al. 2015). However, net autotrophy is also reported from some intermittent low-order streams when terrestrial organic matter inputs decrease (Busch and Fisher 1981; Webster and Meyer 1997; Velasco et al. 2003). In addition, in headwater streams, the benthic and hyporheic zone play a major role in carbon processing (Battin et al. 2008). Particularly, during summer low-flow periods microbial activity in the hyporheic zone is reported to contribute substantially to the CO_2 export from headwater streams (Peter et al. 2014; Argerich et al. 2016). Therefore, the connectivity between remaining surface water and the hyporheic zone is of even higher importance for the source-sink dynamics of dissolved organic carbon during low-flow periods in headwater streams (Figure 1.2).

1.4 In-stream carbon processing: the importance of the hyporheic zone

Defining the boundaries of the hyporheic zone is difficult because the boundaries variate in space and time. Boulton et al. (1998) defined the hyporheic zone "as a spatially fluctuating ecotone between the surface stream and the deep groundwater where important ecological processes and their requirements and products are influenced at a number of scales by water movement, permeability, substrate particle size, resident biota, and the physiochemical features of the overlying stream and adjacent aquifers." From a hydrological perspective, the hyporheic zone is the zone of sediments underlying the surface stream, where stream water that has entered recently the subsurface, may mix with groundwater and will return to the stream channel relatively quickly (Wondzell and Gooseff 2013). Along these hyporheic flow paths, the biogeochemical signature of the water can change considerably (Figure 1.3). While surface water is characterized by light availability, high daily amplitudes of temperature and current velocities, these characteristics are absent or buffered in the hyporheic zone, but conversely to ground water environments the physicochemical gradients are steep and the food webs are rather complex (Krause et al. 2011).

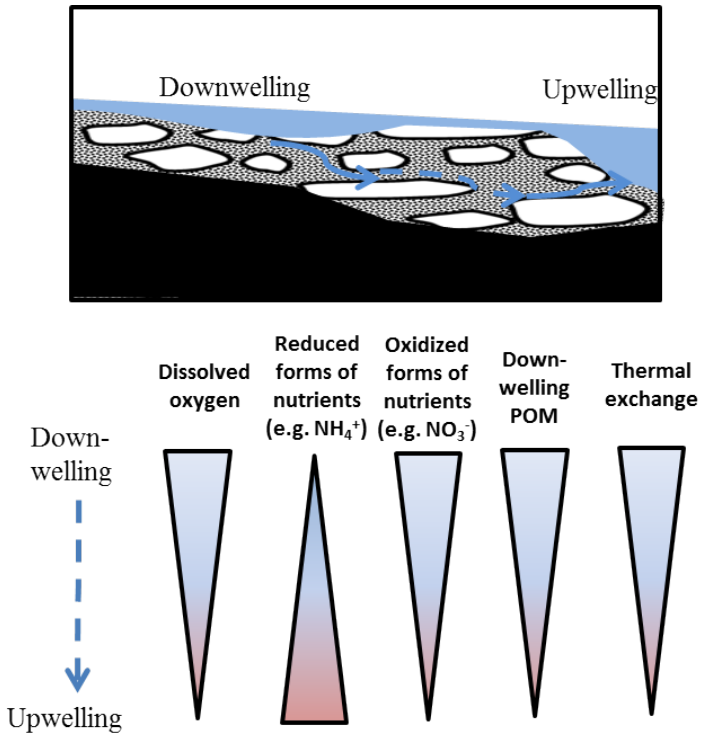

Figure 1.3: Comparison between downwelling and upwelling locations and environmental gradients along hyporheic flowpaths. Modified from Boulton et al. (2008).

Biogeochemical processes occurring in the hyporheic zone are mediated by dissolved oxygen levels that are regulated by the supply from surface water and rates of dissolved oxygen consumption during organic matter decomposition (Jones 1995). Various mesocosm and reach-scale studies have shown that dissolved organic carbon concentrations decrease along hyporheic flowpaths demonstrating that the hyporheic zone is an important compartment of dissolved organic carbon processing in streams (Findlay et al. 1993; Findlay 1995; Naegeli and Uehlinger 1997; Schindler and Krabbenhoft 1998; Baker et al. 1999; Sobczak and Findlay 2002; Zarnetske et al. 2011b; De Falco et al. 2016). Dissolved oxygen is high in downwelling locations and generally low in upwelling locations after subsurface water flows through the hyporheic zone (Valett et al. 1990) and organic matter is processed in the sediments (De Falco et al. 2016). Under these circumstances, denitrification and methanogenesis can occur in the interstitial waters (Harvey and Fuller 1998; Zarnetske et al. 2011a). By contrast, under aerobic conditions, when downwelling surface water supplies dissolved oxygen and nutrients, hyporheic sediments change from a nitrate sink to source (Triska et al. 1990; Merbt et al. 2016). Apart from that, the source and lability of DOM plays a key role for microbial metabolism (Chafiq et al. 1999; Hall and Tank 2003). In this sense,

allochthonous DOM is typically considered resistant to microbial metabolism compared to autochthonous DOM (Fischer et al. 2002). Nevertheless, it had also been suggested that the mixture of fresh labile and accumulated refractory DOM naturally occurring in the hyporheic zone could be the reason for the enhanced bacterial DOM removal (Farjalla et al. 2009).

The amount of water passing through the hyporheic zone and the water residence time are determined by the geomorphological situation (Wondzell and Gooseff 2013) and discharge (Zarnetske et al. 2007). Microbial activity in the hyporheic zone can play an even more important role in watershed ecosystem functions when surface flow ceases, because the hyporheic zone is often the only wet area that remains for microbial activity and subsequent organic carbon processing and nitrogen cycling (Burrows et al. 2017; Romaní et al. 2017). The intensification of organic carbon processing in the hyporheic zone during drought periods might explain the high CO_2 evasions recently reported from drying riverbeds (von Schiller et al. 2014; Gómez-Gener et al. 2015, 2016a). However, triggers of CO_2 evasions from drying riverbeds still remain unclear, partly because of the high spatial and temporal variability of microbial activity reported from drying stream bed sediments (Zoppini et al. 2010; Gómez et al. 2012).

1.5 Towards a general concept of DOM source-sink dynamics during drought

Climate change is generally expected to enhance DOM retention and mineralization in aquatic ecosystems due to the higher probability of drought periods (Lambert et al. 2016; Danczak et al. 2016; Wohl et al. 2017). The main drivers are higher temperatures, narrower wetted channel perimeters and overall dry conditions that reduce DOM inputs (Figure 1.4): Lower drainage from the catchment due to reduced moisture will lead to less DOM transport towards the active stream channel. Increasing water temperature increases metabolic rates in the active channel (Yvon-Durocher et al. 2012), whereby it is not yet clear if primary production and respiration will be affected equally (Acuña et al. 2004; Demars et al. 2016). The severe reduction of discharge during drought will also enhance water residence time in the stream that is equally reported to increase metabolic rates (Sabater et al. 2008; Gómez-Gener et al. 2015; Proia et al. 2016). Specifically, increased water residence times in the hyporheic zone were reported to retain significant amounts of DOM (Baker et al. 1999; Sobczak and Findlay 2002). However, a recent comparison of studies from fluvial ecosystems worldwide revealed that organic carbon decay rates are negatively related with water residence times (Catalán et al. 2016).

Hence, within this conceptual picture of flow reduction and DOM mineralization, there are different mechanisms reported in literature. On the one hand, an increase of DOC concentrations was found in the remaining surface waters during hydrological contraction periods, partly due to an increase of primary production (Jones et al. 1996; Velasco et al. 2003; Von Schiller et al. 2015). On the other hand, intermittent streams were found to be underestimated CO_2 sources to the atmosphere (von Schiller et al. 2014; Gómez-Gener et al. 2015; Looman et al. 2016), which can be triggered partly by increased warming that accelerate heterotrophic metabolism (Acuña et al. 2008; Freixa et al. 2017). Within this debate, the four chapters of this thesis aimed to elucidate some of the complex mechanism driving DOC release and retention under low discharge scenarios.

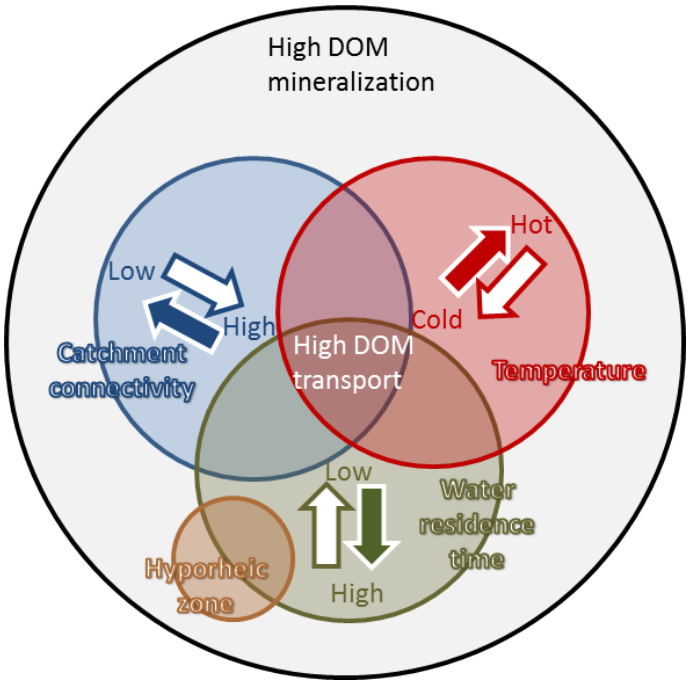

Figure 1.4: Conceptual figure of DOM mineralization versus transport in streams under climate change (modified from Wohl et al., 2017). Colored arrows indicate predicted conditions in regions that will experience more and longer drought periods with climate change. The brown cycle indicates the increasing importance of the hyporheic zone for in-stream carbon cycling with drought.

General Objectives

Lunzer Rinnen (by Masumi Stadler)

2 General Objectives

This doctoral thesis was performed with the goal to improve the understanding of carbon processing in headwater streams under drought scenarios. To approach this goal we studied dissolved organic matter quantity and transformation during the drying phase of an intermittent stream and during flow reduction in an artificial experimental set-up consisting of stream-side flumes. As outlined in the introduction, headwater streams play an important role in global carbon cycling. In this context, dissolved organic carbon dynamics under high flow reflect terrestrial carbon inputs from upstream and the surrounding catchment. On the other hand, the processing, sources and sinks of dissolved organic carbon during severe flow reduction remain yet largely unknown. Particularly, if headwater streams retain or release dissolved organic carbon when they are subjected to drought is an ongoing discussion with contradicting results. Within this discussion, the hyporheic zone is suggested as an organic carbon sink (CO_2 source) but the remaining surface water might be rather a source due to enhanced primary production (CO_2 sink). Therefore, the focus of this thesis lies on the dissolved organic matter processing in the hyporheic zone and on net ecosystem production in the remaining surface water and, finally, on the interaction of these two components.

The first three chapters explore carbon processing in the surface water and the interstitial pore water of the hyporheic zone of a Mediterranean intermittent stream during the drying period. Taking the knowledge gained from these three chapters about the Mediterranean stream into account, a flow reduction experiment in flumes next to a subalpine stream was designed and performed. The fourth chapter evaluates changes in carbon processing with different flow levels at stream-side flumes in the European Alps.

These chapters aim to answer the following questions:

- What are the source-sink dynamics of dissolved organic matter in the hyporheic zone during a summer drought period? (Chapter 1 & 2)
- What are the environmental conditions determining these source-sink dynamics? (Chapter 2 & 3)
- How do dissolved organic matter quality and origin change with flow reduction and subsequent increasing water residence time? (Chapter 1 & 4)
- How does the dissolved organic matter quality of the surface water influence the dissolved organic matter processing in the hyporheic zone? (all Chapters and General Discussion)

- Can we see common patterns in the Mediterranean intermittent stream and the stream-side flume experiment in the Alps? How transferable are findings from the Mediterranean regions to other regions under climate change? (General Discussion)

The first chapter entitled *"Hydrological connectivity drives dissolved organic matter processing in an intermittent stream"* aims to quantify dissolved organic carbon retention and release in the hyporheic zone during different drying phases and to identify Hot Moments and changes in dissolved organic matter quality. In line with previous findings, we expect the hyporheic zone to act as a net sink of dissolved organic carbon, whereby the most labile fractions will show higher retention rates. The lability of the dissolved organic matter from surface water source entering the hyporheic zone will increase with drought severity, because of its autochthonous origin.

The second chapter entitled *"Capturing hot moments of carbon processing across the surface-subsurface interface of an intermittent stream during summer drought"* aims to complement the findings of the first chapter with continuous in-situ measurements of dissolved organic matter fluorescence and partial pressure of CO_2 with the goal to identify Hot Moments of CO_2 production from heterotrophic respiration. We expect that the triggers of these Hot Moments will be the availability of dissolved oxygen and dissolved organic matter.

The third chapter entitled *"Responses of microbial activity across the surface-subsurface interface to biogeochemical changes in a drying headwater stream"* aspires to explain the biogeochemical changes occurring during the drying period with changes in microbial activity. Specifically, this chapter describes the microbial activity across the surface-subsurface interface with the hypothesis that the hyporheic zone represents a hub for microbial activity during drought and thereby explaining enhanced dissolved organic matter processing rates.

Following the research findings from Mediterranean regions, the fourth chapter entitled *"Experimental evidence reveals impact of drought periods on dissolved organic matter quality and ecosystem metabolism in subalpine streams"* presents the stream-side flume experiment, designed to evaluate the impact of different drought levels on dissolved organic matter quantity and quality, as well as on the net ecosystem production in a subalpine stream. We hypothesized that we would find similar high primary production rates as reported from Mediterranean and desert streams. Consequently, we expect to find an increase of dissolved organic carbon concentrations paralleled with a change towards more labile dissolved organic matter characteristics in the flumes with lower discharge.

In the general discussion section, parallels between findings from the natural drought occurring in the Mediterranean stream and from the discharge reduction experiment in the stream-side flumes will be discussed. Even though the geographical locations, scales and environmental setting of the study sites are very different from each other, we expect to identify common patterns with drying and similar drivers of dissolved organic matter processing in the natural stream and the flumes. Furthermore, these results will be embedded with findings in literature on carbon fluxes of headwater streams and the function of the hyporheic zone, allowing a more global view on the findings of this thesis.

General Methods

Lunzer Rinnen (left)

Laboratory test of the flow through cell (right)

Field equipment on dry streambed in Fuirosos (bottom)

3 General Methods

In this part we aim to provide a general overview on methodologies that were used in the four chapters. The specific methodology can be found in detail in every of the four chapters. The field work for this thesis was performed in summer 2014 and 2015 (Figure 3.1). The Chapters 1 to 3 were performed in the Fuirosos catchment and Chapter 4 was performed at a stream-side flumes installation next to the subalpine stream 'Oberer Seebach' (see Chapter 4).

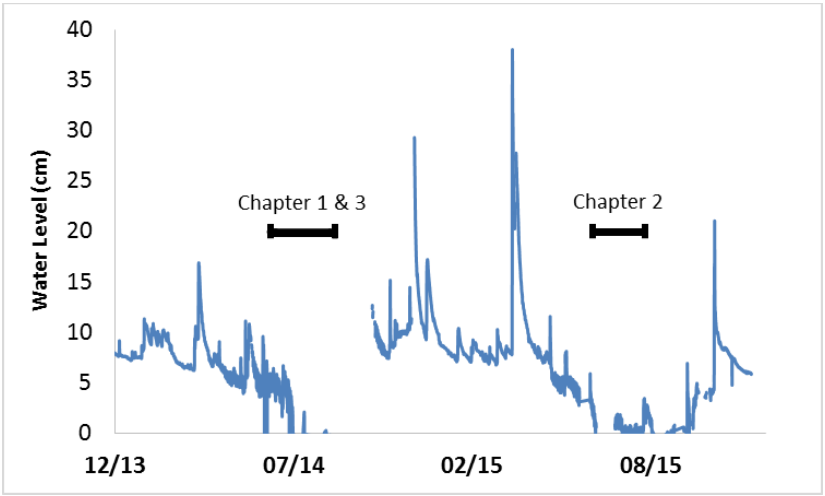

Figure 3.1: Water level at a monitoring station (approximately 1 km upstream of the study site) from the years 2014-15 (Butturini, unpublished data) with the study periods of the chapters indicated above.

3.1 The Fuirosos catchment

Chapters 1, 2 and 3 present research carried out at the Fuirosos stream. Fuirosos is a third order stream that drains a 15 km^2 large catchment located in the Montnegre Natural Park 60 km north of Barcelona. The dense forest vegetation comprises cork oak (*Quercus suber*) and pine tree (*Pinus halepensis*) and the riparian vegetation flanking the stream channel is dominated by plane tree (*Platanus hispanica*) and alder (*Alnus glutinosa*). At the top of the mountain range chestnut (*Castanea sativa*), hazel (*Corylus avellana*) and oak (*Quercus pubescens*) can be found. Less than 2% of the area is used for extensive agriculture. The underlying geology of the catchment is composed of leucogranite and granodiorite (Vazquez et al. 2013). The catchment is located between

50-770 m above sea level, characterized by steep slopes at the valley top and gentler slopes at the valley bottom (Figure 3.2). Most of the active stream channel at the valley bottom is covered by a well-developed alluvial sediment layer (gravel and sand) and there are only few reaches where the hyporheic zone connectivity is interrupted by the exposed granitic bed rock (Medici et al. 2008).

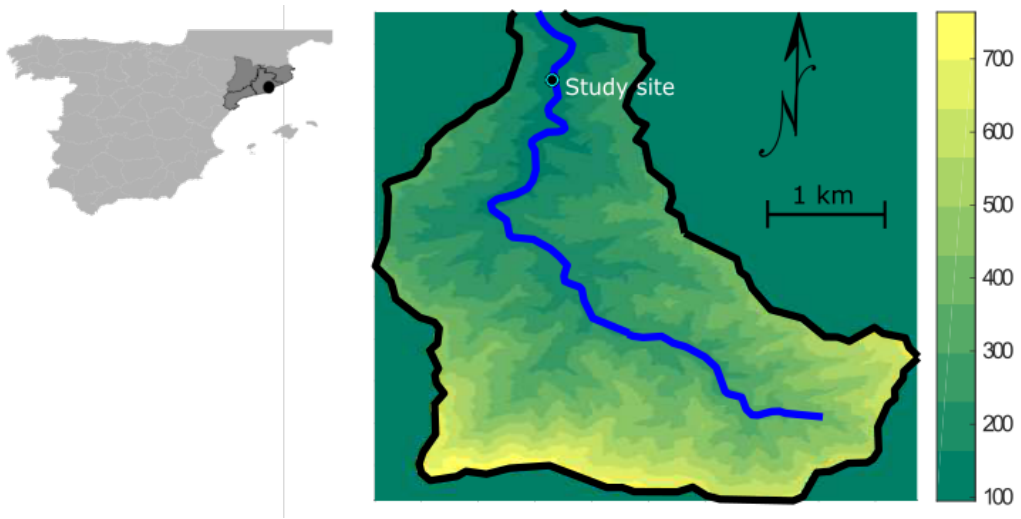

Figure 3.2: Location of the Fuirosos catchment on the Iberian Peninsula (left) and the stream valley with the catchment (black line) and the main stem (blue line) on the right. The point indicates the location of the study site (Figure 3.3). The color bar shows the elevation (m a.s.l.).

The winter average temperature is of 7°C in January and February and the summer average temperature is of 22°C in August and July. Annual precipitation ranges between 500 mm and 900 mm that mainly fall during storm events in spring and autumn. By contrast, the summer months are characterized by a severe drought period with high evaporation rates (total annual evapotranspiration is of 950 mm/yr; Medici et al. 2008). These drought periods account for approximately 20% of the year (Butturini et al. 2008). The severe hydrological changes are also reflected in the groundwater level that ranges from 0.5 m depth with respect to the ground surface in winter to 3.4 m depth in summer. In the same way, the soil–water volumetric content ranges from 8% in summer to 25% in winter (Butturini et al. 2002a). Therefore, during summer rain events there is no relationship between the precipitation intensity and discharge observed (Butturini et al. 2003). In fact, during the summer drought periods the stream becomes hydrologically disconnected from its surrounding catchment (Bernal and Sabater 2012a).

Table 3.1: Some studies that are related to the topics of this thesis and were performed in the Fuirosos catchment.

Study	Topic	Compartment	Hydrological conditions	Findings
Acuña et al. 2004	Stream metabolism	Main channel	Whole year	net heterotrophy due to riparian shading
Álvarez et al. 2010	Inorganic nutrients	Main channel	Whole year	low P retention, nutrient uptake increases with dispersion
Artigas et al. 2008	Microbial activity	Streambed	Flow period	relationship between EEA's and nutrient molar ratios
Artigas et al. 2009	Microbial activity	Streambed	Whole year	heterotrophic activity peaked in autumn
Bernal et al. 2002	DOM and inorganic nutrients	Main channel	Whole year	highest NO_3 export during storm, DOC export during baseflow
Bernal et al. 2005	DOM and inorganic nutrients	Main channel	Whole year	DOC:DON ratios highest during baseflow
Bernal et al. 2006	Inorganic nutrients	Catchment	Whole year	NO_3 retention in near-stream zones during low discharge
Bernal et al. 2007	Inorganic nutrients	Riparian/stream	Whole year	only denitrification in riparian soil during winter and high groundwater table
Bernal and Sabater 2012	Inorganic nutrients	Main channel	Baseflow	DIN retention under baseflow (38%)
Butturini and Sabater 2000	DOM	Riparian/stream	Whole year	during baseflow the DOC in the HZ is higher than in stream water
Butturini et al. 2002	Hydrology	Riparian/stream	Whole year	during summer no relationship between rain intensity and discharge
Butturini et al. 2003	Inorganic nutrients	Riparian/stream	Whole year	NO_3 release of riparian zone during discharge towards the stream
Butturini et al. 2005	Hydrology	Riparian/stream	Stormflow	development of concentration-discharge model
Butturini et al. 2008	DOM and inorganic nutrients	Main channel	Whole year	DOC and NO_3 discharge responses can be categorized, but follow random pattern
Fazi et al. 2013	Microbial activity	Main channel	Drought	community shift between summer and autumn
González-Pinzón et al. 2016	Stream metabolism	Main channel	Baseflow	high respiration in HZ buffer temperature amplitudes
Guarch-Ribot and Butturini 2016	DOM	Main channel	Stormflow	DOM-discharge relationships depend on antecedent conditions
Medici et al. 2008	Hydrology	Riparian/stream	Whole year	non-linear hydrological behavior
Medici et al. 2010	Inorganic nutrients	Riparian/stream	Whole year	riparian zone as important NO_3 source after summer drought
Sabater et al. 2005	Stream metabolism	Main channel	Baseflow	nutrient enrichment increases autochthonous bio mass even with light limitation
Sabater et al. 2008	Stream metabolism	Main channel	Baseflow	light limitation of primary production
Sabater et al. 2011	Stream metabolism	Main channel	Whole year	Autotrophy initiated during spring maintains with long-term nutrient additions
Romaní et al. 2004	Microbial activity	Streambed	Baseflow	different nutrient retention of biofilms grown on rocks and on sand

Study	Topic	Compartment	Hydrological conditions	Finding
Romaní et al. 2006	Microbial activity	Riparian/stream	Stormflow	efficient DOM use with reflow after drought
Romaní et al. 2008	Microbial activity	Streambed	Baseflow	enzyme activity reduces with biofilm age
Vázquez et al. 2007	DOM	Riparian/stream	Dry/Rewetting	dry phase favored DOM retention from riparian zone
Vázquez et al. 2011	DOM	Main channel	Drought	heterogeneity of DOM quality increases with drought among isolated pools
Vázquez et al. 2015	DOM	Main channel	Dry/Rewetting	high DOM bioavailability during rewetting
Von Schiller et al. 2008	Inorganic nutrients	Main channel	Whole year	DIN is dominated by NO3, NH4 and NO2 generally low
Von Schiller et al. 2011	Inorganic nutrients	Main channel	Dry/Rewetting	NO3 limitation drought, but high with runoff
Von Schiller et al. 2015	DOM	Main channel	Drought	hydrological phases shape DOM quality
Ylla et al. 2010	Microbial activity	Streambed	Dry/Rewetting	benthic substrata as refuge for microorganisms
Ylla et al. 2011	Microbial activity	Streambed	Dry/Rewetting	benthic OM quality decreased during drought

The Fuirosos catchment is one of the best studied pristine, intermittent streams in the Iberian Peninsula. Over the past 20 years, more than 30 studies were published investigating the climate, the hydrology, the biology and in particular, the biogeochemistry in relationship with hydrological conditions. The research performed along Fuirosos therefore fitted an important gap of knowledge about the peculiarity of intermittent streams and serves as a reference for streams with similar characteristics. The stream is generally net heterotrophic, because of the abundant shading by riparian vegetation and the high leaf litter input fuelling heterotrophic metabolism (Acuña et al. 2004). While streamwater DOC concentrations during baseflow range between 2 and 4 mg L^{-1}, DOC concentrations can rise up to 20 mg L^{-1} during the transition between dry and wet phases (Bernal et al. 2002). The inorganic nutrient concentrations are generally low but show wide ranges (N-NO3: 14 – 2143 μg L^{-1}; N-NH4: 5 - 201 μg L^{-1}; P-PO4: 0 - 21 μg L^{-1}) over the course of the year (von Schiller et al. 2008). The most relevant studies for this thesis, relating hydrology, biogeochemistry and microbial activity are summarized in Table 3.1.

3.2 The peculiarity of the chosen study site

The study site, the specific sampling points and the sampling strategy are detailed in each chapter. Therefore, this subsection should only provide a brief overview: The studied reach is located at the valley bottom between 160-165 m above sea level

(latitude 41º42'23"-28", longitude 2º34'81"-86"). This location is characterized by an exposed impermeable bedrock channel of 63 m length, flanked by shallow sandy sediments and then covered again forming a channel of alluvial sediments of approximately 1 to 2 m depth. Due to the missing hyporheic connectivity, the flow is restricted to the surface by the uplift of the bedrock acting as a natural barrier. Due to the impermeability of the bedrock channel surface water is still captured in small pools (5-7 m^3) and in the hyporheic zone, even when there is no surface flow present in the rest of the stream.

Figure 3.3: Photo of the study site (location see Figure 3.2). The uplift of the granitic bedrock is clearly visible in the back of the photo with the outlet of the pool. In the front part of the photo, a sampling well (HZ_{inf} that is described in Chapter 3) installed in the alluvial sediments downstream of the pool.

In Chapters 1 to 3 we focussed on two locations (other sampling locations are presented in detail in the according chapter) that maintained hydrological connectivity throughout the drought period: The location pool is located within the impermeable bedrock (Figure 3.3) and well HZ_{dw} is located 25 m downstream of the pool. This reach was ideal for our objectives because the uplift of the impermeable bedrock confined the surface water and the alluvial sediment body. Hence, this situation enabled us to delineate the hyporheic flow paths and investigate biogeochemical changes along these.

We verified the hydrological disconnection of the hyporheic zone from riparian inflows by measuring the water level installed in the riparian zone next to HZ_{dw} and in the well of HZ_{dw} (Figure 3.4). These measurements confirmed that the stream reach was a losing reach during the study period.

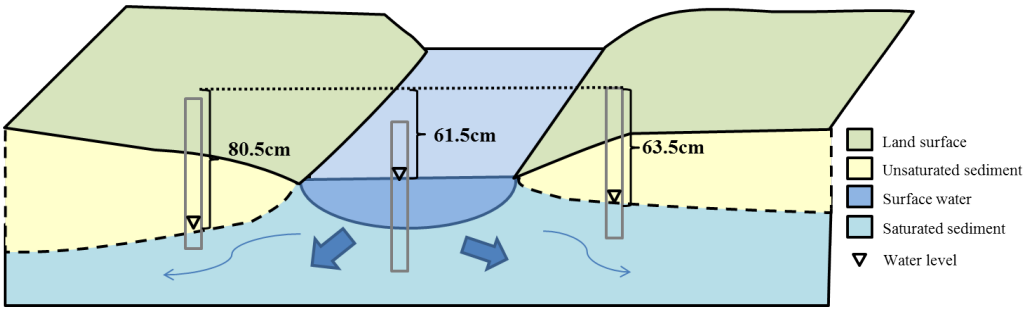

Figure 3.4: Scheme with the location HZ_{dw} in the middle and the riparian wells left and right. The dotted line on top shows the comparison of water levels between these three wells. The water levels are examples from the 3rd of July 2014 that was the start of the contraction phase.

Furthermore, we investigated hydrological connectivity between the pool that served as our reference water source to the hyporheic zone and the well with means of electrical conductivity measurements (see Chapter 1) and stable water isotopes (Figure 3.5). Stable water isotopes are widely used as tracers because they allow following the water transport through a catchment. The reason for this is that the water has a characteristic isotopic fingerprint of its origin and therefore can be used to identify where the water in the stream comes from. Additionally, for our application this was especially important, once in the subsurface and away from evaporative effects, this isotopic fingerprint is conservative and reflect the mixing relationships of water sources (McGuire and Mcdonnell 2008). Specifically, this method uses the ratio of heavy (Deuterium ^{2}H and ^{18}O) to light isotopes (^{1}H and ^{16}O) and the ratio of each sample is then compared and reported in relationship to the international standard ratio (VSMOW) and reported in δ‰ (Gat et al. 1981).

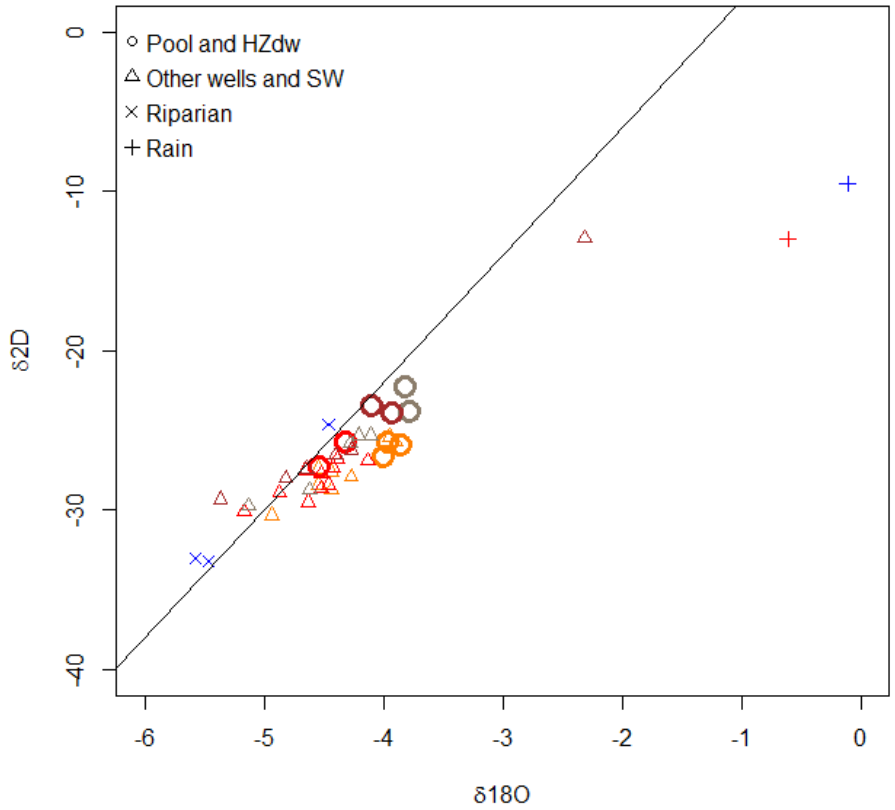

Figure 3.5: The stable water isotope ratios with colors indicating the sampling day. The pool and the HZ_{dw} are highlighted compared to the other wells and surface water samples in the study reach (data from 2014). The proximity of the circles gave us further evidence that the conclusions taken from electrical conductivity were correct and the hydrological connectivity was given during the whole sampling period without riparian inflow or evaporation losses. The black line indicates the global meteoric water line with the formula $\delta D = 8\ \delta^{18}O + 10$ that is based on precipitation data from locations all around the world (Stor and Craig 1961).

3.3 Dissolved organic matter characterization

For the sake of clarity, the analytical protocols of chemical characterization of the water samples are detailed in each chapter because some analyses were performed in different laboratories. Throughout this thesis, we used dissolved organic carbon concentrations [DOC] and optical properties of DOM to describe the DOM composition of the water samples. DOC is assumed to account for 45 to 50% of the DOM mass and is therefore used widely as a proxy to evaluate DOM quantity (McDonald et al. 2004). We calculated from absorbance spectra and fluorescence excitation-emission matrices

(EEM) the indices presented in Table 3.2. These quality indices are based on the fact that chromophoric DOM components absorb light thereby decreasing the amount of energy exiting the sample. Moreover, fluorescence can be detected when a molecule absorbs energy causing an electron to be excited to a higher energy level. As the electron returns to ground state, energy is lost as an emission of a photon, whereby the excitation and emission wavelengths at which this happens can be measured and assigned to specific molecular structures (Fellman et al. 2010; Hansen et al. 2016). Fluorescence excitation-emission matrices data treatment was performed with Matlab (version R2015b, Mathworks). Correction of fluorescence spectra is an important part of the analysis and we used the procedure explained by Goletz et al. (2011). The raw fluorescence data were divided by a correction file obtained for the lamp in use following the protocol of Gardecki and Maroncelli (1998). All samples were normalized to the Raman area to account for lamp decay over time (Lawaetz and Stedmon 2009) and Fluorescence Intensity is given in Raman Units (R.U.). Absorbance data of the respective samples were used to correct for the inner-filter effect (Lakowicz 2006). MilliQ water blanks were subtracted to remove Raman scattering (Goletz et al. 2011). The specific indices that were used in each chapter are described in the according chapter's method section.

Apart from the above mentioned indices, we used parallel factor analysis (PARAFAC) to extract the most dominant components of Fuirosos water samples in chapter 1 and the experimental flumes presented in chapter 4 (Figure 3.6). Again the specific model characteristics and the components found are described in the according chapter. PARAFAC is a statistical analysis of EEM datasets, whereby the fluorescence intensities are separated into individual constituents assigned to fixed excitation-emission wavelength pairs (Bro 1997). The fundamental assumption behind is that the fluorophores are independent from each other according to the Beer-Lamberts law (Stedmon and Bro 2008). This means that every component represents a group of wavelengths that vary independently to the rest of the wavelengths found in the data set. Although widely used, it should be mentioned that this approach is very sensitive to outliers. This disadvantage makes a careful removing of outliers necessary that might obscure the occurrence of very rare components. However, we chose this method because of its wide usage that allowed us to compare our modelled components with the components and the related DOM component characteristics found in other studies with the 'OpenFluor' database (Murphy et al. 2014).

Table 3.2: Summary of the optical indices used in this thesis.

Parameter	Abbreviation	Calculation	Description	Literature
Specific Ultraviolet Absorbance	$SUVA_{254}$	$\frac{Abs254}{[DOC] \times l}$	higher absorbance indicates higher aromatic carbon content	Weishaar et al. (2003)
Spectral slope ratio	S_R	$\frac{slope(275:285)}{slope(350:400)}$	generally increases with DOM being subjected to irradiation	Helms et al. (2008)
Fluorescence Index	FI	$\mathrm{ex}370\frac{em470}{em520}$	indicates the relative contributions of allochtonous vs. autochthonous	Mcknight et al. (2001)
Humification Index	HIX	$\mathrm{ex}254\frac{\sum(em435:480)}{\sum(em300:345)+\sum(em435:480)}$	increases with humification of DOM	Ohno 2002
Freshness Index	$\alpha:\beta$	$\mathrm{ex}310\frac{em380}{max(em420:435)}$	higher values representing a higher proportion of fresh DOM	Wilson and Xenopoulos 2009
Biological Index	BIX	$\mathrm{ex}310\frac{em380}{em430}$	indicates freshly produced DOM in the aquatic environment	Huguet et al. 2009
Absorbance slope	$E_2:E_3$	$\frac{Abs250}{Abs365}$	negatively related to the aromaticity and molecular weight of humic substances	Peuravuori and Pihlaja 1997

Abs = Absorbance at specified wavelength. l = path length of cuvette. ex = excitation. em = emission.

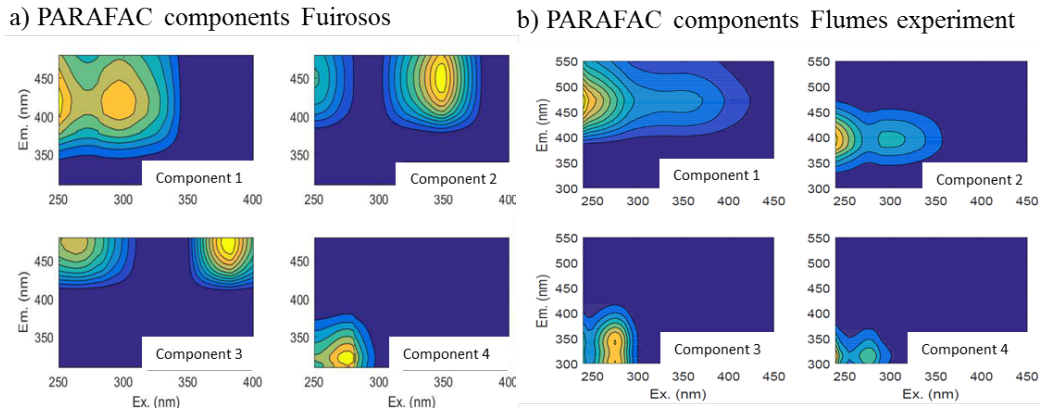

Figure 3.6: Fingerprints of PARAFAC components modeled for the a) Fuirosos data set and b) for the experimental flumes data set. Details on the components are explained in the according chapters.

3.4 Net ecosystem production - Measuring stream metabolism with continuous dissolved oxygen measurements

Since its publication in 1956, the use of diel cycles of dissolved oxygen concentrations to measure stream metabolism (Odum 1956) has been applied in an enormous amount of studies and has become one of the most important tools for the evaluation of ecosystem health in aquatic environments (Hoellein et al. 2013). One of the major challenges is the accurate estimation of the gas exchange coefficient k when using continuous dissolved oxygen concentration measurements in open systems (Raymond and Cole 2001; Schelker et al. 2016). However, this method is of great interest for long-term studies because continuous measurements of oxygen are easy to obtain and allow investigating the change of net ecosystem production between several days or even between seasons. The estimation of k can be done either directly with gas tracer tests, or indirectly by applying empirical equations that include hydraulic parameters to determine k (for a comparison of methods see Aristegi et al. 2009).

In this thesis, we estimated k with two other widely used indirect approaches. One is the nighttime regression method and the other one is a statistical modelling method using Bayesian models. All calculations were performed with R (R Team Development Core 2008). The nighttime regression method uses the change of DO saturation and measured DO during the night (Hornberger and Kelly 1975). The slope of the best regression fit is used as the k (min^{-1}), whereby we put minimum requirements for the linear regression and number of observations that had to be fulfilled ($r^2 > 0.1$ and $n \geq 9$). When these requirements were not fulfilled we took the k from the night before. For the

flumes, *k* was calculated with Bayesian models, using the R toolbox 'streamMetabolizer' provided by Appling et al. (2017) and in addition with the night-time regression method. Both methods gave k-values in the same range (Table 3.3). A similar approach was not possible for Fuirosos because we did not have light data from our measurement point that is necessary for this modelling approach.

Table 3.3: *k* values calculated with Bayesian modelling and nighttime regression method for the flumes in chapter 4

k (min^{-1})	Bayesian	night time regression (r^2)
F1	0.0019	0.0050 (0.58)
F2	0.0032	0.0068 (0.82)
F3	0.0088	0.0095 (0.90)
F4	0.0114	0.0109 (0.76)

For Fuirosos, the single station method was applied, while for the experimental flumes we used the two station method in order to meet the requirements of reach length for each method (Reichert et al. 2009). The two station method is thoroughly explained in chapter 4. For the single station method, estimates were based on 15-min interval measurements by taking the change in DO (ΔO_2) from time1 and time2 divided by the time interval (ti) and subtracting the temperature corrected reaeration coefficient (k_t) multiplied with the oxygen deficit (D) (Bernot et al. 2010; Riley and Dodds 2013).

$$DO_{net\,rate} = \frac{DO_{time1} - DO_{time2}}{ti} - k_t \times D \qquad [mgO_2\ L^{-1}\ min^{-1}]$$

Eq. 1

From this corrected oxygen net rate ($DO_{net\ rate}$) the mean values of each night were taken and temperature corrected with the formula taken from Demars et al. (2016), using the apparent activation energy (0.57 eV) for respiration taken from Yvon-Durocher et al. (2012). These values represent the ecosystem respiration (ER). The Gross Primary Production (GPP) was calculated by adding the absolute values of ER to the $DO_{net\ rate}$. All rates were integrated over 24 h to obtain daily rates.

3.5 Extracellular enzymatic activities

In Chapter 3 we used four extracellular enzymatic activities to investigate microbial activity related with DOM processing. The analytical protocols are described in Chapter 3. Here, we want to provide a brief overview of the activities that were used and explain the choice of these activities for our study.

We chose two polysaccharide degrading enzyme activities, namely β-glucosidase (GLU) and cellobiohydrolase (CBH), one enzyme activity that is related to the degradation of protein-like DOM, namely leucine-aminopeptidase (LEU) and the organic phosphorus degrading enzyme activity phosphatase (PHOS). We considered that these extracellular enzymatic activities resulted to be adequate to study organic matter utilization and microbial activity during the drought period based on their successful use in previous studies. For instance, previous studies showed a strong relationship between the organic matter availability and the extracellular enzymatic activities GLU and LEU in biofilms during spring (Sabater et al. 1997; Ylla et al. 2011) and in surface water during the storm period (Romaní et al. 2006). Likewise, we chose to analyze PHOS because this activity was reported to increase during drought in stream sediments and is therefore a good proxy for microbial activity during this period (Zoppini and Marxsen 2010; Timoner et al. 2012). Similarly, Artigas et al. (2009) found that CBH increased between June and September in relation to the early leaf litter fall in Fuirosos due to water stress during drought periods.

3.6 Statistical methods

The specific statistical method is thoroughly explained in every chapter and therefore only a general overview is provided here: In chapters 1, 2 and 4 we often report or perform statistical analyses with η-values that refer to concentration or DOM quality index changes between the water source and the measurement point. In chapter 1 and 2 the water source is represented by the pool and the measurement point by the well HZ_{dw}. In chapter 4 the former is represented by the inflow and the latter by the outflow of each flume. We used analysis of variance (ANOVA, when assumptions were fulfilled) or otherwise the non-parametric Kruskal-Wallis ANOVA to investigate differences between hydrological phases in chapter 1 and 2, as well as between discharge levels in chapter 4. Normality was evaluated with Shapiro-Wilk tests and histograms. Multivariate statistics included in chapter 1 a principal component analysis to characterize DOM quality of samples in space and time and in chapter 3 a canonical analysis of principal coordinates and a permutational analysis of variance to investigate differences between locations. In chapter 2, we applied generalized least squares with the aim to identify the drivers of pCO_2 dynamics. For details, we refer the reader to the methods section of the according chapters.

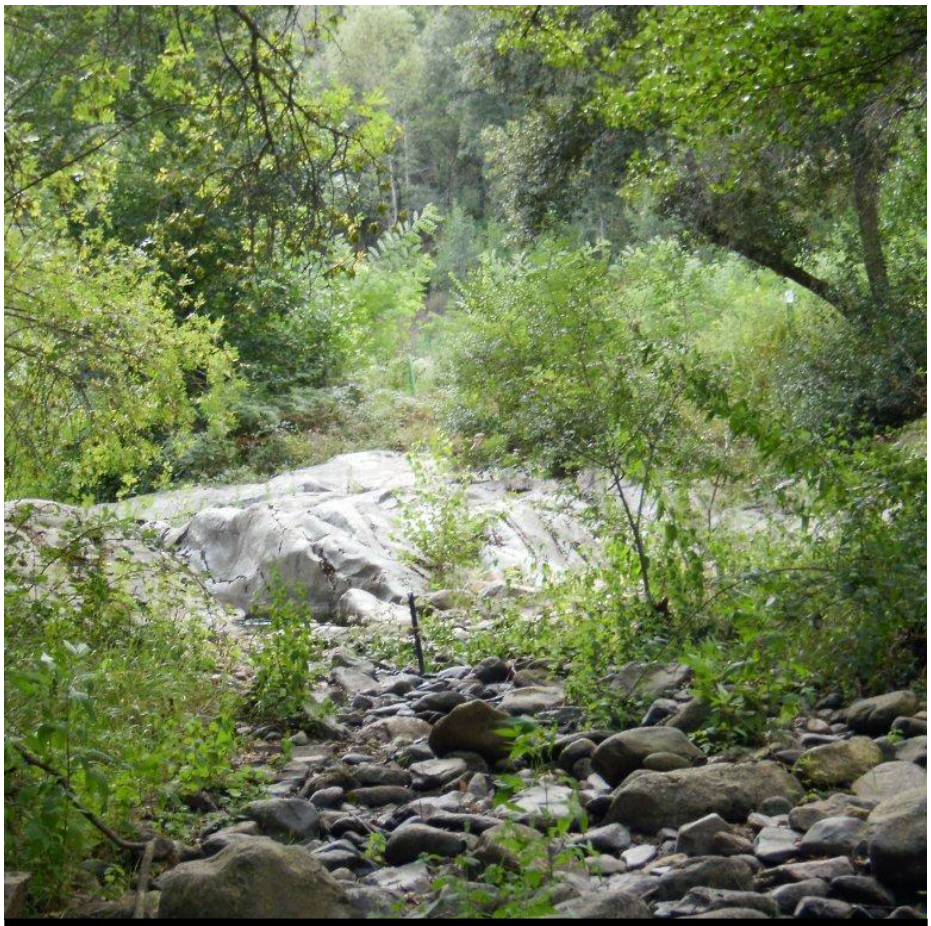

I. Results: Chapter 1

Fuirosos in August (top)

Fuirosos in October (bottom, by Patricia Rodriguez)

4 Hydrological connectivity drives dissolved organic matter processing in an intermittent stream*

Hydrological conditions are key drivers of dissolved organic matter (DOM) processing in intermittent streams. However, there still exist major gaps in knowledge regarding the temporal dynamics of DOM processing during drought periods, as well as the role of the hyporheic zone (HZ). We conducted weekly sampling of surface water and hyporheic pore water during a drying/rewetting cycle and characterized DOM by fluorescence and absorbance properties. Overall, the contribution of allochthonous and humic-like DOM increased during base flow in early summer (pre-drought) and continued increasing throughout the drought period, which covered three phases: contraction, fragmentation and dry. The contribution of autochthonous DOM during this period was restricted to very specific points in space (the HZ) and time (the transition from contraction to fragmentation phase). Hydrological connectivity between the HZ and the surface water was a driver of DOM composition by supplying terrestrial, aromatic DOM to the HZ. The disconnection of the stream from the riparian groundwater enabled us to quantify the DOM retention/release in the HZ. DOM mass balance at the stream-hyporheic interface revealed the occurrence of two time periods with disproportionately high rates for DOM processing (hot moments) during the study period: 1) A short pulse of protein-like, autochthonous DOM net release at the beginning of the disconnection; and 2) A longer time period of increasing net dissolved organic carbon (DOC) retention up to 30% along 25 m of HZ length during fragmentation and dry phase. Remarkably, the net carbon retention was coupled to a decrease of aromatic and high molecular weight compounds, while protein-like, autochthonous DOM was released. This result evidenced that under drought conditions, the HZ becomes a sink for DOM compounds previously assumed to be recalcitrant in aquatic ecosystems and therefore highlights the importance of hydrological drivers on DOM processing.

* *Harjung, A., F. Sabater, and A. Butturini. 2017. Hydrological connectivity drives dissolved organic matter processing in an intermittent stream. Limnol. - Ecol. Manag. Inl. Waters. doi:10.1016/J.LIMNO.2017.02.007*

4.1 Introduction

Intermittent streams are suspected to account for more than half of the global fluvial network, and flow intermittency is predicted to increase with climate change and increasing water use (Palmer et al. 2008; Datry et al. 2014). At the same time, fluvial networks are recognized as an important part of the global carbon cycle (Battin et al. 2008; von Schiller et al. 2014). Consequently, the biogeochemistry of intermittent streams has received increasing attention from the scientific community in recent years (Larned et al. 2010; Leigh et al. 2016). In lotic ecosystems, drought periods strongly influence the quantity and characteristics of dissolved organic matter (DOM) (Vázquez et al. 2007; Fellman et al. 2011b; Butturini et al. 2016; Guarch-Ribot and Butturini 2016). Previous studies report an increase in fresh, non-humic DOM in the remaining surface water as drought proceeds (Vázquez et al. 2011; Von Schiller et al. 2015). Fragmentation of the fluvial continuum generates a set of distinct hydrological hot spots and drought greatly amplifies the qualitative heterogeneity of DOM (Vázquez et al. 2011). However, research has focused mainly on surface water (Fellman et al. 2011a; Von Schiller et al. 2015; Butturini et al. 2016; Casas-Ruiz et al. 2016; Ejarque et al. 2017) or riparian groundwater (Romaní et al. 2006; Vázquez et al. 2007; Fellman et al. 2011b).

In contrast, few studies have tackled the role of the HZ within DOM transport and transformation during drought periods, even though the HZ is recognized as a biogeochemical hot spot (McClain et al. 2003; Boano et al. 2014). Moreover, the efficiency of the HZ to retain labile carbon is positively related to the residence time of hyporheic flow paths (Baker et al. 1999). However, the HZ of perennial streams has also been identified as a source of recalcitrant DOM, but to a lower extent than its overall retention capacity (Battin et al. 2003).

Sobczak and Findlay (2002a) found dissolved organic carbon (DOC) concentration to decrease within a range of 19% to 28% along a HZ length of 4 m in mesocosm experiments. These results highlight the potential of the HZ as an important DOM sink in fluvial systems. Additionally, they have reported significant decreases of DOC concentrations in pore water along hyporheic flow paths for several streams, but the clear delineation between hydrological and biogeochemical controls on DOC in natural systems entail difficulties. DOM retention of the HZ can be overestimated due to dilution with DOM poor ground water. We expected to overcome this uncertainty and tested the potential of the HZ for DOM retention in a natural system, because the HZ is reported to be disconnected from riparian groundwater during drought (Bernal and Sabater 2012b). Additionally, when surface run-off is zero and water flow is restricted

to the HZ, the quantification of DOM retention and release under drought conditions is relatively simple.

We hypothesize that hydrological connectivity along hyporheic flow paths under drought conditions is a major driver of changes in DOM quality and quantity. According to previous studies we predicted an increase in autochthonous, non-humic DOM in the remaining surface water as drought proceeds and the fast retention of this autochthonous input in the HZ. We want to address the lack of knowledge of biogeochemical transformation processes in space (hot spots) and time (hot moments) by exploring the HZ and adjacent surface water during hydrological disconnection of the river continuum caused by a seasonal summer drought and stream bed geomorphology characteristics in a Mediterranean intermittent stream. Our goals were (1) to investigate the DOM quality changes along a hyporheic flow path during different hydrological conditions (2) to use the simplification of the system to perform an in situ DOM mass balance in the HZ.

4.2 Methods

4.2.1 Sampling strategy

This study was performed in Fuirosos, at a reach that is characterized by the uplift of the granitic bedrock, interrupting the permeable streambed composed of alluvial gravel (2-5 cm) with sandy and silty fractions. The exposed impermeable bedrock channel is 67 m long and then covered again by the alluvial sediments forming a HZ of approximately 1 to 2 m of depth with an approximate hydraulic conductivity of 10^{-3} m s^{-1} estimated by pumping of the wells installed in the HZ (Baxter et al., 2003), which is the expected range of gravel (Domenico and Schwartz, 1998). The hyporheic connectivity is restricted to surface flow by the uplift of the bedrock acting as a natural barrier. Due to the impermeability of the bedrock channel surface water is still captured in small pools (5-7 m^3); even when there is no surface flow present in the rest of the stream.

We performed weekly samplings from June until October 2014 to follow the dry-rewetting cycle. The choice for this time period was based on previous investigations of this stream (Butturini et al. 2002b, 2003; Vázquez et al. 2011; Bernal and Sabater 2012b; Von Schiller et al. 2015). Von Schiller et al. (2015) separate the dry-rewetting cycle into the hydrologic phases of contraction, fragmentation, dry and expansion. We followed this scheme, but introduced pre-drought as an additional hydrological phase, which describes the base flow period in June before contraction. We separated these 5 phases based on continuous water level measurements (Campbell Scientific CS451

Stainless-Steel SDI-12/RS-232 Pressure Transducer) in the pool, and presence of surface flow up-and downstream. This information was obtained from continuous electrical conductivity (EC) measurements (Campbell Scientific CS547A-L Water Conductivity and Temperature Probe) installed at the surface of the stream bed (when EC = 0, surface flow = 0) up-and downstream of the bed rock channel. Temperature inside the pool was recorded with a Campbell Scientific 109SS-L Stainless-Steel Temperature Probe for Harsh Environments. The contraction phase starts when the water level in the pool drops and shows a continuous decrease and a corresponding increase of EC measurements. The fragmentation phase is characterized by the absence of surface water at the permeable streambed upstream, while EC and stable water isotope signatures indicate hydrological disconnection. The dry phase is defined by the absence of surface water along the whole reach, with the exception of the pools in the impermeable zones. Rewetting is the phase when the river continuum is re-established after storm events in autumn.

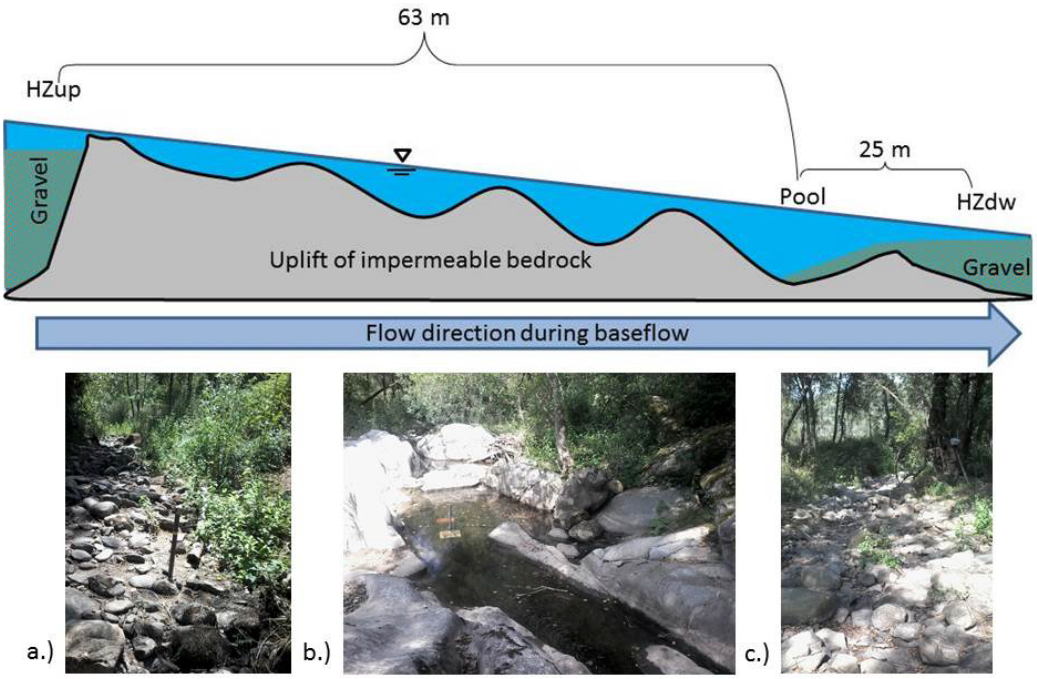

Figure 4.1: Scheme of longitudinal profile of the reach between HZup and HZ_{dw}. Photos of HZ_{up} (a), pool (b) and HZ_{dw} (c).

Discharge (Q) was determined by salt addition (Altendorf and Stauss 2003), measuring EC with a conductivity portable meter WTW ProfiLine Cond 3110 when Q > 1L s^{-1} and by a small gauging weir when Q < 1L s^{-1} (Morgenschweis 2010). The pore water of the

HZ was pumped with a peristaltic pump from PVC tubes installed at a depth of 50 cm in the stream bed. These tubes were screened over the last 30 cm. Before starting the sampling, water level measurements were taken inside and outside of every well. A water level surpassing the level inside of the well (vertical hydraulic gradient (VHG) < 0) suggested downwelling, while higher water level in the well than in the surrounding material represented (VHG > 0) upwelling.

Figure 4.1 shows the sampling points: Measurements and water samples were taken from wells and adjacent surface water when present in the permeable HZ upstream and downstream of the bedrock channel. The sampling point located upstream of the bedrock is called HZup and is characterized by downwelling during flow conditions. The uplift of the bedrock creates a natural barrier trapping water during drought conditions, when the water table falls beyond this barrier. We sampled the last pool in a series of four pools within the impermeable bedrock area located 63 m downstream of this barrier, referred to in the following text simply as pool. A well HZdw was sampled 25 m downstream of the pool, which is subjected to upwelling. Additionally, a well located at the riparian zone right before the inlet of the pool was sampled, representing the inflow of the riparian zone and is in the following referred to as lateral.

Dissolved Oxygen (DO) was measured using a YSI 20 Pro oxygen sensor probe inside the wells immediately after pumping. Both surface and pore water were filtered with ashed GF/F filters 0.7 μm nominal pore size. EC and pH (Thermo Scientific Orion Star A121 pH meter) were measured. Samples for laboratory analysis were collected in pre-washed (MilliQ-water) polyethylene bottles. The samples for NH_4^+ concentration and DOM optical properties were filtered through 0.2 μm Nylon filters and the samples for DOC and total nitrogen (TN) analysis were acidified with 10% HCl. They were stored at 4ºC temperature in the dark and analyzed within a week. Stable water isotopes were stored in new 30 mL conical centrifuge polypropylene tubes and stored at 4ºC temperature until their analysis at the end of the sampling period.

4.2.2 Laboratory analysis

All water samples were analyzed for ammonium (NH_4^+) and DOC concentration, as well as DOM optical properties. DOC and TN concentrations were measured with the high-temperature catalytic oxidation method (Shimadzu TOC analyzer). NH_4^+ was measured using a Shimadzu UV-2401 UV/VIS spectrophotometer with the salicylate method described by Reardon (1969). The samples for DOM optical properties were analyzed at room temperature. Absorbance measurements were conducted using a 1 cm path length cell with the same spectrophotometer over a wavelength range of 200-800 nm. Fluorescence was measured with a Shimadzu RF- 5301PC spectrofluorometer over

(ex/em) wavelengths of 240-420 nm and 280-690 nm respectively using a 1 cm path length cell. Stable water isotopes δD and δ^{18}O were measured by the Scientific and Technologic Center of the University of Barcelona. For δ^{18}O the equilibration was carried out with CO_2 and He and measurements were performed on a MAT253 from Thermofisher. δD was measured by water pyrolysis and analysis of the produced H_2 separated by column chromatography on a EA-TC-IRMS-DELTA PLUS xp (Thermofisher).

4.2.3 Optical Indices

Fluorescence spectroscopy generates Excitation Emission Matrices (EEMs) which in turn provide insight in DOM quality in two ways: 1) through PARAFAC modelling of fluorescence components and 2) through dimensionless indices (Fellman et al. 2010). EEMs were generated over (ex/em) wavelengths of 240-420 nm and 280-690 nm respectively. Excitation spectra at 370 were used to calculate the fluorescence index (FI) values from the ratio of intensities emitted at 470:520 nm (Cory and McKnight 2005); lower values indicate terrestrial origin and higher values correspond to autochthonous DOM (McKnight et al. 2001). Although β:α was suggested by Parlanti et al. (2000) for marine environments, over the past years its use expanded to other environments to describe freshness (higher values refer to more recent production) of DOM (Wilson and Xenopoulos 2009). We applied this index according to them by taking the ratio of 380 nm and the maximum emission between 420 nm and 435 nm em from the excitation spectra at 310 nm. We calculated the humification index (HIX), an index increasing with increasing humification, using the area under the em spectra 435-480 nm divided by the peak area 310-345 nm from the spectra at ex 254 nm (modified from Ohno (2002)). Specific ultra violet absorbance ($SUVA_{254}$) was calculated as the absorbance (measured at 254 nm) normalized to the DOC concentration and reported in units of m^{-1} mg^{-1} L. Higher $SUVA_{254}$ was found to correspond to higher aromaticity of DOM compounds (Weishaar et al. 2003). Spectral Slope Ratio (S_R) was calculated as described by Helms et al. (2008), attributing an increase of this ratio to irradiation. The absorbance ratio E_2:E_3 (the ratio of absorbance at wavelength 250 nm: 365 nm) increases as molecular weight decreases (Peacock et al. 2014).

4.2.4 Data treatment

An index for aerobic/ anaerobic conditions was calculated using the natural logarithm of the ratio of O_2^- versus N-NH_4^+ ($\ln([O_2^-]/[N - NH_4^+])$), based on the assumption that

under low DO concentration, solutes in reduced form will increase (Vázquez et al. 2011).

A parallel factor analysis (PARAFAC) model was set up using the drEEM toolbox (Murphy et al. 2013) to identify fluorescence components. Leverage did not exceed 0.5 and all samples remained in the model. Normalization of each EEM to its total fluorescence signal was necessary, because of the strong correlation of the components. The models were calculated taking the best fit of ten runs. The model of four components was chosen, taking into account the core consistency (45.7%), with special consideration of the spectral loadings of all models from 3 to 7 components, as well as the model residuals for a best capture of the expected com- pounds. For further information on these four components see Table 4.1 and Table SI 1. The split-half analysis was performed randomly alternating validation (validated for some splits) and by splitting the dataset by location and hydrological phase (not validated). Due to high variability in a relatively small data set (119 samples), the validation entailed difficulties for this data set. Hence, several models were calculated with different datasets (only HZ or only surface water) and components did not show the same abundance, but the components had the same em/ex coordinates as calculated by the general model. PARAFAC components of the general model (including all 119 samples) are represented by their relative fluorescence intensity as a percentage (%Ci) of the sum of all four component intensities (C_i) using, $\%C_i = C_i/C_i * 100\%$ (Kothawala et al. 2014).

Table 4.1: Description of PARAFAC components found for the dataset of this study

Component	ex/em	Description	Peaks	Literature
Component 1	296/420	Low molecular weight (LMW),biological activity	Peak M	Coble et al. (1998)
Component 2	251, 349/451	Humic-like FDOM; ubiquitously observed humic substances, predominately terrestrial sources	Peak C	Murphy et al. (2011); Cory and Kaplan (2012)
Component 3	263, 383/476	High molecular weight (HMW), aromatic, fulvic acid, photochemically degradable	Unkown	Cory and McKnight (2005); Murphy et al. (2006); Lapierre and del Giorgio (2014)
Component 4	274, 276/322	Amino acids, free or bound in proteins, may indicate intact proteins	Peak T	Coble et al. (1998)

A principal component analysis (PCA) of optical parameters, namely $SUVA_{254}$, SR, E_2:E_3, FI, β:α, HIX and PARAFAC components, was performed by using the inverse variances of the raw data as weights in order to account for different units (data is available in Table SI 3). We tested the heterogeneity in DOM composition between locations during each sampling campaign by calculating Convex Hull areas (De Berg 2008) of PCA scores for each sampling campaign individually and by dividing this area by the number of samples. Differences in the DOM composition among hydrological phases (factor 1) and locations (factor 2) were tested with a 2-way ANOVA for each index and component, after visual examination of normality and normalization by the Box-Cox technique when necessary. Significance levels were set at $p < 0.01$. Post-hoc analysis was done with Tukey's Honestly Significant Difference Procedure. For DO and $\ln([O_2^-]/[N - NH_4^+])$ no normal distributions could be achieved. Therefore we used the non-parametric Kruskal-Wallis test with the same post-hoc analysis as for the 2-way ANOVA. For testing the similarity of EC and stable water isotopes between sampling locations we used Wilcoxon rank sum test. Relationships were calculated using linear regression models, considering a regression as significant when $p < 0.01$.

EC and stable water isotopes were used to determine the hydrological connection between surface water in the pool and hyporheic water in HZ_{dw} (Pellerin et al. 2008). Both tracers revealed that surface water in the pool is the only water source for HZ_{dw} (Wilcoxon rank sum) and no additional groundwater recharged the hyporheic water (results detailed in subsection 4.3.2). This result allowed to perform a DOM mass balance at the surface-hyporheic water interface comparing the surface water located in the pool (Input) with that measured at HZ_{dw} (Output) according to the following formula:

$$\eta X = \frac{X_{Pool} - X_{HZ}}{X_{Pool}} \pm \frac{EC_{Pool} - EC_{HZ}}{EC_{Pool}} \times 100 \times dx - 1 \quad [\%/m]$$

Eq. 2

where X is the DOC concentration or the optical parameter; EC is the electrical conductivity in the pool (P) and HZ_{dw} (HZ); dx is the linear distance (25 m) between the two sampling sites. For the graphs we represented variation in EC between pool and HZ_{dw} as error bars. If X is DOC concentration or a fluorescent component obtained after PARAFAC modelling (C1, C2, C3 and C4, see section 2.5) and $\eta X < 0$, then the net release of DOC or the according component predominate along the pool-hyporheic transect. The opposite indicates a net DOM retention. Maximum fluorescence intensity in raman units (R.U.) of peaks of PARAFAC components was used for this calculation. If X is a DOM qualitative optical index, then $\eta X < 0$ indicated an increase of the specific optical index in the HZ. The opposite indicates a decrease of that index.

4.3 Results

4.3.1 Hydrological conditions

Pre-drought was marked by several rain events (Table SI 4) and highly fluctuating EC and water level (WL), with a Q ranging from 3.5 to 6 L s^{-1}. Contraction started in the beginning of July. As shown in figure 4.2, during this phase the surface water level in the pool declined constantly and did not recover after storm events. The Q measured during this period ranged between 0.5 L s^{-1} to 2 L s^{-1}, which were clearly below the base flow of 5 L s^{-1} described for Fuirosos by Butturini et al. (2003). During the three weeks of contraction phase the hydraulic gradient between the pool and the HZ_{dw} declined. Temperature in the pool reached maximum values of 26% in the transition phase between contraction and fragmentation, but stayed flat throughout the drought period. Minimum temperature during summer drought was 19% observed after storm events.

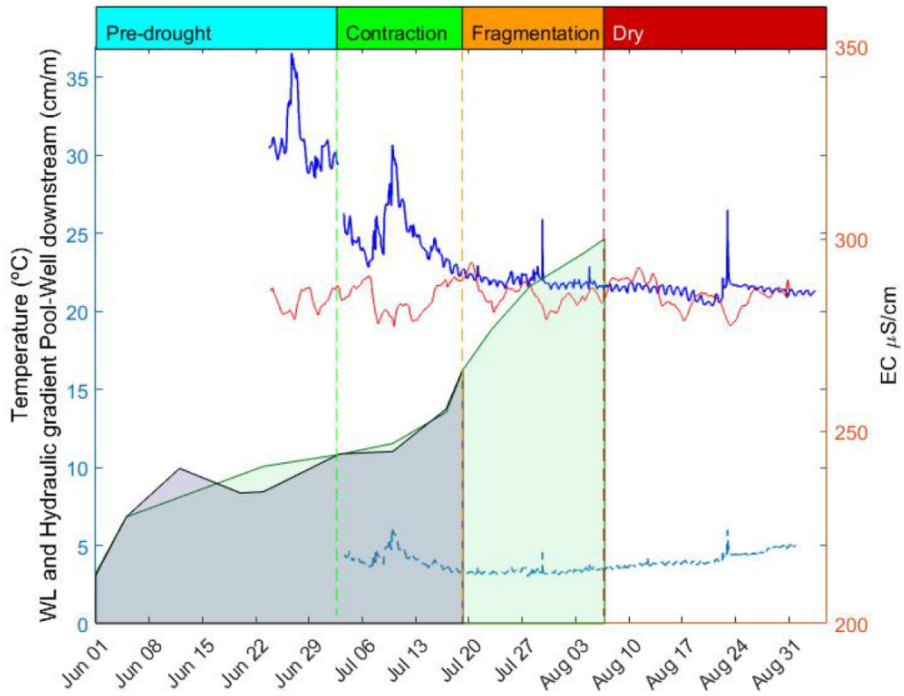

Figure 4.2: Water Level (WL) (dark blue, missing data due to battery failure of data logger), daily mean water temperature (red) in the pool and hydraulic gradient between the WL of the pool and in the well HZ_{dw} (dashed, light blue line). Filled areas represent continuous measurements of EC of the surface water upstream (grey) and downstream (green). When surface flow was zero, the EC dropped to zero as well. The top shows the color scheme of the 4 hydrological phases during drying, separated by dashed lines.

The start of fragmentation was marked by the absence of surface flow upstream of the bedrock channel and a drop in WL in HZ_{dw}, followed by a constantly flat hydraulic gradient between the pool and HZ_{dw} throughout fragmentation. Q measured at the inlet of the pool decreased to 0.06 L s^{-1}. The dry phase started in the beginning of August, when a sharp drop of continuous EC measurements indicated the absence of surface water. During dry phase the hydraulic gradient between the pool and HZ_{dw} rose.

4.3.2 Chemical conditions

The parameter pH showed no significant changes in space (Kruskal-Wallis, $p = 0.27$) or time (p=0.08). EC remained constant in the lateral wells over time, but increased in all other locations during pre-drought and contraction with the same magnitude (Wilcoxon rank sum, p=1, Figure 4.3a). The magnitude of this increase was different among locations with the beginning of the fragmentation phase. EC values of the pool and HZ_{dw} augmented with the same magnitude (Wilcoxon rank sum, p=0.927), but EC values of HZ_{up} climbed significantly more rapid than the values of the pool and the HZ_{dw} (Wilcoxon rank sum, p=0.053 and p=0.012 respectively). EC reliability as a tracer for hydrological connectivity was confirmed by stable water isotopes that demonstrated similar values in the pool and in the HZ_{dw} (Wilcoxon rank sum p=0.524 for δD and p=0.691 for δO), but different values between these locations and HZ_{up} (Wilcoxon rank sum $p<0.1$ for δD and δO). DO concentrations depicted in Figure 4.3b showed significant differences among HZ and Pool (Kruskal-Wallis with post-hoc Tukey-Kramer, $p < 0.01$). Overall, the waters were under-saturated with oxygen. The DO concentration inside the pool fell two times below 4 mg L^{-1}. Once during the fragmentation phase and once during the dry phase when rain events had re-established the hydrological continuum for a short time. The DO concentration in the HZ_{up} ranged from 2.9 mg L^{-1} during pre-drought to anoxic conditions during all three phases of drought. The HZ_{dw} had DO concentrations of 1.5 mg L^{-1} during pre-drought and was anoxic (DO<0.5 mg L^{-1}) from the end of contraction phase on until the start of rewetting. As revealed in Figure 4.3c, $\ln([O_2^-]/[N\text{–}NH_4^+])$ decreased in both sampling locations of the HZ with drying and was significantly lower in the HZ than in the surface water (Kruskal-Wallis with post hoc Tukey-Kramer, $p< 0.01$). The lowest values were observed during the transition from the contraction phase to the fragmentation phase. Figure 4.3d shows that DOC concentration in the HZ_{up} diminished during the fragmentation and the dry phase (linear regression slope = -0.17, $p< 0.01$), while in the pool DOC concentrations rose as drought proceeded (linear regression slope=0.15, $p< 0.01$), whereas in the HZ_{dw} no trend was found. Mean ± SD of all presented parameters for each hydrological phase are presented in Table SI 2.

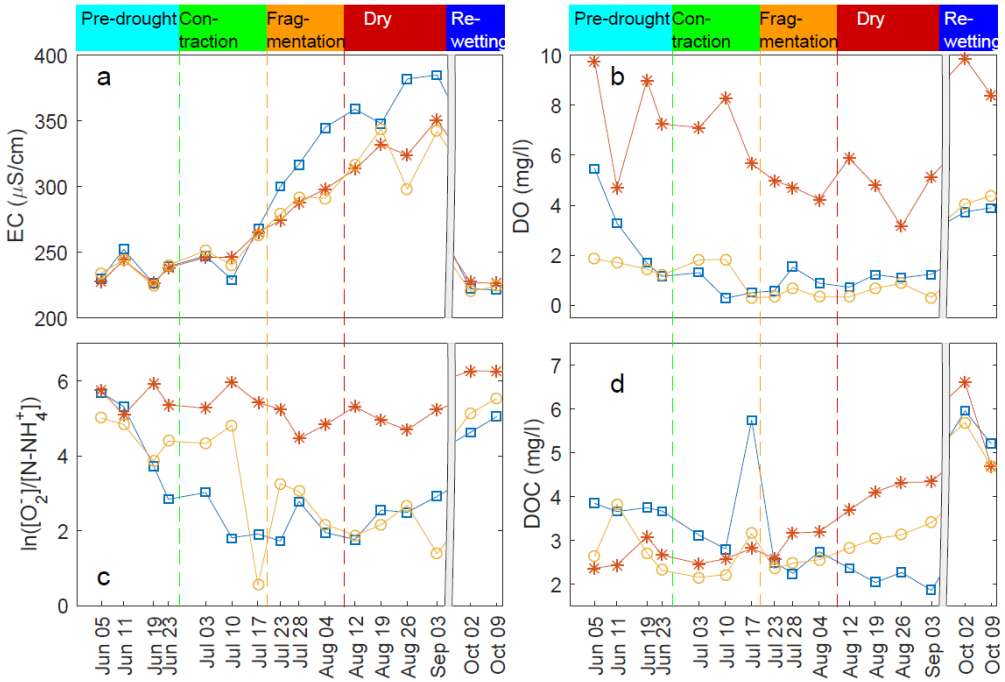

Figure 4.3: Time series of EC (a), DO (b), (c) ln([O_2^-]/[N–NH_4^+]) and DOC (d) for HZ_{up} (blue squares), pool (orange stars) and HZ_{dw} (yellow circles) during the whole sampling period. Hydrological phases are indicated on the top and by dashed lines. Dates refer to sampling dates.

4.3.3 Optical properties of DOM

Principal components 1 and 2 (PC1 and PC2, respectively) explained together 61.3% of the total variance in the dataset of 70 samples. PC 1 explained 38.4% and PC2 22.7% of the total variance. Figure 4.4a depicts that PC1 showed negative loadings for C2, C3 and HIX and positive loadings for C4. PC2 showed negative loadings for C1 and positive loadings for FI, β:α and E_2:E_3. $SUVA_{254}$ and SR showed almost no weight over the PCs. Figure 4.4b reveals that samples from pre-drought and contraction exhibited a higher diversity of DOM characteristics. Samples from the pre-drought and to a certain extent the contraction phase were positive on PC1 axis, while samples from the fragmentation, dry and rewetting phases scored negative on PC1 axis. Surface water samples were divided from the hyporheic pore water samples on PC2. HZ samples exhibited typically positive scores. Convex Hull areas for each sampling campaign further revealed that heterogeneity among sampling locations in DOM composition is highest during pre-drought phase.

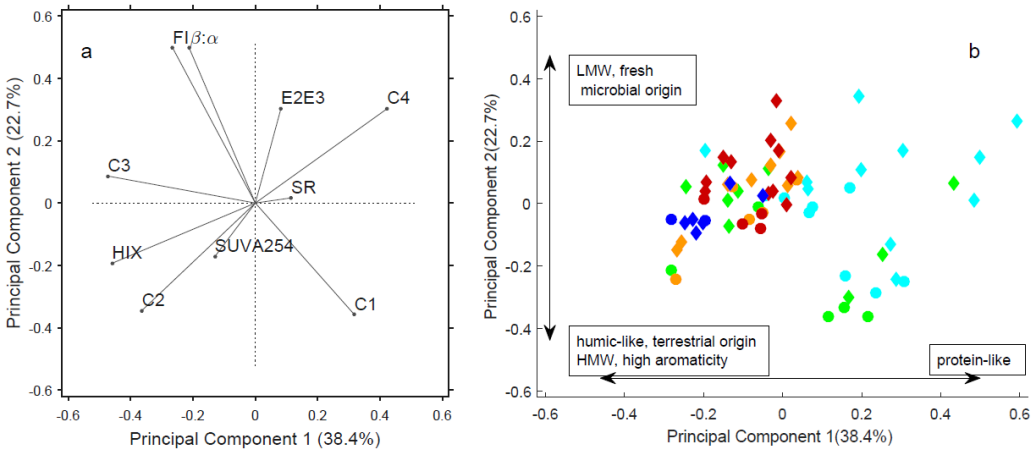

Figure 4.4: Biplots with loadings (a) and scores (b) of PCA. Colors represent the hydrologic phases pre-drought (cyan), contraction (green), fragmentation (orange), dry (red) and rewetting (dark blue). Symbol shapes refer to either HZ (diamonds) or surface water (circles).

Significant changes among hydrological phases were observed for all indices ($F_{4,70} < F_{0.01}$, $p<0.01$), but $E_2:E_3$ ($F_{4,70}=2.29$, $p=0.02$). On the one hand an increase of $\beta:\alpha$ in HZ_{up} was observed, while on the other hand HIX rose in the pool and HZ_{dw}. Further, figure 6 a and c demonstrates that $\beta:\alpha$ and HIX in HZ_{up} decoupled from the pool and HZ_{dw} with the start of fragmentation. As shown in figure 4.5b and d, differences among locations were significant over the whole drought period for $E_2:E_3$ and $SUVA_{254}$ ($F_{6,70} < F_{0.01}$, $p < 0.01$). Visual representation of FI and SR did not indicate specific trends with drought. No correlations with inorganic parameters were observed, but for $\beta:\alpha$ and $\ln([O_2^-]/[N - NH_4^+])$ in HZ_{dw} ($R^2 = 0.45$, $p=0.004$).

The sum of the fluorescence signal of all components was positively related to DOC concentration ($R^2 =0.64$, $p<0.01$), thus the following paragraph describes percentual contribution of each PARAFAC component to the total fluorescence signal. No clear temporal trends were found, but differences between sampling locations were observed: C2 was lower in HZ_{up} than in the pool and HZ_{dw}, while C4 was higher in HZ_{up} than in the pool and HZ_{dw}. Percentage of C1 and C3 of the total fluorescence signal did not exhibit any distinction between locations, but we found these components to be negatively correlated with each other ($R^2 =0.4$, $p<0.01$).

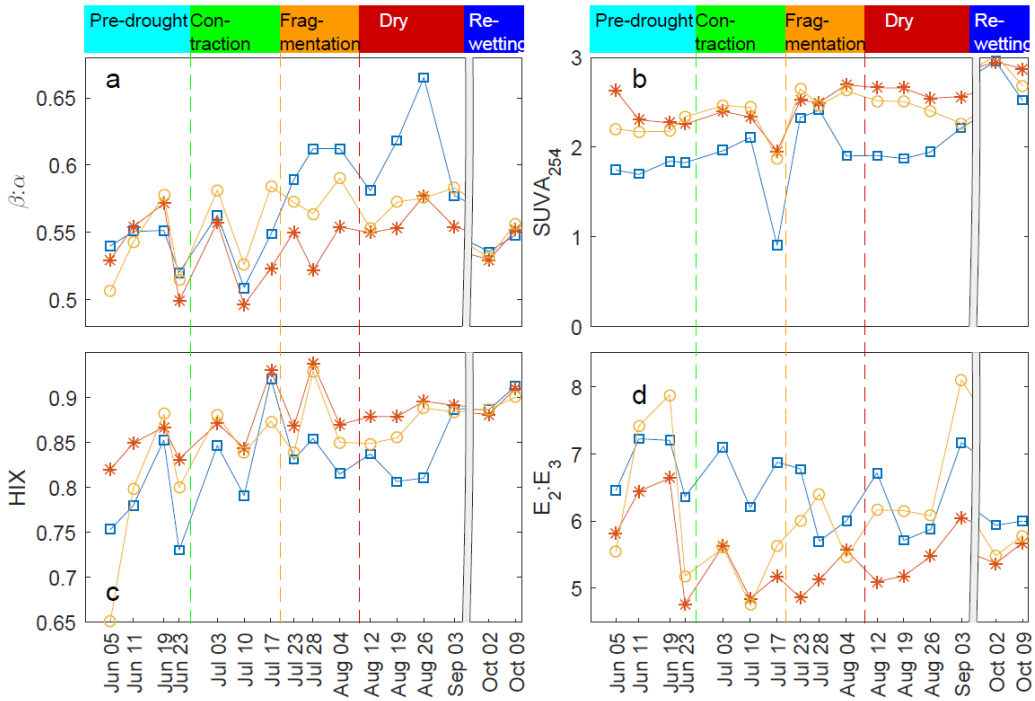

Figure 4.5: Time series of DOM optical parameters *β:α* (a), $SUVA_{254}$ (b), HIX (c) and E_2:E_3 (d) for HZ_{up} (blue squares), pool (orange stars) and HZ_{dw} (yellow circles) during the whole sampling period. Hydrological phases are indicated on the top and by dashed lines. Dates refer to sampling dates.

4.3.4 DOM retention of the HZ

EC (Wilcoxon rank sum, p=0.96) and stable water isotopes (Wilcoxon rank sum, p=0.52 for δD and p=0.69 for δ^{18}O) confirmed that the infiltrating surface water from the pool is the only water source of HZ_{dw} during drought. Figure 4.6a depicts a trend of DOC retention (R^2 = 0.45, p<0.01) with increasing drought intensity. At the beginning of the pre-drought, HZ_{dw} was a net DOC source (ηDOC < 0), but when contraction started the concentration diminished in comparison to the pool. During contraction the ηDOC became positive (ηDOC > 0) and net DOC retention increased up to 1.2%/m ± 0.1%/m. As shown in Figure 4.6b, PARAFAC components revealed that DOM release (ηDOC < 0) was related to release of C4 (ηC4 < 0) and C1 (ηC1 < 0). C2 and C3 were neither retained nor released during pre-drought and contraction, but were retained during the fragmentation and dry phases.

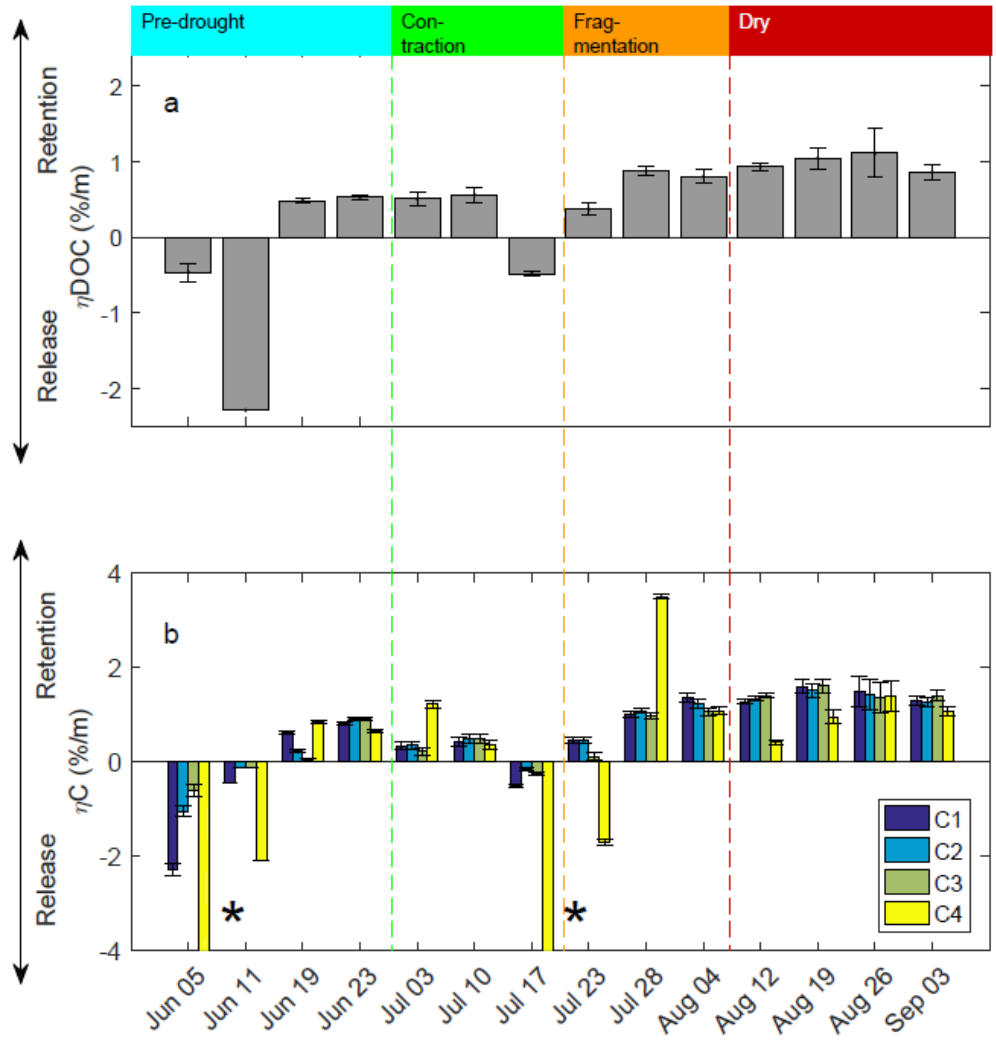

Figure 4.6: Retention or release of DOC (a) and PARAFAC components (b) between the pool and HZdw. Error bars represent uncertainty resulting of differences in EC between both locations. Colors for PARAFAC components are indicated in the legend. Asterisks represent sampling dates without any C4 in the pool and hence high percentage of C4 in the HZ.

In HZdw, DOM was more autochthonous, less degraded ($\eta\beta{:}\alpha < 0$, Figure 4.7a), less aromatic ($\eta SUVA_{254} > 0$, Figure 4.7b) and with a larger proportion of LMW compounds ($\eta E_2{:}E_3 < 0$, Figure 4.7d) than in the pool. On the other hand humification degree did not change significantly across the pool-hyporheic interface ($\eta HIX = 0$, Figure 4.7c). However, these changes did not covary. For instance, $\beta{:}\alpha$ increased gradually in the HZ with respect to the pool, whereas $SUVA_{254}$ decreased during the pre-drought and dry phases. $E_2{:}E_3$ was frequently higher in HZ_{dw} than in the pool, but did not follow any temporal trend.

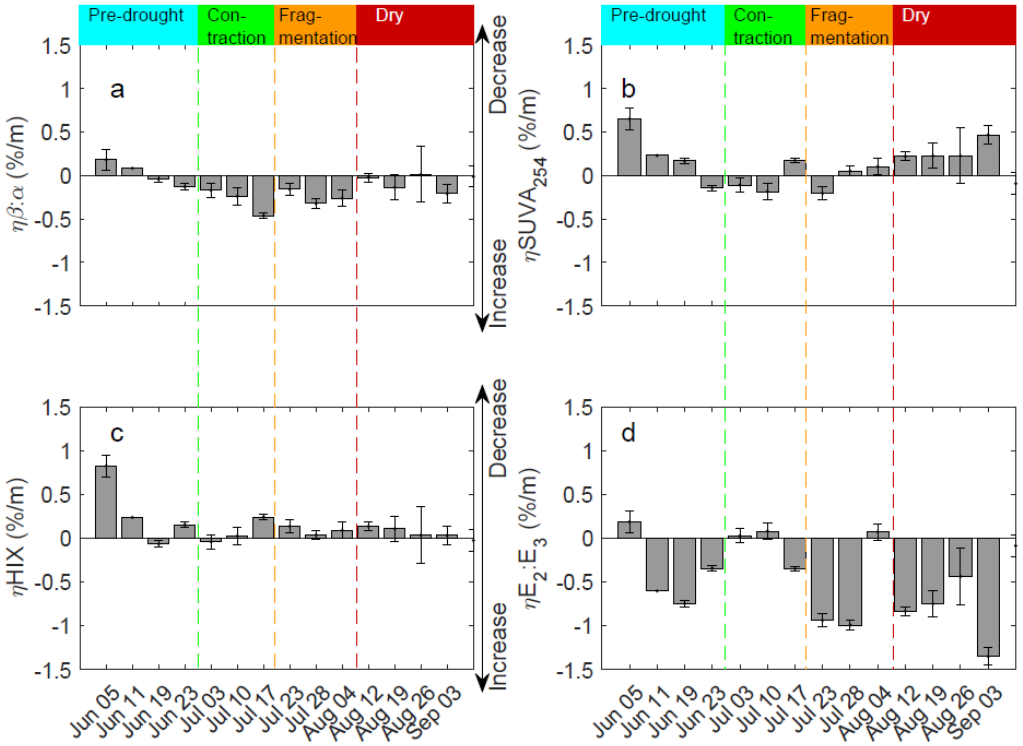

Figure 4.7: Increase or decrease of DOM optical parameters *β: α* (a), $SUVA_{254}$ (b), HIX (c), E_2:E_3 (d) between the pool and HZdw. Error bars represent uncertainty resulting of differences in EC between both locations. Colors are according to hydrological phases. Dates refer to sampling dates.

4.4 Discussion

Source, aromaticity, state of humification and molecular weight are inherent characteristics of DOM and their relationship with the bioavailability of different DOM compounds is an intensively discussed topic (Fellman et al. 2014; Hosen et al. 2014; Hansen et al. 2016). Additionally, this discussion is not limited to the inherent properties of DOM, but expands to external conditions, determining which characteristics favor biodegradation. Hydrology is a key external driver of DOM processing in Mediterranean intermittent rivers (Butturini et al. 2016). Within this context, this study focusses on the impact of hydrological disconnection, as a consequence of seasonal summer drought and local geomorphological uplift of impermeable granitic bed rock, on DOM processing. We will first discuss the hyporheic DOM biogeochemistry up- and downstream of the uplift of the bed rock and then the DOM mass balance, calculated for the HZ downstream.

4.4.1 Hydrological disconnection drives DOM changes in the HZ

In general, PCA indicated a shift from protein-like to more humic-like components with hydrological disconnection of the sampling locations. Contrary to our initial hypothesis, DOM in the HZ generally showed stronger signals of LMW and microbial origin than the surface waters. Further, hydrological disconnection resulted in distinct trends of DOM composition in the HZ up-and downstream of the bedrock channel.

In contrast to previous studies (Jones et al. 1995a) reporting higher DOC concentration in stream water than in the HZ, we found DOC concentration was higher in HZ_{up} than in the adjacent stream surface water and in the other sampling points. However, DOC concentration decreased with the absence of surface flow and reached lower values than in all other sampling locations. In fact, right before surface flow reached zero, DOC concentration peaked in HZ_{up} and declined from this point constantly until the end of drought. This DOC decline with the absence of surface flow suggests that there is important respiration activity (Hynes 1983) and agrees with Gómez-Gener et al. (2016), which showed that the CO2 efflux from stream beds doubled with the absence of surface water. By contrast, $\beta:\alpha$ increased when surface flow was zero. This index is reported to augment with fresh autotrophic (algae/ plant) leaching and to represent a type of DOM highly bioavailable (Wilson and Xenopoulos 2009; Hansen et al. 2016). However, this mechanism can not explain the observed increase of $\beta:\alpha$ in the HZ. Conversely, our findings suggest that the increase of this index corresponds to fresh, autochthonous DOM leachate from heterotrophic microbial community and the observed increase points towards a less bioavailable DOM reservoir.

HZ_{dw} was lower in DOC concentration than HZ_{up} before the hydrological disconnection of these sites. In contrast to HZ_{up}, DOC concentration in HZ_{dw} remained constant until the end of drought. DOC concentration strongly covaried with that of the pool, even though DO concentrations were much lower, pointing towards high respiration rates. With respect to DOM quality, HZ_{dw} followed seemingly the temporal trend of the pool, rather than the one of HZ_{up}. For example, $\beta:\alpha$ values remained stable throughout drought. We are aware of the fact that these conclusions are drawn from the comparison of only two sampling locations. Nevertheless, our results emphasize the importance of hydrological connectivity for creating spatial heterogeneity of DOM processing in the HZ reported from early studies on HZ water chemistry (Valett et al. 1990). Additionally, these results question the direct relationship of certain fluorescence indices with DOM bioavailability. At the same time, they confirm that an important portion of DOM is retained or even respired by the hyporheic microbial community, which is in line with recent research (Gómez-Gener et al. 2016a).

4.4.2 DOM retention across the surface-hyporheic interface

We characterized DOM in the pool and in HZdw and calculated a mass balance, because we found lateral inputs were neglectable during drought period. EC and stable water isotopes confirmed that the input (pool) was the only water source of the output (HZdw) and thereby enabled us to calculate a mass balance. According to previous studies performed in the same stream (Vázquez et al. 2011; Von Schiller et al. 2015), our initial hypothesis was that DOM composition in the pool would become a more autochthonous imprint. On the contrary, in this study optical indices indicating aromatic and HMW DOM composition increased the longer the pool was isolated, suggesting that increasing water residence time in the pool led to an accumulation of these compounds. Primary production in the pool might have been suppressed by factors such as depth and light attenuation by (terrestrial) colored DOM (Karlsson et al. 2009). Consequently, during drought water from the pool infiltrating in the HZ downstream supplies aromatic and HMW-compounds. This DOM moiety is typically considered recalcitrant for aquatic microbiota (Hood et al. 2003; Cammack et al. 2004; Fellman et al. 2009; Hansen et al. 2016).

Overall, DOC was retained most of the time in the HZ. Retention in the HZ started during pre-drought and increased gradually over time, with the exception of DOC release during the transition from the contraction to the fragmentation phase. In other words, the transition phase from contraction to fragmentation is a short hot moment (McClain et al. 2003) for in-stream DOM release. During fragmentation, a second long hot moment of increasing DOC retention started, which was highest during dry phase. Release, as well as retention was related to qualitative changes of DOM composition.

The absorbance indices (E_2:E_3, $SUVA_{254}$) indicated that the relative contribution of LMW fraction increased in the HZ compared to the DOM in the pool. This result suggests that HMW fractions were preferentially retained at the hyporheic interface and that from the breakdown of large DOM fractions, smaller DOM fractions can be released (Amon and Benner 1996). Remarkably, these results are opposite to biodegradation essays from surface waters (Casas-Ruiz et al. 2016) and soils (Kalbitz et al. 2003), which showed that mixtures dominated by LMW fraction had a higher bioavailability. Nevertheless, the experimental ex situ approach of biodegradation essays might not be sufficient to capture all factors affecting biodegradation in natural systems. For example, Zarnetske et al. (2011b) report that $SUVA_{254}$ generally declined along hyporheic flow paths in a gravel bar. In fact, little is known about DOM quality and reactivity in the HZ and our results indicate that aromatic PARAFAC components C2 and C3 and DOM with a high $SUVA_{254}$ index were retained in the HZ under dry conditions. With the mass balance, we detected the increase of $\beta:\alpha$ in HZ_{dw}, which strengthens the idea of in situ autochthonous microbial DOM leaching, observed in

HZ_{up}. HIX, an indicator for humic substances, tended to decrease, but this decrease was very low throughout the drought period. Above all, we found that DOM production or retention is determined by the different hydrological phases during drought. Compounds thought to be recalcitrant were retained, while DOM with characteristics which are thought to be bioavailable, were released.

The temporal shift from fresh DOM release to retention of aromatic HMW-compounds could be the consequence of a severe environmental condition change in HZ. Thus, release of hyporheic fresh DOM (i.e. high $\beta:\alpha$ and C4) during the transition from the contraction to the fragmentation phase co-occurred with the lowest $\ln([O_2^-]/[N–NH_4^+])$ observed in the HZ. This points towards high respiration activity and in situ bacterial C production and leaching and is in line with other studies from intermittent streams, defining this transition phase as a hot moment (Ylla et al. 2011; Von Schiller et al. 2015; Casas-Ruiz et al. 2016). In fact, this hot moment was of short duration (less than a week), but it triggered a second hot moment of DOM retention, that lasted until the end of drought. Therefore, future studies should take a high temporal resolution into account in order to capture these abrupt hot moments. Advances in in situ monitoring of DOM quantity and quality could help to face this challenge (Downing et al. 2009; Sandford et al. 2010; Ruhala and Zarnetske 2017).

Increasing respiration rates during the transition phase led to anoxia, which might have caused a shift in bacterial community. Fazi et al. (2013) reported that shifts of bacterial community in isolated pools of Fuirosos were related to $\ln([O_2^-]/[N–NH_4^+])$ and DOM quality. By the same token, intermittency changed microbial composition within days in the HZ of a Canadian stream (Febria et al. 2012). Moreover, bacterial community shifts are reported from experimental drying of stream bed sediments (Amalfitano and Fazi 2008; Pohlon et al. 2013b) and as a consequence of changes in DOM quality (Findlay et al. 2003). Pohlon et al. (2013a) found that community composition became more similar to soil microbial communities with drying. Soil microorganisms are reported to break down aromatic DOM to fractions that are rapidly mineralized when entering the aquatic environment (Abbott et al. 2014). Indeed, a shift towards a bacterial community adapted to rather recalcitrant DOM, might explain the second hot moment of retention of aromatic and HMW compounds.

In summary, drought and the exposed uplift of impermeable bed rock causes hydrological disconnection in the study site and thereby enhances spatial patchiness of temporal dynamics of DOM processing in the HZ. In situ DOM mass balance at the stream-hyporheic interface revealed the occurrence of two time periods with disproportionately high rates for DOM processing (hot moments) during drought. Contrary to our initial hypothesis that the HZ would be a sink for labile DOM, the first hot moment consisted in a short pulse of protein-like, autochthonous DOM net release.

Nevertheless, the second one was a longer period of increasing net DOM retention, specifically of aromatic and high molecular weight moieties. In the light of predicted temperature and water abstraction increase, we expect to observe these hot moments in other catchments where flow intermittency might become more frequent in future.

II. Results: Chapter 2

Sensors hidden under vegetation (top)

Hyporheic zone (bottom, by Tanja Brandt)

5 Chapter 2: Capturing hot moments of carbon processing across the surface-subsurface interface of an intermittent stream during summer drought

Intermittent streams are increasingly recognized as an important factor for adequate CO_2 emission estimations of aquatic ecosystems but are often neglected or underestimated during summer drought periods. This fact can be partly attributed to the poor understanding of dissolved organic matter (DOM) processing in the remaining surface water and in particular, in the hyporheic zone (HZ). Capturing the carbon processing during drought is a complex task because of the rapid changes occurring during the transition from wet to dry conditions. To investigate the transition between the wet, dry and rewetting phase, we coupled continuous fluorescence DOM and infrared gas analyzer CO_2 sensor measurements with spatially continuous vertical oxygen profiling. Hydrological transitions drive rapid changes in the spatiotemporal distribution of oxygen, and thus creating hot moments of increased biogeochemical processing rates. We observed exponential increases of pCO_2 in hyporheic pore waters when atmospheric oxygen diffused into the unsaturated pore space, co-occurring with a sharp vertical oxygen gradient. The pulse of pCO_2 release in the hyporheic zone during sediment desiccation was of similar magnitude as the pCO_2 release during a period of drying/rewetting cycles that followed the second half of the study period and might be related to the 'Birch effect' observed from soils. Furthermore, we observed that with rewetting of the dry streambed, DOM apparently recalcitrant for the ecosystem metabolism in the surface water was readily respired in the hyporheic zone. Therefore, we conclude that the mineralization of DOM is very different in surface and subsurface environments. In fact, our observations indicate that the microbial community of the hyporheic zone of intermittent streams can switch rapidly from anaerobic to aerobic metabolic pathways and thereby create hot moments of carbon processing during hydrological transitions.

5.1 Introduction

Intermittent streams are subjected to recurrent dry phases of varying duration and spatial extent (Williams 2007). This stream type represents a substantial portion of the total number, length, and discharge of fluvial ecosystems worldwide (Larned et al. 2010) and additionally, the amount of streams with these characteristics is expected to increase because of changes in precipitation regimes and land use (IPCC 2007; Vörösmarty et al. 2010). The rising awareness of the importance to understand and protect these ecosystems is reflected in a growing amount of interdisciplinary studies over the last years (Steward et al. 2012; Nikolaidis et al. 2013; Acuña et al. 2014). As a consequence, the distinct temporal patterns and source-sink dynamics of carbon observed in intermittent streams compared to their perennial counterparts has been revealed in many studies (Ejarque 2014; Casas-Ruiz et al. 2016; Gómez-Gener et al. 2016).

High CO_2 emissions from intermittent streams during summer drought suggest that the predicted spatial and temporal extension of drought could entail a positive feed-back loop that has not been accounted for in present climate models (von Schiller et al. 2014; Gómez-Gener et al. 2015). Within this context, Gómez-Gener et al. 2016a has reported three times higher CO_2 emissions of up to 1500 mmol m^{-2} d^{-1} from dry than from flowing river beds. In their study, variations of CO_2 evasion among stream beds in the catchment were explained by the temperature of the sediment, as well as dissolved organic carbon and total dissolved nitrogen content. However, the temporal extent of these hot moments of over proportional processing rates (McClain et al. 2003) that lead to the observed CO_2 emissions was not targeted by this study. Recent studies have identified inundation events into parafluvial zones as a main driver of CO_2 emissions (Goldman et al. 2017; Stern et al. 2017). Intermittent streams store high amounts of particulate organic matter in their hyporheic zone that is respired with longer water residence times during drought periods (Burrows et al. 2017), whereby even higher respiration rates can be expected due to the 'Birch effect' (Jarvis et al. 2007). This effect is described as an increase of carbon turnover with rewetting of dry soils (Birch 1964). This hot moment also can occur in dry stream beds with rewetting (Gallo et al. 2014) and thereby underlines the temporal variability of carbon turnover in the hyporheic zone that might be encountered during a drought period.

Furthermore, surface water pools retained in impermeable structures can represent another important dissolved organic carbon source for streambeds during drought (Harjung et al. 2017) given that hydrological connectivity with the hyporheic zone (HZ) persists. Nevertheless, controversial findings are reported on the organic matter quality from these pools that might be attributed to the spatial and temporal heterogeneity during drought (Jones et al. 1996; Vázquez et al. 2011; Fellman et al. 2011a; Von

Schiller et al. 2015; Casas-Ruiz et al. 2017). In fact, although to a lesser extent than dry streambeds, these pools can represent hot spots of carbon processing and elevated CO_2 evasions (Dieter et al. 2013; Gómez-Gener et al. 2015; Holgerson and Raymond 2016). The carbon processing and the subsequent dissolved organic matter (DOM) composition that is transported downstream through subsurface flow paths depends on the balance between gross primary production and ecosystem respiration at these pools (Proia et al. 2016). Similar to the hyporheic zone, water residence time, water temperature and organic and inorganic nutrient availability drives metabolism in surface waters (Sabater et al. 2008; Artigas et al. 2012; Tamooh et al. 2013) as well as, the light regime that ultimately determines primary production (Acuña et al. 2004).

Temporal shifts in water level and intermittency were identified as key drivers of carbon dynamics in headwater streams (Looman et al. 2017). Our objective was to understand the temporal dynamics, including disproportional carbon processing rates, that is biogeochemical hot moments, across the surface-hyporheic interface. To investigate the transition between the wet and dry phases, we used a combination of automated pore water sampling and continuous measurements in situ of different field sensors. Our approach coupled continuous fluorescence DOM (protein-like and colored) and infrared CO_2 sensor measurements with spatially continuous vertical oxygen profiling in situ. We expected that the hydrological phases of drying would shape the carbon processing in the surface water and in the subsurface differently: The pool would show close links to the balance between gross primary production and ecosystem respiration, while in the hyporheic zone the heterotrophic respiration would be driven by temperature and DOM availability. Furthermore, we hypothesized that the occurrence of hot moments could be linked to subsurface oxygen concentrations in response to changing water saturation conditions.

5.2 Methods

5.2.1 Experimental set-up

Measurements were conducted in Fuirosos, a semi-pristine, forested catchment that exhibits higher annual evapotranspiration than annual precipitation, which is manifested in regular summer droughts. These periods of flow intermittency are typically of two to three months duration with few rain events during summer that are usually not intense enough to restore surface flow continuum. Only in autumn, storm events reestablish the lateral and longitudinal hydrological connectivity (Vázquez et al. 2007).

The specific study site is described in detail in Methods 3.2 and Chapter 1 (Harjung et al. 2017), where also the different hydrological phases are presented and the description

of the surface-subsurface connectivity between surface water captured in an exposed bedrock channel and the hyporheic zone. The drought period comprised of a contraction, fragmentation, dry and a stagnant phase. The latter phase was not described previously and refers to the phase when the water level in the hyporheic zone dropped dramatically below the well depth because of missing water flow from upstream. The pool got hydrologically disconnected hence, stagnant. However, three rain events during august reestablished the hydrological connectivity in the subsurface. The phases of rewetting and subsequent drying are called rewetting1, 2 and 3 (precipitation data in Table SI 5). Measurements and samplings were conducted in a pool and in a well installed in the HZ 25 m downstream from the pool (Figure 5.1). The well in the HZ consisted of a PVC tube with a screened section at a depth between 30 and 50 cm below streambed surface. Oxygen profiling into the substrate was only conducted in the HZ due to the presence of bedrock and inherent lack of sediment in the pool. The general measurement principle as well as the installation and operation procedure of the O_2 profiling system is described in detail in Brandt et al., 2017. Briefly, repeated O_2 profiles of 55 cm length were obtained in continuum along the sediment depth by means of a motorized profiling unit connected to a tubular sensing element, of which the latter permanently remained in the sediment for the course of this study. For temperature compensation of raw O_2 data, depth-resolved temperatures were acquired with a multilevel temperature spear (MLTS, Umwelt- and Ingenieurtechnik GmbH, Dresden, Germany) installed in close proximity to the oxygen profiling unit.

Hyporheic pore water and pool water were pumped alternatingly every 90 min into a flow through cell that shielded the measurements from the light. The hyporheic pore water was passing first through a sediment filter to remove suspended particles and thereby reduce turbidity. The flow through cell was equipped with two fluorescence sensors. One measured at Ex/Em 275 nm/350 nm (PDOM) where the protein-like peak T is located (Stainless Steel Cyclops-7 Tryptophan for Wastewater Monitoring, Turner Designs, Sunnyvale, USA) and the other one at 365 nm/470 nm (CDOM), where the peak of colored DOM is located (Plastic Cyclops-7 FDOM/CDOM, Turner Designs). The CDOM peak generally represents the bulk DOM quantity (Volk et al. 1997). Furthermore, in the flow through cell a CO_2 sensor using infra-red gas analysis technology (GMM220, Vaisala, Helsinki, Finland), a turbidity sensor (OBS-3+ turbidity sensor, Campbell Scientific, Logan, Utah, USA) and a temperature sensor (109SS-L Stainless-Steel Temperature Probe for Harsh Environments, Campbell Scientific) were deployed. The CO_2 sensor was water proof shielded with a semi-permeable PTFE membrane sleeve (International Polymer Engineering, Tempe, Arizona, USA) as described by Johnson et al (2010). Dissolved oxygen was measured continuously in the pool with a ProODO optical dissolved oxygen meter (YSI, Yellow Springs, Ohio) in 15min intervals. The maintenance interval of the experimental set-up,

including the cleaning of all sensor lenses with an optical glass wipe was performed at least once per week. The water level in the HZ was measured manually with an electric contact gauge in an additional piezometer next to the one used for pumping of hyporheic pore water.

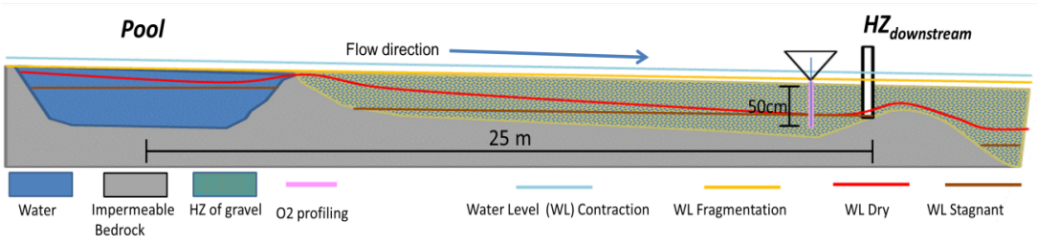

Figure 5.1: Study site with the pool and the well, where water was pumped from to the flow through cell to take continuous measurements. Close to the well the oxygen profiling was installed. Approximated water levels are indicated by different water levels, referring to the hydrological phases.

5.2.2 Sensor data treatment

The output of the fluorescence sensors was corrected for turbidity and temperature as proposed by Downing et al. (2010). To correct for biofouling between the cleaning of the fluorescence sensor lenses, we calculated a drift slope for biofouling and corrected the data with this drift slope. We double-checked the reliability of CDOM-fluorescence sensor outputs with grab samples that were analyzed in the lab for DOC concentrations with the high-temperature catalytic oxidation method on a Shimadzu TOC analyzer (see Figure SI 1). From the data output in voltage of the CO_2 sensor the pressure in μatm was calculated according to manufacturer's instructions. Furthermore, we corrected for temperature (centering around 25ºC) and atmospheric pressure as proposed by Johnson et al. (2010). The sensor data are reported as post-treatment values and as η-values to represent the change of fluorescence intensity or pCO_2 (X) between the pool (X_{pool}) and the HZ_{dw} (X_{HZ}).

$$\eta X = \frac{X_{HZ} - X_{Pool}}{X_{Pool}} \times 100 \quad [\%]$$

Eq. 3

Post-processing of raw data of oxygen profiling was performed in MATLAB (version 2010a).

5.2.3 Net ecosystem production calculation

Metabolic rates in the surface water were estimated from continuous diel dissolved oxygen measurements by taking the change in dissolved oxygen between each 15-min measurement interval (Odum 1956). Reaeration coefficient *k* was calculated with the nighttime regression method by taking the slope between the rate of change and the deficit of dissolved oxygen during each night (Hornberger and Kelly 1975). The change of dissolved oxygen in time was divided by the time interval and the product of the temperature-corrected reaeration coefficient (Riley and Dodds 2013) and the oxygen deficit were subtracted (Bernot et al. 2010). For details see also subsection 3.4. From this corrected oxygen net rate the mean values of each night were taken and temperature-corrected with the formula presented in Demars et al. (2016). The gross primary production (GPP) was then calculated by adding the absolute values of these nighttime values to the corrected net rate (NEP) and integrated over time in order to obtain mg O_2 L^{-1} d^{-1}.

5.2.4 Statistical analysis

All statistical analyses were performed in R (R Team Development Core 2008). To investigate differences between the hydrological phases, we performed non-parametric Kruskal-Wallis tests with Tukey-HSD post-hoc analysis. We identified outliers with the Tukey's method included in the R basic statistics (McGill et al. 1978). These outliers were excluded from the next step, where we evaluated if there are influences other than the hydrological phases on *p*CO2 with generalized least squares. We chose this method because we needed to account for account for the temporal auto-correlation given by the nature of our data set using the R-package 'nlme' (Pinheiro et al. 2011). Since the hydrological phases showed significant differences in the pool, as well as the HZ, we included them in the model as a predictor. We used the Akaike information criterion (AIC) to choose the variables that gave us the best fitted model and to identify the required autocorrelation coefficient (p=2 and p=5 for the pool and the HZ data set, respectively). The model residuals fulfilled the assumptions of normality, homocedasticity and autocorrelation. The graphical representations and a table with AIC values can be found in the supplementary information (Table SI 7and Figure SI 3 and SI4). Explanatory variables for the model were chosen by the dredge function from the R-package 'MuMIn' (Bartoń 2016). To test for the significance of the environmental factors on pCO_2, we calculated type 3 analysis of variance table from the fitted model using Wald $\chi 2$ tests from the R-package 'car'(Fox et al. 2016). The previously mentioned outliers served us to identify so-called hot moments, where we

expect sediment desiccation to play an oversized role for the *p*CO2 in the hyporheic zone.

5.3 Results

5.3.1 Temporal dynamics

Temporal variability of all measured sensor data was closely related to the pre-defined hydrological phases (Table 5.1). The drying period comprised three phases, namely contraction, fragmentation and dry. Following drying, the pool remained stagnant and the well in the HZ fell dry. This stagnant phase persisted for one week, before the first rain event reestablished the hydrological connection between the pool and the HZ. This rain event generally increased most of the measured variables. The following rewetting period comprised three rewetting/drying cycles, thereafter called rewetting 1, 2 and 3. Water and sediment temperature was generally lower during contraction and rewetting3 than during all other phases.

The fluorescence signals of protein-like DOM (PDOM) and colored DOM (CDOM) were highest in both, the pool and the hyporheic zone during rewetting 1 (Figure 5.2: Time series of sensor data from the pool (blue dots) and the hyporheic zone (black dots; a-d). Hydrological phases are separated by dashed lines and indicated in the upper panel. e) shows daily metabolic rates in the pool (GPP in green and ER in blue). The rain events in this panel are indicated by arrows, while the x-Axis indicates the date.a and b). While PDOM remained stable in both locations during all other phases, CDOM showed significant differences among all phases. During contraction, CDOM was similar in the pool and the HZ. However, during fragmentation CDOM increased in the pool, whereas the fluorescence signal in the HZ stayed lower and relatively stable until the well fell dry. Especially, during rewetting 2 and 3 CDOM was significantly higher in the pool than during fragmentation and dry, while in the HZ the opposite applied.

Concerning the dissolved gases (Figure 5.2c and d), the pool and the HZ showed opposite patterns, whereby pCO_2 was always higher and DO lower in the HZ than in the pool. By the end of the dry phase pCO_2 increased exponentially in the HZ during two days before the water level dropped below the well depth. With rewetting period, the high pCO_2 values measured in the hyporheic pore water persisted and peaked during rewetting 2. Conversely, rewetting 2 showed the lowest pCO_2 values measured in the pool. During each drying phase following the three distinct rewetting the DO concentrations in the pool were around 5 mg L^{-1} and around 0 mg L^{-1} in the hyporheic zone. Oxygen concentrations in the hyporheic zone increased gradually during the stagnant phase, i.e. when the sediment became increasingly water-unsaturated due to

rapidly falling water levels (Brandt et al., 2017). Upon rewetting, DO over saturation in the pool was detected, with concentrations above 10 mg L^{-1} during all three rewetting phases, while anoxic conditions were immediately re-established in the hyporheic zone.

Table 5.1: Mean (±SD) values of continuous sensor data for each hydrological phase with the highest value of each variable in bold. On the top the hydrological phases with the number of observations per phase. The letters next to the values indicate the result of the Tukey's HSD post-hoc test of the Kruskal-Wallis analysis.

	Contraction (*n* = 26)	Fragmentation (*n* = 79)	Dry (*n* = 45)	Rewetting 1 (*n* = 54)	Rewetting 2 (*n* = 34)	Rewetting 3 (*n* = 59)
Pool						
PDOM	18 (± 1)^{a}	17 (± 2)^{a}	17 (± 2)^{a}	**22 (± 5)^{b}**	17 (± 2)^{a}	16 (± 2)^{a}
CDOM	115 (± 5)^{a}	133 (± 14)^{b}	138 (± 23)^{b}	**212 (± 18)^{e}**	146 (± 22)^{d}	156 (± 16)^{d}
pCO_2	3298 (± 255)^{bc}	**3737 (± 751)^{bc}**	2914 (± 658)^{ab}	3381 (± 951)^{bc}	2507 (± 542)^{a}	3332 (± 1009)^{bc}
Temperature	22 (± 3)^{ab}	**25 (± 3)^{c}**	**25 (± 2)^{c}**	24 (± 2)^{c}	24 (± 3)^{bc}	21 (± 2)^{a}
Hyporheic zone						
PDOM	17 (± 2)^{a}	16 (± 2)^{a}	16 (± 2)^{a}	**19 (± 3)^{b}**	17 (± 2)^{a}	16 (± 2)^{a}
CDOM	114 (± 4)^{ab}	122 (± 8)^{b}	118 (± 10)^{b}	**139 (± 26)^{c}**	110 (± 22)^{a}	106 (± 10)^{a}
pCO_2	10269 (± 472)^{a}	9820 (± 2268)^{a}	13856 (± 7038)^{bc}	14853 (± 3725)^{bc}	**16565 (± 3585)^{c}**	13554 (± 1772)^{b}
Temperature	21 (± 1)^{a}	23 (± 2)^{b}	24 (± 2)^{c}	24 (± 1)^{c}	23 (± 1)^{c}	21 (± 1)^{a}
Difference						
ηPDOM	-6 (± 11)^{ab}	0 (± 15)^{b}	-1 (± 14)^{b}	**-10 (± 13)^{a}**	-3 (± 13)^{ab}	-4 (± 13)^{ab}
ηCDOM	-1 (± 3)^{d}	-8 (± 5)^{c}	-13 (± 11)^{c}	**-33 (± 17)^{a}**	-25 (± 10)^{b}	-32 (± 4)^{ab}
ηCO_2	213 (± 27)^{ab}	166 (± 53)^{a}	400 (± 291)^{c}	390 (± 244)^{c}	**580 (± 172)^{d}**	344 (± 149)^{bc}

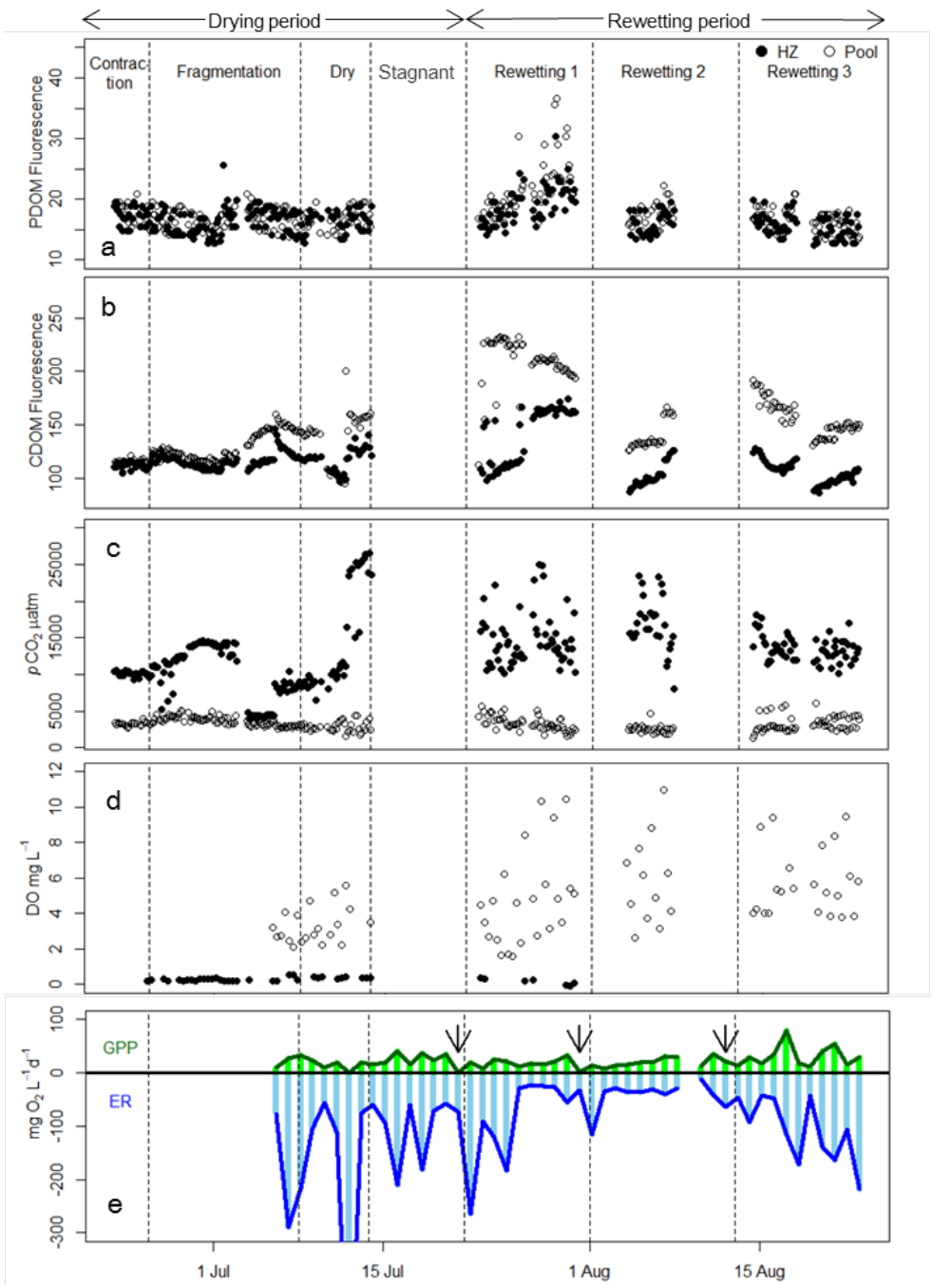

Figure 5.2: Time series of sensor data from the pool (blue dots) and the hyporheic zone (black dots; a-d). Hydrological phases are separated by dashed lines and indicated in the upper panel. e) shows daily metabolic rates in the pool (GPP in green and ER in blue). The rain events in this panel are indicated by arrows, while the x-Axis indicates the date.

The metabolic balance of the pool demonstrated that during the whole study period ER dominated over GPP (Figure 5.2e and Table SI 6). Net heterotrophy was more pronounced during fragmentation and dry phase than during rewetting phases. Especially, rewetting 3 showed some peaks of GPP that transiently balanced the two metabolic processes. Each rain event provoked a drop in GPP that was followed by a steady increase.

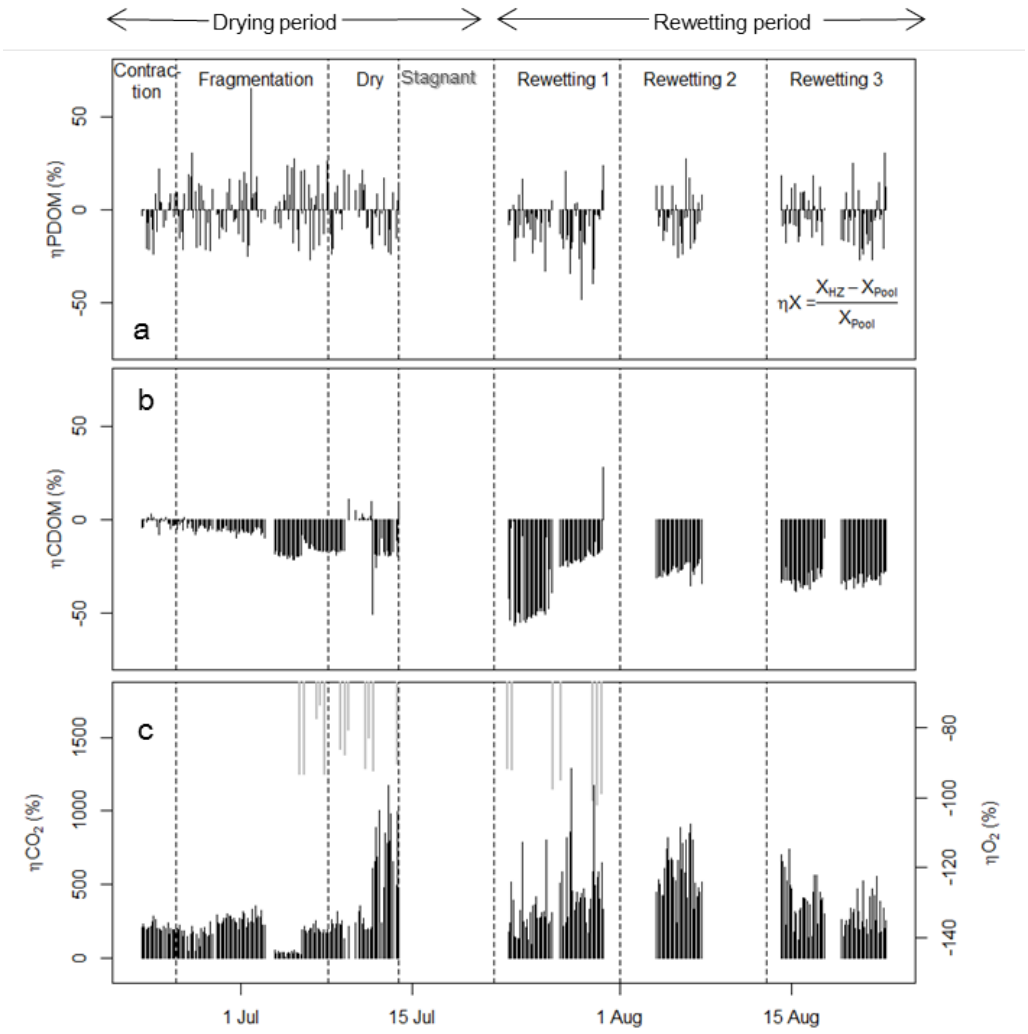

Figure 5.3: Retention or release shown as *η*-values along hyporheic flow paths. The equation is indicated in panel a, as well as the hydrological phases divided by dashed lines.

The comparison between the pool and the hyporheic pore water, expressed as η-values (Figure 5.3) revealed that during the drying phase the HZ acted as both, a source and a sink for PDOM with average positive η-values during the fragmentation phase. Conversely, rewetting 1 showed the most negative ηPDOM. Similarly, ηCDOM was significantly more negative during all three rewetting events than during drying with most negative ηCDOM during rewetting 1. By contrast, ηpCO_2 was always positive and significantly higher during all three rewetting events. Although ηpCO_2 was highest on average during rewetting 2 (Table 5.1), the maximum values of 950% were detected during the dry phase.

5.3.2 pCO_2 dynamics related to temperature and DOM availability

We applied generalized least squares models (GLS), accounting for temporal autocorrelation and differences between hydrological phases, to investigate the drivers of pCO_2 in the pool and the hyporheic pore water (for details see subsection 5.2.4). The pCO_2 release from the pool showed strong differences among hydrological phases with the model after correcting for temporal autocorrelation ($\chi^2_4 = 17.3$, $p < 0.01$) and also showed a significant negative relationship with PDOM ($\chi^2_1 = 12.2$, $p < 0.01$; Table 5.2). The model explained 24% of the variation of pCO_2 in the pool water (*pseudo-*$R^2 = 0.24$; Figure 5.4a), whereby the best fit excluded time as a variable. The other variables, namely CDOM ($\chi^2_1 = 0.6$, $p = 0.44$), NEP ($\chi^2_1 = 0.9$, $p = 0.33$), GPP ($\chi^2_1 = 1.5$, $p = 0.22$) and water temperature were not significant ($\chi^2_1 = 0.1$, $p = 0.77$), but still improved the selected model (AIC = 3154).

Table 5.2: Generalized least squares model on the pCO_2 in the pool.

Variable	Coefficient	Std. Error	*t*	*p*
NEP	-80	82	-0.97	0.333
PDOM	-75	21	-3.49	<0.001*
CDOM	-3	3	-0.77	0.441
GPP	-19	15	-1.23	0.219
Temperature	-10	34	-0.29	0.772
Dry	237	278	0.85	0.395
Rewetting1	-192	236	-0.81	0.417
Rewetting2	256	214	1.20	0.231
Rewetting3	920	245	3.75	<0.001*

Intercept = 4947 ± 996; *pseudo-*$R^2 = 0.24$; $\chi^2 = 24.7$; $p < 0.001$; $n = 200$.

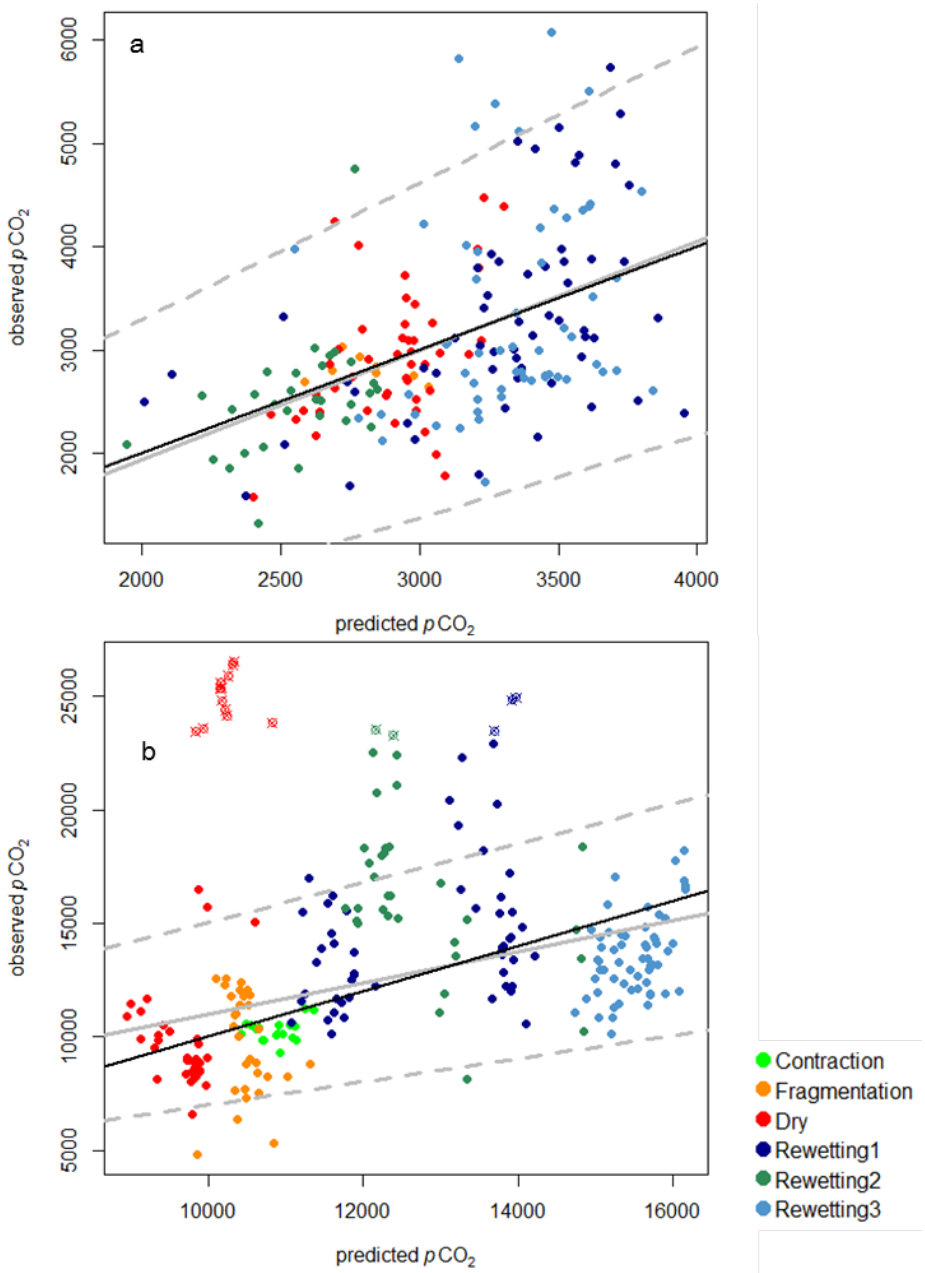

Figure 5.4: Predicted relative to observed pCO_2 for a) the pool (*pseudo*-R^2 = 0.24, the summary of the model is presented in Table 5.2) and b) the hyporheic zone for the model without outliers (*pseudo*-R^2 = 0.21, the summary of the model is presented in Table 5.3). The black line represents the 1:1 line and the grey line the linear regression of observed versus predicted, with dashed lines representing the 95% confidence level. The predicted pCO_2 of the outliers were calculated with this model and are marked with crosses. Colors indicate the hydrological phase.

In the HZ, we expected that temperature and DOM availability would show a significant influence. However, the best fitted GLS (*pseudo-R^2* = 0.21, AIC = 3979; Figure 5.4b) showed no significant effect of the hyporheic temperature on pCO_2 (χ^2_1 = 0.1, p=0.75). In contrast, the CDOM signal of the interstitial pore water was significantly positively related to the pCO_2 (χ^2_1 = 8.4, p<0.01), while PDOM did not show any significant influence (χ^2_1 = 0.1, p=0.79). Time was discarded as a variable and hydrological phases were not significant (χ^2_5 = 6.5, p=0.25).

Table 5.3: Generalized least squares model on the pCO_2 in the hyporheic zone without outliers.

Variable	Coefficient	Std. Error	*t*	*p*
PDOM	-19	72	-0.27	0.791
CDOM	42	14	2.90	0.004*
Temperature	-179	565	-0.32	0.751
Fragmentation	-527	1732	-0.30	0.761
Dry	-794	2250	-0.35	0.724
Rewetting1	1383	2578	0.54	0.592
Rewetting2	2402	2696	0.89	0.374
Rewetting3	4928	2655	1.86	0.006*

Intercept = 10187 ± 12238; *pseudo-R^2* = 0.21; χ^2 = 0.69; p =0.41; n = 224.

5.3.3 Water and oxygen saturation during the Hot Moment

From the sensor data, we detected one hot moment in the HZ of disproportional pCO_2 increase which we could not explain by the generalized linear model. More than 70% of the outliers identified in the pre-analysis occurred during these two days. This hot moment occurred towards the end of the dry phase just before the pool and the HZ became hydrologically disconnected (stagnant phase). Subsurface water levels in the HZ declined continuously throughout the dry phase, most rapidly within the last two days (12th to 14th July 2015). Oxygen profiles in the HZ revealed a stable oxic-anoxic zonation with depth throughout all hydrological phases. The inherent oxygen penetration depth (OPD) was strongly correlated with the depth of water levels (R^2=0.95, Brandt et al. 2017). During the dry phase, the OPD continuously increased, most intensively within two days just before the hot moment (10th – 12th July). During the hot moment, the initially narrow oxygen transition zone expanded, resulting in a

less sharp subsurface oxygen gradient (Figure 5.5). Simultaneously, the shape of the gradient became increasingly non-linear.

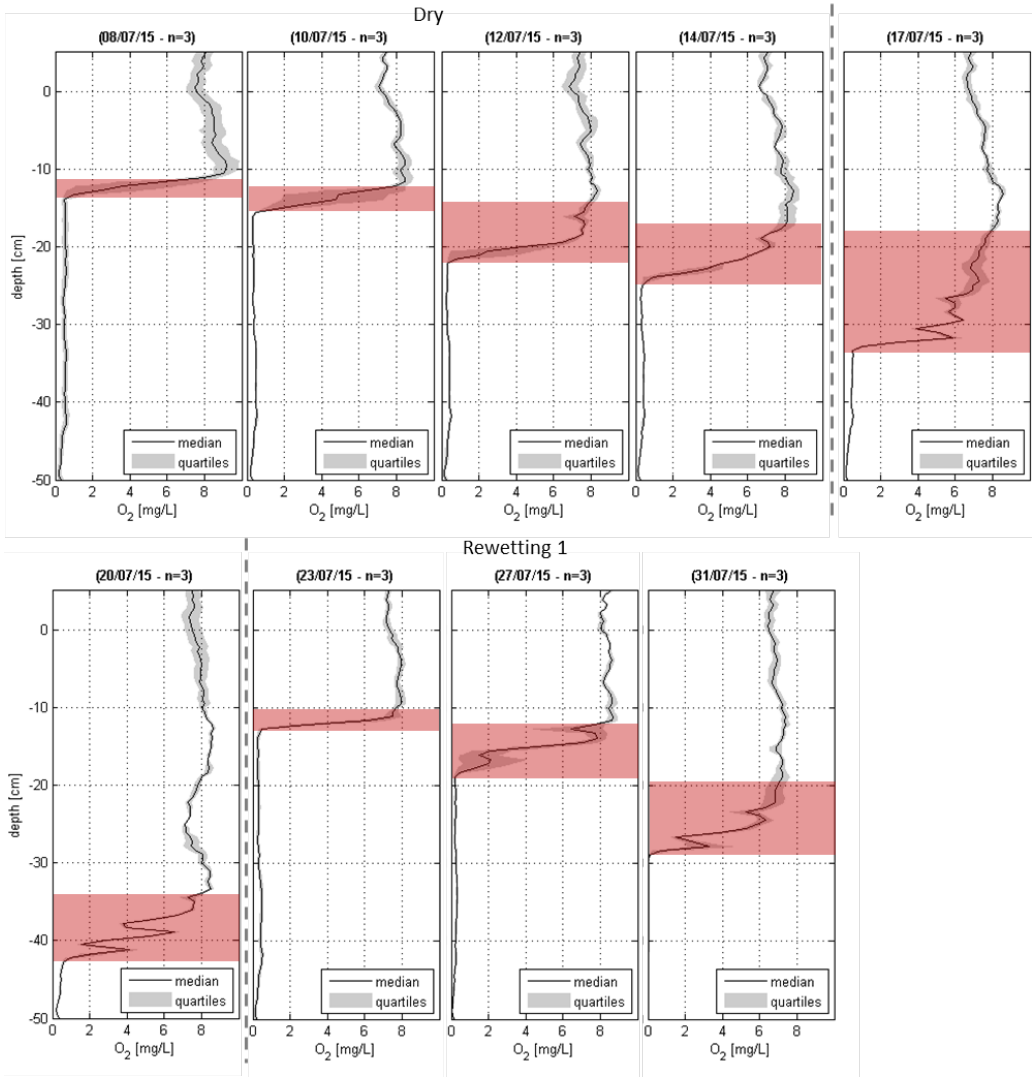

Figure 5.5: Daily oxygen profiles in the Hyporheic Zone (HZ) during the dry and beginning of stagnant phase. Hydrological phases are indicated by the dashed line as defined in Figure 5.1. Red shades areas indicate the extent of the oxygen transition zone. Data is presented as median of *n* measurements per measurement day.

5.4 Discussion

5.4.1 Advantages and limitations of the chosen monitoring approach

Our goals were to identify with continuous measurements moments of disproportionally high carbon processing rates (biogeochemical hot moments; McClain et al. 2003) across the surface-subsurface interface of an intermittent stream during an annual summer drought. Furthermore, we aimed to assign these hot moments to environmental conditions. Our approach demonstrated that the occurrence of these hot moments in surface water was triggered by different factors and therefore occurred during different hydrological phases than in the HZ. This was possible because of the high spatial resolution of oxygen profiling and the comparability of sensor measurements in space and time. The monitoring approach, comprising a whole summer drought period, allowed capturing pCO_2 pulses in the HZ with desiccation and rewetting of this stream compartment. It should be noted that we did not aim to achieve any carbon mass balances because this was not possible with our approach due to inherent limitations. We are aware that during pumping and passing through the silicon tubes and the flow through cell pCO_2 has been outgassed and DOM transformations might have occurred. Furthermore, fluorescence sensor measurements underestimate DOM quantity when abundance of components with other ex/em wavelengths is high. Therefore, we were generally cautious with reporting concentrations and rather interpret the values obtained from the sensors, in accordance with our goals, as relative values in space (pool and HZ_{dw}) and time. Keeping these goals and the limitations in mind, we frame the discussion of our results around the explanation of pCO_2 dynamics in the pool and in the HZ.

5.4.2 Dynamics of pCO_2 in the surface water pool

The pCO_2 values in the pool were generally high in comparison with values reported from other streams (Dinsmore et al. 2013; Peter et al. 2014; Looman et al. 2016). High CO2 super saturation can be found in very slow moving water bodies when the gas exchange velocity with the atmosphere is very low (Gómez-Gener et al. 2016b).We found pCO_2 closely related to protein-like DOM, especially during rewetting 3 when peaks of GPP were followed by high ER. The negative relationship between pCO_2 and protein-like DOM suggests a preferred respiration of this DOM type. Conversely, the bulk DOM quantity represented by the fluorescence signal of CDOM did not show any effect on pCO_2. This observation is in contrast to other studies, suggesting that colored DOM is preferentially respired, while the protein-like DOM is incorporated in the biomass or produced during metabolic processes (Fasching et al. 2014; Wagner et al.

2014). Another mechanism driving pCO_2, even though not measured in this study, could be the abiotic process of photooxidation and subsequent DOM mineralization (Salonen and Vähätalo 1994; Amado et al. 2006). The co-occurrence of DOM mineralization by photooxidation could explain the absent direct relationship between net ecosystem production and pCO_2 (Hessen et al. 2017).

Generally, the fragmentation phase exhibited the highest pCO_2 values in the pool, although rewetting phases showed a similar magnitude. We do not have data from the pre-drought and the contraction phase of the year this study was performed, but data from the previous year showed that NEP was generally higher during pre-drought (Figure SI 2). Fuirosos is reported to exhibit considerable higher ER rates and lower GPP rates compared to similar streams throughout the year (Acuña et al. 2004). However, these authors related the net heterotrophy to the dense riparian vegetation that shaded the stream during the main portion of the year. By contrast, in the stream reach investigated in our study, the shading effect by riparian vegetation is minor because, even though not directly measured, the bedrock channel is fully exposed to sunlight (see Figure 3.3). Therefore, GPP measured in this study was substantially higher (max. 14.4 g O_2 m^{-2} d^{-1}) than the maximums of 1.9 g O_2 m^{-2} d^{-1} measured by Acuña et al. (2004). However, our metabolism estimations still indicated that GPP was exceeded by ER throughout.

Temperature did not show a significant effect on pCO_2 in the pool maybe due to the low variation of surface water temperature during the whole study period or because other drivers might have played a more prominent role (Martí et al. 2009). However, it should be noted that high temperatures have been reported to favor heterotrophic respiration (Sand-Jensen et al. 2007; Acuña et al. 2008; Yvon-Durocher et al. 2012). Similarly, the average water temperature of the pool was higher than 22ºC identified for a Greek intermittent stream as a threshold at which heterotrophic pathways dominated (Skoulikidis et al. 2017b). Within this context, the availability of NO_3 might have limited GPP that is often low in pristine streams of semi-arid and arid environments (Martí et al. 1997; Skoulikidis and Amaxidis 2009; Sabater et al. 2011). While nitrogen to phosphor ratios are high in Fuirosos for most of the year (von Schiller et al. 2008), during drying the ratio of nitrogen to phosphor decreases dramatically (von Schiller et al. 2011). In line with the increases in GPP that we observed after rain events, NO_3 could have been transported to the pool from NO_3-rich riparian soils (Butturini et al. 2003; Moraetis et al. 2010), as well as from the HZ upstream (Gómez et al. 2012).

In summary, our results suggest that the biogeochemical signature of the water exported to the HZ downstream of the pool was high in DOM quantity. However, the DOM mixture was dominated by colored DOM that was recalcitrant to heterotrophic metabolism in the pool (Catalán et al. 2017) rather than protein-like DOM that was

rapidly respired in the surface water. Furthermore, even not measured in this study, previous studies suggest that the surface water might have been low in inorganic nutrients in particular, the electron acceptor NO_3.

5.4.3 Dynamics of pCO_2 in the hyporheic zone driven by drying/rewetting cycles

We detected elevated pCO_2 in the HZ during the dry phase, as well as upon rewetting and subsequent re-drying. These observations are in line with studies from other temporary waterways (Sponseller 2007; Gómez-Gener et al. 2016a). The detected hot moments of carbon processing differed in intensity and duration. While pCO_2 stayed at a constant high level throughout each rewetting event, a hot moment of exponential pCO_2 increase occurred only towards the end of the dry phase, just before the pool and the HZ became hydrologically disconnected. In contrast to pCO_2 during rewetting, this hot moment was not related to DOM quantity in the HZ. Hence, we suggest that this hot moment occurred due to the fact that oxygen had penetrated deeply into the HZ as hyporheic sediments became increasingly water-unsaturated. Previous work found an inverse relationship between CO_2 effluxes and water content, alongside with diffusion serving as the only mechanism for measured CO_2 effluxes (Gómez-Gener et al. 2015). Thus, we can assume that measured pCO_2 in the subsurface will be emitted into the atmosphere.

Rewetting events following the stagnant phase reestablished hydrological connectivity and thus, hyporheic sediments became water-saturated again. Such changes in the hydration status of soils and sediments strongly influence the diffusion of oxygen with depth and thus, aerobic and anaerobic zonation (Ebrahimi and Or 2016). The water level is commonly recognized as sufficient proxy for the depth of oxygen penetration in terrestrial systems, e.g. soils and wetlands (Askaer et al. 2010). Oxygen profiling revealed the validity of this relationship ($R^2 = 0.95$) also for the HZ of an intermittent stream during drought as well as rewetting events (Brandt et al. 2017). However, anaerobic decomposition might still persist under water-unsaturated conditions if oxygen consumption exceeds oxygen diffusion (Fan et al. 2014; Ebrahimi and Or 2016). As a result, the peaks of pCO_2 towards the end of the dry phase might have been caused by two distinct mechanisms or a combination of both: Either elevated oxygen diffusion from the water-unsaturated sediment fueled aerobic decomposition or longer water residence times in the subsurface accelerated anaerobic decomposition. Previous estimations of our study site actually indicated water residence times that exceeded one

day between the pool and the well (see Chapter 3). Anaerobic and aerobic co-metabolism was previously observed in the context of intermittent streams and might play a crucial role in the inorganic nutrient mitigation of these ecosystems (Gómez et al. 2012; Merbt et al. 2016) and in particular, can explain the high DOM mineralization rates found in the HZ (Merbt et al. 2014).

Above all, the HZ showed high DOM retention and respiration rates compared to the pool. Consequently, this zone offered better environmental conditions for a more efficient microbial community, capable of switching fast between aerobic and anaerobic decomposition. Additionally, the HZ has previously been suggested to act as a humid refuge for microbial activity during drought phases of intermittent streams (Romaní et al. 2017). Furthermore, recent evidence proved that extracellular enzymatic activities continue degradation of organic matter even in dry sediments, where this degraded and assumingly labile organic matter accumulates and is readily available when the water level rises again (Stegen et al. 2016). Our observations during the rewetting phase confirm this feature of the HZ microbial community to rapidly recover from hydrologic stress due to desiccation in agreement with studies from Mediterranean soils (Placella et al. 2012). Furthermore, our observations during rewetting suggests the occurrence of the 'Birch effect' in dry streambeds (Gallo et al. 2014).

We found that the HZ of intermittent streams has higher capacities to process organic matter than the surface water and maintains this ability with drying/rewetting cycles. In fact, we suggest that these cycles enhance carbon turnover and increase respiration rates. While recalcitrant CDOM accumulated in the surface water pool, this DOM type was readily respired in the HZ. Additionally, we found that sediment desiccation leads to biogeochemical hot moments that are manifested in disproportional high pCO_2 pulses, explaining the high CO_2 emissions observed in previous studies.

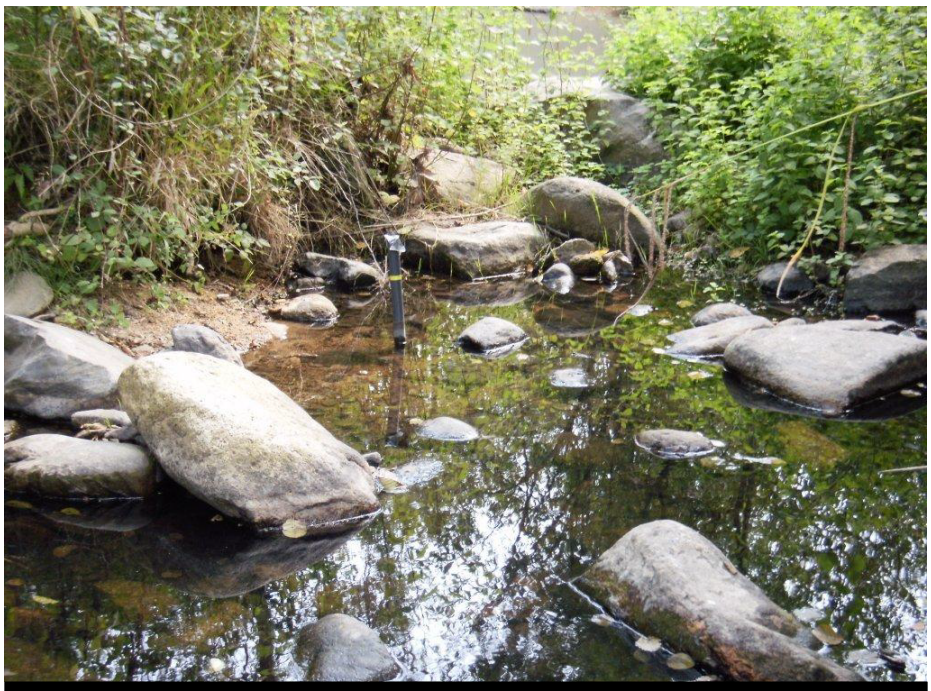

III. Results: Chapter 3

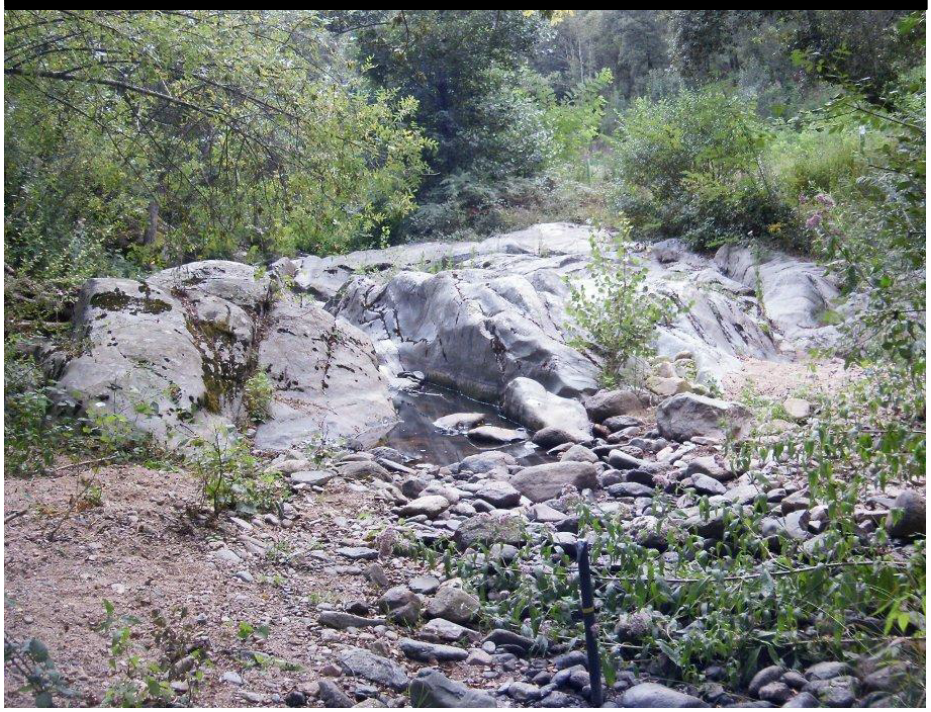

Lateral well (top)

Downstream the bedrock in August (bottom, by Margit Harjung)

6 Responses of microbial activity across the surface-subsurface interface to biogeochemical changes in a drying headwater stream

Microbial heterotrophic activity is a major driver of nutrient and organic matter processing in the hyporheic zone of headwater streams. Additionally, the hyporheic zone might provide humid refuge for microbes when surface flow ceases. We investigated biogeochemistry and microbiological parameters (bacterial density, Live/Dead ratios and extracellular enzyme activities) of surface and interstitial pore water in a period of progressive surface-subsurface disconnection due to summer drying. The biogeochemistry of the subsurface reflected the connectivity with the surface water and was related to the travel time through this interface. Conversely, microbial activity in all subsurface locations was different from the surface waters, suggesting that the microbial signature of the water changes rapidly once the water enters the subsurface. This feature was principally manifested in higher Live/Dead ratios and lower leucine-aminopeptidase (an activity related to nitrogen acquisition) in the interstitial pore waters. Overall, bacterial density and extracellular enzyme activities increased along hyporheic flow paths, with a congruent decrease of inorganic nutrients and dissolved organic matter quantity and apparent molecular size. Therefore, our findings support two ideas of current discussion on the role of the hyporheic zone during drought: First, our results indicate that those deeper (-50 cm) humid layers of the hyporheic zone can act as a refuge for microbial activity. Second, the hyporheic zone shows high rates of carbon and nitrogen turnover related to longer water residence times and these rates might be even boosted by the refuge role of the hyporheic zone during drought.

6.1 Introduction

In fluvial ecosystems, the hyporheic zone is a biogeochemical Hot Spot with high reaction rates of organic matter and inorganic nutrients, because most of microbial heterotrophic activity takes place in this compartment (Boulton et al. 1998; McClain et al. 2003; Danczak et al. 2016). The hyporheic zone plays the role of the river's liver; for instance hyporheic denitrification can comprise up to twice the rate of whole stream denitrification (Fischer et al. 2005; Harvey et al. 2013) and the biggest portion of dissolved organic matter (DOM) is metabolized there (Naegeli and Uehlinger 1997). Additionally, the hyporheic zone of intermittent streams can serve as a humid refuge for microbes, when surface flow ceases in the course of annual summer droughts (Romaní et al. 2013). In the light of today's pressures on fluvial ecosystems that enclose water abstraction and changes in precipitation regime due to global warming (García-Ruiz et al. 2011), it is imperative to understand hydrological and ensuing biogeochemical constrains on microbial activity across the surface-subsurface interface. This understanding is a critical puzzle piece for predicting organic matter and nutrient cycling of fluvial ecosystems under global change.

Microbial activity was found to be related to DOM content of the sediment (Fischer et al. 2002; Eiler et al. 2003). However, the source and lability of DOM plays a key role for microbial metabolism (Chafiq et al. 1999; Hall and Tank 2003). Leaching from microbial assemblages provide an autochthonous DOM source that is assumed to be even more labile for microbes (Anesio et al. 2005). In this respect, allochthonous DOM is typically considered resistant to microbial metabolism, although, this DOM source has been reported to possibly drive shifts in community composition (Eiler et al. 2003) whereas autochthonous DOM seems to affect community composition only transiently (Wagner et al. 2014). Additionally, Farjalla *et al.* (2009) suggested that the mixture of fresh labile and accumulated refractory DOM that naturally occurs in aquatic ecosystems could accelerate bacterial growth and bacterial DOM removal.

So far, the relationship between microbial activity and environmental conditions has been mainly investigated in the laboratory or in mesocosm experiments (Amalfitano et al. 2008; Freixa et al. 2016b; Liu et al. 2017; Perujo et al. 2017). While these experiments target specific physical or chemical parameters that potentially drive microbial activity, we expect that streams offer far more complex interactions (Arce et al. 2014; Zhu and Dittrich 2016). Against this background, the drying period of an intermittent stream offers a set of distinct biogeochemical conditions within a short reach length (Febria et al. 2012). This set of microhabitats at the surface and subsurface is subjected to rapid hydrological changes, driving biogeochemical parameters that

determine microbial activity (Vervier et al. 1993; Lake 2003). For instance, the DOM composition and inorganic nutrient availability undergoes severe changes during the drying of an intermittent stream (Gómez et al. 2009; Vázquez et al. 2011). From prior research carried out at the intermittent study site we were aware of a reach, where the hyporheic zone was confined by impermeable bed rock (Harjung et al. 2017). This situation offered the possibility to investigate the hyporheic zone as a biogeochemical reactor driving dissolved organic carbon (DOC) and inorganic nutrient retention, release and DOM quality changes. In the present study, we linked these biogeochemical changes to the bacterial density, Live/Dead ratio and extracellular enzyme activities in surface and interstitial pore water during a drying period. We expect that the transfer from surface to subsurface will change the chemical and the microbiological signature of the water significantly. We chose to focus on microbial activity in the interstitial pore water rather than attached to the sediment, because in the water the reactions to environmental conditions will be observed immediately (Febria et al. 2012).

In this study, we have two specific objectives, the first one being, to compare spatial heterogeneity of microbial activity with that of biogeochemical characteristics, whereby we hypothesize that we would find the hyporheic zone with different biogeochemical characteristics determining distinct microbial activities. Secondly, we aim to explore spatial and temporal variability of microbial activity during a period of progressive surface-subsurface disconnection with the goal to relate the biogeochemical changes to microbial activity along hyporheic flow paths. We hypothesize the variability of microbial activity would be related to the temporal changes in biogeochemical conditions induced by summer drought and that certain microbial activities can be related to the changing capacity of the hyporheic zone to retain or release DOM and inorganic nutrients.

6.2 Methods

6.2.1 Sampling strategy

The studied reach in Fuirosos is the same as described in chapter1 where the uplift of the bedrock interrupts the hyporheic zone that is composed of alluvial gravel (2-5 cm) with sand and silt fractions. The exposed impermeable bedrock channel is 63 m long, flanked by shallow sandy sediments and then covered again forming a channel of alluvial sediments of approximately 1 to 2 m depth. The hyporheic connectivity is restricted to surface flow by the uplift of the bedrock acting as a natural barrier. Due to the impermeability of the bedrock channel surface water is still captured in small pools (5-7 m^3) and in the hyporheic zone, even when there is no surface flow present in the rest of the stream.

We performed five samplings between June and September 2014 to follow the drying period. The first sampling represents the pre-drought phase in June and the second sampling exemplifies the contraction phase. The approximated water residence times for these phases were estimated from salt slug injections, taking the time that electrical conductivity needed to recover to background values at the measuring point downstream. This tail of the salt tracer curve is indicative for the water volume having passed through the hyporheic zone. It was not possible to achieve a similar estimation for the later samplings, but the absence of diurnal temperature cycles in the hyporheic zone downstream indicates that water residence time exceeded 24 h. The third sampling represents the transition phase from contraction to fragmentation. The fourth sampling was performed during the fragmentation phase and finally, the fifth sampling during the dry phase. The interstitial pore water of the hyporheic zone was pumped with a peristaltic pump from PVC tubes that were perforated over 30 cm on the bottom and were installed at a depth of 50 cm in the hyporheic zone. Figure 6.1 shows the sampling points: The well HZ_{up} is located upstream of the bedrock and is characterized by downwelling during flow conditions. The laterals were represented by two wells: HZ_{lat1} is located at the riparian zone next to the bedrock structure on the left side receiving water from the hillslope and HZ_{lat2} is located on the right lateral receiving mainly surface water from the bedrock channel. The location pool is the most downstream in a series of four pools within the impermeable bedrock. HZ_{inf} refers to the well directly downstream of the pool, where the water of the pool infiltrates into the hyporheic zone. The well HZ_{dw} is located 25 m downstream of the pool and is subjected to upwelling.

Dissolved Oxygen (DO) was measured using an YSI 20 Pro oxygen sensor probe inside the wells immediately after pumping and was deployed in the pool and HZ_{dw} in order to obtain continuous DO and temperature measurements. Surface and interstitial water samples for microbiological analyses were either incubated in the field for the measurement of extracellular enzyme activities, or placed in sterile vials and fixed for bacterial density and viability (see below). Both surface and interstitial pore water samples for chemical analyses were filtered with ashed GF/F filters 0.7 µm nominal pore size and then electrical conductivity (WTW Cond 3310 Conductivity meter) and pH (Thermo Scientific Orion Star A121 pH meter) were measured. Samples for laboratory analysis were collected in pre-washed (MilliQ) polyethylene bottles. The samples for inorganic nutrient concentration and DOM optical properties were filtered through 0.2 μm Nylon filters and the samples for DOC analysis were acidified with 10% HCl. All samples were stored at 4ºC temperature in the dark and analyzed within a week.

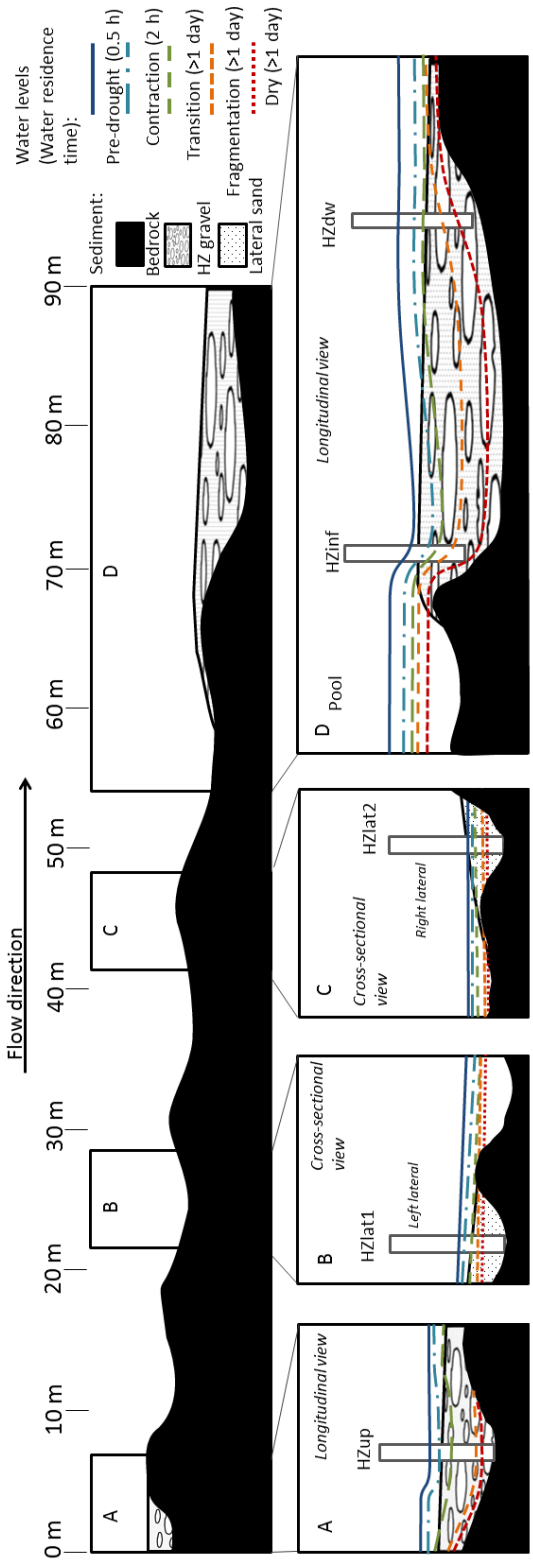

Figure 6.1: Scheme of stream reach, where the top panel is an overview of the complete sampled reach together with the legend for the subsurface type on the right and the individual panels on the bottom represent the magnification of geomorphologic situation of the sampling locations. The colored and differently dashed lines indicate the approx. water level of each phase. Panel A and D show the longitudinal view, while panel B and C present cross-sectional views.

6.2.2 Microbiological analysis

Extracellular enzyme activities β-glucosidase (EC 3.2.1.21) –GLU-, cellobiohydrolase (EC 3.2.1.91) –CBH-, phosphatase (EC 3.1.3.1-2) –PHOS-, and leucine-aminopeptidase (EC 3.4.11.1) –LEU- were measured spectrofluorometrically using fluorescent-linked artificial substrates [Methylumbelliferyl (MUF)-β-D-glucopyranoside, MUF-cellobioside, MUF-phosphate and L-leucine-7-amido-4-methylcoumarin hydrochloride (Leu-AMC), Sigma-Aldrich]. All enzyme activities were measured under saturating conditions (0.3 mM for GLU, PHOS and LEU (Romaní & Sabater, 2000); and 0.9 mM for CBH,(Mora-Gómez et al. 2018)). Water samples (4 mL) were placed in falcon tubes and artificial substrates were added for the determination of extracellular activities (120 µL for GLU, PHOS and LEU and 400 μL for CBH determination). A blank for each artificial substrate with MilliQ water was prepared in order to determine the abiotic hydrolysis of the substrate itself. Samples and blanks were incubated in the field for 1 h in the dark maintaining the same temperature as in the field by placing a tube rack immersed in the stream water. After 1 h incubation, glycine buffer (4 mL, pH 10.4) was added at each sample in order to stop the reaction and maximize MUF and AMC fluorescence. Samples were kept cold and transported to the laboratory for fluorescence readings. Aliquots (350 μL) of each sample were placed into wells of a 96-well black plate (Greiner bio-one). Fluorescence was measured at an excitation/emission wavelength of 365/455 (MUF fluorescence) and 364/445 (AMC fluorescence) in a fluorimeter plate reader (Tecan, infinite M200 Pro). To determine extracellular enzyme activities, MUF and AMC standards were prepared and measured for their fluorescence. Results are given in nmol MUF mL^{-1} h^{-1} or nmol AMC mL^{-1} h^{-1}.Bacterial density was determined by flow cytometry as described below, adapted from Amalfitano et al. (2009). Water samples (1 mL) were placed in sterilized glass vials and detaching solution (9 mL) was added to each water sample. Detaching solution consisted of NaCl (130 mM), Na2HPO4 (7 mM), NaH2PO4 (3 mM), formaldehyde (37%), sodium pyrophosphate decahydrate 99% (0.1% final concentration), and tween 20 (0.5% final concentration) which fix the sample and helps to avoiding bacterial aggregates. Samples were vortexed and an aliquot (400 μL) of each sample was stained with Syto 13 (4 μL Fisher, 5 μM), and incubated in the dark for 15 minutes. To calculate bacterial density an internal standard (10 μL of beads solution 106 beads ml^{-1}, Fisher, 1.0 μm) was added to each sample. Bacterial density was measured by flow cytometry (FACSCalibur, Becton–Dickinson). Results are reported as bacteria cells mL^{-1}.

Bacterial viability was determined by microscope counting. Water samples (2 ml) were stained (3 μl) using the Live/Dead BacLight Bacterial Viability Kit which includes Syto 9 and propidium iodide stains. Samples were incubated for 15 min in the dark. Samples

were filtrated (Black-polycarbonate filter, 0.2 μm) and each filter was prepared for counting in an epifluorescence microscope (Nikon E 600 at 1000X magnification). Syto 9 penetrates all bacterial membranes and stains the cells fluorescent green, while propidium iodide only penetrates cells with damaged membranes, and the combination of the two stains produces red fluorescing cells (Boulos et al. 1999). Results are presented as the ratio of the counted live cells (in green) to the counted dead ones (in red) (Live/Dead ratio).

6.2.3 Chemical analysis

All water samples were analyzed for ammonium (NH_4), nitrate (NO_3), soluble reactive phosphorus (SRP) and DOC concentration, as well as DOM optical properties. DOC concentrations were measured with the high-temperature catalytic oxidation method (Shimadzu TOC analyser). NO_3 was measured using the cadmium reduction method (Keeney and Nelson 1982) with a Technicon Autoanalyzer (Technicon, Tarrytown, NewYork, USA). SRP and NH_4 were measured using a Shimadzu UV-2401 UV-Vis spectrophotometer using the method of the molibdate of Murphy & Riley (1962) for SRP and the salicylate method described by Reardon (1966) for NH_4^+. The samples for DOM optical properties were analyzed at room temperature. Absorbance measurements were conducted using a 1 cm path length cell with the same spectrophotometer over a wavelength range of 200-800 nm. Fluorescence was measured with a Shimadzu RF-5301PC spectrofluorometer over (ex/em) wavelengths of 240-420 nm and 280-690 nm respectively using a 1 cm path length cell.

6.2.4 DOM quality indices

We applied the following optical indices as described in chapter 1: FI, HIX, $SUVA_{254}$, S_R, E_2:E_3. Furthermore, we calculated BIX taking the ratio of emissions 380 nm and 430 nm from the excitation spectra at 310 nm. This index describes freshness (higher values refer to more recent production) and biological activity as origin of DOM (Huguet et al. 2009).

6.2.5 Statistical analysis

Differences between locations were investigated with a PERMANOVA and a canonical analysis of principal coordinates with location as a factor using the PRIMER 6 + PERMANOVA (v. 6.1.11) computer program (Primer-E Ltd., Plymouth, UK)

(Anderson et al. 2008). The values were log(x+1)-transformed to achieve normality. To assess if the location significantly affected water chemistry and microbial activity, a resemblance matrix based on the normalized Euclidean distance was calculated for a one-way analysis of similarity (ANOSIM), which calculates a global R statistic that assesses the differences in variability between groups compared to the variability within the group and checks for the significance of R using permutation tests. A canonical analysis of principal coordinates (CAP) was performed to visualize and classify the locations. CAP is a constrained ordination tool that discriminates locations defined a priori and determines the level of misclassification among sampling locations. Appropriate axis (m) was chosen by minimizing the *p*-value from the permutation test based upon the trace statistic and maximizing the leave-one-out allocation success, as suggested by Ratkowsky (2016). This approach tests how good the locations were discriminated using CAP. To quantify the effect of each variable to potential differences among locations, Spearman correlations were calculated for all variables and the CAP axes. Only the variables with a correlation coefficient $r^2 > 0.4$ were considered. Additionally, one way ANOVA with Tukey's post-hoc analysis was used to evaluate differences between sampling locations at a significance level of $p < 0.01$. All data can be found in Table SI 8.

A redundancy analysis (RDA) using the R-package "vegan" (Oksanen et al. 2013) was performed, whereby the environmental biogeochemical conditions were explanatory variables for the microbiological variables. Pretreatment consisted in the exclusion of environmental variables that showed collinearity and Hellinger transformation of microbiological variables to meet the requirements for RDA (Legendre and Gallagher 2001). The function "envfit" was used to evaluate which biogeochemical variables were significantly correlated with the first two RDA axes ($p < 0.05$). For testing correlations between biogeochemical parameters with microbiological parameters in the hyporheic zone pearson correlation from the R-package "Hmisc" (Harrell Jr 2015) has been used on data of the wells, being significant when $r^2 > 0.5$ and $p < 0.05$.

6.3 Results

6.3.1 Spatial heterogeneity of biogeochemical characteristics and microbial activities across the surface-subsurface interface

We explored the spatial heterogeneity of biogeochemical characteristics and microbial activity. The differences among locations were strong enough to assign the biogeochemical characteristics (ANOSIM R = 0.394, $p < 0.001$) and microbial activity (ANOSIM R = 0.272, $p < 0.001$) to the sampling locations. In both CAP analyses

shown in Figure 6.2, 53% of the observations were assigned correctly. HZ_{up} was poorest classified by biogeochemical variables and the pool was poorest classified by microbial activity. This result suggests that temporal variability of biogeochemical conditions was highest in HZ_{up} and temporal variability of microbial activity was highest in the pool.

Biogeochemical characteristics did not separate surface water samples from the subsurface (ANOSIM R = 0.053, p = 0.216 for factor surface-subsurface, Figure 6.2a). The first axis separated surface water samples and HZ_{inf} from the laterals with high loadings for DO, SRP and NO_3 concentration. HZ_{up} and HZ_{dw} plotted negative side on the second axis, opposite of humification index HIX. The lateral samples plotted together with NH_4, E_2:E_3 and FI.

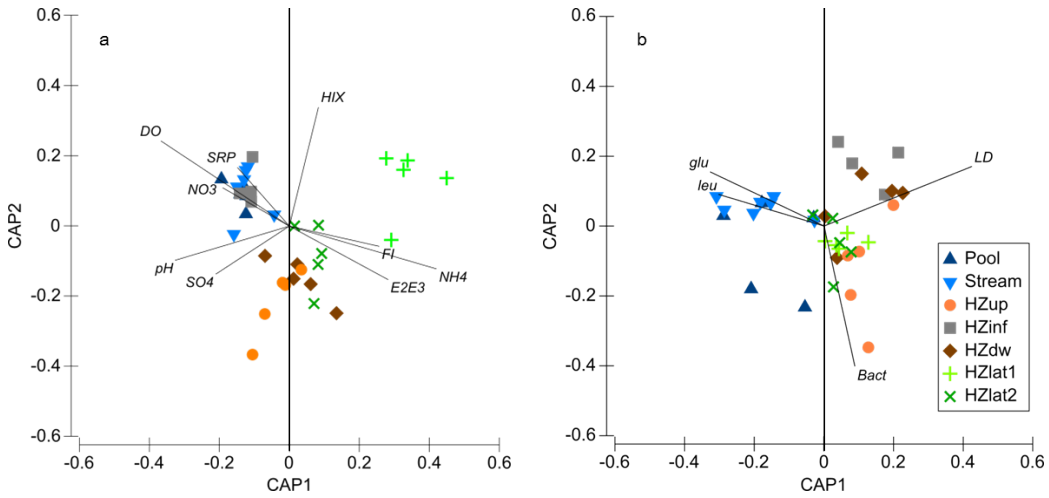

Figure 6.2: Canonical analysis of principal components with location as a factor for a) biogeochemical variables with an overall correct prediction rate of 53% (m = 9, p< 0.001) and b) microbiological variables with an overall correct prediction rate of 53% (m = 4, p< 0.001). Vector overlay are Spearman correlations of variables with canonical axes are shown if |r| > 0.40.

Microbial activities (Figure 6.2b), showed a distinction between surface water and the interstitial pore water samples on the first axis (ANOSIM R = 0.412, p<0.001 for factor surface-subsurface). The surface waters were characterized by higher GLU and LEU, while the interstitial pore waters exhibited a higher Live/Dead ratio. Bacterial density was the only variable that weighted negative on the second axis.

Table 6.1: Mean ± standard deviation of all sampling locations. Asterisks highlight significant differences between sampling locations detected with the one way ANOVA ($p < 0.01$) and letters next to the means indicate the results of Tukey's post-hoc analysis. The highest value for each variable is marked in bold.

Location	HZ_{up} (n = 5)	HZ_{lat1} (n = 5)	HZ_{lat2} (n = 5)	HZ_{inf} (n = 4)	HZ_{dw} (n = 5)	Pool (n = 5)	Stream (n = 7)
Bacteria* 10^6 cells mL^{-1}	**5.9^{b} ± 8.9**	1.1^{ab} ± 0.3	1.3^{ab} ± 1.0	0.4^{a} ± 0.5	1.1^{ab} ± 0.7	2.8^{ab} ± 2.9	0.6^{ab} ± 0.1
Live/Dead ratio*	0.41^{b} ± 0.29	0.22^{ab} ± 0.13	0.19^{ab} ± 0.08	0.69^{b} ± 0.38	**0.74^{b} ± 0.4**	0.06^{a} ± 0.06	0.09^{ab} ± 0.05
GLU* nmol mL^{-1} h^{-1}	0.01^{a} ± 0.00	0.02^{a} ± 0.02	0.01^{a} ± 0.01	0.01^{a} ± 0.01	0.05^{a} ± 0.05	**0.08^{a} ± 0.05**	**0.08^{a} ± 0.03**
PHOS nmol mL^{-1} h^{-1}	0.42 ± 0.68	0.04 ± 0.06	0.07 ± 0.09	0.10 ± 0.09	**0.31 ± 0.32**	0.23 ± 0.18	0.15 ± 0.10
CBH nmol mL^{-1} h^{-1}	0.00 ± 0.00	0.00 ± 0.00	0.00 ± 0.00	0.00 ± 0.00	0.00 ± 0.00	0.00 ± 0.00	0.01 ± 0.02
LEU* nmol mL^{-1} h^{-1}	0.23^{ab} ± 0.29	0.03^{a} ± 0.03	0.19^{ab} ± 0.12	0.26^{ab} ± 0.28	0.27^{ab} ± 0.33	**0.82^{b} ± 0.61**	0.76^{b} ± 0.57
FI	1.52 ± 0.03	**1.58 ± 0.03**	1.53 ± 0.08	1.49 ± 0.01	1.53 ± 0.05	1.49 ± 0.01	1.50 ± 0.08
HIX *	0.87^{a} ± 0.03	**0.95^{b} ± 0.02**	0.91^{ab} ± 0.02	0.92^{ab} ± 0.03	0.89^{ab} ± 0.02	0.90^{ab} ± 0.03	0.91^{ab} ± 0.02
BIX	0.58 ± 0.02	0.58 ± 0.01	0.59 ± 0.01	0.59 ± 0.01	**0.60 ± 0.02**	0.58 ± 0.02	**0.60 ± 0.03**
Slope Ratio	1.01 ± 0.24	0.87 ± 0.07	0.95 ± 0.13	**1.07 ± 0.31**	1.06 ± 0.32	0.98 ± 0.19	0.94 ± 0.17
$SUVA_{254}$	1.87 ± 0.58	2.05 ± 0.40	**2.34 ± 0.28**	2.06 ± 0.74	2.25 ± 0.25	**2.34 ± 0.24**	2.32 ± 0.35
E_2E_3	6.81 ± 0.63	**7.23 ± 1.03**	7.22 ± 0.89	5.98 ± 0.82	6.72 ± 1.20	5.73 ± 0.63	6.05 ± 0.57
DOC mg L^{-1}	3.34 ± 1.54	**5.15 ± 1.54**	2.70 ± 0.57	3.08 ± 1.28	2.78 ± 0.50	3.17 ± 0.70	2.68 ± 0.42
DO* mg L^{-1}	1.25^{ab} ± 0.46	1.03^{ab} ± 0.47	2.49^{abc} ± 1.37	4.20^{abc} ± 2.38	0.91^{a} ± 0.68	**6.33^{c} ± 1.75**	6.23^{bc} ± 3.04
NO_3* mg L^{-1}	0.11^{a} ± 0.07	0.09^{a} ± 0.05	0.09^{a} ± 0.06	**0.71^{b} ± 0.30**	0.23^{ab} ± 0.15	0.14^{ab} ± 0.09	0.15^{ab} ± 0.09
SRP mg L-1	0.02 ± 0.01	0.02 ± 0.00	0.01 ± 0.01	**0.03 ± 0.01**	0.02 ± 0.01	0.02 ± 0.01	0.02 ± 0.00
SO_4* mg L^{-1}	**7.57^{b} ± 4.93**	1.96^{a} ± 1.03	5.87^{b} ± 1.16	5.72^{b} ± 0.46	5.58^{b} ± 0.55	5.67^{b} ± 0.55	5.69^{b} ± 0.40
NH_4* mg L^{-1}	0.09^{bc} ± 0.03	**0.33^{d} ± 0.10**	0.13^{cd} ± 0.03	0.03^{a} ± 0.01	0.09^{abc} ± 0.08	0.04^{ab} ± 0.02	0.03^{ab} ± 0.01
pH*	**7.02^{b} ± 0.16**	6.55^{a} ± 0.10	6.75^{ab} ± 0.12	6.97^{b} ± 0.13	6.92^{b} ± 0.15	6.98^{b} ± 0.14	6.99^{b} ± 0.10
Temperature	20.0 ± 1.9	19.8 ± 1.7	20.0 ± 1.8	20.2 ± 2.3	21.0 ± 1.9	**21.3 ± 3.3**	20.8 ± 3.3
EC* µS cm^{-1}	289^{ab} ± 64	**398^{b} ± 23**	280^{ab} ± 31	259^{a} ± 28	274^{a} ± 45	275^{a} ± 48	251^{a} ± 23

Overall, the one-way ANOVA confirmed that the variables defined by spearman correlation with the CAP axes had significant differences between locations (p<0.01), except for optical indices FI and E_2:E_3. The post-hoc analysis and the mean ± SD values are presented in Table 6.1.

6.3.2 Biogeochemical constrains on microbial activity

We investigated the relationships between environmental variables and microbial activity with a RDA (Figure 6.3a). The first two axes were significant (p<0.001), whereby the first axis explained 16 % and the second axis 16 % of the variation. Out of the 14 environmental variables, six showed a high correlation with the first two RDA axes, namely DO, NO_3, SRP, pH, NH_4 and E_2:E_3 (all p<0.05). E_2:E_3 weighted negative on the first axis and plotted together with the Live/Dead ratio. This was in contrast to DO concentration, which weighted positive on the first axis and was related to LEU and GLU. The second axis separated SRP, NO_3 and pH weighting positive, from E_2:E_3 and NH_4 that were weighting negative. Bacterial density plotted together with E_2E_3 and NH_4 concentration.

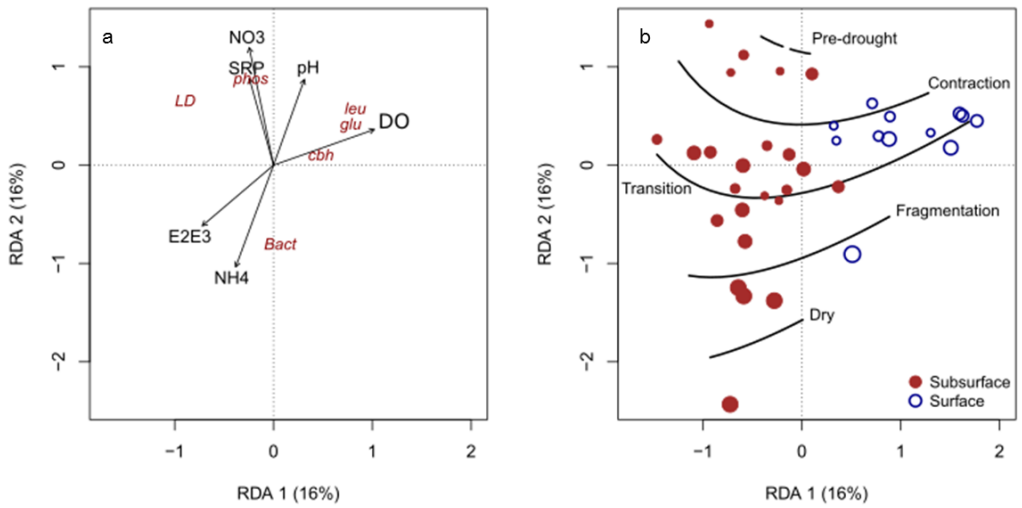

Figure 6.3: RDA with biological data from wells fitted with biogeochemical data, in a) only constrained variables are shown with black arrows, which had a significant correlation with RDA axes (p < 0.05). Unconstrained variables are shown in dark red/italic. b) shows samples distributed in the RDA space with colors indicating subsurface vs. surface. The isolines represent samplings phases and the size of the symbols increase with time (drier).

In Figure 6.3b the scores are shown, demonstrating that the first axis divided surface (plotting positive) from subsurface water samples (plotting negative). The isolines (smoothed) mark the five samplings performed during the different phases of the drying period and therefore indicate that the second axis reflects the changes in time. Both, surface and subsurface water samples shifted during the drying period towards lower SRP and NO_3 concentrations and lower pH, but higher NH_4 concentration. This shift was related to a lower Live/Dead ratio and lower PHOS, but higher bacterial density.

6.3.3 Biogeochemical and microbial changes along hyporheic flow paths with increasing water residence time

We investigated the temporal variability of the hyporheic zone with drying by plotting the biogeochemical and microbiological parameters for the pool, HZ_{inf} (10 m after the pool) and HZ_{dw} (upwelling location 25 m after the pool) for pre-drought, contraction, transition and fragmentation separately (Figure 6.4). For the dry phase the water level in HZ_{inf} was already below the well bottom.

As already demonstrated in both multivariate analyses, the Live/Dead ratio was higher in the hyporheic zone than in the pool. With longer water residence time, the Live/Dead ratio decreased to half of the initial values in HZ_{inf}, but remained stable above 0.8 in HZ_{dw}. Extracellular enzyme activities were generally lower in HZ_{inf} compared to the pool, but PHOS and GLU recovered along the hyporheic flow paths. Generally, these extracellular enzyme activities decreased in the hyporheic zone with longer water residence times and during fragmentation they were nearly undetectable for both hyporheic zone locations. Only LEU showed maximum values in HZ_{dw} during the transition phase that was when water residence time already exceeded a day. The value of 0.84 nmol L^{-1} h^{-1} measured this day represents three times the mean value in HZ_{dw} over the whole sampling period. During the transition phase also a peak of bacterial density of 2.3 x 10^6 cells mL^{-1} that is twice the mean bacterial density of HZ_{dw} was detected.

The change in concentrations between the pool and HZ_{dw} revealed that the hyporheic zone acted as a sink for DO and both, as a sink and as a source, for DOC and inorganic nutrients (Table 6.2). During contraction, anoxic conditions were detected at night time in HZ_{dw}, but still the DO concentration would recover to values above 0.5 mg L^{-1} during the day (Data not shown). When water residence time exceeded one day, the DO was completely consumed in HZ_{dw} at any time of the day. In general, DOC was retained in the hyporheic zone, only interrupted by DOC pulses from HZ_{inf} during the transition phase and from HZ_{dw} during fragmentation. Conversely, SRP and NO_3 concentrations always increased when surface water entered the hyporheic zone at HZ_{inf}. This increase

between pool and HZ_{inf} was higher with longer water residence time, leading to twice the SRP concentration and five times the NO_3 concentration of the pool during fragmentation. Between HZ_{inf} and HZ_{dw}, SRP concentrations decreased back to pool concentrations. The same applied to NO_3, but the magnitude of this decrease was not sufficient to remove all the NO_3 produced at HZ_{inf}. Overall, the NO_3 concentration increased by 260 %, 230 % and 59 % between the pool and HZ_{dw}, during pre-drought, contraction and the transition phase, respectively. Conversely, during fragmentation, the NO_3 concentration decreased by 35 % between pool and HZ_{dw}, even though the concentration was highest in HZ_{inf} during this phase. Contrariwise, NH_4 concentrations were lowest at HZ_{inf} and increased along hyporheic flow paths with a peak in HZ_{dw} during the transition phase.

Three optical indices are plotted that represent how DOM quality changed between the pool and HZ_{dw}: E_2:E_3 increased along hyporheic flow paths, but the magnitude of this increase was not associated to water residence time. FI did not show any change between HZ_{inf} and the pool, but clearly increased between HZ_{inf} and HZ_{dw}. HIX showed a similar pattern as the inorganic nutrients, whereby this index increased between the pool and HZ_{inf}, but decreased between HZ_{inf} and HZ_{dw}. In line with the pattern of the inorganic nutrients, the increase/decrease sequence of HIX showed higher magnitudes with higher water residence time.

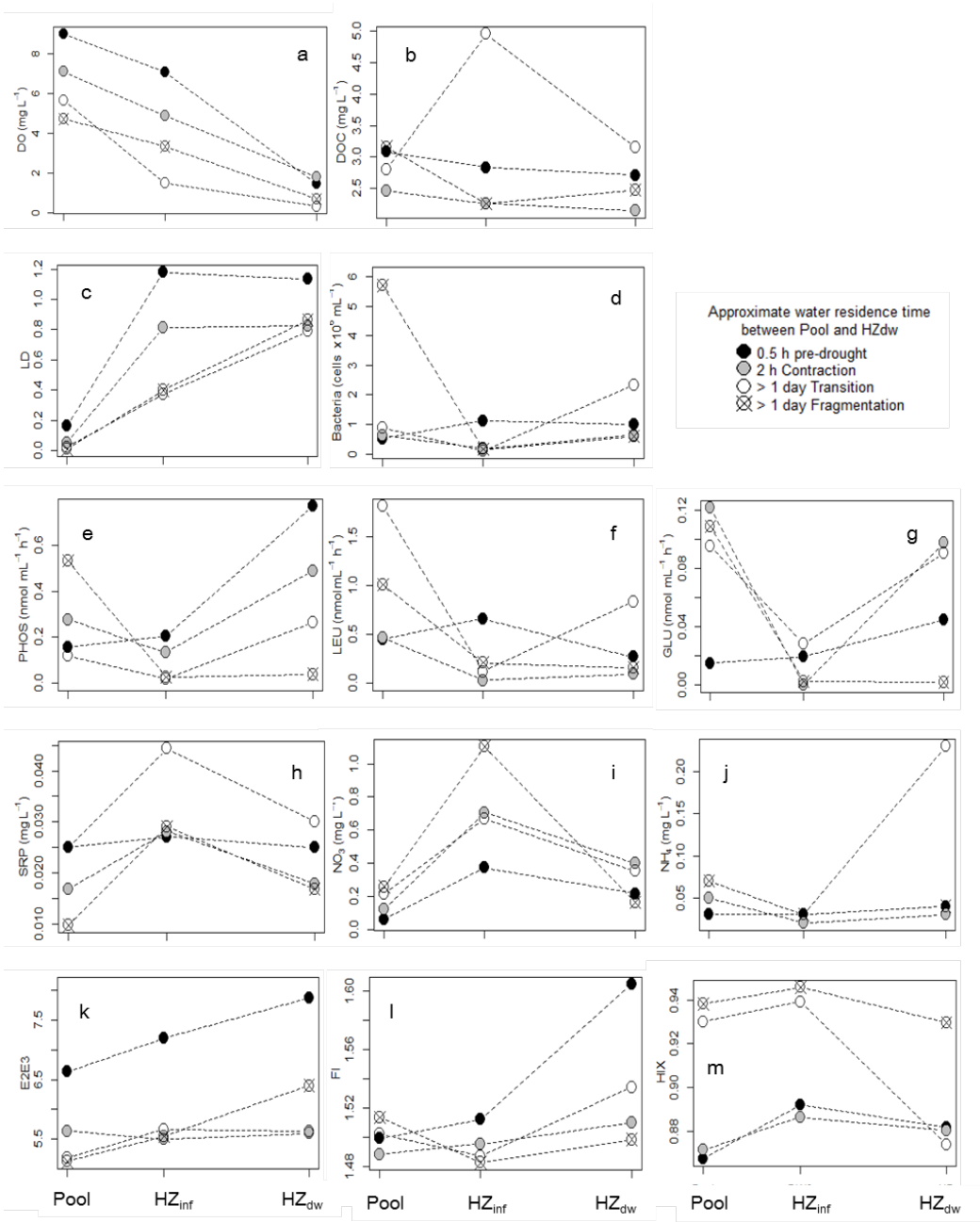

Figure 6.4: Biogeochemical and microbiological variables for the locations pool, HZ_{inf} and HZ_{dw} during pre-drought, contraction, transition and fragmentation.

Table 6.2: Percentage (%) difference between Pool and HZ_{inf} (infiltration surface water) and between HZ_{inf} and HZ_{dw} (Upwelling subsurface). Negative values indicate retention (in bold) and positive values indicate release. Arrows indicate if median of all four values was positive or negative. Rows on the bottom show temperature and oxygen ranges continuously measured at HZ_{dw}. Asterisks indicate that these values were not taken exactly from the sampling day, but the closest date due to technical problems.

	Concentration difference in infiltration surface water					Concentration difference in upwelling subsurface				
Sampling	Pre-drought	Con-traction	Trans-ition	Frag-mentation	Ten-dency	Pre-drought	Con-traction	Trans-ition	Frag-mentation	Ten-dency
				Biogeochemical changes (%)						
DOC	**-8**	**-8**	+77	**-29**	↓	**-4**	**-5**	**-36**	+10	↓
DO	**-21**	**-31**	**-74**	**-29**	↓	**-80**	**-63**	**-79**	**-79**	↓
NO_3	+516	+468	+207	+327	↑	**-42**	**-44**	**-47**	**-85**	↓
NH_4	0	**-60**	0	**-57**	↓	+33	+50	+667	+33	↑
SRP	+8	+67	+77	+199	↑	**-8**	**-36**	**-32**	**-42**	↓
E_2:E_3	+8	**-2**	+9	+8	↑	+9	+2	**-1**	+15	↑
HIX	+3	+2	+1	+1	↑	**-1**	**-1**	**-7**	**-2**	↓
FI	+1	+1	**-1**	-2	–	+6	+1	+3	+1	↑
				Microbial changes (%)						
L/D ratio	+624	+1474	+1491	+4482	↑	**-4**	+2	+112	+117	↑
Bact. density	+113	**-71**	**-89**	**-97**	↓	**-11**	+251	+2261	+279	↑
GLU	+29	**-100**	**-71**	**-98**	↓	+130	+Inf	+222	**-22**	↑
PHOS	+29	**-52**	**-84**	**-95**	↓	+277	+263	+1272	+50	↑
LEU	+48	**-93**	**-93**	**-79**	↓	**-59**	+192	+593	**-25**	↑
				Daily ranges in HZ_{dw}						
	Pre-drought		Contraction			Transition		Fragmentation		
Temperature ºC	25.4 - 16.8 *		21.8 -17.8			21.6 - 20.9		21.2 - 20.8		
DO mg L^{-1}	4.89 - 1.10 *		1.68 - 0.33			0.33 - 0.30		0.33 - 0.31		

6.4 Discussion

6.4.1 Microbial activity and biogeochemistry across the surface-subsurface interface in an intermittent system

We aimed to improve the understanding of microbial processes related to environmental conditions across the surface-subsurface interface during a drying period. Very few studies have compared extracellular enzyme activities and bacterial density in surface and interstitial pore water of natural stream ecosystems (Romaní et al. 2006; Ann 2015). It should be noted that we found pronounced differences in microbial activity between hydrological periods that emphasizes the high variability of microbial activity in intermittent streams. Extracellular enzyme activities GLU and LEU from Fuirosos stream surface water in spring season during baseflow were twice the maximum values of this study (Ylla et al. 2010). Furthermore, Romaní et al. (2006) report LEU values in both surface and subsurface waters that were even tenfold higher during a flooding episode in fall ($Q = 400$ L s^{-1}). In literature, we only found comparably low extracellular enzyme activities reported from the larger Tordera River during low flow phase in July (Ann 2015). The author of this study suggested a close connection between extracellular enzyme activities and DOM availability, as reported from different aquatic environments (Sabater and Romani 1996; Ylla et al. 2011; Baltar et al. 2017). In this context, photooxidized DOM could result less labile to bacterial metabolism if amino-acids were destroyed (Amado et al. 2015) or extracellular enzyme activities themselves can be photodegraded in the surface waters due to the shallow water level (Fernández Zenoff et al. 2006; Dieter et al. 2013). Additionally, LEU exhibits a very narrow pH range around 7.5 as optimal (Cunha et al., 2010). The pH was mostly below 7, because the low buffering capacity of the water in the granitic catchment favors acidic conditions when humic acids are abundant. Hence, DOM quality could have affected the occurrence of extracellular enzyme activities directly via energy availability or indirectly by decreasing the pH.

We hypothesized that we would find different biogeochemical characteristics and microbial activities in the surface waters versus the interstitial pore waters. However, the surface locations did not separate from the subsurface locations based on their distinct biogeochemical characteristics, but based on differences in microbial activity. The hyporheic zone of the main channel is fed exclusively by the surface water during the study period, but offers a habitat for microbial activity that is similar to the laterals (depth, solid surfaces). This situation was reflected in our results as followed: HZ_{inf}, the location where surface water infiltrated into the hyporheic zone, showed similar biogeochemical characteristics as the surface waters. On the other hand, longer

hyporheic flow paths might explain the separation of HZ_{up} and HZ_{dw} from the other locations. This biogeochemical imprint of the hyporheic zone is manifested in lower DO, as well as less humification degree of the DOM than all other locations. Conversely, the microbiological variables denoted a strong influence of the hyporheic zone, since all interstitial pore water samples showed a clear division from the surface waters. Hence, we suggest a delay between the change in microbial activity that occurs immediately once the water enters the hyporheic zone and the legacy of biogeochemical response observed along the hyporheic flow paths.

6.4.2 Linking chemical characteristics and microbial activities during drying: The hyporheic zone as a biogeochemical Hot Spot

6.4.2.1 Nutrient retention and DOM mineralization in the hyporheic zone

The drying period in Mediterranean streams is reported to show distinct biogeochemical conditions that can be assigned to hydrological phases (Vázquez et al. 2011; von Schiller et al. 2011). Drying and its consequences, as e.g. disconnection of flow paths laterally and longitudinally, as well as longer water residence times (Fisher et al. 1998; Harvey et al. 2003) provoked a decrease of SRP and NO_3 concentrations that is also observed in other studies from intermittent streams (Martí et al. 1997; von Schiller et al. 2008; Bernal and Sabater 2012b). Additionally, in intermittent streams the absence of surface flow can involve the diffusion of oxygen into the pore space of the hyporheic zone that triggers ammonia oxidation (Merbt et al., 2016). Similarly, Storey et al. (2004) reported differences in DO concentration and nitrogen removal between up- and downwelling locations, with downwelling sites as Hot Spots of nitrification (Triska et al. 1990; Edwardson et al. 2003). Both, nitrification preceding denitrification in the hyporheic zone increases with water residence times (Zarnetske et al., 2011a). Similarly, the downwelling location HZ_{inf} was characterized by high inorganic nutrient concentrations, which might have made extracellular enzyme activities redundant to achieve them. On the other hand, at the upwelling location HZ_{dw} the nutrient concentration was so depleted that extracellular enzyme activities were produced to obtain the nutrients from the organic matter pool. We observed NO_3 removal of up to 0.21 mg N L^{-1} during fragmentation between Hzinf and HZdw when water residence time exceeded a day.

Labile DOC can additionally enhance hyporheic denitrification, with rates of up to 0.37 mg-N L^{-1} in 10 hours (Zarnetske et al., 2011b) that is higher, but still in a similar magnitude as found in this study. Conversely, DOM infiltrating with the surface water showed a high humification degree in HZ_{inf}, in line with high nitrification rates reported when recalcitrant DOM is abundant (Strauss & Lamberti 2002). However, the DOM

quality was improving along hyporheic flow paths, as indicated by decreasing humification, but increasing FI (autochtonous) and E_2:E_3 (smaller molecules) values. The FI values showed similar dynamics as GLU, an extracellular enzyme activity that is reported to correlate with autochthonous DOM availability (Proia et al. 2016; Freixa et al. 2016a) and higher pCO_2 levels (Grossart et al., 2006). The dynamics of GLU, a drop at HZ_{inf} and an increase in HZ_{dw}, are consistent with the DOM retention and the pCO_2 release that occurred in this hyporheic zone reach (unpublished data). DOM derived from surface water can fuel hyporheic metabolism (Clinton, Edwards & Findlay, 2010), but DOM can also be leached from particulate organic matter, extracellular enzymes or released during anabolic processes in the hyporheic zone (Stegen et al. 2016; Burrows et al. 2017). Fischer et al. (2002) suggested that the cycling of these autochthonous DOM fractions might be faster and consequently their contribution to bacterial metabolism would be higher than inferred from the apparent DOM retention.

Moreover, bacterial density increased in all sampling locations with drying that is in contrast to continuous flow column experiments, where bacterial density rapidly decreased with depth (Perujo et al. 2017). Conversely, an reported increase of bacterial density in the interstitial pore water of a sediment desiccation laboratory experiment (Pohlon et al. 2013a), suggests that microbial activity in intermittent streams follow a different distribution pattern of microbial activity than their perennial counterparts. Furthermore, Pohlon et al. (2013a) suggested a community shift towards bacteria that are more efficient in carbon and nutrient acquisition. This described community shift could explain the decrease of nutrient concentrations and apparent DOM molecular size on the temporal axis that we have observed in this study and further suggests that deeper humid layers are important Hot Spots of DOM and nutrient retention during drought.

6.4.2.2 The hyporheic zone as a refuge

The hyporheic zone appeared to have acted as a humid refuge for the bacteria during the drying period of the stream indicated by higher Live/Dead ratio of subsurface waters compared to the surface water. The sediment desiccation of intermittent rivers is reported to drastically reduce living bacteria, when experimentally tested in mesocosms (Amalfitano et al. 2008). However, we suggest that natural streams and rivers often maintain deeper, humid layers of the hyporheic zone as a refuge for microbial activity during drought as suggested by Romaní et al. (2013). We found significantly higher Live/Dead ratios in the interstitial pore water compared to surface water that points towards this survival mechanism of bacteria and is further evidenced by the increase of the Live/Dead ratio along the hyporheic flow path between HZ_{inf} and HZ_{dw}. Similarly,

the bacterial community in the hyporheic zone (at 10 cm depth) of Fuirosos showed higher resistance to drying than the upper layers of sandy sediment cores (Timoner et al. 2014). Furthermore, Ann (2015) reports higher extracellular enzyme activities in interstitial water of the Tordera River with absence of surface flow from sediment depths similar to those of this study (-30 to -50 cm). Concerning the resistance mechanisms of microbial metabolism during drought, there is a gap of studies reporting Live/Dead ratios and bacterial density in interstitial pore water. This would be particularly of interest, as prokaryotes are able to travel greater distances and deeper into the hyporheic zone with the water flow, because of their ubiquitous nature (Febria et al. 2012; Peralta-Maraver et al. 2017; Romaní et al. 2017). In this sense, prokaryotes might have a survival advantage compared to larger microbes that makes them the essential actors of nutrient retention and DOM mineralization in intermittent streams as well as other environments with fluctuating water levels (Stegen et al. 2016; Goldman et al. 2017). The spatial flexibility of prokaryotes to travel to humid regions (deeper, upwelling locations) of the hyporheic zone, as proposed by the results of this study, might indicate an underestimation of bacterial survival of droughts and point towards Hot Spots in the hyporheic zone that can show enhanced carbon turnover rates (Ylla et al. 2010; Gómez-Gener et al. 2016a). This idea is further corroborated by the much lower microbial activity that we found in the interstitial pore water in October when the fluvial continuum had reestablished (data shown in Table SI 9). Still, we have to acknowledge the fact that the number of observations in this study is small and similar studies from other intermittent streams are needed to fully understand the hyporheic zone as a refuge for microbial activity. Nevertheless, our results emphasize the importance of the hyporheic zone during drought: not just that remaining humid locations are biogeochemical Hot Spots during drought that act as DOM and nutrient sinks, but they can also provide a refuge for microbial activity that can explain enhanced DOM and nutrient turnover rates upon rewetting.

IV. Results: Chapter 4

Nationalpark Gesäuse (top)

Outlet of the flumes (bottom, Masumi Stadler)

7 Experimental evidence reveals impact of drought periods on dissolved organic matter quality and ecosystem metabolism in subalpine streams

Subalpine streams are predicted to experience lower summer discharge following climate change and water extractions. In this study, we aimed to understand how drought periods impact dissolved organic matter (DOM) processing and ecosystem metabolism of subalpine streams. We mimicked a gradient of drought conditions in stream-side flumes and evaluated implications of drought on DOM composition, gross primary production and ecosystem respiration. Our experiment demonstrated a production and release of DOM from biofilms and leaf litter decomposition at low discharges, increasing dissolved organic carbon concentrations in stream water by up to 50%. Absorbance and fluorescence properties suggested that the released DOM was labile for microbial degradation. Dissolved organic carbon mass balances revealed a high contribution of internal processes to the carbon budget during low flow conditions. The flumes with low discharge were transient sinks of atmospheric CO_2 during the first two weeks of drought. After this autotrophic phase, the metabolic balance of these flumes turned heterotrophic, suggesting a nutrient limitation for primary production, while respiration remained high. Overall our experimental findings suggest that droughts in subalpine streams will enhance internal carbon cycling by transiently increasing primary production and more permanently respiration as the drought persists. We propose that the duration of a drought period combined with inorganic nutrient availability are key variables that determine if more carbon is respired in situ or exported downstream.

7.1 Introduction

Mountainous regions are estimated to provide more than 30% of the global water runoff from the continents to the oceans (Meybeck et al. 2001). At the same time, these regions are predicted to be most affected by climate change, as more precipitation will fall as rain rather than snow (Barnett et al. 2005), resulting in a potential loss of stream flow during spring and summer (Berghuijs et al. 2014). In addition, streams in the European Alps are subject to direct human impacts on the hydrological regime, such as water extractions and hydroelectric power production (Maiolini and Bruno 2008). Hence, there is an increasing need to understand the implications of hydrological regime change and in particular, the occurrence of droughts, on alpine stream ecosystem functioning (Hannah et al. 2007; Ulseth et al. 2017).

Subalpine streams are considered net heterotrophic (Uehlinger and Naegeli 1998; Fellows et al. 2001; Hall et al. 2015), with ecosystem respiration (ER) exceeding gross primary production (GPP) resulting in a negative net ecosystem production (NEP). Net heterotrophy is also reported for most other fluvial ecosystems (Mulholland et al. 2001; Hoellein et al. 2013) where high ER is maintained by a steady supply of particulate and dissolved organic matter (DOM) from the terrestrial ecosystem (Battin et al. 2008). The DOM supply from the surrounding catchment is determined by the availability of DOM in soils (Schelker et al. 2013) and its transport with surface runoff and subsurface flow into the main channel (Aitkenhead-Peterson et al. 2003). Hence, heterotrophy largely depends on the hydrological connectivity of soils and streams. Autochthonous DOM has been found to contribute less than 5% of the DOM pool of headwater streams (Mulholland 1997).

The effects of hydrological variation on DOM quantity have been well studied in the context of stormflow events. For example, several studies report that DOM quantity increases with discharge (Ågren et al. 2008; Wiegner et al. 2009; Bass et al. 2011; Guarch-Ribot and Butturini 2016). DOM quality changed towards a terrestrial, more humified composition, with probably lower biodegradability for heterotrophic metabolism (Saraceno et al. 2009; Fasching et al. 2016; Raymond et al. 2016). However, little is known about how extended periods of reduced flow may affect DOM quantity and quality, particularly in humid regions (Larned et al. 2010).

Streams regularly subject to flow intermittency, such as those of the Mediterranean biome, show distinct patterns of DOM processing. DOC concentrations have been found to increase with decreasing discharge during summer drying (Von Schiller et al. 2015). Although this DOC increase during drying is less prominent than during storm events, the former is paralleled with a change in DOM composition towards labile characteristics (Vázquez et al. 2011; Butturini et al. 2016; Ejarque et al. 2017).

Additionally, some Mediterranean and semi-arid streams have been characterized to transiently shift to net autotrophy (Webster and Meyer 1997; Velasco et al. 2003), acting as sources of aquatic DOM. Phases of net autotrophy are partly explained by high water temperatures that enhance GPP (Busch and Fisher 1981; Acuña et al. 2004). Similarly, Proia et al. (2016) report higher autochthonous carbon loads in a Mediterranean river during summer low-flow associated with lower water residence times.

To identify the potential effects of drought conditions on subalpine stream ecosystem functioning, we designed an experiment in stream-side flumes. We recreated six hydrological conditions, ranging from baseflow to drought, and evaluated changes in DOM quantity and quality, as well as in whole-flume metabolism. We expected the ecosystem response to drought to be similar to the responses reported for drier regions (Jones Jr et al. 1996; Mulholland et al. 2001; Velasco et al. 2003; Pastor et al. 2017) and predicted that discharge reduction will increase water residence time and water temperature. Following these alterations, we expected higher in-stream DOC production and an increase of autochthonous DOM in the flumes with low discharges, as well as an increase in autotrophic metabolic pathways.

7.2 Methods

7.2.1 Experimental setup

This study consisted of simulating decreasing flow conditions from base flow to drought in six streamside flumes located in the subalpine region of lower Austria (47º 15'N 15º04'E). All flumes were fed with stream water of the 'Oberer Seebach', a pristine, second-order stream draining a karst catchment of 25 km^2 located between 600-1900 m above sea level (Schelker et al. 2016). Previous studies have identified hydrological conditions as a major driver of dissolved CO_2 concentrations (Peter et al. 2014). Generally low production and high respiration result in a low autotrophic contribution to the carbon budget (Ulseth et al. 2017). DOC concentration ranges from 1.11 - 5.43 mg C L^{-1} and increases with discharge. DOM composition is typically terrestrially-derived and humic-like, with some autochthonous imprints during base flow (Fasching et al. 2016). Summer stream water temperature ranges from 6.6 - 15.0ºC, inorganic nutrient concentrations (mean ± SD) are generally low ($N\text{-}NO_3$ = 1197 ± 261 μg L^{-1}; $N\text{-}NO_2$ = 0.8 ± 0.5 μg L^{-1}; $N\text{-}NH_4$ = 10 ± 8 μg L^{-1}; $P\text{-}PO_4$ = 5 ± 2.5 μg L^{-1}) and the stream is commonly supersaturated in O_2 (12.1 ± 0.8 mg L^{-1}) (Müllner and Schagerl 2003).

The flumes (40 m length, 0.4 m width) were filled with a mixture of sand (d_{50} = 0.2 - 0.4 mm) and leaf-litter (*Fagus sylvatica* and *Acer pseudoplatanus*), representing the streambed sediment containing a typical source of particulate organic matter of terrestrial origin. We chose a total organic carbon to sediment ratio of approximately 1.5 g C kg^{-1} that is within the range of 0.8 to 2.1 g C kg^{-1} found in the bed sediments of 'Oberer Seebach' (Leichtfried 1996). The sand-leaf-litter mixture was distributed as a series of dunes (2 m long, maximum height of 0.15 m and minimum height of 0.05 m above the bottom of the flumes) in order to create a sequence of pools and riffles (Figure 7.1a, b, c and d). A thin layer of gravel was added the tops to avoid erosion.

Figure 7.1: a) Flume outlets with discharge ascending from the left (F1) to the right (F6). b) Set up of flumes before water flow and c) underwater photo of biofilm after two weeks of treatment (17th of September 2015). d) Scheme of F1 during treatment with black arrows indicating the enforced water flow through the stream bed. e) Scheme of F6 during treatment with black arrows indicating the water flow predominantly above the stream bed.

The experiment was performed during August and September of 2015 and consisted of three phases: First, a two-week pre-treatment phase with constant discharge (2.65 L s^{-1}) in all flumes to allow colonization by bacteria and establishment of biofilms. Second, a three-week treatment phase with different levels of decreased discharge (Table 7.1) in each flume, except for the control flume (F6) remaining with the initial discharge.

Third, a reflow phase where all flumes received pre-treatment discharge levels for three days.

Table 7.1: Discharge (Q), flow velocity (v), water residence time (WRT), water volume (WV) and the percentage of water volume being interstitial water (IW) in flumes during treatment

Flume	Q (L s^{-1})	v (cm s^{-1})	WRT (min)	WV (m^3)	IW (%)
F1	0.03	0.19	351	0.63	100
F2	0.10	0.34	196	1.18	63
F3	0.35	1.11	66	1.39	54
F4	0.73	2.27	29	1.29	58
F5	1.45	4.07	16	1.39	53
F6	2.65	6.67	10	1.59	47

7.2.2 Flume ecosystem monitoring

We used a combination of high-frequency monitoring with sensors and grab sampling. Light intensity and temperature were measured continuously in each flume over the whole duration of the experiment by a HOBO Pendant Temperature/Light 64K Data Logger (Onset Computer Corporation, Massachusetts). Dissolved oxygen concentrations were recorded continuously during treatment and reflow with one HOBO Dissolved Oxygen Data Logger at the end of each flume, as well as at the inlet of control flume F6. A UV-Vis probe (Spectro::lyser, S::can Messtechnik GmbH, Austria) was installed in a flow through cell, measuring absorbance spectra from the water at the outflow of each flume (once per hour) and from the inflow (twice per hour) during the last week of the treatment phase. From UV-Vis spectral data hourly DOC and NO_3 concentrations were estimated using the manufacturer's algorithms. Surface water was sampled manually every three days during pre-treatment and during treatment, and every day during the reflow phase. Temperature and dissolved oxygen concentration were measured at every manual sampling at the inflow and the outflow with a FiresStingO2 optical oxygen meter (Pyro Science GmbH, Germany). Manual measurements of dissolved oxygen agreed well with automated measurements (r^2 = 0.94; slope= 0.99, y-intercept = 0.27; data not shown). Discharge was measured volumetrically at the inflow and at the outflow. Salt slug injections were used to measure flow velocity during treatment. Samples, collected with three replicates at the inflow and one at each outflow for DOC and optical properties were stored in borosilicate vials, which were prepared by soaking in 0.1 N HCl, rinsing with MilliQ water and combusting at 450ºC for 4 hours. Inorganic nutrient samples were collected into sterile conical base centrifuge tubes. All manual samples were filtered with 0.7 μm

Whatman GF/F filters directly in the field. Manual samples for dissolved gases (CO_2 and CH_4) were collected in clear glass serum bottles with unfiltered stream water without a headspace and closed with a gas-tight rubber septum.

7.2.3 Laboratory analyses

We analyzed for DOC, N-NO_3, N-NO_2, N-NH_4 and P-PO_4 concentrations and measured DOM fluorescence and absorbance. DOC concentration was measured on a TOC analyzer with an inorganic carbon removal unit (GE-Sievers 900). DOM absorbance spectra over 200 to 700 nm wavelength were obtained from an UV-Vis spectrophotometer (ShimadzuUV 17000), using 5-cm cuvettes and MilliQ water as a blank. Fluorescence intensities were measured on a Hitachi F-7000 spectrofluorometer with 1-cm quartz cuvettes at excitation wavelengths ranging from 240 to 450 nm and emission wavelengths from 250 to 550 nm. N-NO_3, N-NO_2, N-NH_4 and P-PO_4 concentrations were measured on a continuous flow nutrient analyzer (Alliance Instruments). Dissolved gas (CO_2 and CH_4) partial pressure of manual gas samples was measured in a manually generated headspace on a Cavity RingDown Spectrometer (CRDS) G2310 (Picarro cooperation, CA, USA).

7.2.4 DOM spectroscopic data treatment

DOM quality was investigated using its specific fluorescence and absorbance characteristics as described in the following. Excitation-emission-matrices were subtracted by MilliQ water blanks to remove Raman scattering (Goletz et al. 2011) and were corrected for the inner filter effect using corresponding absorbance spectra (Lakowicz 2006). Raw fluorescence data was converted into Raman units by dividing by the area of the Raman peak of a MilliQ sample measured on the same day of analysis. All fluorescence measurements were corrected for wavelength-dependent lamp inefficiencies using manufacturer's built-in functions. From absorbance and fluorescence measurements the following parameters were determined: $SUVA_{254}$, S_R, FI, BIX and HIX. Parallel factor analysis (PARAFAC) components were calculated with the MATLAB toolbox drEEM by Murphy et al. (2013). A 4-component model was validated using split-half analysis with four random split combinations (Murphy et al. 2013). PARAFAC components are expressed as relative fluorescence intensities (ΣCi) using, $\%Ci = Ci \setminus \Sigma Ci \times 100\%$ (Table 7.2).

Table 7.2: Description of PARAFAC components modelled from the data set. The model included surface and streambed samples.

Parallel factor analysis	PARAFAC	Excitation/ Emission	Peak	Description	Literature
Component 1	C1	<240, (350)/ 476	Peak C	ubiquitously humic-substances, associated with predominately terrestrial sources	Coble (1996); Yamashita et al. (2010)
Component 2	C2	300/ 396	Peak M	Low molecular weight, biological activity	Lapierre and Del Giorgio (2014); Cory and Mcknight (2005)
Component 3	C3	275/ 342	Peak T	Amino acids, free or bound in proteins, may indicate intact proteins	Cory and Mcknight (2005); Yamashita et al. (2010); Lapierre and Del Giorgio (2014)
Component 4	C4	<240, (275)/ 314	Peak B	Tyrosine-like fluorophore, Amino acids, free or bound in proteins	Yamashita et al. (2011)

7.2.5 Statistical analyses

To focus on the net changes in water chemistry occurring within each flume, rather than on the variability in the incoming water, data are reported relative to the inflow as

$$\eta X = \frac{X_f - X_{in}}{X_{in}} \times 100 \qquad [\%]$$

Eq. 4

where ηX is the percentage of change of the parameter at the outlet of the flume X_f compared to the mean value of three replicates of the inflow X_{in}.

The effects of hydrology (discharge, 6-level factor) on ηX were tested using non-parametric Kruskal-Wallis tests, followed by Tukey-Kramer post-hoc analysis when significant differences were found (all data in tables SI10 and SI11). Specifically, we compared discharge levels from F1 to F5 during treatment with the control discharge (2.65 L s^{-1}) that covered data from F6 during the whole experimental period and from F1 to F5 during pre-treatment and reflow. The flumes were subject to the prevailing light conditions. Therefore we performed Kruskal-Wallis tests, followed by Tukey-Kramer post-hoc analysis with the daily sum of light intensity as the response variable and flume as the main effect. F1 showed a higher light intensity, while all the other flumes were not significantly different (p>0.1). This was the same for all three experimental phases (pre-treatment, treatment and reflow). Hence, we assume that any trends seen during treatment, but not during pre-treatment or reflow are a sole result of differences in discharge and that difference in light availability between the flumes had a negligible impact on the variability in ηX. Linear trends of variables over time and with discharge were tested with non-parametric Mann-Kendall test using MATLAB with the curve fitting toolbox (MATLAB 2016). Variables which were found to be affected by the drought treatment with the Kruskal-Wallis test (p<0.01), were also tested with a two-way ANOVA on the influence of two independent variables (discharge and days of treatment) and the interaction of these two. Normality of residuals was evaluated with the Shapiro-Wilk test (significance level α = 0.01) and with histograms. Data not fulfilling normality were power transformed with the most suitable exponent to meet the assumptions (Helsel and Hirsch 2002; post-transformation histograms see Figure SI 6). Whereas no transformation was required for ηDOC (Shapiro-Wilk test p=0.77), ηNO3 (post-transformation p = 0.07) was transformed to the power of 2, ηC3 (post-transformation p = 0.07) and ηSUVA254 (post-transformation p=0.02) to the power of -2. This analysis was performed with the R-package car (R Team Development Core 2008).

7.2.6 Estimation of net ecosystem production

NEP was estimated from continuous diel dissolved oxygen measurements (Odum 1956). Estimates were based on 5-min interval by taking the change in dissolved oxygen from the inflow (represented by dissolved oxygen measurements at the inflow of F6) and the outlet of each flume. Reaeration coefficient k was calculated with Bayesian models, using the R toolbox 'streamMetabolizer' (Appling et al. 2017) and in addition with the nighttime regression method by taking the slope between the rate of change and the deficit of dissolved oxygen during each night. Both methods gave k-values in the same range (Table 2.3). For simplicity, we decided to only use the robust k's of the Bayesian models with the best fit.

We used the two-station-method to account for the short reach length of the flumes. According to Reichert et al. (2009) the minimal reach length depends on flow velocity and the reaeration coefficient. This criterion was not fulfilled for flumes F5 and F6. Hence, NEP was only calculated for flumes F1 to F4 during treatment. The change of dissolved oxygen ($DO_{outflow}$ - DO_{inflow}) was divided by the travel time (tt_f) of each flume and subtracting the temperature corrected reaeration coefficient (k_t) multiplied with the oxygen deficit (D) (Odum 1956; Bernot et al. 2010)

$$DO_{net} = \frac{DO_{outflow} - DO_{inflow}}{tt_f} - k_t \times D \qquad [\text{mg } O_2\ L^{-1}\ \text{min}^{-1}]$$

Eq. 5

From this corrected oxygen net rate (DO_{net}) the mean values of each night were taken and temperature-corrected with the following formula after Demars et al. (2016), centering the values around the overall average temperature T_{all} of 10.26ºC, representing the ER at every minute.

$$ER = mean(DO_{net,night}) \times exp[E \times (\frac{1}{Bk \times T_{all}} - \frac{1}{Bk \times T_{mean}})] \qquad [\text{mg } O_2\ L^{-1}\ \text{min}^{-1}]$$

Eq. 6

where E is the apparent activation energy (0.57 eV) for respiration taken from Yvon-Durocher et al. (2012) for rivers and Bk is the Boltzmann constant (8.62 x 10^{-5} eV K^{-1}). The GPP_{daily} was then calculated by adding the absolute values of ER to the corrected net rate and integrating the resulting values over time in order to obtain mg O_2 L^{-1} d^{-1}.

7.2.7 Estimation of DOC mass balance

To illustrate carbon fluxes at different discharge levels, we estimated carbon mass balances for 24 hours at the end of the treatment (17th day). This day was chosen because of the availability of sensor and laboratory measurements and stable light conditions during that day. DOC generated from the flumes (ηDOC_{gen}) was calculated with DOC estimates from absorbance spectra as:

$$\eta DOC_{gen} = Q_f \times \int_{t2}^{t1} (DOC_f - DOC_{in})dt \qquad [\text{mg C d}^{-1}]$$

Eq. 7

where t_1 is the time before sunrise and t_2 the same time on the next day; DOC_f the DOC concentration at the outflow of each flume and DOC_{in} the mean DOC concentration at the inflow measured by the UV-Vis probe (DOC_{in_r1} and DOC_{in_r2}). As some inaccuracies in optical measurements can occur (e.g. by particles blocking the optical path), data treatment included the removal of out-of-range values, whereby only (DOC_f – DOC_{in}) values which were higher than max|DOC_{in_r1} - DOC_{in_r2}| were included in equation 7. Further, DOC mass exports since the beginning of the treatment until the day of the DOC balance were quantified as the following: First, ηDOC was interpolated for every day. Second, ηDOC_{gen} was calculated by multiplying ηDOC with a correction factor accounting for reduced DOC release during nighttime. This correction factor (0.833 and 0.64 for F1 and F2, respectively) was estimated as the ratio of manually measured ηDOC_{gen} calculated from daytime DOC concentrations and ηDOC_{gen} from continuous measurements (UV-Vis probe) for the entire day as presented in equation 7. Third, DOC mass exports [g] were then calculated by summing up daily ηDOC_{gen}.

NEP estimations were converted into carbon concentrations by multiplying them with the molar ratio of CO_2 and with the photosynthetic quotient PQ of 1/1.2 for GPP and the respiration coefficient RQ of 1/0.85 for ER (Dodds et al. 1996). The concentration was converted into mass by multiplying them with the water volume (WV) of each flume as

$$GPP_{daily} = \frac{12}{32} \times PQ \times WV \; x \; GPP_{daily} \qquad [\text{mg C d}^{-1}]$$

Eq. 8

and

$$ER_{daily} = \frac{12}{32} \times RQ \times WV \times ER_{daily} \qquad [\text{mg C d}^{-1}]$$

Eq. 9

Finally, for the mass balance MB_{daily} we assumed that GPP_{daily} would be equal to the amount of carbon respired (ER_{daily}) and exported (ηDOC_{gen}).

$$MB_{daily} = GPP_{daily} - (ER_{daily} + \eta DOC_{gen}) \qquad [\text{mg C d}^{-1}]$$

Eq. 10

If the MB_{daily} was negative, we assumed that DOC was supplied by autotrophs or by leaf litter in the sediment.

7.3 Results

7.3.1 Drought effect on nutrient concentrations and DOM composition

Drought impacted DOM and nutrient composition (Figure 7.2). Low discharge levels (0.03 L s^{-1} in F1 (n = 5) and 0.1 L s^{-1} in F2 (n = 5) during treatment) resulted in significantly higher ηDOC (χ^2 = 41.1, df = 5, p < 0.01), lower ηNO_3 (χ^2 = 36.9, df = 5, p < 0.01) and lower $\eta SUVA_{254}$ (χ^2 = 29.7, df = 5, p<0.01) compared to the control discharge during the whole experimental period (2.65 L s^{-1}, n = 53). Additionally, PARAFAC component ηC3 in F1 (χ^2 = 17.7, df = 5, p<0.01) and ηDOC in F3 (Q = 0.35 L s^{-1}, n = 5) during treatment were significantly higher compared to the control discharge. Overall, the variation of ηDOC with the six discharge levels could be best described by an exponential function, where average ηDOC(%) = $41 * e^{-5.6 * Q}$ (linear model with log(Q): r2 = 0.90, p<0.01, n = 6; Figure SI 5). Water residence time showed a positive, linear relationship with average ηDOC (r^2 = 0.98, p <0.01, n = 6), as well as ηwater temperature with all ηDOC values during the whole treatment phase (r^2 = 0.75, p<0.01, n = 30). By contrast, ηSR, ηHIX, ηBIX and ηFI and the PARAFAC components ηC1, ηC2 and ηC4 did not show significant differences between discharge levels.

Moreover, we found that ηDOC was also significantly related to the interaction between discharge level and treatment duration (two-way ANOVA, $F_{(5,8)}$ = 56.2, p < 0.01). Over time, flumes with the lowest discharge (F1 and F2) showed a continuous increase in ηDOC (Figure 7.2a), reaching values of almost 50 % in F1 ([DOC] = 1513 μg L^{-1}, compared to the inflow [DOC] = 1034 μg L^{-1}) by the end of the treatment. In F1 and F2, variation over time followed a significant linear trend (Mann-Kendall test, both p = 0.02) where the increase in F1 had a steeper slope (slope = 1.5) than in F2 (slope = 1.2). ηNO_3 was also related to the interaction between discharge and treatment duration ($F_{(5,18)}$ = 7.2, p < 0.01). ηNO_3 declined by 25% in the beginning of the treatment in F1, but gradually returned to pre-treatment levels (Figure 7.2d). The interaction effect of treatment duration and discharge was not significant for DOM indices ηC3 ($F_{(5,18)}$ = 0.2, p = 0.9) and $\eta SUVA_{254}$ ($F_{(5,18)}$ = 0.6, p = 0.7), indicating that the quality of the released DOC did not follow an overarching temporal change. During treatment, protein-like ηC3 was on average (±SD) +160 (± 98)% and +135 (± 105)% in F1 and F2, respectively. In contrast, $SUVA_{254}$ was -12 ± 3% and -8 ± 4% in these flumes.

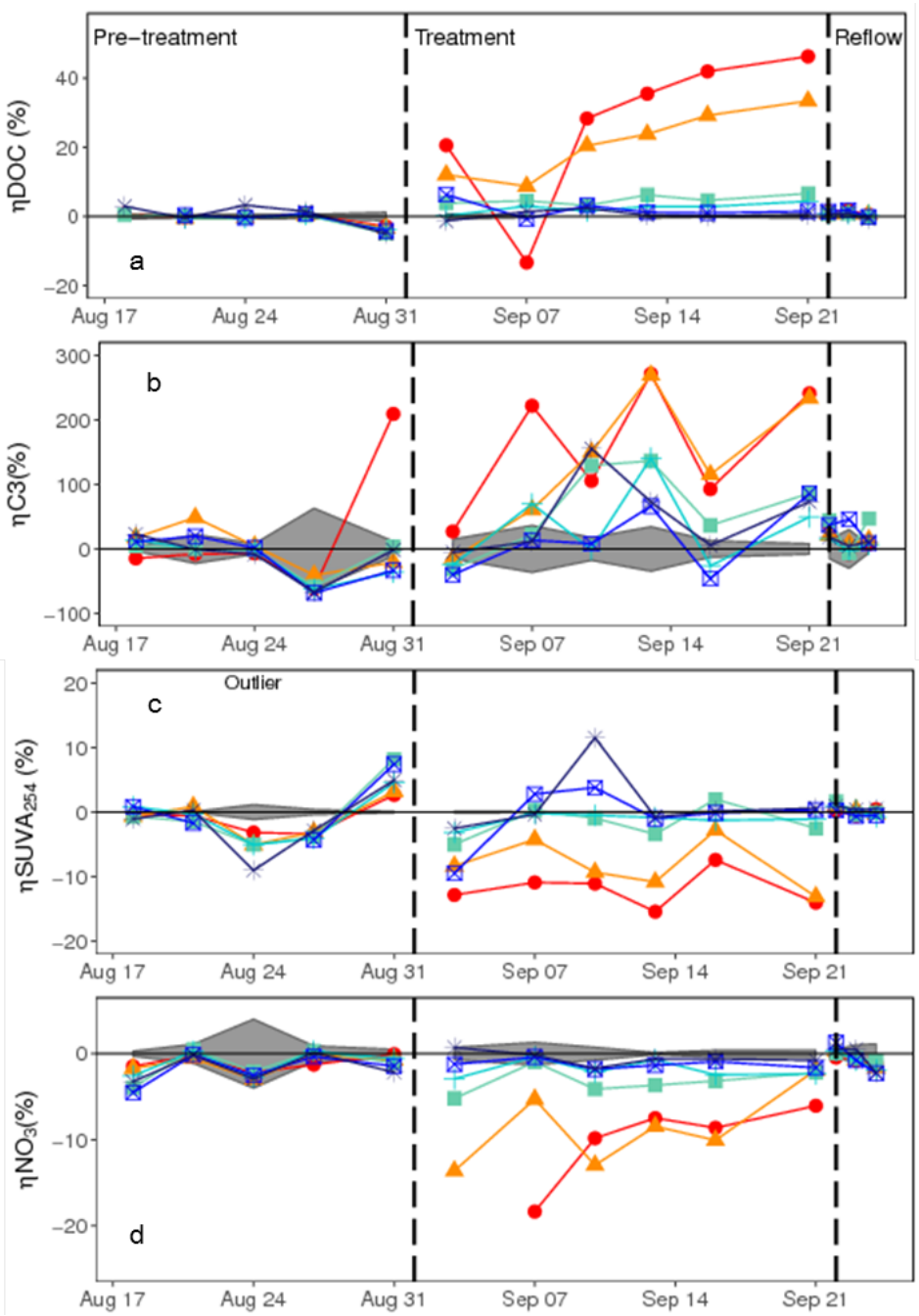

Figure 7.2: η values for a) DOC concentration, b) $SUVA_{254}$, c) C3 (peak T, labile) and d) N-NO_3 concentrations in the flumes F1 (red circle), F2 (orange triangle), F3-F6 (light to dark blue squares and crosses) relative to the inflow (the SD replicates of the inflow as grey area) over the whole experimental period. Dashed lines indicate the start and the end of the treatment.

Table 7.3: Concentrations of DOC and nutrients and DOM optical properties during the treatments (means ± standard deviation). Bold letters indicate that the main effect of discharge (Q) was significant in the Kruskal-Wallis test. Daggers indicate the results of the post-hoc analysis. Asterisks indicate if the interaction of Q and treatment duration was significant in the 2-way ANOVA.

	F1	F2	F3	F4	F5	F6	Inflow
Q ($L\ s^{-1}$)	0.03	0.10	0.35	0.73	1.45	2.65	
DOC ($\mu g\ L^{-1}$)*	**1517† ± 196**	**1488† ± 331**	**1299† ± 359**	**1272 ± 359**	**1261 ± 328**	**1249 ± 358**	**1240 ± 346**
$N\text{-}NO_3$ ($\mu g\ L^{-1}$)*	**892† ± 96**	**930† ± 53**	**986 ± 40**	**1000 ± 37**	**1006 ± 34**	**1013 ± 29**	**1019 ± 37**
$N\text{-}NH_4$ ($\mu g\ L^{-1}$)	10 ± 5	11 ± 5	10 ± 13	11 ± 10	7 ± 8	7 ± 7	6 ± 3
$P\text{-}PO_4$ ($\mu g\ L^{-1}$)	0.1 ± 0.0	0.1 ± 0.0	0.2 ± 0.3	0.2 ± 0.2	0.2 ± 0.2	0.1 ± 0.1	0.3 ± 0.4
C1 (%)	51.7 ± 2.5	52.5 ± 3.3	54.2 ± 2.2	54.3 ± 2.3	54.4 ± 2.9	54.5 ± 2.1	53.9 ± 2.4
C2 (%)	37.0 ± 1.6	37.5 ± 1.6	38.6 ± 1.0	39.2 ± 0.7	39.5 ± 0.7	39.1 ± 0.7	39.4 ± 0.8
C3 (%)	**5.4† ± 1.8**	**4.7 ± 1.3**	**3.3 ± 0.8**	**2.7 ± 0.9**	**2.3 ± 0.7**	**3.2 ± 1.0**	**2.3 ± 0.9**
C4 (%)	5.9 ± 3.6	5.3 ± 3.7	3.9 ± 2.5	3.8 ± 2.6	3.9 ± 2.9	3.2 ± 1.8	4.4 ± 2.1
$SUVA_{254}$ ($L\ mg\text{-}C^{-1}\ m^{-1}$)	**2.48† ± 0.17**	**2.59† ± 0.20**	**2.78 ± 0.19**	**2.79 ± 0.17**	**2.81 ± 0.26**	**2.86 ± 0.23**	**2.82 ± 0.14**
S_R	**0.92 ± 0.04**	**0.90 ± 0.04**	**0.86 ± 0.04**	**0.84 ± 0.03**	**0.85 ± 0.02**	**0.86 ± 0.05**	**0.83 ± 0.04**
HIX	0.86 ± 0.03	0.87 ± 0.03	0.90 ± 0.03	0.91 ± 0.02	0.91 ± 0.02	0.90 ± 0.02	0.90 ± 0.02
BIX	0.68 ± 0.02	0.69 ± 0.02	0.68 ± 0.02	0.69 ± 0.02	0.68 ± 0.03	0.70 ± 0.03	0.69 ± 0.02
FI	1.75 ± 0.06	1.71 ± 0.03	1.73 ± 0.05	1.69 ± 0.02	1.74 ± 0.07	1.68 ± 0.07	1.71 ± 0.04

7.3.2 Drought effect on water temperature

During pre-treatment and reflow, ηwater temperature was less than ±10%. Discharge reduction increased water residence time, resulting in a high positive ηwater temperature and diurnal variability (maximum daily range of water temperature between 9 ºC and 18 ºC in F1 compared to 8 ºC and 11 ºC in F6). During the treatment phase, the flumes with the lowest discharge (F1 and F2) had a significantly higher ηwater temperature (χ^2 = 24.1, df = 5, p < 0.01) than the control discharge over the whole experimental period. The highest ηwater temperature observed in F1 was +77% (equals to approx. 20 ºC).

7.3.3 Gas concentrations and metabolic balance

Flume gas concentrations of O_2 and pCO_2 showed strong variation over time and with treatment. During pre-treatment, ηpCO_2 decreased continuously to ηpCO_2 -50%, whereas ηO_2 remained near zero (Figure 7.3). During treatment, ηpCO_2 increased in all flumes with a more pronounced increase in F1, F2 and F5 and reached values of up to 120% in F1 at the end of the treatment. With the beginning of reflow ηpCO_2 immediately dropped to 0 % in all flumes which coincided with a rapid reduction in water temperature from 10 ºC to 7.5 ºC (Figure 7.3c). The temporal dynamics of ηO_2 consisted of a strong increase in the beginning of the treatment phase in F1 and F2 and a decrease over time (Figure 7.3b). Dissolved Oxygen went up in F1 (ηO_2 = 35%) immediately after the beginning of the treatment phase and in F2 by 40% by the end of the first week. After that, ηO_2 declined to negative ηO_2 values in both flumes after three weeks of treatment.

The dynamics of the dissolved gases were reflected in the dynamics of the production-respiration-ratio (P/R ratio, Figure 7.3d). In F1 and F2, the P/R ratio reached values above 2 in the first week of treatment but declined to values below 1 during the third week. By contrast, the P/R ratio in F3 and F4 remained close to 1 (0.9 ± 0.4 and 1.1 ± 0.4, respectively), indicating that no process (production or respiration) was dominating. In F1, GPP showed a significant negative linear trend with treatment duration (Mann-Kendall test, p<0.001). However, ER did not follow this trend, indicating a decoupling of GPP and ER during treatment.

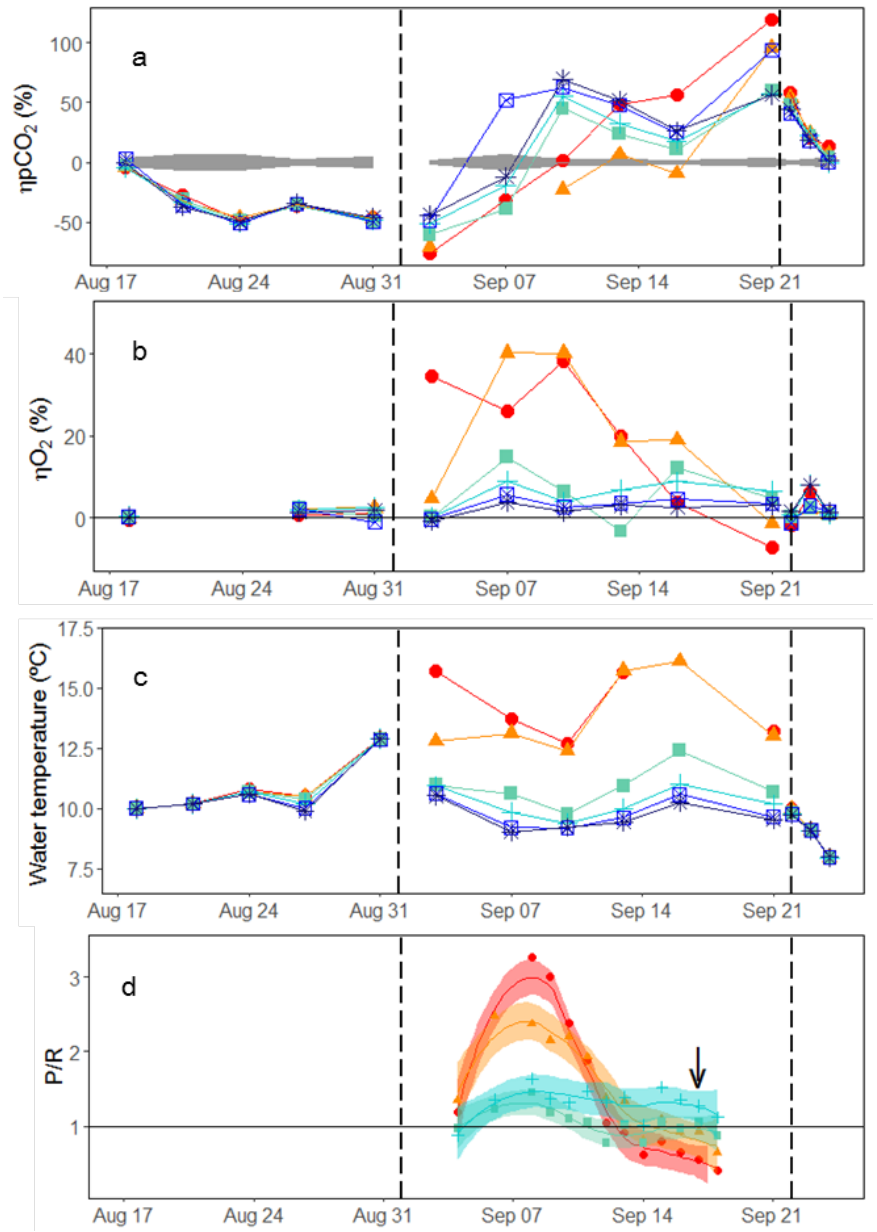

Figure 7.3: a) shows the *ηp*CO_2 relative to the mean of the inflow (the SD of all six inflows as grey shaded area). b) O_2 measured at the outflow of each flume compared to inflow as *η* values for F1 (red circles), F2 (orange triangles), and F3 - F6 (light to dark blue squares and crosses) over the whole experiment period. c) Water temperature (ºC) at the outflow of flumes (same scheme as in a and b) and inflow (black line). d) Daily P/R values for flumes F1 (red circles), F2 (orange triangles), F3 (green squares) and F4 (cyan crosses) during the treatment period. Arrow indicates the day of the mass balance. Dashed lines indicate the start and the end of the treatment.

7.3.4 DOC mass balance

The reduction of discharge had a pronounced effect on sources and sinks of carbon, as exemplified by DOC mass balances integrating carbon fluxes of 24 h at the end of the experiment. Hourly UV-Vis sensor data revealed that ηDOC and ηNO_3 in F1 and F2 followed clear diel cycles during treatment, which disappeared immediately with reflow (Figure 7.4). The ηDOC estimated from the absorbance spectra peaked during daytime at +48% in F1 (8 pm) and at +34% in F2 (5 pm). At nighttime, ηDOC decreased to 10% in F1 and to 5% in F2. In terms of production rate per day (ηDOC_{gen}), we estimated a ηDOC_{gen} of approximately 1.0 g C d^{-1} from F1 and 1.8 g C d^{-1} from F2. When we calculated ηDOC_{gen} for the same day by extrapolating the lab measurement of one grab sample taken during daytime, ηDOC_{gen} from F1 (1.2 g C d^{-1}) and F2 (2.8 g C d^{-1}) were notably higher. This demonstrates that omitting diel cycles alters estimations of daily DOC exports.

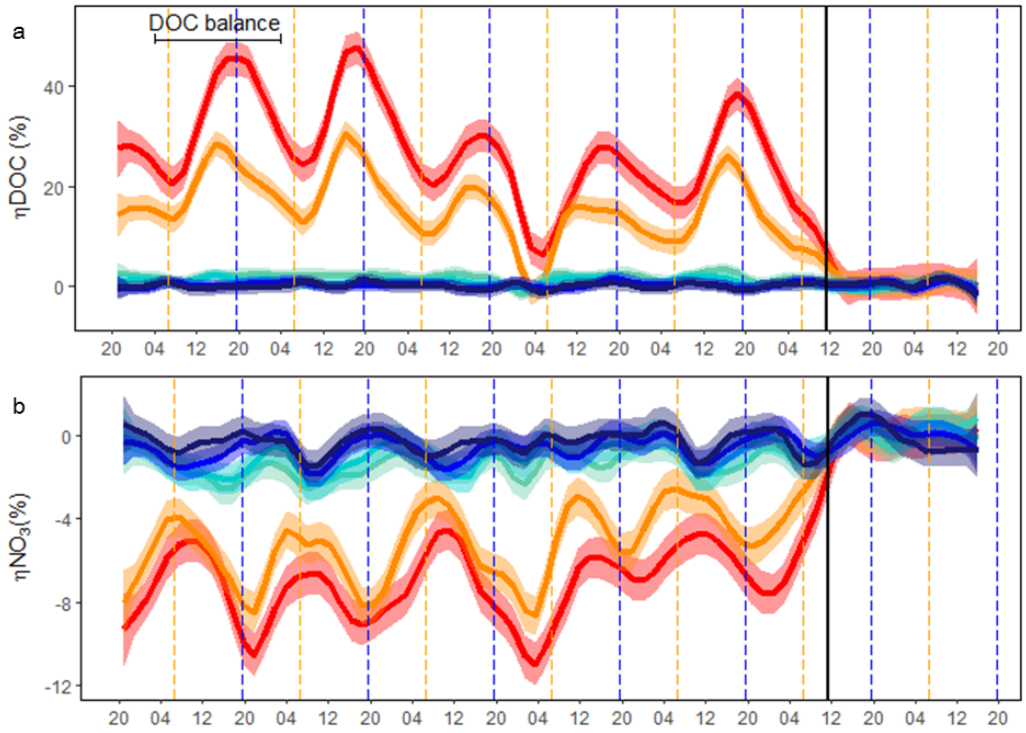

Figure 7.4: Diel cycles of a) ηDOC with the time of the DOC balance indicated on the top and b) ηNO3 in the flumes F1 (red), F2 (orange), F3-F6 (light to dark blue). Both are calculated from hourly measurements of the UV-Vis sensor installed for the last 5 days of the treatment phase (16th to 21st of September). The start of the reflow phase is indicated by the black, solid line. The dashed lines indicate sunrise (yellow) and sunset (purple). The x-axis indicates the hour of the day.

F1 never reached positive NEP on the day of the DOC mass balance but released relatively more DOC coming from either autotrophic production or previously stored DOC than F2 (Table SI 10). In F1, 35% more DOC than inflowing was exported (Figure 7.5a), while this export was only 21% in F2 (Figure 7.5b). Moreover, we found that there was almost three times as much carbon respired (5.8 g C d^{-1}) than incorporated by photosynthesis in F1 (2.1 g C d^{-1}). In general, GPP and ER were important fluxes in the carbon budget of F1 and F2, while in flumes with higher discharge these fluxes were relatively lower. For example in F1, GPP and ER represented 72% and 200% of the DOC mass entering the flume, whereas in F4 these fluxes only represented 13% and 15%, respectively (Figure 7.5c).

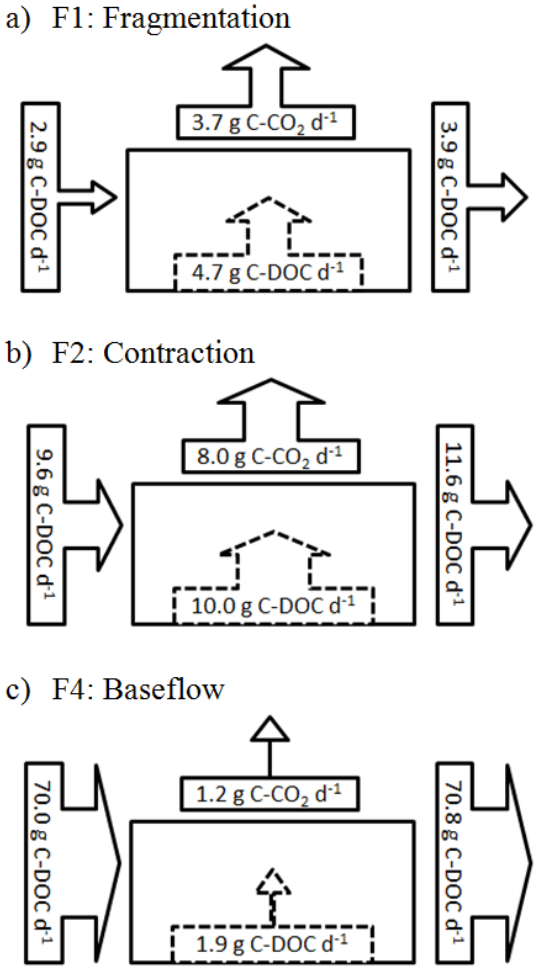

Figure 7.5: Mass balances for F1 (a), F2 (b) and F4 (c) on the 17th day of treatment, where numbers represent daily carbon flux in g. Horizontal arrows represent in- and outflow, solid vertical arrow NEP and dashed vertical arrow missing carbon, originating from the flume.

Since daily NEP was negative in F1 on the day of the DOC mass balance, the export and respiration of carbon was supported by DOM from a surplus of GPP stored since the onset of drought or from microbial processing and leaf litter. We estimated a surplus of biomass originating from NEP of 1.9 g in F1 and 5.6 g in F2 that could maintain excess ηDOC_{gen} and ER. However, a rough estimation of ηDOC_{gen} since the beginning of the treatment suggested that 7.5 g and 15.2 g were already exported during the same time period from F1 and F2, respectively. This estimation demonstrates that export and respiration of DOC relied on leaf litter as a carbon source and that the microbial utilization of this source was likely higher in the flumes with low discharge than in the others.

7.4 Discussion

Our experiment demonstrated an increase of DOC concentration with discharge reduction that originated from autochthonous sources (high C3 and low $SUVA_{254}$) with assumingly high availability for heterotrophic metabolism. The change in DOM bioavailability during drought was paralleled by an initial phase of increased GPP that was superimposed with high ER. The latter persisted until the end of the experiment, despite a decline in GPP. These findings show that summer droughts in subalpine streams might enhance in-stream carbon processing and that longer drought periods can facilitate the decomposition of organic matter stored in stream sediments.

7.4.1 Potential drivers of labile DOM increase during low flow

We found net DOC releases (ηDOC_{gen}) of up to 65 and 113 mg C m^{-2} d^{-1} for F1 and F2, respectively. These values are in the same range as the net DOC export from GPP reported from a desert stream (70 - 209 mg C m^{-2} d^{-1}; Jones et al. 1996). Similarly, DOC mass balances from a Mediterranean river have revealed pulses of net DOC release of up to 800 mg C m^{-2} d^{-1} during a low-flow period (Butturini et al. 2016). Nutrient-rich, urban streams were even found to exceed these values with DOC releases of up to 1344 mg C m^{-2} d^{-1} (Sivirichi et al. 2011). In our experiment, ηDOC had a positive, linear relationship with water residence time and water temperature, suggesting that these two factors were the main drivers of DOM release and composition change.

GPP has been found to be affected by water residence time and water temperature. For example, rivers with high flow velocities and resulting bottom shear stress sustain GPP by benthic algae, whereas in large and slow flowing rivers plankton and long filamentous algae dominate (Larned et al. 2004; Hall et al. 2015). We do not have

explicit information on the autotrophic community structure in our experiment but observed floating, filamentous algae only in F1 and F2. Similarly, Müllner and Schagerl (2003) reported from the 'Oberer Seebach' that pioneer-algae communities of *Synurophyceae* and *Bacillariophyceae* dominated at riffle sections and during high flow conditions. Under intermediate and stable flow conditions, growth of filamentous *Chlorophyta* and *Cyanoprokaryota* was common. Algae community and the velocity of algal colonization can also change with water temperature (Villanueva et al. 2011), whereby higher water temperature increases GPP when light is not a limiting factor (Murphy 1998). We assume that light was not limiting in our setting because measured light availability was higher than the light saturation threshold of 90 μE m^{-2} s^{-1} suggested by Acuña et al. (2004) during most days. This assumption is further corroborated by the GPP curves showing a steep increase with sunrise followed by the formation of a plateau in the morning, while light availability further increased.

Diurnal increases of DOC similar to this study are known from desert streams, with high DOC releases from algal production (Jones et al. 1996). Kaplan and Bott (1982) reported daily increases of DOM by 40 % in a piedmont stream, which is similar to the increase observed in F1. They showed in microcosm experiments using carbon isotopes that this gained DOM was composed of exudates of benthic algae modified by heterotrophic bacteria. Furthermore, Fasching et al. (2016) observed DOC concentrations to peak before sunset in the 'Oberer Seebach' during summer baseflow. This daily increase was found to vary as a function of light availability, water temperature and time span since the last storm event. In this study, we identified similar environmental controls of daily DOC variation under controlled experimental conditions. Specifically, our observed increases of daily DOC release with treatment time highlights the influence of time span since last hydrological disturbance.

Higher temperatures enhance microbial activity, as for example the enzymes that catalyze the oxidation of phenolic compounds to quinines, thereby increasing the transformation rate from particulate organic matter to DOM (Freeman et al. 2001; Kane et al. 2014). This mechanism was reported from experiments using particulate organic matter from peatlands, where an increase of 10 °C in water temperature resulted in an increase of 33% of DOC concentration (Freeman et al. 2001). The results are similar to our observations of a 40% increase in DOC concentration with a temperature difference between inflow and outflow of up to 8 ºC. DOM quality was also observed to change as a function of temperature, in the form of a decrease in $SUVA_{254}$ and aromaticity (Kane et al. 2014) due to enhanced microbial activity (Kim et al. 2006). Therefore, the low $SUVA_{254}$ detected in F1 and F2 might be related to microbial activity favored by increased stream temperature.

Diel cycles of ηDOC that were mirror-inverted with ηNO_3 and the inverse trend of ηNO_3 and GPP over the whole drought period suggests that NO_3 concentration was controlled by the uptake by autotrophs. At high GPP, up to 25 % of the available NO_3 was taken up, suggesting that at some point during the day the primary production was nutrient limited. We suspect that this limitation was caused by the lack of inorganic P, because of the high nitrogen to phosphorus ratio (> 100:1) and the fact that P-PO_4 concentrations were continuously below the detection limit in F1. Nutrient limitation is often present when inorganic nutrients are not supplied from the surrounding soils or groundwater (Roberts et al. 2007). Further, high light to nutrient ratios have been found to stimulate the release of algal carbon exudates as DOM because nutrient uptake is unable to keep pace with carbon fixation (Sterner et al. 1997; Lyon and Ziegler 2009). This supports our idea that algal exudates substantially contributed to increased DOC fluxes.

As a secondary pathway, the availability of algal exudates might have favored the degradation of complex organic matter. This effect known as 'priming' is a process, where inputs of bioavailable organic matter (e.g. algal exudates) can increase the rate at which microbes consume more stable organic matter (e.g. particulate organic matter) (Guenet et al. 2014; Hotchkiss et al. 2014). While the process is well documented for soil microbial communities (Wolfaardt et al. 1994), the existence of the priming effect in stream ecosystems is currently questioned (Bengtsson et al. 2015; Wagner et al. 2017). However, the steady gain of labile DOM parallel to the increase of CO_2 and ER in this study, lead us to suggest a potential contribution of at least 'apparent priming' (Catalán et al. 2015) and thereby enhanced degradation of sediment leaf litter during drought.

7.4.2 Shift in metabolic balance

Streams are generally assumed to be net heterotrophic (Hoellein et al. 2013), but exceptions are reported, mainly from desert and Mediterranean streams (Busch and Fisher 1981; Velasco et al. 2003). The DOC mass balance indicated that F1 and F2 had a higher contribution of GPP to their carbon budget than the other flumes even after the P/R ratio of F1 and F2 remained below 1. The phase of net autotrophy in F1 and F2 enabled to store and export carbon that was generated within the flumes. However, the excess DOC stored during the first week of the experiment was rapidly respired or exported from the flumes during the third week. The quantity of ER and ηDOC_{gen} even suggests that more of the sediment leaf litter had to be degraded in F1 and F2 than in the other flumes.

The increase of ER and the decrease of GPP indicate a decoupling of these two metabolic rates. GPP can decline or even collapse due to light or nutrient limitation. Light limitation in streams is not only caused by riparian vegetation but also by organic matter accumulation (e.g. dead algal mats) in the stream that can lower the performance of the underlying autotrophs (Acuña et al. 2004). Sabater et al. (2008) report that algal biomass increased until spring in an intermittent stream and reduced with summer drying. In this stream, floods washed away the overlying materials and algae could grow again readily, when light availability to the bed surface was restored. Apart from that, bacterial growth and the availability of DOM was observed to lead to higher ratios of bacterial biomass to algal biomass in lakes when light to nutrient ratios rose (Elser et al. 2003). However, this shift was not confirmed in a flume experiment that simulated streams with a flow velocity of 10 cm s^{-1} (Hill et al. 2011). Taking into account that this flow velocity is ten times higher than the velocity present in F2 during treatment, we suggest that the metabolism of flumes with high water residence time might include mechanisms more commonly found in lakes than in lotic systems.

Coupling between ER and biofilm growth has been reported in experimental flumes (Singer et al. 2010; Haggerty et al. 2014), which may explain the rise of ER and $\eta pCO2$ over time in all flumes. In our study the consistent increase in ER and ηDOC in F1 and F2 may be explained by increased primary production and release of labile DOM leading to high ηpCO_2. However, ER (and resulting pCO_2) remained high even after primary production declined. Following this observation, we propose that high ER is fueled by the added allochtonous particulate organic matter in the sediment, rather than DOM from primary production.

Microbial respiration of newly moistured leave litter is described to peak after 20 days (Suberkropp 1998). This timeframe would approximately coincide with the time period of the shift in metabolic balance in F1 and F2 that took place three weeks after the start of the water flow in the flumes. Additionally, the second and third week were characterized by warmer streamwater temperatures than the first week. Temperature affects ER more than GPP because of the higher apparent activation energy for ER (Sand-Jensen et al. 2007; Acuña et al. 2008; Yvon-Durocher et al. 2012). Consequently, Skoulikidis et al. (2017) identified a threshold temperature of 22ºC for respiration dominating over production. Certainly, the highest water temperature observed in this study was lower (~20º C). However, such a threshold could well be reduced for microbial communities of subalpine streams that are adapted to a different temperature regime.

Finally, in carbonate rich karst streams, high rates of photosynthesis can cause CO_2 contributions from carbonate precipitation (de Montety et al. 2011). We cannot discriminate such a contribution to stream pCO_2 from those of ER in our study.

However, given that neither calcite nor aragonite precipitation was observed at the sediment surface or on in situ sensors, we assume this contribution to be minor in our experiment.

Overall, we suggest that a superposition of the drivers (biofilm growth and subsequent labile organic matter availability, leaf litter decomposition, temperature increase with associated modification of the balance of ER and GPP) caused the increase of ER and thereby the shift in the metabolic balance of F1 and F2.

7.4.3 From a flume experiment to stream ecosystem functioning

Mimicking the drying phase of an intermittent stream with flumes poses challenges, at the same time as it provides the opportunity to study the effects of hydrological variability beyond the range naturally present in the past. Our selected range of discharge covered the stages of baseflow (F4 to F6) and drying, namely contraction (F2 and F3) and fragmentation (F1), while complete desiccation was not recreated. Natural drying of intermittent streams includes receding of wetted perimeters and the gradual weakening of connectivity between laterals and the main channel (Mcdonough et al. 2011). We argue that a summer drought period, when reaches only receive water from upstream sections, can be well represented within a flume experiment. By contrast, we did not recreate the gradual decrease of lateral and groundwater inputs in the experiment. Likewise, our experimental design mimicked streams with a shallow permeable streambed constrained by concrete, bedrock or clay soils and therefore neglects a larger hyporheic zone. Hyporheic respiration can contribute more than half of the total respiration of mountainous streams, depending on the vertical exchange (Uehlinger and Naegeli 1998; Fellows et al. 2001). Further, we acknowledge that this experiment simulated only low gradient stream reaches. Higher slopes could have decreased water residence time substantially and thus would have likely changed the exponent of the relationship of ηDOC with discharge. In fact, it shall be noted, that streams of this area often have steeper slopes than the ones present in the experiment, increasing their gas exchange velocity and flow velocity (Schelker et al. 2016). Another difference between our flumes and a natural stream may be the enhanced exposure of the flumes to air temperature, potentially causing an additional warming. However, high water temperature and enhanced daily amplitudes, especially in isolated pools, are found commonly in intermittent streams during drought conditions (Ward and Stanford 1982). Also, high amplitudes of water temperature have been reported from some alpine intermittent streams (Robinson et al. 2016). Nevertheless, all these aspects have to be taken into account when trying to transfer our findings to natural subalpine streams.

Our experimental results expand earlier work on carbon cycling during baseflow in the 'Oberer Seebach' (Fasching et al. 2016). In the light of climate change, our objective was to experimentally extend a baseflow situation of the 'Oberer Seebach' to a summer drought. We found our results in agreement with studies of Mediterranean and desert streams; this refers specifically to the increase in labile DOM and the shift to autotrophy. Contrary to our initial hypothesis, this trophic state did not persist throughout the treatment phase. In fact, a large portion of the accumulated biomass was respired and a smaller portion exported downstream. Putting our findings into the context of climate change, this would suggest that flow intermittency can lead to enhanced carbon fixation in the remaining surface water, but only for a limited period of time. Consequently, the gain of aquatic respiration with increasing temperature might not be countered by photosynthesis as suggested previously in the literature (Demars et al. 2016), if the streams are affected by drought. The fate and pathways of newly fixed carbon then depend on the one hand, on the light to nutrient ratio in a stream reach, a ratio that, together with water temperature might have caused the shift of the metabolic balance in this study. Low inorganic nutrient concentration in subalpine streams could limit GPP substantially even with otherwise favorable conditions for high GPP under climate change, meaning more carbon would be respired or exported downstream. After all, the time span until reflow, that is, the event when the organic material will be flushed downstream to fuel downstream reaches appears crucial. If this time span is long, a large proportion of the freshly produced biomass will likely be respired and might also enhance respiration of allochthonous organic matter stored in sediments.

General Discussion

Riejka Crnojevica (top)

Rio grey (bottom)

8 General Discussion

8.1 DOM source-sink dynamics during drought scenarios

Terrestrial DOM originates from catchment vegetation and organic soils, and its transport to the stream is principally regulated by the surface runoff and the subsurface water flow. The annual carbon input that rivers receive from terrestrial ecosystems is approximately 2.7 Pg, and more than 75% of this carbon input is actively transformed, stored and outgassed within the fluvial network (Borges et al. 2015). Generally, these terrestrial DOM fluxes have been considered to represent the main energy source for aquatic metabolism as they quantitatively dominate over in-stream produced DOM in low-order streams and deep, turbid rivers (Vannote et al. 1980). By contrast, the consequences of severe reduction of terrestrial DOM fluxes due to drought and the subsequent amplified role of in-stream processes contributing to the stream's carbon budget are not well understood (Brett et al. 2017). We approached this gap by the evaluation of two aspects that we found essential for understanding DOM processing in streams subjected to drought periods.

First, we considered the DOM release from in-stream processes related to the metabolic balance of the remaining surface water because high rates of primary production and DOM release from aquatic production have been found in semi-arid and arid streams (Webster and Meyer 1997; Pastor et al. 2017). In both study sites, Fuirosos and the experimental flumes in the Alps, we observed an increase in DOC concentration under low discharge conditions. This concentration increase was paralleled by an increase/decrease sequence of net ecosystem production. However, the quality of the DOM changed differently in Fuirosos compared to the experimental flumes as drought proceeded.

The hyporheic zone is the second aspect that we considered because its role is enlarged with the reduction of surface flow (Burrows et al. 2017). The hyporheic zone is generally reported to show high carbon processing rates (Sobczak and Findlay 2002), but there is little information on how these rates are affected by the drying of an intermittent stream. Since the hyporheic zone is commonly described as a DOC sink and CO_2 source (Naegeli and Uehlinger 1997; Baker et al. 1999), we would expect enhanced DOC retention when surface flow ceases (Acuña et al. 2015). Given that in this thesis, we focussed on the retention/release dynamics of DOM in the hyporheic zone of a stream reach in Fuirosos, we want to extend the general discussion by comparing these dynamics with observations from the pool-riffle sediment sequence that was installed in the flume experiment. The partly controversial results, high

retention in the hyporheic zone in Fuirosos and release from the flume sediments, will be discussed considering findings from the literature.

8.2 Discharge reduction and autochthonous DOC release

Understanding solute concentration-discharge relationships is a major goal in the research field of fluvial biogeochemistry, whereby the availability of large data sets has improved substantially the knowledge of solute concentration-discharge relationships in recent years (Godsey et al. 2009; Moatar et al. 2017; Abbott et al. 2018). For many solutes it has been shown advantageous to split the hydrograph at the median daily flow and to compute separate concentration-discharge slopes because that enables to account for nonlinearity, as well as for potential shifts from hydrological to biogeochemical drivers under different hydrological conditions (Meybeck and Moatar 2012). In fact, that applies to DOC-discharge relationships (Doyle et al. 2005; Andrews et al. 2011), whereby rivers can be either a net source to the atmosphere or downstream sections, or a sink of organic carbon that is stored in the fluvial sediment (Wohl et al. 2017). Therefore, achieving consistent predictions on DOC-discharge curves for a wide range of catchments is a complex task, but necessary to improve the understanding of the global carbon cycle (Stanley et al. 2012; Creed et al. 2015). For example, in-stream DOC retention and release with low water residence time (Casas-Ruiz et al. 2016) represent biogeochemical dynamics that are not detectable when hydrological transport dominates DOC-discharge slopes (Moatar et al. 2013). However, the heterogeneity of DOC-discharge relationships reported from Mediterranean catchments demonstrates the difficulties that are encountered in intermittent streams (Casas-Ruiz et al. 2016; Guarch-Ribot and Butturini 2016; Ejarque et al. 2017).

While the positive relationship of DOC concentrations and discharge is explained by allochthonous inputs (Butturini et al. 2008; Andrews et al. 2011), the negative relationship during low discharge periods derives from in-stream processes (Mulholland and Hill 1997; Figure 8.1), such as primary production, leaching from microbial assemblages or enhanced microbial processing of particulate organic matter (Jones et al. 1995b; Butturini et al. 2016; Burrows et al. 2017). Our study sites exhibited a surprisingly similar relationship between DOC increase rate and discharge reduction, with the discharge threshold of conservative transport to an increase in DOC concentration found at roughly 1 L s^{-1} both in Fuirosos, and in the flumes experiment (Figure 8.2). In both sites, this discharge represents a flow velocity of 0.2 cm/s. In the experimental flumes, DOC increase rates can be related directly to biotic in-stream processes, due to the exclusion of evaporation by comparing inflow and outflow rates. Conversely, in Fuirosos the observed DOC increase is partly due to evaporation that

can equally enhance DOC concentrations in the remaining surface water pools of intermittent streams (Siebers et al. 2016).

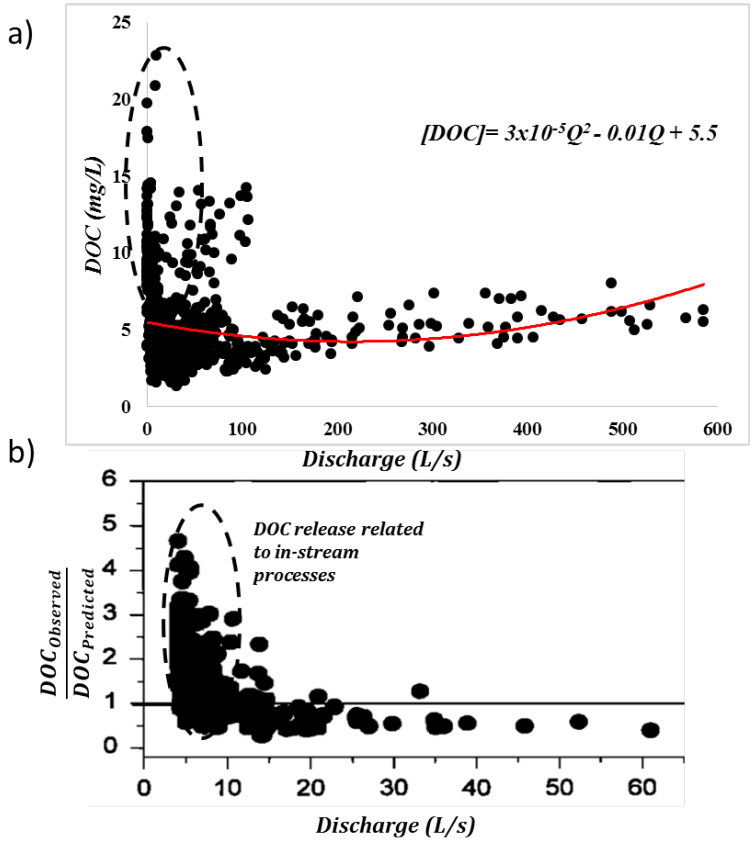

Figure 8.1: a) DOC increase observed under high flow conditions and under very low discharge conditions (dashed ellipse) plotted with observations from Fuirosos between 1998-2003 (data from Butturini et al. 2008). b) Example for DOC release attributed to in-stream processing at low discharge from first- and second order temperate forest catchments (Mulholland and Hill 1997). Rate from DOC above one indicates that there was more DOC measured than predicted from discharge.

Therefore, this comparison of the two sites should be merely seen as a starting point to unravel magnitudes of DOC release with discharge reduction and low flow velocities. There is a lack of studies reporting slopes of DOC concentration increase and discharge reduction, days of drought or water residence times (Raymond and Saiers 2010). This lack of information surprises, since from several streams in Mediterranean and arid regions DOC concentration increases during summer drought are reported (Jones et al. 1996; Vázquez et al. 2011; Von Schiller et al. 2015). Information from different streams and climate zones might enable the scientific community to identify patterns

(temperature, water residence time, light conditions, inorganic nutrient availability) and predict DOM increases from autochthonous sources related to flow reduction. The different magnitudes of DOM pulses from in-stream production presented in Table 8.1 indicate different drivers of labile DOM pulses to downstream reaches, while the most important driver seems to be inorganic nutrient availability. For instance, Dupas et al. (2017) reported higher respiration rates in upstream sections of a German river due to light and nutrient limitation, and autochthonous DOM pulses downstream because of increase in light and nutrient availability. Indeed, light availability is the key factor driving algae growth (Sabater et al. 2000; von Schiller et al. 2007), but it should be reminded that light limitation did not apply to our study sites, neither the stream reach in Fuirosos nor the experimental flumes. Contrasting to our findings, Casas-Ruiz et al., (2017) found that water residence time was positively related to DOC removal in surface water of a Mediterranean stream. However, they report that autochthonous DOC concentrations increased with nitrate concentrations. Furthermore, inhibition of DOM release due to high DOC/nitrogen ratios was even reported from the human impacted Tordera River during drought (Ejarque 2014).

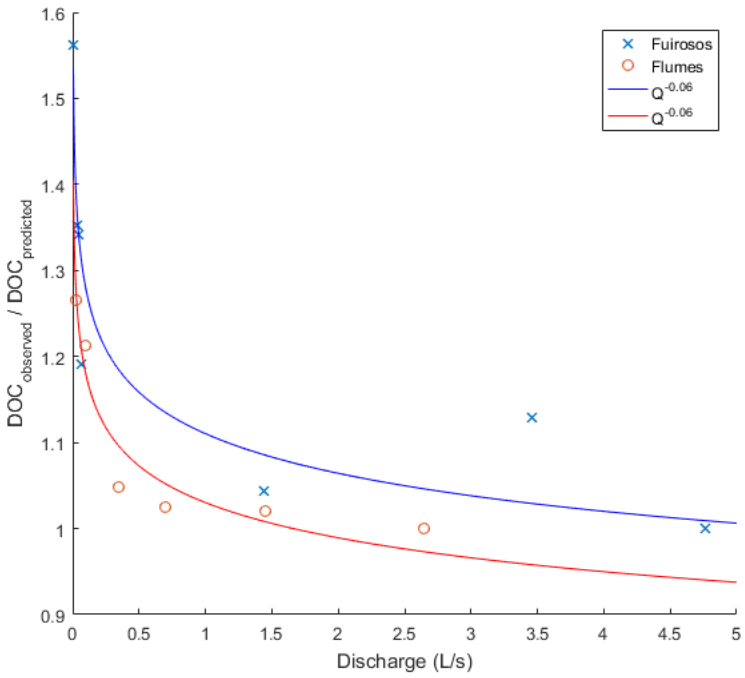

Figure 8.2: The relationship of $DOC_{observed}/DOC_{predicted}$ with discharge. Blue crosses are observations from Fuirosos and red points are the mean observations of the flumes. The accordingly colored lines represent the power relationships with the formula shown in the legend. $DOC_{predicted}$ concentrations from Fuirosos are the baseflow concentrations and the $DOC_{predicted}$ from the flumes are the concentrations of the inflow.

Table 8.1: Net DOC exports from in-stream production found in different studies and in chapter 4.

Study	Nutrient status	Ecosystem	Net DOC export from in-stream production (mg C m^{-2} d^{-1})
Chapter 4	Low	Flume 1	65
Chapter 4	Low	Flume 2	113
Jones et al. 1996	Low	Sycamore	70 - 209
Brett et al., 2012	Low	Oligotrophic lakes	29 - 137
Morling et al. 2017	Low	Reservoir	3
Morling et al. 2017	Moderate	Reservoir	150 - 168
Gawne et al. 2007	Moderate	Large River Australia	173 - 408
Brett et al. 2017	Moderate	Rivers	63 - 514
Brett et al. 2017	High	Lakes	152 - 711
Butturini et al. 2016	High	Tordera	800
Sivirichi et al. 2011	Very high	Urban stream	1344

8.3 The metabolic balance of the surface water determines DOM release during drought

Fundamentally, the DOM source and sink dynamics of a stream are connected to its ecosystem metabolism. Consequently, this discussion continues by comparing the net ecosystem production (NEP) of the pool in Fuirosos and the experimental flumes. The trend of NEP with drought was similar in both study sites. Specifically, during drought both ecosystems ultimately turned net heterotrophic. Ejarque et al. (2017) reported a release of autochthonous DOM during baseflow in the Tordera River followed by DOM retention due to high respiration rates during drought. In general, net heterotrophy of intermittent streams was assigned to the respiration rates of the hyporheic zone that plays an oversized role with surface flow ceasing (Acuña et al. 2015). By contrast, in this thesis low contribution of the hyporheic zone to the calculated NEP is expected. The sediment layer in the flumes was shallow (max. 20 cm) and the oxygen sensor in Fuirosos was deployed in a pool without any sediment layer. During pre-drought (June 2014), Fuirosos was moderately heterotrophic with values ranging from -1 to -7 g O_2 m^{-2} d^{-1}. The flume associated with pre-drought (Q=0.7 L s^{-1}) remained autotrophic (Figure 8.3). During contraction, the NEP decreased in both systems and continued decreasing as long as drought persisted. In Fuirosos, only with the rain events (August 2015) did NEP start to notably increase again; reaching even positive values after the second rain event (see Chapter 2).

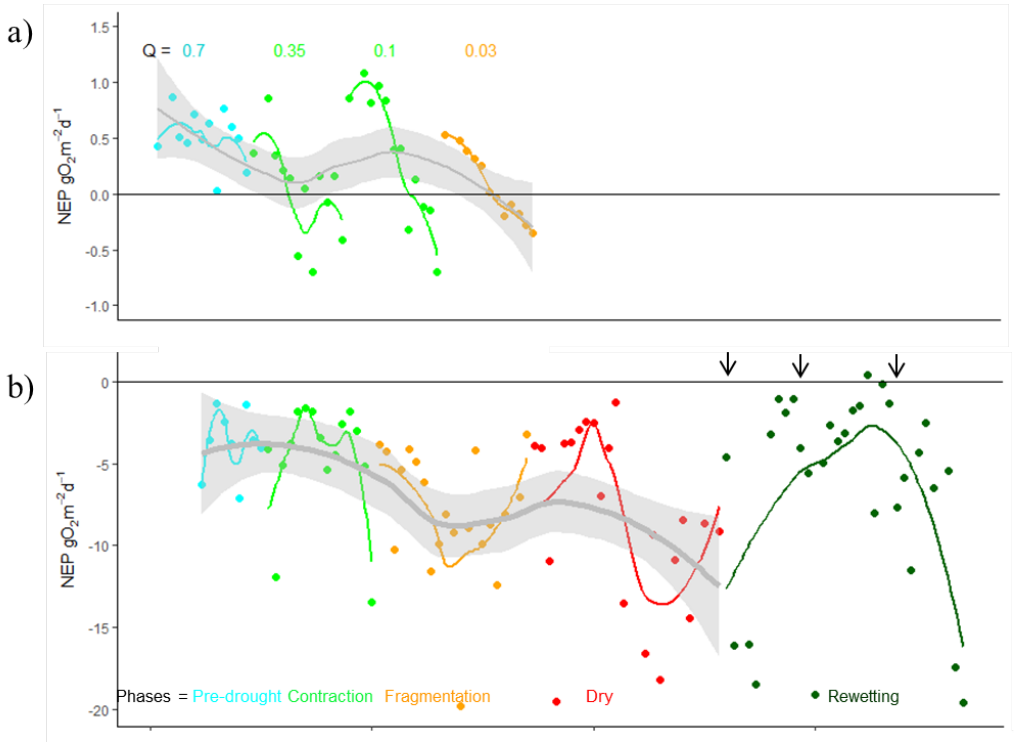

Figure 8.3: Comparison of NEP results from a) Flumes and from b) Fuirosos (data from summer 2014 and 2015). The colors indicate the drying phases with pre-drought (cyan), contraction (green), fragmentation (orange), dry (red) and rewetting (dark green). Rewetting includes three major rain events (>15 mm) with subsequent re-drying that are indicated by arrows. The grey line with shades indicates the smoothed trend of NEP over the whole discharge range in panel a and over the whole drying period in panel b.

In Chapter 4, we suggested that the shift towards net heterotrophy might have been owing to inorganic nutrient limitation of primary producers, and/or light limitation caused by organic matter accumulation (Murphy 1998; Elser et al. 2003; Sabater et al. 2008). Both suggestions are supported by the increase in net ecosystem production, when rain events might have introduced nutrients from the surrounding catchment and washed away decomposing, dead primary producers and accumulated colored DOM. Colored DOM was the key factor reducing primary production in nutrient-poor lakes through light attenuation (Karlsson et al. 2009). By contrast, Chapter 2 showed that during rewetting colored DOM was much higher than during drying, suggesting that the decrease of NEP was merely due to nutrient limitation. Similarly, Moraetis et al. (2010) report that nitrate pulses coming from the riparian zone during rain events were processed in only a few hours, while elevated oxygen levels persisted slightly longer. Especially in Fuirosos NO_3 exports from the riparian zone to the main channel can

increase stream NO_3 concentrations substantially after long drought periods (Butturini et al. 2003).

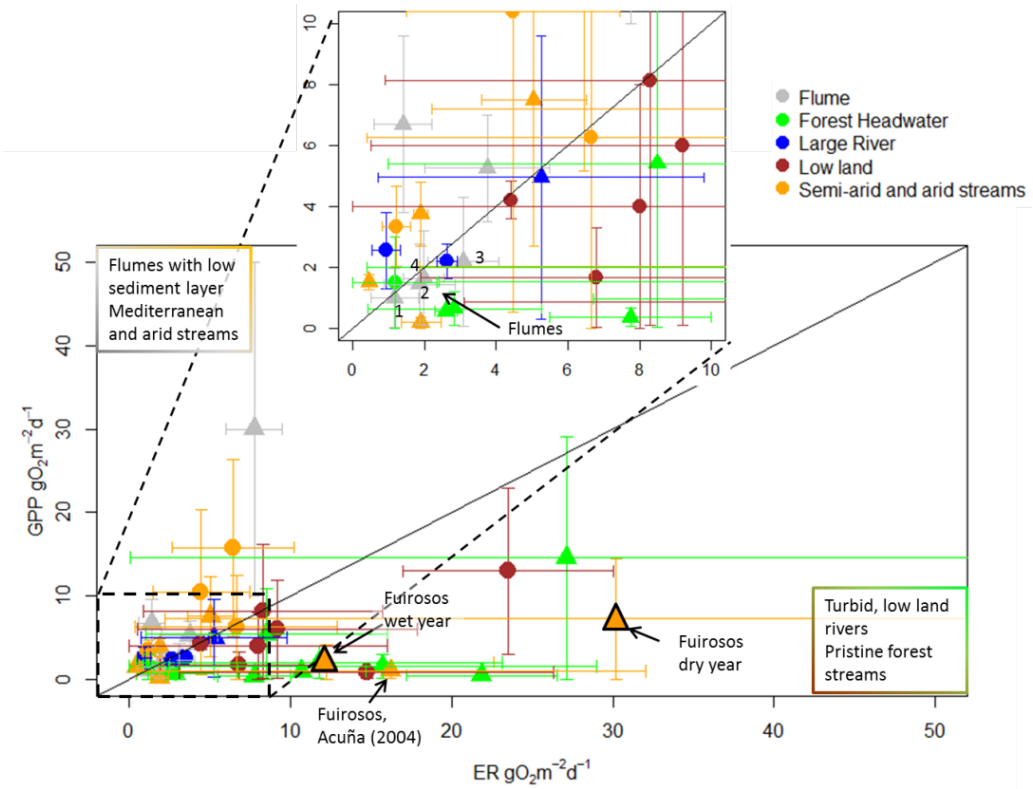

Figure 8.4: Comparison of gross primary production (GPP) and ecosystem respiration (ER) found in this thesis with data from literature. The error bars indicate minimum and maximum values of GPP and ER. The colors indicate the ecosystem type the study sites were affiliated to. The dots (high inorganic nutrient status) and triangles (low inorganic nutrient status) are the mean of the minimum/maximum values (*n*=2). The black line represents a 1:1 separation, where no process (GPP or ER) is dominating. The inlet on the top is a zoom to the area where the values of the flumes are plotted. The metadata can be found in Table SI 13: Metadata of the literature review to plot figure 8.5..

The comparison of GPP and ER data from literature revealed similar trends as have been shown by Webster and Meyer (1997). In their review, arid streams plotted close to high GPP and DOM budgets with high autochthonous contribution. Conversely, the study sites from this thesis plot both towards higher respiration than what we would expect from the ecosystem group they are affiliated with (Figure 8.4): Our flumes plotted below other flume studies and the Fuirosos pool plotted together with examples from temperate and boreal forested catchments, even though the pool was not shaded

by riparian vegetation. Furthermore, the respiration rates found in Fuirosos were high in comparison with all other examples and even higher in the dry year (2015). Many studies are performed during baseflow conditions and neglect isolated pools of intermittent streams, thereby not accounting for the high respiration rates that these water bodies can exhibit (see Chapter 2). The distinction between nutrient loads further highlighted that in the group of semi-arid and arid streams a high nutrient status increased autotrophy, while this did not apply to turbid, lowland streams.

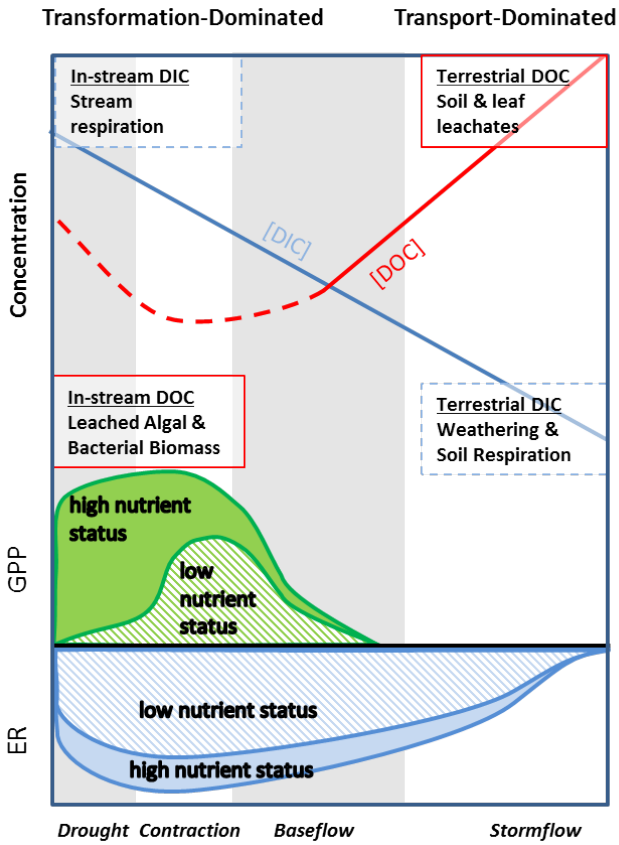

Figure 8.5: Streamflow-based conceptual model adapted from Smith & Kaushal, (2015) of processes and factors that affect carbon transport and transformation in intermittent streams based on the general discussion of the chapters. The upper lines represent dissolved inorganic carbon (blue) and dissolved organic carbon (red). The shaded areas below represent GPP (green with high nutrient status and striped green with low nutrient status) and ER (blue/striped blue). The grey shadings indicate the hydrological period.

In summary, we propose that inorganic nutrient availability is a key predictor for quantifying autochthonous DOM pulses and DOM source/sink dynamics of the

remaining surface water of drying streams, given that light availability is not a limiting factor. The patterns discussed here are collated into a conceptual model adopted from Smith & Kaushal, 2015 by extending the baseflow to the drought period and adding nutrient availability as a key factor (Figure 8.5). Clearly, this adopted conceptual model neglected the overarching effect of light availability that was emphasized by the authors and other studies (Sabater et al. 2000; von Schiller et al. 2007; Wagner et al. 2017) and represents a collection of hypotheses that emerge from the results of the four chapters of this thesis. These speculations are supported by a long-term nutrient-addition study performed in Fuirosos that revealed persisting net autotrophy with nutrient additions even under light limitation (Sabater et al. 2011). In fact, we found that even when light is not a limiting factor, the streamflow-window of GPP balancing or even exceeding ER during summer drying is very short in streams with low nutrient status and switches to net heterotrophy when drought persists. This high respiration rates are then fueled by the labile DOM from autochthonous production pulses that might also increase the degradation of more recalcitrant organic matter (see Chapters 1, 2 and 4). By contrast, even not studied in this thesis, in nutrient rich streams we expect that this window expands to severe drought levels and fuels downstream reaches and especially the hyporheic zone when connectivity persists. Hence, connectivity with downstream hyporheic zone reaches persisting during drought can mitigate nutrient loads by supplying labile DOM to the subsurface with sufficient hyporheic residence times to allow for biogeochemical reactions, such as denitrification and organic matter respiration (Harvey and Gooseff 2015).

8.4 DOM processing along hyporheic flow paths

The DOM composition of water infiltrating in the hyporheic zone of Fuirosos and the sediment layer of the experimental flumes was different. These differences became even more pronounced with drought. In Fuirosos, we observed that respiration and/or photooxidation in the surface water increased the humification degree of the DOM molecules that subsequently infiltrated into the hyporheic zone (Chapters 1 to 3). Conversely, in the experimental flumes and particularly in flumes with low discharge, the DOM was of rather fresh and labile characteristics. Furthermore, in Fuirosos, a decrease of DOM along hyporheic flow paths was observed that increased with drying. However, in the experimental flumes we observed a release of DOM from the sediments (hyporheic zone). The DOM release was most pronounced in the flumes that simulated the contraction phase (Figure 8.6).

DOC release from hyporheic zones is reported less frequent than retention in literature (see Table 8.2). For instance, in the comparison of the hyporheic zone from five

different streams, only one stream showed DOC release from the hyporheic zone (Sobczak and Findlay 2002). The latter stream had significantly lower DOC concentrations in the surface water than the other streams. In fact, the DOC concentration from this stream (1.2 mg L^{-1}) was similar to the source water of our flumes but three times less than in the Fuirosos pool. The flume that simulated the fragmentation phase showed the highest DOC concentrations at the downwelling location and in this flume DOC concentration showed no change as water moved through the sediment. This observation indicates that DOC release occurred readily when surface water entered into the hyporheic zone and the reaction was completed before the water returned to the surface (Harvey and Gooseff 2015). DOC is released from stream sediments with increasing temperature due to enhanced leaf litter degradation by microbes (Mas-Martí et al. 2015), whereby a congruent increase in organic P mineralization was observed (Argerich et al. 2008; Duan and Kaushal 2013). This mechanism was also observed at the infiltration location described in chapter 3, where NO_3 and SRP were released. Therefore, we suggest that nutrient availability for heterotrophic metabolism in the hyporheic zone is secured by this mechanism when sufficient organic matter is stored in the sediments.

With regards to DOM quality, the trends were similar in both sites: the DOM quality changed towards more labile characteristics (higher BIX and lower HIX) along hyporheic flowpaths during all hydrological phases (Figure 8.6). Respiration rates were high in the hyporheic zone of Fuirosos. We measured partial pressure of CO_2 of up to 26,000 μatm (pCO_2 reported in the literature in the hyporheic zone were max. 2000 and 4500; Baker et al. (1999); Peter et al. (2014)) together with DOM retention of up to 50% along hyporheic flow paths (Chapters 1 and 2). These findings indicate that hyporheic respiration changed the properties of the DOM, in line with recent evidence that humic-like fractions are preferentially mineralized and low molecular weight components are incorporated into biomass (Fasching et al. 2014) or released along hyporheic flow paths (Schindler and Krabbenhoft 1998). Within this context, leaching from microbial assemblages in the hyporheic zone can provide an autochthonous DOM source that is assumed to be even more labile for microbes (Anesio et al. 2005). Rudolf von Rohr et al. (2014) report that increases in temperature promoted oxygen consumption associated with the degradation of particulate organic matter. In their study, river water was infiltrated into sediment columns with a particulate organic matter source buried and subjected to different temperatures. Particulate organic matter hydrolysis released bioavailable DOM that was rapidly mineralized. By contrast, the DOM infiltrated into the sediment columns was not respired, which was attributed by the authors to its low bioavailability. Generally, bioavailability of DOM was found not to be the same for every environment and microbial community that makes it difficult to predict the fate of a certain DOM type upon its characteristics (Guillemette and del

Giorgio 2011). Consequently, bacterial degradation of organic matter can represent either a source or a sink for protein- and humic-like DOM (Cory and Kaplan 2012).

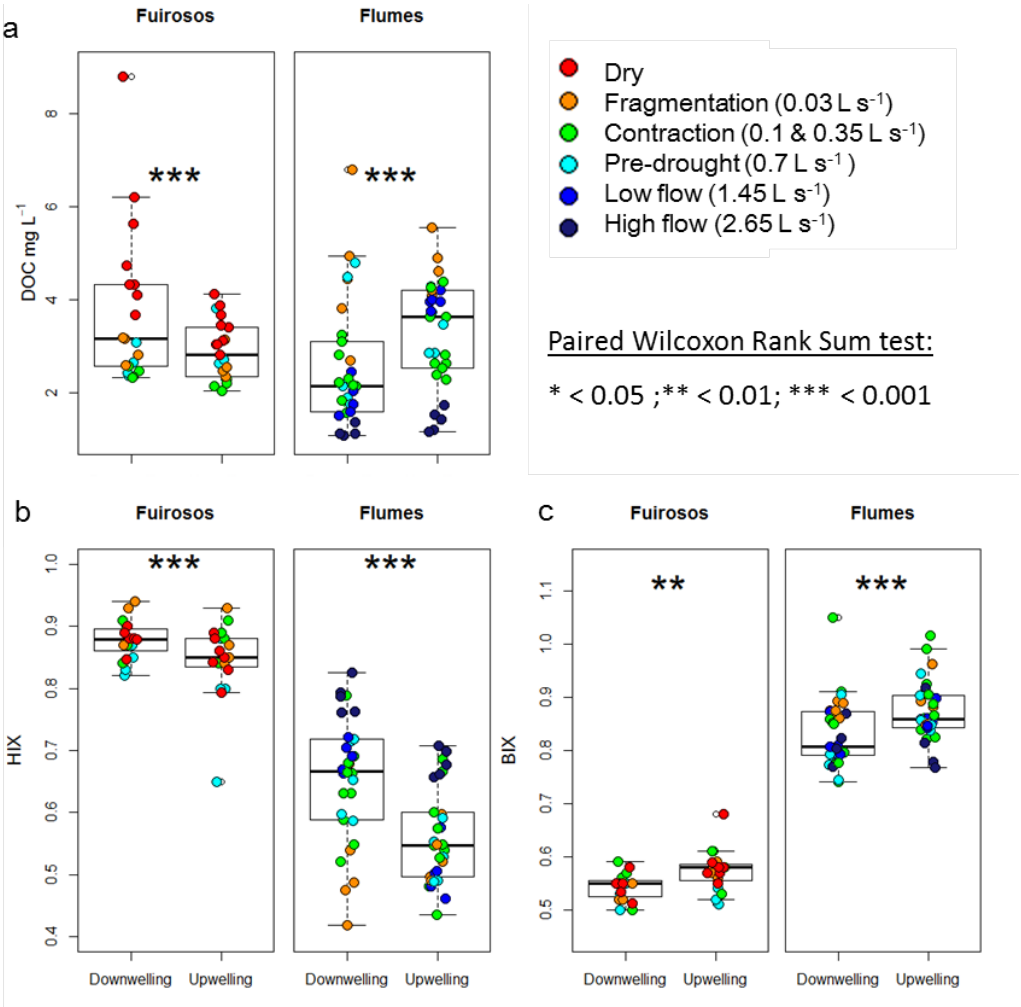

Figure 8.6: Boxplots comparing downwelling and upwelling locations in Fuirosos and the Flumes, demonstrating the transformation of DOM in hyporheic flow paths. a) shows DOC concentrations (mg L^{-1}), b) HIX and c) BIX. The colors indicate the hydrological phase and the asterisks the results of the non-parametric paired Wilcoxon Rank Sum test having "downwelling" and "upwelling" as groups.

Table 8.2: Comparison of DOC transformation in the hyporheic zone found in different studies

Ecosystem	DOC retention	DOC release	CO2 release	Trend observations	Studies
Literature					
Columns/ Microcosm	45%	0.38 g $Cm^{-2}d^{-1}$	28%;	preferred respiration of labile DOC; increased retention with water residence time; hydrolysis of POC increased with temperature	Bengtsson et al 2014; Sleighter et al 2014; von Rohr et al 2014; Duan and Kaushal 2014
Mesocosm	28%; 26.6 g $Cm^{-2}d^{-1}$	9%		release from POC leaching in flume with lowest DOC concentration; higher retention with higher flow velocity	Sobczak and Findlay, 2002; De Falco et al 2016
Gravel bar	43%; 60%		Outflux: 0.9 g $Cm^{-2}d^{-1}$	CO_2 evasion increased with higher temperature	Zarnetske et al 2011; Boodoo et al 2017; Claret et al 1997
Upper sediment layer	1.25 g $Cm^{-2}d^{-1}$		0.1 g $Cm^{-2}d^{-1}$; 2.2 g $Cm^{-2}d^{-1}$	DOC retention increased with temperature	Bott and Kaplan 1985; Naegeli and Uehlinger 1997
Dry river bed			Outflux: 34.4 g $Cm^{-2}d^{-1}$; 9.3 g $Cm^{-2}d^{-1}$		Gomez-Gener et al 2016; Von Schiller et al 2014
Hyporheic zone	100%; 50%; 0.34 g $Cm^{-2}d^{-1}$	74.4 g $Cm^{-2}d^{-1}$	30%; 34.7 g $Cm^{-2}d^{-1}$	DOC retention increased with water residence time and DOC concentration of streamwater; reduction of molecular weight; CO2 increased with water residence time	Baker et al1999; Sobczak and Findlay, 2002; Rasilo et al 2017; Battin 1999; Peter et al 2014; Schindler and Krabbenhoft 1998; Findlay and Sobczak 1996
This thesis					
Hyporheic zone	50%; ≈4 mg-C L^{-1}	10%	950%; ≈35 mg-C L^{-1}	DOC retention increased with water residence time and DOC concentration of streamwater; reduction of molecular weight; CO2 increased with water residence time	Chapter 1; Chapter 2; Chapter 3
Mesocosm		40%; ≈1.2 g $Cm^{-2}d^{-1}$		released DOM has more labile characteristics; higher release with higher temperature and water residence time	Chapter 4

Additionally, this process can create anoxic zones, where denitrification occurs, and thereby can influence the abundance of inorganic forms of nitrogen (Rudolf von Rohr et al. 2014). For instance, in the flume with the lowest discharge an increase of 100% of N-NO_2 between down-and upwelling occurred (0.0012 mg L^{-1}). The completion of the denitrification process is enhanced by water flow from aerobic to anaerobic pockets and determined by a combination of residence time and organic matter availability, showing that the interplay of DOM and nutrients is extremely close (Storey et al. 1999).

8.5 DOM dynamics and nutrient availability in the hyporheic zone

Biogeochemical processes control low-flow NO_3 concentration because water residence time and the ratio of streambed surface to water volume are high, favouring NO_3 uptake by primary producers at the interface as well as denitrification in the hyporheic zones (Zarnetske et al. 2011a). In general, organic matter decomposition is more efficient under aerobic conditions, while anaerobic decomposition requires for example nitrate as an electron donor (Storey et al. 1999). However, down- and upwelling sites proved to create optimal conditions for both processes to occur, whereby the higher the water residence time is, the more DOC and NO_3 will be retained (Figure 8.7; Harvey and Fuller 1998).

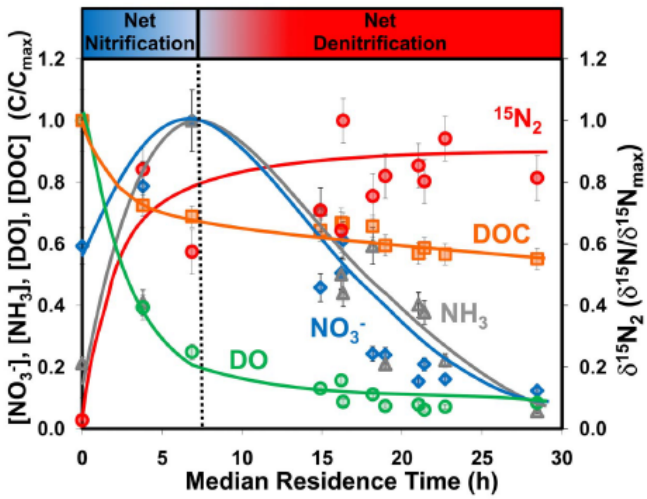

Figure 8.7 Nitrification and denitrification as a function of water residence time along hyporheic flow paths, related to DOC respiration (figure from Zarnetske et al. (2011)).

Likewise, the down-and upwelling sequence in Fuirosos followed this pattern that got more pronounced with the drying of the stream and subsequent increase of water residence time along hyporheic flow paths (Figure 8.8).Additionally, we showed in Chapters 2 and 3 that the oxygen penetration depth played an important role in determining carbon and nitrate cycling. Hence, streambeds that transition between saturated and unsaturated conditions, such as sections that are influenced by summer droughts or dam operations, showed to be highly dynamic in nutrient cycling. Therefore, intermittent streams might not only represent Hot Spots of CO_2 outgassing, but also of the greenhouse gas N_2O, as shown for riparian soils subjected to drying/rewetting cycles (Poblador et al. 2017).

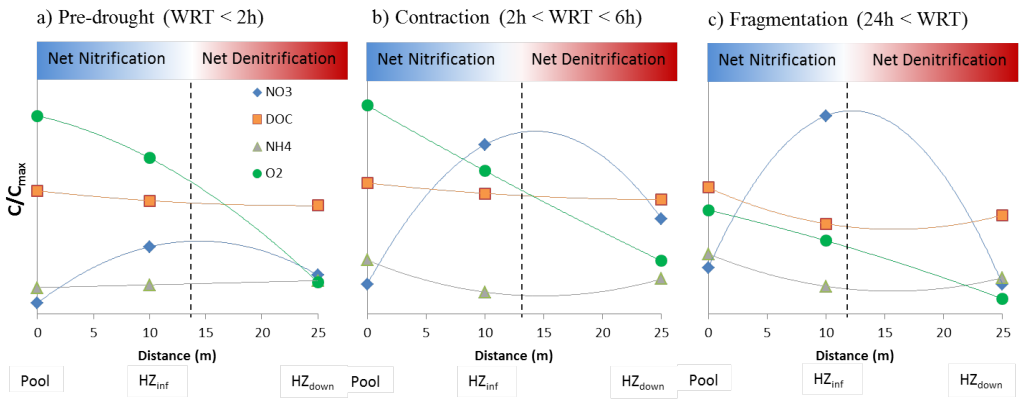

Figure 8.8: Nitrification and denitrification as a function of distance and water residence time along hyporheic flow paths, related to DOC respiration (same representation as in Figure 8.7, but with data from Fuirosos and distance on the x-axis). The three points represent the pool, the downwelling location HZ_{inf} (see Chapter 3) and the upwelling location HZ_{dw} (see Chapter 1 and 3). These snapshots show a) pre-drought, b) contraction and c) fragmentation with the according estimated water residence time (WRT).

8.6 Biogeochemical coupling of surface water and the hyporheic zone during drought period

On the one hand, DOM regulates bacterial nutrient uptake (Bernhardt et al. 2002) but in the same way, we found DOM availability closely related to nutrient availability when terrestrial solute fluxes are restricted during drought (Chapter 4). As outlined, the connectivity of surface water and interstitial pore water can promote nutrient cycling and metabolism in the stream by the exchange of oxygen (surface water) and nutrients (subsurface). Although the connectivity between surface water and the hyporheic zone for stream ecosystem services and functioning is recognized, only a small number of

studies employ integrated sampling regimes considering both stream compartments (Robertson and Wood 2010; Argerich et al. 2011; Krause et al. 2017). We found this especially the case for intermittent streams, where surface-subsurface connectivity is restricted by natural and human-made barriers during summer droughts. In fact, these environmental transition zones often result in resource mixtures that overcome limitations to microbial metabolism (Stegen et al. 2016). Consequently, these zones become even more important during drought.

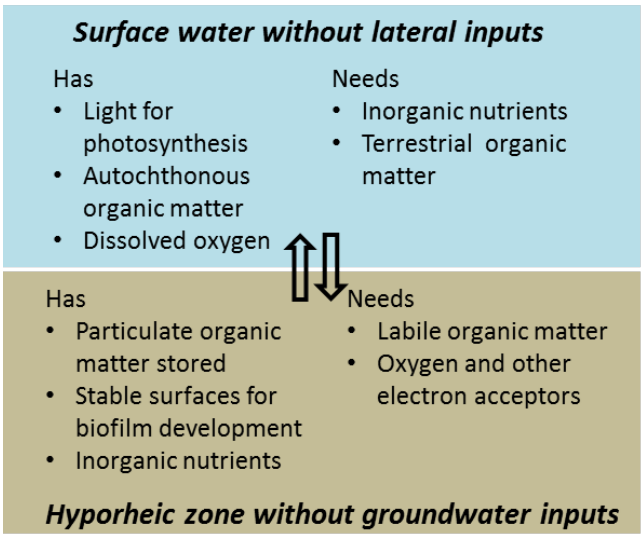

Figure 8.9: Conceptual summary of the functions and demands of metabolic activity driving carbon processing in remaining surface water pools and the hyporheic zone, and the importance of connectivity between these two compartments. In each of the compartments, it is listed what they can provide to the other compartment and what they lack during drought and subsequent disconnection from the surrounding watershed.

The heterotrophic bacterial community relied on primary production as a carbon supplier and catalyser for particulate organic matter degradation (Figure 8.9). In the same way, primary production relied on nutrient supply from upstream sections. While heterotrophic bacteria in the hyporheic zone were able to achieve nutrients from the particulate organic matter stored in the hyporheic zone (Duan and Kaushal 2013) or from abiotic desorption (von Schiller et al. 2015), this might have not been possible for primary producers in the remaining surface water (Chapter 3). This thesis shows that processes happening with drought are fundamentally different in the surface waters and the interstitial pore water of the hyporheic zone. However, in many streams, likewise the systems presented in this thesis, surface water pools remain connected with

hyporheic flowpaths. Taking the biogeochemical coupling of surface and subsurface into account can help improve the study design of future works and the understanding of stream functioning under summer drought conditions. The rapid activation of biogeochemical processes with rewetting is especially important when drying affects headwater streams, as shown in Chapters 2 and 3, where we stressed the high resilience of these ecosystem processes. By contrast, intermittent streams are still insufficiently protected, evidenced by rubbish dumping, sand and gravel extraction activities and, in the context of this thesis particularly relevant, the impermeabilization of parts of the streambed (Gómez et al. 2005). Actually, the protection and restoration of surface-subsurface connectivity must be of upmost priority because these connections maintain vital ecosystem services during drought.

General Conclusions

Fuirosos during contraction (by Tanja Brandt)

9 General Conclusions

Chapter 1: Hydrological connectivity drives dissolved organic matter processing in an intermittent stream

1. The geomorphological setting allows to perform a DOM mass balance and to investigate qualitative transformation during the drought period. The source water captured in the pool resulted to be the same as in the well 25 m downstream.
2. The DOM dynamics across the surface-subsurface interface can be categorized and related to drying phases. Specifically, these phases are contraction (lateral disconnection), fragmentation (longitudinal disconnection) and dry (surface flow is restricted to impermeable structures).
3. DOC concentrations in the remaining surface water increased as drought persisted. The DOC input of the surface water had an impact on DOM quality in the hyporheic zone, as shown when comparing the hyporheic water in locations up-and downstream the bedrock formation.
4. The DOC concentrations decreased along hyporheic flow paths and the DOM quality of the hyporheic zone showed a more autochthonous imprint and labile characteristics. The retention capacity of the hyporheic zone increased with drying to up to 1.2%/m. Only during the transition phase between contraction and fragmentation a pulse of DOM with labile characteristics was detected.

Chapter 2: Capturing hot moments of carbon processing across the surface-subsurface interface of an intermittent stream during summer drought

5. In the surface-water protein-like DOM was rapidly respired, while coloured DOM was accumulated. The overall metabolic balance of the surface water was dominated by high respiration. Rain events led to a drop of primary production followed by a slight increase.

6. Colored DOM was respired efficiently along hyporheic flow paths. DOM composition that was assumed to be recalcitrant for the surface water metabolism fueled hyporheic metabolism.
7. The exponential increase of pCO_2 by up to 1000% ($26x10^3$ μatm) along hyporheic flow paths during sediment desiccation could be related to the co-occurrence of aerobic and anaerobic metabolism, demonstrating that the microbial community of the hyporheic zone of intermittent streams can switch fast from anaerobic to aerobic pathways.
8. The respiration activity started immediately with rewetting. The pCO_2 increase along hyporheic flowpaths was related to colored DOM availability and was promoted by short rewetting events.

Chapter 3: Responses of microbial activity across the surface-subsurface interface to biogeochemical changes in a drying headwater stream

9. Microbial activity changed immediately once the water entered the hyporheic zone, while the biogeochemical imprint of the surface water remained and changed slower along hyporheic flow paths.
10. The hyporheic zone can provide a refuge for microbial activity, explaining enhanced DOM and nutrient turnover rates upon rewetting. Specifically, we observed that microbial viability and extracellular enzymatic activities increased along hyporheic flow paths during the drought period.
11. The increasing DOM retention was paralleled with the retention of inorganic nutrients along hyporheic flowpaths. This was most reflected in the down-upwelling sequence, where we found nitrate and soluble reactive phosphorus release at the downwelling location and subsequent retention that increased with water residence time in the hyporheic zone.

Chapter 4: Experimental evidence reveals impact of drought periods on dissolved organic matter quality and ecosystem metabolism in subalpine streams

12. An increase of 50% of DOC concentration in the flume with the lowest discharge was observed. This translates in a net DOC release rate of autochthonous DOC of up to 65 mg C L^{-1} d^{-1}. The threshold of DOC

concentration increase due to discharge reduction was at 0.7 L s^{-1} or at a flow velocity of 0.2 cm s^{-1}. A similar threshold was found in the surface water of Fuirosos.

13. High DOC production and leaf litter decomposition can be explained by a combination of drivers that include temperature increase and priming by algal exudates that enhances particulate organic matter decomposition.
14. The metabolic balance of flumes with low flow was characterized by a transient increase of gross primary production and therefore net autotrophy, followed by a switch to net heterotrophy that is most probably associated with phosphorus limitation and temperature.
15. Carbon fluxes of in-stream processes were higher in the flumes with lower discharge compared to the amount of DOC entering the flume. In the flume with the lowest discharge, daily GPP and daily ER represented 72% and 200% of the DOC mass entering the flume, respectively.
16. DOC concentration increased along subsurface flowpaths, contrasting the findings of Fuirosos. However, DOM quality changed towards more labile characteristics, likewise the observations from Fuirosos.

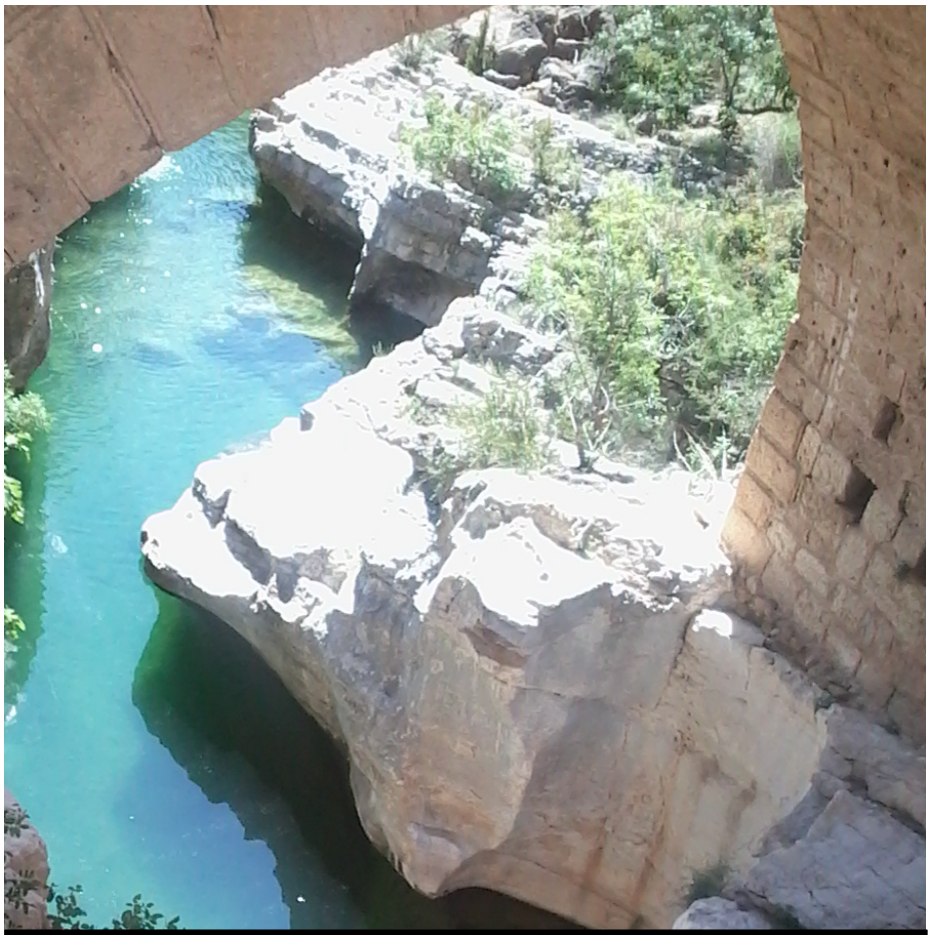

Bibliography

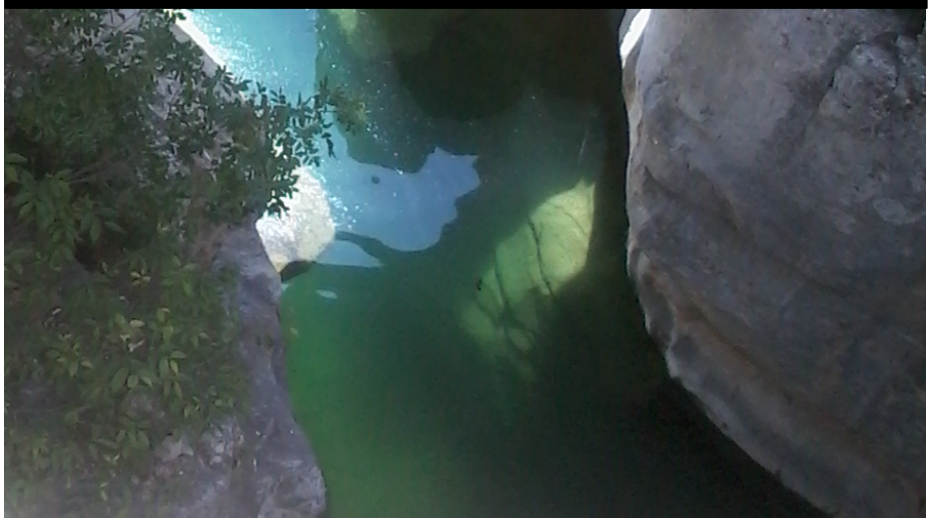

Matarranya in spring

10 Bibliography

Abbott, B. W., G. Gruau, J. P. Zarnetske, and others. 2018. Unexpected spatial stability of water chemistry in headwater stream networks J. Grover [ed.]. Ecol. Lett. **21**: 296–308. doi:10.1111/ele.12897

Abbott, B. W., J. R. Larouche, J. B. Jones, W. B. Bowden, and A. W. Balser. 2014. Elevated dissolved organic carbon biodegradability from thawing and collapsing permafrost. J. Geophys. Res. Biogeosciences **119**: 2049–2063.

Acuña, V., M. Casellas, N. Corcoll, X. Timoner, and S. Sabater. 2015. Increasing extent of periods of no flow in intermittent waterways promotes heterotrophy. Freshw. Biol. **60**. doi:10.1111/fwb.12612

Acuña, V., T. Datry, J. Marshall, and others. 2014. Conservation. Why should we care about temporary waterways? Science **343**: 1080–1. doi:10.1126/science.1246666

Acuña, V., A. Giorgi, I. Munoz, U. Uehlinger, and S. Sabater. 2004. Flow extremes and benthic organic matter shape the metabolism of a headwater Mediterranean stream. Freshw. Biol. **49**: 960–971. doi:10.1111/j.1365-2427.2004.01239.x

Acuña, V., C. Vilches, and a. Giorgi. 2011. As productive and slow as a stream can be—the metabolism of a Pampean stream. J. North Am. Benthol. Soc. **30**: 71–83. doi:10.1899/09-082.1

Acuña, V., A. Wolf, U. Uehlinger, and K. Tockner. 2008. Temperature dependence of stream benthic respiration in an Alpine river network under global warming. Freshw. Biol. **53**: 2076–2088.

Ågren, A., M. Jansson, H. Ivarsson, K. Bishop, and J. Seibert. 2008. Seasonal and runoff-related changes in total organic carbon concentrations in the River Öre, Northern Sweden. Aquat. Sci. **70**: 21–29. doi:10.1007/s00027-007-0943-9

Aitkenhead-Peterson, J. A., W. H. McDowell, and J. C. Neff. 2003. Sources, Production, and Regulation of Allochthonous Dissolved Organic Matter Inputs to Surface Waters, p. 25–70. *In* Aquatic Ecosystems. Elsevier.

Altendorf, M., and T. Stauss. 2003. Durchfluss-Handbuch: Ein Leitfaden für die Praxis: Messtechniken - Anwendungen - Lösungen, 4. Aufl.,. Endress und Hauser.

Álvarez, M., L. Proia, A. Ruggiero, F. Sabater, and A. Butturini. 2010. A comparison between pulse and constant rate additions as methods for the estimation of nutrient uptake efficiency in-streams. J. Hydrol. **388**: 273–279. doi:10.1016/J.JHYDROL.2010.05.006

Amado, A. M., J. B. Cotner, R. M. Cory, B. L. Edhlund, and K. McNeill. 2015.

Disentangling the Interactions Between Photochemical and Bacterial Degradation of Dissolved Organic Matter: Amino Acids Play a Central Role. Microb. Ecol. **69**: 554–566. doi:10.1007/s00248-014-0512-4

Amado, A. M., V. F. Farjalla, F. D. A. Esteves, R. L. Bozelli, F. Roland, and A. Enrich-Prast. 2006. Complementary pathways of dissolved organic carbon removal pathways in clear-water Amazonian ecosystems: Photochemical degradation and bacterial uptake. FEMS Microbiol. Ecol. **56**: 8–17. doi:10.1111/j.1574-6941.2006.00028.x

Amalfitano, S., and S. Fazi. 2008. Recovery and quantification of bacterial cells associated with streambed sediments. J. Microbiol. Methods **75**: 237–243. doi:10.1016/j.mimet.2008.06.004

Amalfitano, S., S. Fazi, A. Zoppini, A. Barra Caracciolo, P. Grenni, and A. Puddu. 2008. Responses of Benthic Bacteria to Experimental Drying in Sediments from Mediterranean Temporary Rivers. Microb. Ecol. **55**: 270–279. doi:10.1007/s00248-007-9274-6

Amon, R. M. W., and R. Benner. 1996. Bacterial utilization of different size classes of dissolved organic matter. Limnol. Oceanogr. **41**: 41–51. doi:10.4319/lo.1996.41.1.0041

Anderson, M. J., R. N. Gorley, and K. R. Clarke. 2008. PERMANOVA+ for PRIMER: Guide to Software and Statistical Methods, p. 1–214. *In* Plymouth, UK.

Andrews, D. M., H. Lin, Q. Zhu, L. Jin, and S. L. Brantley. 2011. Hot Spots and Hot Moments of Dissolved Organic Carbon Export and Soil Organic Carbon Storage in the Shale Hills Catchment. Vadose Zo. J. **10**: 943. doi:10.2136/vzj2010.0149

Anesio, A. M., W. Granéli, G. R. Aiken, D. J. Kieber, and K. Mopper. 2005. Effect of humic substance photodegradation on bacterial growth and respiration in lake water. Appl. Environ. Microbiol. **71**: 6267–75. doi:10.1128/AEM.71.10.6267-6275.2005

Ann, V. 2015. Linking river sediment physical properties to biofilm biomass and activity. TDX (Tesis Dr. en Xarxa).

Appling, A. P., R. O. Hall, M. Arroita, and C. B. Yackulic. 2017. streamMetabolizer: Models for Estimating Aquatic Photosynthesis and Respiration.

Arce, M. I., M. del M. Sánchez-Montoya, M. R. Vidal-Abarca, M. L. Suárez, and R. Gómez. 2014. Implications of flow intermittency on sediment nitrogen availability and processing rates in a Mediterranean headwater stream. Aquat. Sci. **76**: 173–186. doi:10.1007/s00027-013-0327-2

Argerich, A., R. Haggerty, S. L. Johnson, and others. 2016. Comprehensive multiyear carbon budget of a temperate headwater stream. J. Geophys. Res. G

Biogeosciences **121**: 1306–1315. doi:10.1002/2015JG003050

Argerich, A., R. Haggerty, E. Martí, F. Sabater, and J. Zarnetske. 2011. Quantification of metabolically active transient storage (MATS) in two reaches with contrasting transient storage and ecosystem respiration. J. Geophys. Res. Biogeosciences **116**. doi:10.1029/2010JG001379

Argerich, A., E. Martí, F. Sabater, M. Ribot, D. von Schiller, and J. L. Riera. 2008. Combined effects of leaf litter inputs and a flood on nutrient retention in a Mediterranean mountain stream during fall. Limnol. Oceanogr. **53**: 631–641. doi:10.4319/lo.2008.53.2.0631

Aristegi, L., O. Izagirre, and A. Elosegi. 2009. Comparison of several methods to calculate reaeration in streams, and their effects on estimation of metabolism. Hydrobiologia **635**: 113–124. doi:10.1007/s10750-009-9904-8

Aristi, I., M. Arroita, A. Larrañaga, L. Ponsatí, S. Sabater, D. von Schiller, A. Elosegi, and V. Acuña. 2014. Flow regulation by dams affects ecosystem metabolism in Mediterranean rivers. Freshw. Biol. **59**: 1816–1829. doi:10.1111/fwb.12385

Arthington, A. H., J. M. Bernardo, and M. Ilhéu. 2014. Temporary rivers: Linking ecohydrology, ecological quality and reconciliation ecology. River Res. Appl. **30**: 1209–1215. doi:10.1002/rra.2831

Artigas, J., A. M. Romaní, A. Gaudes, I. Muñoz, and S. Sabater. 2009. Organic matter availability structures microbial biomass and activity in a Mediterranean stream. Freshw. Biol. **54**: 2025–2036. doi:10.1111/j.1365-2427.2008.02140.x

Artigas, J., A. M. Romaní, and S. Sabater. 2008. Relating nutrient molar ratios of microbial attached communities to organic matter utilization in a forested stream. Fundam. Appl. Limnol. / Arch. für Hydrobiol. **173**: 255–264. doi:10.1127/1863-9135/2008/0173-0255

Artigas, J., S. Soley, M. C. Pérez-Baliero, A. M. Romaní, C. Ruiz-González, and S. Sabater. 2012. Phosphorus use by planktonic communities in a large regulated Mediterranean river. Sci. Total Environ. **426**: 180–187. doi:10.1016/J.SCITOTENV.2012.03.032

Askaer, L., B. Elberling, R. N. Glud, M. Kühl, F. R. Lauritsen, and H. P. Joensen. 2010. Soil heterogeneity effects on O2distribution and CH4emissions from wetlands: In situ and mesocosm studies with planar O2optodes and membrane inlet mass spectrometry. Soil Biol. Biochem. **42**: 2254–2265. doi:10.1016/j.soilbio.2010.08.026

Aufdenkampe, A. K., E. Mayorga, P. A. Raymond, J. M. Melack, S. C. Doney, S. R. Alin, R. E. Aalto, and K. Yoo. 2011. Riverine coupling of biogeochemical cycles between land, oceans, and atmosphere. Front. Ecol. Environ. **9**: 53–60. doi:10.1890/100014

Baker, M. A., C. N. Dahm, and H. M. Valett. 1999. Acetate retention and metabolism in the hyporheic zone of a mountain stream. Limnol. Oceanogr. **44**: 1530–1539. doi:10.4319/lo.1999.44.6.1530

Baltar, F., X. A. G. Morán, and C. Lønborg. 2017. Warming and organic matter sources impact the proportion of dissolved to total activities in marine extracellular enzymatic rates. Biogeochemistry **133**: 307–316. doi:10.1007/s10533-017-0334-9

Barnett, T. P., J. C. Adam, and D. P. Lettenmaier. 2005. Potential impacts of a warming climate on water availability in snow-dominated regions. Nature **438**: 303–309. doi:10.1038/nature04141

Bartoń, K. 2016. MuMIn: Multi-model inference. R package version 1.15.6. Version **1**: 18. doi:citeulike:11961261

Bass, A. M., M. I. Bird, M. J. Liddell, and P. N. Nelson. 2011. Fluvial dynamics of dissolved and particulate organic carbon during periodic discharge events in a steep tropical rainforest catchment. Limnol. Oceanogr. **56**: 2282–2292. doi:10.4319/lo.2011.56.6.2282

Bates, B. 2006. Climate Change, Water Flows and the Environment Paper prepared for presentation at the " Water For Irrigated Agriculture And The Environment: Finding a Flow for All " conference conducted by the Crawford Fund for International Agricultural Resea.

Battin, T. J., L. A. Kaplan, S. Findlay, C. S. Hopkinson, E. Marti, A. I. Packman, J. D. Newbold, and F. Sabater. 2008. Biophysical controls on organic carbon fluxes in fluvial networks. Nat. Geosci. **1**: 95–100. doi:10.1038/ngeo101

Battin, T. J., L. A. Kaplan, J. D. Newbold, and S. P. Hendricks. 2003. A mixing model analysis of stream solute dynamics and the contribution of a hyporheic zone to ecosystem function. Freshw. Biol. **48**: 995–1014. doi:10.1046/j.1365-2427.2003.01062.x

Battin, T. J., S. Luyssaert, L. A. Kaplan, A. K. Aufdenkampe, A. Richter, and L. J. Tranvik. 2009. The boundless carbon cycle. Nat. Geosci. **2**: 598–600. doi:10.1038/ngeo618

Beaulieu, J. J., C. P. Arango, D. A. Balz, and W. D. Shuster. 2013. Continuous monitoring reveals multiple controls on ecosystem metabolism in a suburban stream. Freshw. Biol. **58**: 918–937. doi:10.1111/fwb.12097

De Beer, D., P. Stoodley, and Z. Lewandowski. 1996. Liquid flow and mass transport in heterogeneous biofilms. Water Res. **30**: 2761–2765. doi:10.1016/S0043-1354(96)00141-8

Bengtsson, M. M., K. Wagner, N. R. Burns, E. R. Herberg, W. Wanek, L. A. Kaplan, and T. J. Battin. 2015. No evidence of aquatic priming effects in hyporheic zone

microcosms. Sci. Rep. **4**: 5187. doi:10.1038/srep05187

De Berg, M. 2008. Computational geometry: Algorithms and applications, 3rd ed. Springer.

Berghuijs, W. R., R. A. Woods, and M. Hrachowitz. 2014. A precipitation shift from snow towards rain leads to a decrease in streamflow. Nat. Clim. Chang. **4**: 583–586. doi:10.1038/nclimate2246

Bernal, S., A. Butturini, and F. Sabater. 2002. Variability of DOC and nitrate responses to storms in a small Mediterranean forested catchment. Hydrol. Earth Syst. Sci. **6**: 1031–1041.

Bernal, S., A. Butturini, and F. Sabater. 2005. Seasonal variations of dissolved nitrogen and DOC:DON ratios in an intermittent Mediterranean stream. Biogeochemistry **75**: 351–372. doi:10.1007/s10533-005-1246-7

Bernal, S., A. Butturini, and F. Sabater. 2006. Inferring nitrate sources through end member mixing analysis in an intermittent Mediterranean stream. Biogeochemistry **81**: 269–289. doi:10.1007/s10533-006-9041-7

Bernal, S., and F. Sabater. 2012a. Changes in discharge and solute dynamics between hillslope and valley-bottom intermittent streams. Hydrol. Earth Syst. Sci. **16**: 1595–1605. doi:10.5194/hess-16-1595-2012

Bernal, S., and F. Sabater. 2012b. Changes in discharge and solute dynamics between hillslope and valley-bottom intermittent streams. Hydrol. Earth Syst. Sci **16**: 1595–1605. doi:10.5194/hess-16-1595-2012

Bernal, S., F. Sabater, A. Butturini, E. Nin, and S. Sabater. 2007. Factors limiting denitrification in a Mediterranean riparian forest. Soil Biol. Biochem. **39**: 2685–2688. doi:10.1016/J.SOILBIO.2007.04.027

Bernhardt, E. S., R. O. Hall, and G. E. Likens. 2002. Whole-system estimates of nitrification and nitrate uptake in streams of the Hubbard Brook Experimental Forest. Ecosystems **5**: 419–430. doi:10.1007/s10021-002-0179-4

Bernot, M. J., D. J. Sobota, R. O. Hall, P. J. Mulholland, W. K. Dodds, J. R. Webster, J. L. Tank, and L. R. Ashkenas. 2010. Inter-regional comparison of land-use effects on stream metabolism. Freshw. Biol. **55**: 1874–1890. doi:10.1111/j.1365-2427.2010.02422.x

Birch, H. F. 1964. Mineralisation of plant nitrogen following alternate wet and dry conditions. Plant Soil **20**: 43–49. doi:10.1007/BF01378096

Bishop, P. L., J. T. Gibbs, and B. E. Cunningham. 1997. Relationship Between Concentration and Hydrodynamic Boundary Layers over Biofilms. Environ. Technol. **18**: 375–385. doi:10.1080/09593331808616551

Boano, F., J. W. Harvey, A. Marion, A. I. Packman, R. Revelli, L. Ridolfi, and A. Wörman. 2014. Hyporheic flow and transport processes: Mechanisms, models, and biogeochemical implications. Rev. Geophys. **52**: 603–679. doi:10.1002/2012RG000417

Boodoo, K. S., N. Trauth, C. Schmidt, J. Schelker, and T. J. Battin. 2017. Gravel bars are sites of increased CO2outgassing in stream corridors. Sci. Rep. **7**. doi:10.1038/s41598-017-14439-0

Borges, A. V., F. Darchambeau, C. R. Teodoru, and others. 2015. Globally significant greenhouse-gas emissions from African inland waters. Nat. Geosci. **8**. doi:10.1038/ngeo2486

Boulêtreau, S., M. Sellali, A. Elosegi, and others. 2010. Temporal Dynamics of River Biofilm in Constant Flows: A Case Study in a Riverside Laboratory Flume. Int. Rev. Hydrobiol. **95**: 156–170. doi:10.1002/iroh.200911203

Boulos, L., M. Prévost, B. Barbeau, J. Coallier, R. Desjardins, L. Boulos, and B. Barbeau. 1999. Methods LIVE / DEAD ® Bac Light E : application of a new rapid staining method for direct enumeration of viable and total bacteria in drinking water. J. Microbiol. Methods **37**: 77–86. doi:10.1016/S0167-7012(99)00048-2

Boulton, A. J., G. D. Fenwick, P. J. Hancock, and M. S. Harvey. 2008. Biodiversity, functional roles and ecosystem services of groundwater invertebrates. Invertebr. Syst. **22**: 103–116. doi:10.1071/IS07024

Boulton, A. J., S. Findlay, P. Marmonier, E. H. Stanley, and H. M. Valett. 1998. THE FUNCTIONAL SIGNIFICANCE OF THE HYPORHEIC ZONE IN STREAMS AND RIVERS. Annu. Rev. Ecol. Syst. **29**: 59–81. doi:10.1146/annurev.ecolsys.29.1.59

Brandt, T., M. Vieweg, G. Laube, R. Schima, T. Goblirsch, J. H. Fleckenstein, and C. Schmidt. 2017. Automated in Situ Oxygen Profiling at Aquatic-Terrestrial Interfaces. Environ. Sci. Technol. **51**: 9970–9978. doi:10.1021/acs.est.7b01482

Brett, M. T., G. B. Arhonditsis, S. Chandra, and M. J. Kainz. 2012. Mass flux calculations show strong Allochthonous support of freshwater Zooplankton production is unlikely. PLoS One **7**. doi:10.1371/journal.pone.0039508

Brett, M. T., S. E. Bunn, S. Chandra, and others. 2017. How important are terrestrial organic carbon inputs for secondary production in freshwater ecosystems? Freshw. Biol. **62**: 833–853. doi:10.1111/fwb.12909

Bro, R. 1997. PARAFAC. Tutorial and applications. Chemom. Intell. Lab. Syst. **38**: 149–171. doi:10.1016/S0169-7439(97)00032-4

Bunn, S. E., P. M. Davies, and M. Winning. 2003. Sources of organic carbon

supporting the food web of an arid zone floodplain river. Freshw. Biol. **48**: 619–635. doi:10.1046/j.1365-2427.2003.01031.x

Burrows, R. M., H. Rutlidge, N. R. Bond, S. M. Eberhard, A. Auhl, M. S. Andersen, D. G. Valdez, and M. J. Kennard. 2017. High rates of organic carbon processing in the hyporheic zone of intermittent streams. Sci. Rep. **7**. doi:10.1038/s41598-017-12957-5

Busch, D. E., and S. G. Fisher. 1981. Metabolism of a desert stream. Freshw. Biol. **11**: 301–307. doi:10.1111/j.1365-2427.1981.tb01263.x

Butman, D., S. Stackpoole, E. Stets, C. P. McDonald, D. W. Clow, and R. G. Striegl. 2016. Aquatic carbon cycling in the conterminous United States and implications for terrestrial carbon accounting. Proc. Natl. Acad. Sci. **113**: 58–63. doi:10.1073/pnas.1512651112

Butturini, A., M. Alvarez, S. Bernal, E. Vazquez, and F. Sabater. 2008. Diversity and temporal sequences of forms of DOC and NO_3 -discharge responses in an intermittent stream: Predictable or random succession? J. Geophys. Res. **113**: G03016. doi:10.1029/2008JG000721

Butturini, A., S. Bernal, C. Hellin, E. Nin, L. Rivero, S. Sabater, and F. Sabater. 2003. Influences of the stream groundwater hydrology on nitrate concentration in unsaturated riparian area bounded by an intermittent Mediterranean stream. Water Resour. Res. **39**. doi:10.1029/2001WR001260

Butturini, A., S. Bernal, and F. Sabater. 2005. Modeling storm events to investigate the influence of the stream-catchment interface zone on stream biogeochemistry. Water Resour. Res. **41**: 1–12. doi:10.1029/2004WR003842

Butturini, A., S. Bernal, S. Sabater, and F. Sabater. 2002a. The influence of riparian-hyporheic zone on the hydrological responses in an intermittent stream. Hydrol. Earth Syst. Sci. **6**: 515–526. doi:10.5194/hess-6-515-2002

Butturini, A., S. Bernal, S. Sabater, and F. Sabater. 2002b. The influence of riparian-hyporheic zone on the hydrological responses in an intermittent stream. Hydrol. Earth Syst. Sci. **6**: 515–526. doi:10.5194/hess-6-515-2002

Butturini, A., A. Guarch, A. M. Romaní, A. Freixa, S. Amalfitano, S. Fazi, and E. Ejarque. 2016. Hydrological conditions control in situ DOM retention and release along a Mediterranean river. Water Res. **99**: 33–45. doi:10.1016/j.watres.2016.04.036

Butturini, A., and F. Sabater. 2000. Seasonal variability of dissolved organic carbon ina Mediterranean stream. Biogeochemistry **51**: 303–321. doi:10.1023/A:1006420229411

Cammack, W. L., J. Kalff, Y. T. Prairie, and E. M. Smith. 2004. Fluorescent dissolved

organic matter in lakes: relationships with heterotrophic metabolism. Limnol. Oceanogr. **49**: 2034–2045.

Casas-Ruiz, J. P., N. Catalán, L. Gómez-Gener, and others. 2017. A tale of pipes and reactors: Controls on the in-stream dynamics of dissolved organic matter in rivers. Limnol. Oceanogr. **62**: S85–S94. doi:10.1002/lno.10471

Casas-Ruiz, J. P., J. Tittel, D. von Schiller, and others. 2016. Drought-induced discontinuities in the source and degradation of dissolved organic matter in a Mediterranean river. Biogeochemistry **127**: 125–139. doi:10.1007/s10533-015-0173-5

Catalán, N., J. P. Casas-Ruiz, D. von Schiller, L. Proia, B. Obrador, E. Zwirnmann, and R. Marcé. 2017. Biodegradation kinetics of dissolved organic matter chromatographic fractions in an intermittent river. J. Geophys. Res. Biogeosciences **122**: 131–144. doi:10.1002/2016JG003512

Catalán, N., A. M. Kellerman, H. Peter, F. Carmona, and L. J. Tranvik. 2015. Absence of a priming effect on dissolved organic carbon degradation in lake water. Limnol. Oceanogr. **60**: 159–168. doi:10.1002/lno.10016

Catalán, N., R. Marcé, D. N. Kothawala, and L. J. Tranvik. 2016. Organic carbon decomposition rates controlled by water retention time across inland waters. Nat. Geosci. **9**. doi:10.1038/ngeo2720

Chafiq, M., J. Gibert, and C. Claret. 1999. Interactions among sediments, organic matter, and microbial activity in the hyporheic zone of an intermittent stream. Can. J. Fish. Aquat. Sci. **56**: 487–495. doi:10.1139/f98-208

Coble, P. G., C. E. Del Castillo, and B. Avril. 1998. Distribution and optical properties of CDOM in the Arabian Sea during the 1995 Southwest Monsoon. Deep. Res. Part II Top. Stud. Oceanogr. **45**: 2195–2223. doi:10.1016/S0967-0645(98)00068-X

Cole, J. J., Y. T. Prairie, N. F. Caraco, and others. 2007. Plumbing the Global Carbon Cycle: Integrating Inland Waters into the Terrestrial Carbon Budget. Ecosystems **10**: 172–185. doi:10.1007/s10021-006-9013-8

Cory, R. M., and L. A. Kaplan. 2012. Biological lability of streamwater fluorescent dissolved organic matter. Limnol. Oceanogr. **57**: 1347–1360. doi:10.4319/lo.2012.57.5.1347

Cory, R. M., and D. M. McKnight. 2005. Fluorescence Spectroscopy Reveals Ubiquitous Presence of Oxidized and Reduced Quinones in Dissolved Organic Matter. Environ. Sci. Technol. **39**: 8142–8149. doi:10.1021/es0506962

Creed, I. F., D. M. McKnight, B. A. Pellerin, and others. 2015. The river as a chemostat: fresh perspectives on dissolved organic matter flowing down the river

continuum R. Smith [ed.]. Can. J. Fish. Aquat. Sci. **72**: 1272–1285. doi:10.1139/cjfas-2014-0400

Dai, A., T. Qian, K. E. Trenberth, J. D. Milliman, A. Dai, T. Qian, K. E. Trenberth, and J. D. Milliman. 2009. Changes in Continental Freshwater Discharge from 1948 to 2004. J. Clim. **22**: 2773–2792. doi:10.1175/2008JCLI2592.1

Danczak, R. E., A. H. Sawyer, K. H. Williams, J. C. Stegen, C. Hobson, and M. J. Wilkins. 2016. Seasonal hyporheic dynamics control coupled microbiology and geochemistry in Colorado River sediments. J. Geophys. Res. Biogeosciences **121**: 2976–2987. doi:10.1002/2016JG003527

Datry, T., S. T. Larned, and K. Tockner. 2014. Intermittent Rivers: A Challenge for Freshwater Ecology. Bioscience **64**: 229–235. doi:10.1093/biosci/bit027

Demars, B. O. L., G. M. Gíslason, J. S. Ólafsson, J. R. Manson, N. Friberg, J. M. Hood, J. J. D. Thompson, and T. E. Freitag. 2016. Impact of warming on CO2 emissions from streams countered by aquatic photosynthesis. Nat. Geosci. **9**: 758–761. doi:10.1038/ngeo2807

Dey, P., and A. Mishra. 2017. Separating the impacts of climate change and human activities on streamflow: A review of methodologies and critical assumptions. J. Hydrol. **548**: 278–290. doi:10.1016/J.JHYDROL.2017.03.014

Dieter, D., K. Frindte, A. Krüger, and C. Wurzbacher. 2013. Preconditioning of leaves by solar radiation and anoxia affects microbial colonisation and rate of leaf mass loss in an intermittent stream. Freshw. Biol. **58**: 1918–1931. doi:10.1111/fwb.12180

Dinsmore, K. J., M. B. Wallin, M. S. Johnson, M. F. Billett, K. Bishop, J. Pumpanen, and A. Ojala. 2013. Contrasting CO<inf>2</inf> concentration discharge dynamics in headwater streams: A multi-catchment comparison. J. Geophys. Res. Biogeosciences **118**: 445–461. doi:10.1002/jgrg.20047

Dodds, W. K., R. E. Hutson, A. C. Eichem, M. A. Evans, D. A. Gudder, K. M. Fritz, and L. Gray. 1996. The relationship of floods, drying, flow and light to primary production and producer biomass in a prairie stream. Hydrobiologia **333**: 151–159. doi:10.1007/BF00013429

Downing, B. D., E. Boss, B. A. Bergamaschi, J. A. Fleck, M. A. Lionberger, N. K. Ganju, D. H. Schoellhamer, and R. Fujii. 2009. Quantifying fluxes and characterizing compositional changes of dissolved organic matter in aquatic systems in situ using combined acoustic and optical measurements. Limnol. Oceanogr. Methods **7**: 119–131.

Doyle, M. W., E. H. Stanley, D. L. Strayer, R. B. Jacobson, and J. C. Schmidt. 2005. Effective discharge analysis of ecological processes in streams. Water Resour. Res. **41**. doi:10.1029/2005WR004222

Duan, S.-W., and S. S. Kaushal. 2013. Warming increases carbon and nutrient fluxes from sediments in streams across land use. Biogeosciences **10**: 1193–1207. doi:10.5194/bg-10-1193-2013

Dudgeon, D., A. H. Arthington, M. O. Gessner, and others. 2006. Freshwater biodiversity: importance, threats, status and conservation challenges. Biol. Rev. **81**: 163. doi:10.1017/S1464793105006950

Dupas, R., A. Musolff, J. W. Jawitz, P. S. C. Rao, C. G. Jäger, J. H. Fleckenstein, M. Rode, and D. Borchardt. 2017. Carbon and nutrient export regimes from headwater catchments to downstream reaches. Biogeosciences **14**: 4391–4407. doi:10.5194/bg-14-4391-2017

Ebrahimi, A., and D. Or. 2016. Microbial community dynamics in soil aggregates shape biogeochemical gas fluxes from soil profiles - upscaling an aggregate biophysical model. Glob. Chang. Biol. **22**: 3141–3156. doi:10.1111/gcb.13345

Edwardson, K. J., W. B. Bowden, C. Dahm, and J. Morrice. 2003. The hydraulic characteristics and geochemistry of hyporheic and parafluvial zones in Arctic tundra streams, north slope, Alaska. Adv. Water Resour. **26**: 907–923. doi:10.1016/S0309-1708(03)00078-2

Eiler, A., S. Langenheder, S. Bertilsson, and L. J. Tranvik. 2003. Heterotrophic bacterial growth efficiency and community structure at different natural organic carbon concentrations. Appl. Environ. Microbiol. **69**: 3701–9. doi:10.1128/AEM.69.7.3701-3709.2003

Ejarque, E., A. Freixa, E. Vazquez, A. Guarch, S. Amalfitano, S. Fazi, A. M. Romaní, and A. Butturini. 2017. Quality and reactivity of dissolved organic matter in a Mediterranean river across hydrological and spatial gradients. Sci. Total Environ. **599–600**: 1802–1812. doi:10.1016/J.SCITOTENV.2017.05.113

Ejarque Gonzalez, E. 2014. From flood to drought: Transport and reactivity of dissolved organic matter along a Mediterranean river. TDX (Tesis Dr. en Xarxa).

Elser, J. J., M. Kyle, W. Makino, T. Yoshida, and J. Urabe. 2003. Ecological stoichiometry in the microbial food web: A test of the light: nutrient hypothesis. Aquat. Microb. Ecol. **31**: 49–65.

De Falco, N., F. Boano, and S. Arnon. 2016. Biodegradation of labile dissolved organic carbon under losing and gaining streamflow conditions simulated in a laboratory flume. Limnol. Oceanogr. **61**: 1839–1852. doi:10.1002/lno.10344

Fan, Z., J. C. Neff, M. P. Waldrop, A. P. Ballantyne, and M. R. Turetsky. 2014. Transport of oxygen in soil pore-water systems: implications for modeling emissions of carbon dioxide and methane from peatlands. Biogeochemistry **121**: 455–470. doi:10.1007/s10533-014-0012-0

Farjalla, V. F., C. C. Marinho, B. M. Faria, A. M. Amado, F. de A. Esteves, R. L. Bozelli, and D. Giroldo. 2009. Synergy of Fresh and Accumulated Organic Matter to Bacterial Growth. Microb. Ecol. **57**: 657–666. doi:10.1007/s00248-008-9466-8

Fasching, C., B. Behounek, G. A. Singer, and T. J. Battin. 2014. Microbial degradation of terrigenous dissolved organic matter and potential consequences for carbon cycling in brown-water streams. Sci. Rep. **4**. doi:10.1038/srep04981

Fasching, C., A. J. Ulseth, J. Schelker, G. Steniczka, and T. J. Battin. 2016. Hydrology controls dissolved organic matter export and composition in an Alpine stream and its hyporheic zone. Limnol. Oceanogr. **61**: 558–571. doi:10.1002/lno.10232

Fazi, S., E. Vázquez, E. O. Casamayor, S. Amalfitano, and A. Butturini. 2013. Stream Hydrological Fragmentation Drives Bacterioplankton Community Composition. PLoS One **8**. doi:10.1371/journal.pone.0064109

Febria, C. M., P. Beddoes, R. R. Fulthorpe, and D. D. Williams. 2012. Bacterial community dynamics in the hyporheic zone of an intermittent stream. ISME J. **6**: 1078–1088. doi:10.1038/ismej.2011.173

Fellman, J. B., S. Dogramaci, G. Skrzypek, W. Dodson, and P. F. Grierson. 2011a. Hydrologic control of dissolved organic matter biogeochemistry in pools of a subtropical dryland river. Water Resour. Res. **47**. doi:10.1029/2010WR010275

Fellman, J. B., E. Hood, D. V D'Amore, R. T. Edwards, and D. White. 2009. Seasonal changes in the chemical quality and biodegradability of dissolved organic matter exported from soils to streams in coastal temperate rainforest watersheds. Biogeochemistry **95**: 277–293.

Fellman, J. B., E. Hood, and R. G. M. Spencer. 2010. Fluorescence spectroscopy opens new windows into dissolved organic matter dynamics in freshwater ecosystems: A review. Limnol. Oceanogr. **55**: 2452–2462. doi:10.4319/lo.2010.55.6.2452

Fellman, J. B., K. C. Petrone, and P. F. Grierson. 2011b. Source, biogeochemical cycling, and fluorescence characteristics of dissolved organic matter in an agro-urban estuary. Limnol. Oceanogr. **56**: 243–256. doi:10.4319/lo.2011.56.1.0243

Fellman, J. B., R. G. M. Spencer, P. A. Raymond, N. E. Pettit, G. Skrzypek, P. J. Hernes, and P. F. Grierson. 2014. Dissolved organic carbon biolability decreases along with its modernization in fluvial networks in an ancient landscape. Ecology **95**. doi:10.1890/13-1360.1

Fellows, C. S., J. E. Clapcott, J. W. Udy, S. E. Bunn, B. D. Harch, M. J. Smith, and P. M. Davies. 2006. Benthic Metabolism as an Indicator of Stream Ecosystem Health. Hydrobiologia **572**: 71–87. doi:10.1007/s10750-005-9001-6

Fellows, C. S., M. H. Valett, and C. N. Dahm. 2001. Whole stream metabolism in two montane streams: Contribution of the hyporheic zone. Limnol. Oceanogr. **46**:

523–531. doi:10.4319/lo.2001.46.3.0523

Fernández Zenoff, V., F. Siñeriz, and M. E. Farías. 2006. Diverse responses to UV-B radiation and repair mechanisms of bacteria isolated from high-altitude aquatic environments. Appl. Environ. Microbiol. **72**: 7857–63. doi:10.1128/AEM.01333-06

Ficklin, D. L., I. T. Stewart, and E. P. Maurer. 2013. Climate Change Impacts on Streamflow and Subbasin-Scale Hydrology in the Upper Colorado River Basin V. Shah [ed.]. PLoS One **8**: e71297. doi:10.1371/journal.pone.0071297

Findlay, S. 1995. Importance of surface-subsurface exchange in stream ecosystems: The hyporheic zone. Limnol. Oceanogr. **40**: 159–164. doi:10.4319/lo.1995.40.1.0159

Findlay, S. E. G., R. L. Sinsabaugh, W. V. Sobczak, and M. Hoostal. 2003. Metabolic and structural response of hyporheic microbial communities to variations in supply of dissolved organic matter. Limnol. Oceanogr. **48**: 1608–1617. doi:10.4319/lo.2003.48.4.1608

Findlay, S., D. Strayer, C. Goumbala, and K. Gould. 1993. Metabolism of streamwater dissolved organic carbon in the shallow hyporheic zone. Limnol. Oceanogr. **38**: 1493–1499. doi:10.4319/lo.1993.38.7.1493

Fischer, H., F. Kloep, S. Wilzcek, and M. T. Pusch. 2005. A River's Liver – Microbial Processes within the Hyporheic Zone of a Large Lowland River. Biogeochemistry **76**: 349–371. doi:10.1007/s10533-005-6896-y

Fischer, H., A. Sachse, C. E. W. Steinberg, and M. Pusch. 2002. Differential retention and utilization of dissolved organic carbon by bacteria in river sediments. Limnol. Oceanogr. **47**: 1702–1711. doi:10.4319/lo.2002.47.6.1702

Fisher, S. G., N. B. Grimm, E. Martí, and R. Gómez. 1998. Hierarchy, spatial configuration, and nutrient cycling in a desert stream. Austral Ecol. **23**: 41–52. doi:10.1111/j.1442-9993.1998.tb00704.x

Fox, J., S. Weisberg, D. Adler, and others. 2016. Package "car." CRAN Repos. 171.

Freeman, C., C. D. Evans, D. T. Monteith, B. Reynolds, and N. Fenner. 2001. Export of organic carbon from peat soils. Nature **412**: 785–785. doi:10.1038/35090628

Freixa, A., V. Acuña, M. Casellas, S. Pecheva, and A. M. Romaní. 2017. Warmer night-time temperature promotes microbial heterotrophic activity and modifies stream sediment community. Glob. Chang. Biol. **23**: 3825–3837. doi:10.1111/gcb.13664

Freixa, A., E. Ejarque, S. Crognale, S. Amalfitano, S. Fazi, A. Butturini, and A. M. Romaní. 2016a. Sediment microbial communities rely on different dissolved

organic matter sources along a Mediterranean river continuum. Limnol. Oceanogr. **61**: 1389–1405. doi:10.1002/lno.10308

Freixa, A., S. Rubol, A. Carles-Brangarí, D. Fernàndez-Garcia, A. Butturini, X. Sanchez-Vila, and A. M. Romaní. 2016b. The effects of sediment depth and oxygen concentration on the use of organic matter: An experimental study using an infiltration sediment tank. Sci. Total Environ. **540**: 20–31. doi:10.1016/J.SCITOTENV.2015.04.007

Fuß, T., B. Behounek, A. J. Ulseth, and G. A. Singer. 2017. Land use controls stream ecosystem metabolism by shifting dissolved organic matter and nutrient regimes. Freshw. Biol. **62**: 582–599. doi:10.1111/fwb.12887

Gallart, F., N. Prat, E. M. Garca-Roger, and others. 2012. A novel approach to analysing the regimes of temporary streams in relation to their controls on the composition and structure of aquatic biota. Hydrol. Earth Syst. Sci. **16**: 3165–3182. doi:10.5194/hess-16-3165-2012

Gallo, E. L., K. A. Lohse, C. M. Ferlin, T. Meixner, and P. D. Brooks. 2014. Physical and biological controls on trace gas fluxes in semi-arid urban ephemeral waterways. Biogeochemistry **121**. doi:10.1007/s10533-013-9927-0

García-Ruiz, J. M., J. I. López-Moreno, S. M. Vicente-Serrano, T. Lasanta–Martínez, and S. Beguería. 2011. Mediterranean water resources in a global change scenario. Earth-Science Rev. **105**: 121–139. doi:10.1016/J.EARSCIREV.2011.01.006

Gardecki, J. A., and M. Maroncelli. 1998. Set of secondary emission standards for calibration of the spectral responsivity in emission spectroscopy. Appl. Spectrosc. **52**: 1179–1189. doi:10.1366/0003702981945192

Gasith, A., and V. H. Resh. 1999. Streams in Mediterranean Climate Regions: Abiotic Influences and Biotic Responses to Predictable Seasonal Events. Annu. Rev. Ecol. Syst. **30**: 51–81. doi:10.1146/annurev.ecolsys.30.1.51

Gat, J. R., R. Gonfiantini, and International Hydrological Programme. Working Group on Nuclear Techniques in Hydrology. 1981. Stable isotope hydrology : deuterium and oxygen-18 in the water cycle : a monograph prepared under the aegis of the IAEA/UNESCO Working Group on Nuclear Techniques in Hydrology of the International Hydro-logical Programme, International Atomic Energy Agency.

Gawne, B., C. Merrick, D. G. Williams, and others. 2007. Patterns of primary and heterotrophic productivity in an arid lowland river. River Res. Appl. **23**: 1070–1087. doi:10.1002/rra.1033

Godsey, S. E., J. W. Kirchner, and D. W. Clow. 2009. Concentration-discharge relationships reflect chemostatic characteristics of US catchments. Hydrol. Process. **23**: 1844–1864. doi:10.1002/hyp.7315

Goldman, A. E., E. B. Graham, A. R. Crump, and others. 2017. Biogeochemical cycling at the aquatic-terrestrial interface is linked to parafluvial hyporheic zone inundation history. Biogeosciences **14**: 4229–4241. doi:10.5194/bg-14-4229-2017

Goletz, C., M. Wagner, A. Grübel, W. Schmidt, N. Korf, and P. Werner. 2011. Standardization of fluorescence excitation–emission-matrices in aquatic milieu. Talanta **85**: 650–656. doi:10.1016/j.talanta.2011.04.045

Gómez-Gener, L., B. Obrador, R. Marcé, and others. 2016a. When Water Vanishes: Magnitude and Regulation of Carbon Dioxide Emissions from Dry Temporary Streams. Ecosystems **19**: 710–723. doi:10.1007/s10021-016-9963-4

Gómez-Gener, L., B. Obrador, D. Von Schiller, and others. 2015. Hot spots for carbon emissions from Mediterranean fluvial networks during summer drought. Biogeochemistry **125**: 409–426. doi:10.1007/s10533-015-0139-7

Gómez-Gener, L., D. von Schiller, R. Marcé, and others. 2016b. Low contribution of internal metabolism to carbon dioxide emissions along lotic and lentic environments of a Mediterranean fluvial network. J. Geophys. Res. Biogeosciences **121**: 3030–3044. doi:10.1002/2016JG003549

Gómez, R., M. I. Arce, J. J. Sánchez, and M. del Mar Sánchez-Montoya. 2012. The effects of drying on sediment nitrogen content in a Mediterranean intermittent stream: a microcosms study. Hydrobiologia **679**: 43–59. doi:10.1007/s10750-011-0854-6

Gómez, R., V. García, R. Vidal-Abarca, and L. Suárez. 2009. Effect of intermittency on N spatial variability in an arid Mediterranean stream. J. North Am. Benthol. Soc. **28**: 572–583. doi:10.1899/09-016.1

Gómez, R., I. Hurtado, M. L. Suárez, and M. R. Vidal-Abarca. 2005. Ramblas in south-east Spain: threatened and valuable ecosystems. Aquat. Conserv. Mar. Freshw. Ecosyst. **15**: 387–402. doi:10.1002/aqc.680

González-Pinzón, R., M. Peipoch, R. Haggerty, E. Martí, and J. H. Fleckenstein. 2016. Nighttime and daytime respiration in a headwater stream. Ecohydrology **9**: 93–100. doi:10.1002/eco.1615

Graeber, D., J. R. Poulsen, M. Heinz, J. J. Rasmussen, D. Zak, B. Gücker, B. Kronvang, and N. Kamjunke. 2018. Going with the flow: Planktonic processing of dissolved organic carbon in streams. Sci. Total Environ. **625**: 519–530. doi:10.1016/j.scitotenv.2017.12.285

Guarch-Ribot, A., and A. Butturini. 2016. Hydrological conditions regulate dissolved organic matter quality in an intermittent headwater stream. From drought to storm analysis. Sci. Total Environ. **571**: 1358–1369. doi:10.1016/j.scitotenv.2016.07.060

Guenet, B., M. Danger, L. Harrault, and others. 2014. Fast mineralization of land-born

C in inland waters: first experimental evidences of aquatic priming effect. Hydrobiologia **721**: 35–44. doi:10.1007/s10750-013-1635-1

Guillemette, F., and P. A. del Giorgio. 2011. Reconstructing the various facets of dissolved organic carbon bioavailability in freshwater ecosystems. Limnol. Oceanogr. **56**: 734–748. doi:10.4319/lo.2011.56.2.0734

Haggerty, R., M. Ribot, G. A. Singer, E. Martí, A. Argerich, G. Agell, and T. J. Battin. 2014. Ecosystem respiration increases with biofilm growth and bed forms: Flume measurements with resazurin. J. Geophys. Res. Biogeosciences **119**: 2220–2230. doi:10.1002/2013JG002498

Hall, R. O., and J. L. Tank. 2003. Ecosystem metabolism controls nitrogen uptake in streams in Grand Teton National Park, Wyoming. Limnol. Oceanogr. **48**: 1120–1128. doi:10.4319/lo.2003.48.3.1120

Hall, R. O., C. B. Yackulic, T. A. Kennedy, M. D. Yard, E. J. Rosi-Marshall, N. Voichick, and K. E. Behn. 2015. Turbidity, light, temperature, and hydropeaking control primary productivity in the Colorado River, Grand Canyon. Limnol. Oceanogr. **60**: 512–526. doi:10.1002/lno.10031

Halliday, S. J., R. A. Skeffington, A. J. Wade, and others. 2015. High-frequency water quality monitoring in an urban catchment: hydrochemical dynamics, primary production and implications for the Water Framework Directive. Hydrol. Process. **29**: 3388–3407. doi:10.1002/hyp.10453

Hannah, D. M., L. E. Brown, A. M. Milner, A. M. Gurnell, G. R. McGregor, G. E. Petts, B. P. G. Smith, and D. L. Snook. 2007. Integrating climate–hydrology–ecology for alpine river systems. Aquat. Conserv. Mar. Freshw. Ecosyst. **17**: 636–656. doi:10.1002/aqc.800

Hansen, A. M., T. E. C. Kraus, B. A. Pellerin, J. A. Fleck, B. D. Downing, and B. A. Bergamaschi. 2016. Optical properties of dissolved organic matter (DOM): Effects of biological and photolytic degradation. Limnol. Oceanogr. **61**: 1015–1032. doi:10.1002/lno.10270

Harjung, A., F. Sabater, and A. Butturini. 2017. Hydrological connectivity drives dissolved organic matter processing in an intermittent stream. Limnol. - Ecol. Manag. Inl. Waters. doi:10.1016/J.LIMNO.2017.02.007

Harrell Jr, F. E. 2015. CRAN - Package Hmisc.

Harvey, J., and M. Gooseff. 2015. River corridor science: Hydrologic exchange and ecological consequences from bedforms to basins. Water Resour. Res. **51**: 6893–6922. doi:10.1002/2015WR017617

Harvey, J. W., J. K. Böhlke, M. A. Voytek, D. Scott, and C. R. Tobias. 2013. Hyporheic zone denitrification: Controls on effective reaction depth and

contribution to whole-stream mass balance. Water Resour. Res. **49**: 6298–6316. doi:10.1002/wrcr.20492

Harvey, J. W., M. H. Conklin, and R. S. Koelsch. 2003. Predicting changes in hydrologic retention in an evolving semi-arid alluvial stream. Adv. Water Resour. **26**: 939–950. doi:10.1016/S0309-1708(03)00085-X

Harvey, J. W., and C. C. Fuller. 1998. Effect of enhanced manganese oxidation in the hyporheic zone on basin-scale geochemical mass balance. Water Resour. Res. **34**: 623–636. doi:10.1029/97WR03606

Hassan, M. A., and R. Egozi. 2001. Impact of wastewater discharge on the channel morphology of ephemeral streams. Earth Surf. Process. Landforms **26**: 1285–1302. doi:10.1002/esp.273

Helms, J. R., A. Stubbins, J. D. Ritchie, E. C. Minor, D. J. Kieber, and K. Mopper. 2008. Absorption spectral slopes and slope ratios as indicators of molecular weight, source, and photobleaching of chromophoric dissolved organic matter. Limnol. Oceanogr. **53**: 955–969. doi:10.4319/lo.2008.53.3.0955

Hertig, E., S. Seubert, A. Paxian, G. Vogt, H. Paeth, and J. Jacobeit. 2013. Changes of total versus extreme precipitation and dry periods until the end of the twenty-first century: statistical assessments for the Mediterranean area. Theor. Appl. Climatol. **111**: 1–20. doi:10.1007/s00704-012-0639-5

Hessen, D. O., J. P. Håll, J.-E. Thrane, and T. Andersen. 2017. Coupling dissolved organic carbon, CO_2 and productivity in boreal lakes. Freshw. Biol. **62**: 945–953. doi:10.1111/fwb.12914

Hill, B. H., F. H. Mccormick, B. C. Harvey, S. L. Johnson, M. L. Warren, and C. M. Elonen. 2010. Microbial enzyme activity, nutrient uptake and nutrient limitation in forested streams. Freshw. Biol. **55**: 1005–1019. doi:10.1111/j.1365-2427.2009.02337.x

Hill, W. R., B. J. Roberts, S. N. Francoeur, and S. E. Fanta. 2011. Resource synergy in stream periphyton communities. J. Ecol. **99**: no-no. doi:10.1111/j.1365-2745.2010.01785.x

Hisdal, H., K. Stahl, L. M. Tallaksen, and S. Demuth. 2001. Have streamflow droughts in Europe become more severe or frequent? Int. J. Climatol. **21**: 317–333. doi:10.1002/joc.619

Hoellein, T. J., D. A. Bruesewitz, and D. C. Richardson. 2013. Revisiting Odum (1956): A synthesis of aquatic ecosystem metabolism. Limnol. Oceanogr. **58**: 2089–2100. doi:10.4319/lo.2013.58.6.2089

Holgerson, M. A., and P. A. Raymond. 2016. Large contribution to inland water CO2and CH4emissions from very small ponds. Nat. Geosci. **9**: 222–226.

doi:10.1038/ngeo2654

Hood, E., D. M. Mcknight, and M. W. Williams. 2003. Sources and chemical character of dissolved organic carbon across an alpine/subalpine ecotone, Green Lakes Valley, Colorado Front Range, United States. Water Resour. Res. **39**.

Hornberger, G. M., and M. G. Kelly. 1975. Atmospheric Reaeration in a River Using Productivity Analysis. J. Environ. Eng. Div. **101**: 729–739.

Hosen, J. D., O. T. McDonough, C. M. Febria, and M. A. Palmer. 2014. Dissolved organic matter quality and bioavailability changes across an urbanization gradient in headwater streams. Environ. Sci. Technol. **48**. doi:10.1021/es501422z

Hotchkiss, E. R., R. O. Hall, M. A. Baker, E. J. Rosi-Marshall, and J. L. Tank. 2014. Modeling priming effects on microbial consumption of dissolved organic carbon in rivers. J. Geophys. Res. Biogeosciences **119**: 982–995. doi:10.1002/2013JG002599

Hotchkiss, E. R., R. O. Hall Jr, R. A. Sponseller, D. Butman, J. Klaminder, H. Laudon, M. Rosvall, and J. Karlsson. 2015. Sources of and processes controlling CO2 emissions change with the size of streams and rivers. Nat. Geosci. **8**: 696–699. doi:10.1038/ngeo2507

Huguet, A., L. Vacher, S. Relexans, S. Saubusse, J. M. Froidefond, and E. Parlanti. 2009. Properties of fluorescent dissolved organic matter in the Gironde Estuary. Org. Geochem. **40**: 706–719. doi:10.1016/j.orggeochem.2009.03.002

Hynes, H. B. N. 1983. Groundwater and stream ecology. Hydrobiologia **100**: 93–99.

IPCC. 2007. Climate Change 2007 Synthesis Report,.

Jarvis, P., A. Rey, C. Petsikos, and others. 2007. Drying and wetting of Mediterranean soils stimulates decomposition and carbon dioxide emission: The “Birch effect.” *Tree Physiology*. Oxford University Press. 929–940.

Jones, J. B. 1995. Factors controlling hyporheic respiration in a desert stream. Freshw. Biol. **34**: 91–99. doi:10.1111/j.1365-2427.1995.tb00426.x

Jones, J. B., S. G. Fisher, and N. B. Grimm. 1995a. Vertical Hydrologic Exchange and Ecosystem Metabolism in a Sonoran Desert Stream. Ecology **76**: 942–952.

Jones, J. B., S. G. Fisher, and N. B. Grimm. 1995b. Nitrification in the Hyporheic Zone of a Desert Stream Ecosystem. J. North Am. Benthol. Soc. **14**: 249–258. doi:Cited By (since 1996) 92\nExport Date 4 April 2012

Jones, J. B., S. G. Fisher, and N. B. Grimm. 1996. A long-term perspective of dissolved organic carbon transport in Sycamore Creek, Arizona, USA. Hydrobiologia **317**: 183–188.

Jones Jr, J. B., S. G. Fisher, and N. B. Grimm. 1996. A long-term perspective of dissolved organic carbon transport in Sycamore Creek, Arizona, USA. Hydrobiologia **317**: 183–188.

Kalbitz, K., J. Schmerwitz, D. Schwesig, and E. Matzner. 2003. Biodegradation of soil-derived dissolved organic matter as related to its properties. Geoderma **113**: 273–291.

Kane, E. S., L. R. Mazzoleni, C. J. Kratz, J. A. Hribljan, C. P. Johnson, T. G. Pypker, and R. Chimner. 2014. Peat porewater dissolved organic carbon concentration and lability increase with warming: a field temperature manipulation experiment in a poor-fen. Biogeochemistry **119**: 161–178. doi:10.1007/s10533-014-9955-4

Kaplan, L. A., and T. L. Bott. 1982. Diel fluctuations of DOC generated by algae in a piedmont stream. Limnol. Oceanogr. **27**: 1091–1100. doi:10.4319/lo.1982.27.6.1091

Karlsson, J., P. Byström, J. Ask, P. Ask, L. Persson, and M. Jansson. 2009. Light limitation of nutrient-poor lake ecosystems. Nature **460**: 506–509. doi:10.1038/nature08179

Keeney, D. R., and D. W. Nelson. 1982. Nitrogen-inorganic forms. In A. L. Page, D. R. Keeney, D.E. Baker, R. H. Miller, R. J. Ellis and J. D. Rhoades (Eds.), Methods of Soil Analysis, p. 1982. *In* Methods of Soil Analysis Part 2.

Kim, S., L. A. Kaplan, and P. G. Hatcher. 2006. Biodegradable dissolved organic matter in a temperate and a tropical stream determined from ultra-high resolution mass spectrometry. Limnol. Oceanogr. **51**: 1054–1063.

Kothawala, D. N., C. A. Stedmon, R. A. Müller, G. A. Weyhenmeyer, S. J. Köhler, and L. J. Tranvik. 2014. Controls of dissolved organic matter quality: Evidence from a large-scale boreal lake survey. Glob. Chang. Biol. **20**: 1101–1114. doi:10.1111/gcb.12488

Krause, S., D. M. Hannah, J. H. Fleckenstein, and others. 2011. Inter-disciplinary perspectives on processes in the hyporheic zone. Ecohydrology **4**: 481–499. doi:10.1002/eco.176

Krause, S., J. Lewandowski, N. B. Grimm, and others. 2017. Ecohydrological interfaces as hot spots of ecosystem processes. Water Resour. Res. **53**: 6359–6376. doi:10.1002/2016WR019516

Kurz, M. J., J. D. Drummond, E. Martí, and others. 2017. Impacts of water level on metabolism and transient storage in vegetated lowland rivers: Insights from a mesocosm study. J. Geophys. Res. Biogeosciences **122**: 628–644. doi:10.1002/2016JG003695

Lake, P. S. 2003. Ecological effects of perturbation by drought in flowing waters.

Freshw. Biol. **48**: 1161–1172. doi:10.1046/j.1365-2427.2003.01086.x

Lakowicz, J. R. 2006. Principles of fluorescence spectroscopy, 3rd ed. Springer.

Lambert, T., C. R. Teodoru, F. C. Nyoni, S. Bouillon, F. Darchambeau, P. Massicotte, and A. V Borges. 2016. Along-stream transport and transformation of dissolved organic matter in a large tropical river. Biogeosciences **13**: 2727–2741. doi:10.5194/bg-13-2727-2016

Lapierre, J.-F., and P. A. del Giorgio. 2014. Partial coupling and differential regulation of biologically and photochemically labile dissolved organic carbon across boreal aquatic networks. Biogeosciences **11**: 5969–5985. doi:10.5194/bg-11-5969-2014

Larned, S. T., T. Datry, D. B. Arscott, and K. Tockner. 2010. Emerging concepts in temporary-river ecology. Freshw. Biol. **55**: 717–738. doi:10.1111/j.1365-2427.2009.02322.x

Larned, S. T., V. I. Nikora, and B. J. F. Biggs. 2004. Mass--transfer--limited nitrogen and phosphorus uptake by stream periphyton: A conceptual model and experimental evidence. Limnol. Oceanogr. **49**: 1992–2000.

Lawaetz, A. J., and C. A. Stedmon. 2009. Fluorescence intensity calibration using the Raman scatter peak of water. Appl. Spectrosc. **63**: 936–940.

Ledger, M. E., L. E. Brown, F. K. Edwards, A. M. Milner, and G. Woodward. 2012. Drought alters the structure and functioning of complex food webs. Nat. Clim. Chang. **3**: 223–227. doi:10.1038/nclimate1684

Legendre, P., and E. D. Gallagher. 2001. Ecologically meaningful transformations for ordination of species data. Oecologia **129**: 271–280. doi:10.1007/s004420100716

Leichtfried, M. 1996. Organic matter in bed-sediments of the River Danube and a small unpolluted stream, the Oberer Seebach. River Syst. **10**: 87–98. doi:10.1127/lr/10/1996/87

Leigh, C., A. J. Boulton, J. L. Courtwright, K. Fritz, C. L. May, R. H. Walker, and T. Datry. 2016. Ecological research and management of intermittent rivers: an historical review and future directions. Freshw. Biol. **61**: 1181–1199. doi:10.1111/fwb.12646

Ligon, F. K., W. E. Dietrich, and W. J. Trush. 1995. Downstream Ecological Effects of Dams. Bioscience **45**: 183–192. doi:10.2307/1312557

Liu, Y., C. Liu, W. C. Nelson, and others. 2017. Effect of Water Chemistry and Hydrodynamics on Nitrogen Transformation Activity and Microbial Community Functional Potential in Hyporheic Zone Sediment Columns. Environ. Sci. Technol. **51**: 4877–4886. doi:10.1021/acs.est.6b05018

Looman, A., D. T. Maher, E. Pendall, A. M. Bass, and I. R. Santos. 2017. The carbon

dioxide evasion cycle of an intermittent first-order stream : contrasting water – air and soil – air exchange. Biogeochemistry **1**–**2**: 87–102. doi:10.1007/s10533-016-0289-2

Looman, A., I. R. Santos, D. R. Tait, J. R. Webb, C. A. Sullivan, and D. T. Maher. 2016. Carbon cycling and exports over diel and flood-recovery timescales in a subtropical rainforest headwater stream. Sci. Total Environ. **550**: 645–657. doi:10.1016/j.scitotenv.2016.01.082

Lowe, W., and G. E. Likens. 2005. Moving Headwater Streams to the Head of the Class. Bioscience **55**: 196. doi:10.1641/0006-3568(2005)055[0196:MHSTTH]2.0.CO;2

Ludwig, W., E. Dumont, M. Meybeck, and S. Heussner. 2009. River discharges of water and nutrients to the Mediterranean and Black Sea: Major drivers for ecosystem changes during past and future decades? Prog. Oceanogr. **80**: 199–217. doi:10.1016/J.POCEAN.2009.02.001

Lupon, A., E. Martí, F. Sabater, and S. Bernal. 2016. Green light: Gross primary production influences seasonal stream N export by controlling fine-scale N dynamics. Ecology **97**. doi:10.1890/14-2296.1

Lyon, D. R., and S. E. Ziegler. 2009. Carbon cycling within epilithic biofilm communities across a nutrient gradient of headwater streams. Limnol. Oceanogr. **54**: 439–449. doi:10.4319/lo.2009.54.2.0439

Maiolini, B., and M. Bruno. 2008. The river continuum concept revisited: Lessons from the Alps, p. 67–76. *In* The Water Balance of the Alps, Alp. Space Man Environ. Innsbruck Univ. Press.

Martí, E., P. Fonollà, D. von Schiller, F. Sabater, A. Argerich, M. Ribot, and J. L. Riera. 2009. Variation in stream C, N and P uptake along an altitudinal gradient: a space-for-time analogue to assess potential impacts of climate change. Hydrol. Res. **40**: 123. doi:10.2166/nh.2009.090

Martí, E., N. B. Grimm, and S. G. Fisher. 1997. Pre- and Post-Flood Retention Efficiency of Nitrogen in a Sonoran Desert Stream. J. North Am. Benthol. Soc. **16**: 805–819. doi:10.2307/1468173

Mas-Martí, E., I. Muñoz, F. Oliva, and C. Canhoto. 2015. Effects of increased water temperature on leaf litter quality and detritivore performance: a whole-reach manipulative experiment. Freshw. Biol. **60**: 184–197. doi:10.1111/fwb.12485

MATLAB. 2016. version 7.10.0 (R2016a), The MathWorks Inc.

McClain, M. E., E. W. Boyer, C. L. Dent, and others. 2003. Biogeochemical Hot Spots and Hot Moments at the Interface of Terrestrial and Aquatic Ecosystems. Ecosystems **6**: 301–312. doi:10.1007/s10021-003-0161-9

McDonald, S., A. G. Bishop, P. D. Prenzler, and K. Robards. 2004. Analytical chemistry of freshwater humic substances. Anal. Chim. Acta **527**: 105–124. doi:10.1016/J.ACA.2004.10.011

Mcdonough, O. T., J. D. Hosen, and M. A. Palmer. 2011. Temporary streams: the hydrology, geography, and ecology of non-perennially flowing waters, p. 259–289. *In* River Ecosystems: Dynamics, Management and Conservation.

McGill, R., J. W. Tukey, and W. A. Larsen. 1978. Variations of Box Plots. Am. Stat. **32**: 12. doi:10.2307/2683468

McGuire, K. J., and J. Mcdonnell. 2008. Stable Isotope Tracers in Watershed Hydrology, p. 334–374. *In* Stable Isotopes in Ecology and Environmental Science: Second Edition.

McKnight, D. M., E. W. Boyer, P. K. Westerhoff, P. T. Doran, T. Kulbe, and D. T. Andersen. 2001. Spectrofluorometric characterization of dissolved organic matter for indication of precursor organic material and aromaticity. Limnol. Oceanogr. **46**: 38–48. doi:10.4319/lo.2001.46.1.0038

Medici, C., S. Bernal, A. Butturini, F. Sabater, M. Martin, A. J. Wade, and F. Frances. 2010. Modelling the inorganic nitrogen behaviour in a small Mediterranean forested catchment, Fuirosos (Catalonia). Hydrol. Earth Syst. Sci **14**: 223–237.

Medici, C., A. Butturini, S. Bernal, E. Vázquez, F. Sabater, J. I. Vélez, and F. Francés. 2008. Modelling the non-linear hydrological behaviour of a small Mediterranean forested catchment. Hydrol. Process. **22**: 3814–3828. doi:10.1002/hyp.6991

Merbt, S. N., J. C. Auguet, A. Blesa, E. Martí, and E. O. Casamayor. 2014. Wastewater Treatment Plant Effluents Change Abundance and Composition of Ammonia-Oxidizing Microorganisms in Mediterranean Urban Stream Biofilms. Microb. Ecol. **69**: 66–74. doi:10.1007/s00248-014-0464-8

Merbt, S. N., L. Proia, J. I. Prosser, E. Marti, E. O. Casamayor, and D. Von Schiller. 2016. Stream drying drives microbial ammonia oxidation and first-flush nitrate export. Ecology **97**: 2192–2198. doi:10.1002/ecy.1486

Meybeck, M. 1982. Carbon, nitrogen, and phosphorus transport by world rivers. Am. J. Sci. **282**: 401–450. doi:10.2475/ajs.282.4.401

Meybeck, M., P. Green, and C. Vörösmarty. 2001. A new typology for mountains and other relief classes: An application to global continental water resources and population distribution. Mt. Res. Dev. **21**: 34–45. doi:10.1659/0276-4741

Meybeck, M., and F. Moatar. 2012. Daily variability of river concentrations and fluxes: Indicators based on the segmentation of the rating curve. Hydrol. Process. **26**: 1188–1207. doi:10.1002/hyp.8211

Moatar, F., B. W. Abbott, C. Minaudo, F. Curie, and G. Pinay. 2017. Elemental properties, hydrology, and biology interact to shape concentration-discharge curves for carbon, nutrients, sediment, and major ions. Water Resour. Res. **53**: 1270–1287. doi:10.1002/2016WR019635

Moatar, F., M. Meybeck, S. Raymond, F. Birgand, and F. Curie. 2013. River flux uncertainties predicted by hydrological variability and riverine material behaviour. Hydrol. Process. **27**: 3535–3546. doi:10.1002/hyp.9464

de Montety, V., J. B. Martin, M. J. Cohen, C. Foster, and M. J. Kurz. 2011. Influence of diel biogeochemical cycles on carbonate equilibrium in a karst river. Chem. Geol. doi:10.1016/j.chemgeo.2010.12.025

Moody, C. S. S., F. Worrall, C. D. D. Evans, and T. G. G. Jones. 2013. The rate of loss of dissolved organic carbon (DOC) through a catchment. J. Hydrol. **492**: 139–150. doi:10.1016/j.jhydrol.2013.03.016

Mora-Gómez, J., S. Duarte, F. Cássio, C. Pascoal, and A. M. Romaní. 2018. Microbial decomposition is highly sensitive to leaf litter emersion in a permanent temperate stream. Sci. Total Environ. **621**: 486–496. doi:10.1016/j.scitotenv.2017.11.055

Moraetis, D., D. Efstathiou, F. Stamati, O. Tzoraki, N. P. Nikolaidis, J. L. Schnoor, and K. Vozinakis. 2010. High-frequency monitoring for the identification of hydrological and bio-geochemical processes in a Mediterranean river basin. J. Hydrol. **389**: 127–136. doi:10.1016/j.jhydrol.2010.05.037

Morgenschweis, G. 2010. Hydrometrie: Theorie und Praxis der Durchflussmessung in offenen Gerinnen, Springer.

Morling, K., P. Herzsprung, and N. Kamjunke. 2017. Discharge determines production of, decomposition of and quality changes in dissolved organic carbon in pre-dams of drinking water reservoirs. Sci. Total Environ. **577**: 329–339. doi:10.1016/j.scitotenv.2016.10.192

Mulholland, P. J. 1997. Organic Matter Dynamics in the West Fork of Walker Branch, Tennessee, USA. J. North Am. Benthol. Soc. **16**: 61–67. doi:10.2307/1468235

Mulholland, P. J., C. S. Fellows, J. L. Tank, and others. 2001. Inter-biome comparison of factors controlling stream metabolism. Freshw. Biol. **46**: 1503–1517. doi:10.1046/j.1365-2427.2001.00773.x

Mulholland, P. J., and W. R. Hill. 1997. Seasonal patterns in streamwater nutrient and dissolved organic carbon concentrations: Separating catchment flow path and in-stream effects. Water Resour. Res. **33**: 1297–1306. doi:10.1029/97WR00490

Müllner, A. N., and M. Schagerl. 2003. Abundance and Vertical Distribution of the Phytobenthic Community within a Pool and Riffle Sequence of an Alpine Gravel Stream. Int. Rev. Hydrobiol. **88**: 243–254. doi:10.1002/iroh.200390022

Murphy, J., and J. P. Riley. 1962. A modified single solution method for the determination of phosphate in natural waters. Anal. Chim. Acta **27**: 31–36. doi:10.1016/S0003-2670(00)88444-5

Murphy, K. R., A. Hambly, S. Singh, R. K. Henderson, A. Baker, R. Stuetz, and S. J. Khan. 2011. Organic matter fluorescence in municipal water recycling schemes: toward a unified PARAFAC model. Environ. Sci. Technol. **45**: 2909–2916.

Murphy, K. R., G. M. Ruiz, W. T. M. Dunsmuir, and T. D. Waite. 2006. Optimized parameters for fluorescence-based verification of ballast water exchange by ships. Environ. Sci. Technol. **40**: 2357–2362.

Murphy, K. R., C. A. Stedmon, D. Graeber, and R. Bro. 2013. Fluorescence spectroscopy and multi-way techniques. PARAFAC. Anal. Methods **5**: 6557. doi:10.1039/c3ay41160e

Murphy, K. R., C. A. Stedmon, P. Wenig, and R. Bro. 2014. OpenFluor– an online spectral library of auto-fluorescence by organic compounds in the environment. Anal. Methods **6**: 658–661. doi:10.1039/C3AY41935E

Murphy, M. L. 1998. Primary production, p. 144–168. *In* R.E. Bilby and R.J. Naiman [eds.], River ecology and management: lessons from the Pacific coastal ecoregion. Springer-Verlag.

Naegeli, M. W., and U. Uehlinger. 1997. Contribution of the Hyporheic Zone to Ecosystem Metabolism in a Prealpine Gravel-Bed-River. J. North Am. Benthol. Soc. **16**: 794–804. doi:10.2307/1468172

Nikolaidis, N. P., L. Demetropoulou, J. Froebrich, and others. 2013. Towards sustainable management of Mediterranean river basins: policy recommendations on management aspects of temporary streams. Water Policy **15**: 830. doi:10.2166/wp.2013.158

Odum, H. T. 1956. Primary production in flowing waters. Limnol. Oceanogr. **1**: 102–117.

Ohno, T. 2002. Fluorescence Inner-Filtering Correction for Determining the Humification Index of Dissolved Organic Matter. Environ. Sci. Technol. **36**: 742–746. doi:10.1021/es0155276

Oksanen, J., F. G. Blanchet, R. Kindt, and others. 2013. Package "vegan." R Packag. ver. 2.0–8 254. doi:10.4135/9781412971874.n145

Pachauri, R. K., L. Meyer, J.-P. Van Ypersele, S. Brinkman, L. Van Kesteren, N. Leprince-Ringuet, and F. Van Boxmeer. 2014. Climate Change 2014 Synthesis Report The Core Writing Team Core Writing Team Technical Support Unit for the Synthesis Report, IPCC.

Palmer, M. A., D. P. Lettenmaier, N. L. Poff, S. L. Postel, B. Richter, and R. Warner. 2009. Climate Change and River Ecosystems: Protection and Adaptation Options. Environ. Manage. **44**: 1053–1068. doi:10.1007/s00267-009-9329-1

Palmer, M. A., C. A. Reidy Liermann, C. Nilsson, M. Flörke, J. Alcamo, P. S. Lake, and N. Bond. 2008. Climate change and the world's river basins: anticipating management options. Front. Ecol. Environ. **6**: 81–89. doi:10.1890/060148

Parlanti, E., K. Wörz, L. Geoffroy, and M. Lamotte. 2000. Dissolved organic matter fluorescence spectroscopy as a tool to estimate biological activity in a coastal zone submitted to anthropogenic inputs. Org. Geochem. **31**: 1765–1781. doi:10.1016/S0146-6380(00)00124-8

Pastor, A., A. Lupon, L. Gomez-Gener, and others. 2017. Local and regional drivers of headwater streams metabolism: Insights from the first AIL collaborative project. Limnetica **36**: 67–85. doi:10.23818/limn.36.06

Peacock, M., C. D. Evans, N. Fenner, C. Freeman, R. Gough, T. G. Jones, and I. Lebron. 2014. UV-visible absorbance spectroscopy as a proxy for peatland dissolved organic carbon (DOC) quantity and quality: considerations on wavelength and absorbance degradation. Environ. Sci. Process. Impacts **16**: 1445. doi:10.1039/c4em00108g

Pellerin, B. A., W. M. Wollheim, X. Feng, and C. J. Vörösmarty. 2008. The application of electrical conductivity as a tracer for hydrograph separation in urban catchments. Hydrol. Process. **22**: 1810–1818.

Peralta-Maraver, I., J. Reiss, and A. L. Robertson. 2017. Interplay of hydrology, community ecology and pollutant attenuation in the hyporheic zone.doi:10.1016/j.scitotenv.2017.08.036

Perujo, N., X. Sanchez-Vila, L. Proia, and A. M. Romaní. 2017. Interaction between Physical Heterogeneity and Microbial Processes in Subsurface Sediments: A Laboratory-Scale Column Experiment. Environ. Sci. Technol. **51**: 6110–6119. doi:10.1021/acs.est.6b06506

Peter, H., G. A. Singer, C. Preiler, P. Chifflard, G. Steniczka, and T. J. Battin. 2014. Scales and drivers of temporal p CO 2 dynamics in an Alpine stream. J. Geophys. Res. Biogeosciences **119**: 1078–1091. doi:10.1002/2013JG002552

Peuravuori, J., and K. Pihlaja. 1997. Molecular size distribution and spectroscopic properties of aquatic humic substances. Anal. Chim. Acta **337**: 133–149. doi:10.1016/S0003-2670(96)00412-6

Pinheiro, J., D. Bates, S. DebRoy, and D. Sarkar. 2011. R Development Core Team. 2010. nlme: Linear and Nonlinear Mixed Effects Models. R Packag. version 3 1–97.

Placella, S. A., E. L. Brodie, and M. K. Firestone. 2012. Rainfall-induced carbon dioxide pulses result from sequential resuscitation of phylogenetically clustered microbial groups. Proc. Natl. Acad. Sci. **109**: 10931–10936. doi:10.1073/pnas.1204306109

Poblador, S., A. Lupon, S. Sabaté, and F. Sabater. 2017. Soil water content drives spatiotemporal patterns of CO 2 and N 2 O emissions from a Mediterranean riparian forest soil. Biogeosciences **145194**: 4195–4208. doi:10.5194/bg-14-4195-2017

Poff, N. L., and J. K. H. Zimmerman. 2010. Ecological responses to altered flow regimes: A literature review to inform the science and management of environmental flows. Freshw. Biol. **55**: 194–205. doi:10.1111/j.1365-2427.2009.02272.x

Pohlon, E., A. O. Fandino, and J. Marxsen. 2013a. Bacterial community composition and extracellular enzyme activity in temperate streambed sediment during drying and rewetting. PLoS One **8**. doi:10.1371/journal.pone.0083365

Pohlon, E., C. Mätzig, and J. Marxsen. 2013b. Desiccation affects bacterial community structure and function in temperate stream sediments. Fundam. Appl. Limnol. / Arch. für Hydrobiol. **182**: 123–134. doi:10.1127/1863-9135/2013/0465

Preiner, S., I. Drozdowski, M. Schagerl, F. Schiemer, and T. Hein. 2008. The significance of side-arm connectivity for carbon dynamics of the River Danube, Austria. Freshw. Biol. **53**: 238–252. doi:10.1111/j.1365-2427.2007.01888.x

Proia, L., D. von Schiller, C. Gutierrez, and others. 2016. Microbial carbon processing along a river discontinuum. Freshw. Sci. **35**. doi:10.1086/689181

Rasilo, T., R. H. S. Hutchins, C. Ruiz-González, and P. A. del Giorgio. 2017. Transport and transformation of soil-derived CO2, CH4 and DOC sustain CO2 supersaturation in small boreal streams. Sci. Total Environ. **579**: 902–912. doi:10.1016/J.SCITOTENV.2016.10.187

R Team Development Core. 2008. R: A Language and Environment for Statistical Computing.

Ratkowsky, D. A. 2016. Choosing the number of principal coordinates when using CAP, the canonical analysis of principal coordinates. Austral Ecol. **41**: 842–851. doi:10.1111/aec.12378

Raymond, P. A., and J. J. Cole. 2001. Gas Exchange in Rivers and Estuaries: Choosing a Gas Transfer Velocity. Estuaries **24**: 312. doi:10.2307/1352954

Raymond, P. A., J. Hartmann, R. Lauerwald, and others. 2013. Global carbon dioxide emissions from inland waters. Nature **503**: 355–359. doi:10.1038/nature12760

Raymond, P. A., and J. E. Saiers. 2010. Event controlled DOC export from forested watersheds. Biogeochemistry **100**: 197–209. doi:10.1007/s10533-010-9416-7

Raymond, P. A., J. E. Saiers, and W. V Sobczak. 2016. Hydrological and biogeochemical controls on watershed dissolved organic matter transport: pulse-shunt concept. Ecology **97**: 5–16. doi:10.1890/14-1684.1

Reardon, J. 1966. Salicylate method for the quantitative determination of ammonia nitrogen.

Reichert, P., U. Uehlinger, and V. Acuña. 2009. Estimating stream metabolism from oxygen concentrations: Effect of spatial heterogeneity. J. Geophys. Res. Biogeosciences **114**: n/a--n/a. doi:10.1029/2008JG000917

Riley, A. J., and W. K. Dodds. 2013. Whole-stream metabolism: strategies for measuring and modeling diel trends of dissolved oxygen. Freshw. Sci. **32**: 56–69. doi:10.1899/12-058.1

Roberts, B. J., P. J. Mulholland, and W. R. Hill. 2007. Multiple scales of temporal variability in ecosystem metabolism rates: Results from 2 years of continuous monitoring in a forested headwater stream. Ecosystems **10**: 588–606.

Robertson, A. L., and P. J. Wood. 2010. Ecology of the hyporheic zone: origins, current knowledge and future directions. Fundam. Appl. Limnol. / Arch. für Hydrobiol. **176**: 279–289. doi:10.1127/1863-9135/2010/0176-0279

Robinson, C. T., D. Tonolla, B. Imhof, R. Vukelic, and U. Uehlinger. 2016. Flow intermittency, physico-chemistry and function of headwater streams in an Alpine glacial catchment. Aquat. Sci. **78**: 327–341. doi:10.1007/s00027-015-0434-3

Romaní, A. M., S. Amalfitano, J. Artigas, S. Fazi, S. Sabater, X. Timoner, I. Ylla, and A. Zoppini. 2013. Microbial biofilm structure and organic matter use in mediterranean streams, Springer Netherlands.

Romaní, A. M., E. Chauvet, C. Febria, J. Mora-Gómez, U. Risse-Buhl, X. Timoner, M. Weitere, and L. Zeglin. 2017. The Biota of Intermittent Rivers and Ephemeral Streams: Prokaryotes, Fungi, and Protozoans, p. 161–188. *In* Intermittent Rivers and Ephemeral Streams. Elsevier.

Romaní, A. M., K. Fund, J. Artigas, T. Schwartz, S. Sabater, and U. Obst. 2008. Relevance of polymeric matrix enzymes during biofilm formation. Microb. Ecol. **56**: 427–436. doi:10.1007/s00248-007-9361-8

Romaní, A. M., A. Giorgi, V. Acuña, and S. Sabater. 2004. The influence of substratum type and nutrient supply on biofilm organic matter utilization in streams. Limnol. Oceanogr. **49**: 1713–1721. doi:10.4319/lo.2004.49.5.1713

Romaní, A. M., E. Vázquez, and A. Butturini. 2006. Microbial Availability and Size

Fractionation of Dissolved Organic Carbon After Drought in an Intermittent Stream: Biogeochemical Link Across the Stream–Riparian Interface. Microb. Ecol. **52**: 501–512. doi:10.1007/s00248-006-9112-2

Rudolf von Rohr, M., J. G. Hering, H. P. E. Kohler, and U. Von Gunten. 2014. Column studies to assess the effects of climate variables on redox processes during riverbank filtration. Water Res. **61**: 263–275. doi:10.1016/j.watres.2014.05.018

Ruhala, S. S., and J. P. Zarnetske. 2017. Using in-situ optical sensors to study dissolved organic carbon dynamics of streams and watersheds: A review. Sci. Total Environ. **575**: 713–723. doi:10.1016/j.scitotenv.2016.09.113

Sabater, F., A. Butturini, E. MartÍ, I. Muñoz, A. Romaní, J. Wray, and S. Sabater. 2000. Effects of riparian vegetation removal on nutrient retention in a Mediterranean stream. J. North Am. Benthol. Soc. **19**: 609–620. doi:10.2307/1468120

Sabater, S., V. Acuna, A. Giorgi, E. Guerra, I. Munoz, and A. M. Romani. 2005. Effects of nutrient inputs in a forested Mediterranean stream under moderate light availability. Arch. Fur Hydrobiol. **163**: 479–496. doi:10.1127/0003-9136/2005/0163-0479

Sabater, S., J. Artigas, A. Gaudes, I. Muñoz, G. Urrea, and A. M. Romaní. 2011. Long-term moderate nutrient inputs enhance autotrophy in a forested Mediterranean stream. Freshw. Biol. **56**: 1266–1280. doi:10.1111/j.1365-2427.2010.02567.x

Sabater, S., A. Butturini, I. Muñoz, A. Romaní, J. Wray, and F. Sabater. 1997. Effects of removal of riparian vegetation on algae and heterotrophs in a Mediterranean stream. J. Aquat. Ecosyst. Stress Recover. **6**: 129–140. doi:10.1023/A:1009938511352

Sabater, S., A. Elosegi, V. Acuña, A. Basaguren, I. Muñoz, and J. Pozo. 2008. Effect of climate on the trophic structure of temperate forested streams. A comparison of Mediterranean and Atlantic streams. Sci. Total Environ. **390**: 475–484. doi:10.1016/j.scitotenv.2007.10.030

Sabater, S., and A. M. Romani. 1996. Metabolic changes associated with biofilm formation in an undisturbed Mediterranean stream. Hydrobiologia **335**: 107–113. doi:10.1007/BF00015272

Sabater, S., and K. Tockner. 2009. Effects of Hydrologic Alterations on the Ecological Quality of River Ecosystems, p. 15–39. *In* Springer, Berlin, Heidelberg.

Salonen, K., and A. Vähätalo. 1994. Photochemical mineralisation of dissolved organic matter in lake Skjervatjern. Environ. Int. **20**: 307–312. doi:10.1016/0160-4120(94)90114-7

Sand-Jensen, K., N. L. Pedersen, and M. Sondergaard. 2007. Bacterial metabolism in small temperate streams under contemporary and future climates. Freshw. Biol.

52: 2340–2353. doi:10.1111/j.1365-2427.2007.01852.x

Sandford, R. C., R. Bol, and P. J. Worsfold. 2010. In situ determination of dissolved organic carbon in freshwaters using a reagentless UV sensor. J. Environ. Monit. **12**: 1678–1683. doi:10.1039/C0EM00060D

Saraceno, J. F., B. A. Pellerin, B. D. Downing, E. Boss, P. Am Bachand, and B. A. Bergamaschi. 2009. High-frequency in situ optical measurements during a storm event: Assessing relationships between dissolved organic matter, sediment concentrations, and hydrologic processes. J. Geophys. Res. Biogeosciences **114**.

Schädler, B., and R. Weingartner. 2010. Impact of Climate Change on Water Resources in the Alpine Regions of Switzerland, p. 59–69. *In* Springer, Berlin, Heidelberg.

Schelker, J., T. Grabs, K. Bishop, and H. Laudon. 2013. Drivers of increased organic carbon concentrations in stream water following forest disturbance: Separating effects of changes in flow pathways and soil warming. J. Geophys. Res. Biogeosciences **118**: 1814–1827. doi:10.1002/2013JG002309

Schelker, J., G. A. Singer, A. J. Ulseth, S. Hengsberger, and T. J. Battin. 2016. CO 2 evasion from a steep, high gradient stream network: importance of seasonal and diurnal variation in aquatic pCO 2 and gas transfer. Limnol. Oceanogr. **61**: 1826–1838. doi:10.1002/lno.10339

von Schiller, D., V. Acuña, D. Graeber, E. Martí, M. Ribot, S. Sabater, X. Timoner, and K. Tockner. 2011. Contraction, fragmentation and expansion dynamics determine nutrient availability in a Mediterranean forest stream. Aquat. Sci. **73**: 485–497. doi:10.1007/s00027-011-0195-6

von Schiller, D., S. Bernal, F. Sabater, and E. Martí. 2015. A round-trip ticket: the importance of release processes for in-stream nutrient spiraling. Freshw. Sci. **34**: 20–30. doi:10.1086/679015

von Schiller, D., D. Graeber, M. Ribot, X. Timoner, V. Acuña, E. Martí, S. Sabater, and K. Tockner. 2015. Hydrological transitions drive dissolved organic matter quantity and composition in a temporary Mediterranean stream. Biogeochemistry **123**: 429–446. doi:10.1007/s10533-015-0077-4

von Schiller, D., R. Marcé, B. Obrador, L. Gómez-Gener, J. Casas-Ruiz, V. Acuña, and M. Koschorreck. 2014. Carbon dioxide emissions from dry watercourses. Inl. Waters **4**: 377–382. doi:10.5268/IW-4.4.746

von Schiller, D., E. Martí, J. L. Riera, M. Ribot, A. Argerich, P. Fonollà, and F. Sabater. 2008. Inter-annual, annual, and seasonal variation of P and N retention in a perennial and an intermittent stream. Ecosystems **11**: 670–687. doi:10.1007/s10021-008-9150-3

von Schiller, D., E. Martí, J. L. Riera, and F. Sabater. 2007. Effects of nutrients and

light on periphyton biomass and nitrogen uptake in Mediterranean streams with contrasting land uses. Freshw. Biol. **52**: 891–906. doi:10.1111/j.1365-2427.2007.01742.x

Schindler, J. E., and D. P. Krabbenhoft. 1998. The Hyporheic Zone as a Source of Dissolved Organic Carbon Gases to a Temperate Forest Stream. Biogeochemistry **43**: 157–174. doi:10.1023/A:1006005311257

Siebers, A. R., N. E. Pettit, G. Skrzypek, J. B. Fellman, S. Dogramaci, and P. F. Grierson. 2016. Alluvial ground water influences dissolved organic matter biogeochemistry of pools within intermittent dryland streams. Freshw. Biol. **61**: 1228–1241. doi:10.1111/fwb.12656

Singer, G., K. Besemer, P. Schmitt-Kopplin, I. Hödl, and T. J. Battin. 2010. Physical Heterogeneity Increases Biofilm Resource Use and Its Molecular Diversity in Stream Mesocosms T. Bell [ed.]. PLoS One **5**: e9988. doi:10.1371/journal.pone.0009988

Sivirichi, G. M., S. S. Kaushal, P. M. Mayer, C. Welty, K. T. Belt, T. A. Newcomer, K. D. Newcomb, and M. M. Grese. 2011. Longitudinal variability in streamwater chemistry and carbon and nitrogen fluxes in restored and degraded urban stream networks. J. Environ. Monit. **13**: 288–303. doi:10.1039/C0EM00055H

Skoulikidis, N., and Y. Amaxidis. 2009. Origin and dynamics of dissolved and particulate nutrients in a minimally disturbed Mediterranean river with intermittent flow. J. Hydrol. **373**: 218–229. doi:10.1016/J.JHYDROL.2009.04.032

Skoulikidis, N. T., S. Sabater, T. Datry, and others. 2017a. Non-perennial Mediterranean rivers in Europe: Status, pressures, and challenges for research and management. Sci. Total Environ. **577**: 1–18. doi:10.1016/J.SCITOTENV.2016.10.147

Skoulikidis, N. T., L. Vardakas, Y. Amaxidis, and P. Michalopoulos. 2017b. Biogeochemical processes controlling aquatic quality during drying and rewetting events in a Mediterranean non-perennial river reach. Sci. Total Environ. **575**: 378–389. doi:10.1016/j.scitotenv.2016.10.015

Sleighter, R. L., R. M. Cory, L. A. Kaplan, H. A. N. Abdulla, and P. G. Hatcher. 2014. A coupled geochemical and biogeochemical approach to characterize the bioreactivity of dissolved organic matter from a headwater stream. J. Geophys. Res. Biogeosciences **119**: 1520–1537. doi:10.1002/2013JG002600

Smith, R. M., and S. S. Kaushal. 2015. Carbon cycle of an urban watershed: exports, sources, and metabolism. Biogeochemistry **126**: 173–195. doi:10.1007/s10533-015-0151-y

Sobczak, W. V., and S. Findlay. 2002. Variation in Bioavailability of Dissolved Organic Carbon among Stream Hyporheic Flowpaths. Ecology **83**: 3194.

doi:10.2307/3071853

Solomon, S., G.-K. Plattner, R. Knutti, and P. Friedlingstein. 2009. Irreversible climate change due to carbon dioxide emissions. Proc. Natl. Acad. Sci. U. S. A. **106**: 1704–9. doi:10.1073/pnas.0812721106

Sponseller, R. A. 2007. Precipitation pulses and soil CO2 flux in a Sonoran Desert ecosystem. Glob. Chang. Biol. **13**: 426–436. doi:10.1111/j.1365-2486.2006.01307.x

Stanley, E. H., S. M. Powers, N. R. Lottig, I. Buffam, J. T. Crawford, E. I. L Y H St A N Le Y, and C. Ford. 2012. Contemporary changes in dissolved organic carbon (DOC) in human-dominated rivers: Is there a role for DOC management? Freshw. Biol. **57**: 26–42. doi:10.1111/j.1365-2427.2011.02613.x

Stedmon, C. A., and R. Bro. 2008. Characterizing dissolved organic matter fluorescence with parallel factor analysis: a tutorial. Limnol. Oceanogr. Methods **6**: 572–579. doi:10.4319/lom.2008.6.572

Stegen, J. C., J. K. Fredrickson, M. J. Wilkins, and others. 2016. Groundwater–surface water mixing shifts ecological assembly processes and stimulates organic carbon turnover. Nat. Commun. **7**: 11237. doi:10.1038/ncomms11237

Stern, N., M. Ginder-Vogel, J. C. Stegen, E. Arntzen, D. W. Kennedy, B. R. Larget, and E. E. Roden. 2017. Colonization Habitat Controls Biomass, Composition, and Metabolic Activity of Attached Microbial Communities in the Columbia River Hyporheic Corridor. Appl. Environ. Microbiol. **83**: e00260-17. doi:10.1128/AEM.00260-17

Sterner, R. W., J. J. Elser, E. J. Fee, S. J. Guildford, and T. H. Chrzanowski. 1997. The Light: Nutrient Ratio in Lakes: The Balance of Energy and Materials Affects Ecosystem Structure and Process. Am. Nat. **150**: 663–684. doi:10.1086/286088

Steward, A. L., D. von Schiller, K. Tockner, J. C. Marshall, and S. E. Bunn. 2012. When the river runs dry: human and ecological values of dry riverbeds. Front. Ecol. Environ. **10**: 202–209. doi:10.1890/110136

Stor, D., and H. Craig. 1961. Isotopic Variations in Meteoric Waters. Sci. New Ser. **133**: 1702–1703.

Storey, R. G., R. R. Fulthorpe, and D. D. Williams. 1999. Perspectives and predictions on the microbial ecology of the hyporheic zone. Freshw. Biol. **41**: 119–130. doi:10.1046/j.1365-2427.1999.00377.x

Storey, R. G., D. D. Williams, and R. R. Fulthorpe. 2004. Nitrogen processing in the hyporheic zone of a pastoral stream. Biogeochemistry **69**: 285–313. doi:10.1023/B:BIOG.0000031049.95805.ec

Suberkropp, K. F. 1998. Microorganisms and organic matter decomposition, p. 144–168. *In* R.E. Bilby and R.J. Naiman [eds.], River ecology and management: lessons from the Pacific coastal ecoregion. Springer-Verlag.

Tamooh, F., A. V. Borges, F. J. R. Meysman, K. Van Den Meersche, F. Dehairs, R. Merckx, and S. Bouillon. 2013. Dynamics of dissolved inorganic carbon and aquatic metabolism in the Tana River basin, Kenya. Biogeosciences **10**: 6911–6928. doi:10.5194/bg-10-6911-2013

Timoner, X., V. Acuña, D. Von Schiller, and S. Sabater. 2012. Functional responses of stream biofilms to flow cessation, desiccation and rewetting. Freshw. Biol. **57**: 1565–1578. doi:10.1111/j.1365-2427.2012.02818.x

Timoner, X., C. M. Borrego, V. Acuña, and S. Sabater. 2014. The dynamics of biofilm bacterial communities is driven by flow wax and wane in a temporary stream. Limnol. Oceanogr. **59**: 2057–2067. doi:10.4319/lo.2014.59.6.2057

Triska, F. J., J. H. Duff, and R. J. Avanzino. 1990. Influence of Exchange Flow Between the Channel and Hyporheic Zone on Nitrate Production in a Small Mountain Stream. Can. J. Fish. Aquat. Sci. **47**: 2099–2111. doi:10.1139/f90-235

Tzoraki, O., N. P. Nikolaidis, Y. Amaxidis, and N. T. Skoulikidis. 2007. In-stream biogeochemical processes of a temporary river. Environ. Sci. Technol. **41**: 1225–1231. doi:10.1021/es062193h

Uehlinger, U., and M. W. Naegeli. 1998. Ecosystem Metabolism, Disturbance, and Stability in a Prealpine Gravel Bed River. J. North Am. Benthol. Soc. **17**: 165–178. doi:10.2307/1467960

Ulseth, A. J., E. Bertuzzo, G. A. Singer, J. Schelker, and T. J. Battin. 2017. Climate-Induced Changes in Spring Snowmelt Impact Ecosystem Metabolism and Carbon Fluxes in an Alpine Stream Network. Ecosystems 1–18. doi:10.1007/s10021-017-0155-7

Valett, H. M., S. G. Fisher, and E. H. Stanley. 1990. Physical and Chemical Characteristics of the Hyporheic Zone of a Sonoran Desert Stream Published by : The North American Benthological Society Sonoran Desert stream. J. North Am. Benthol. Soc. **9**: 201–215.

Vannote, R. R. L., G. W. Minshall, K. W. Cummins, J. R. Sedell, and C. E. Cushing. 1980. The river continuum concept. Can. J. Fish. Aquat. Sci. **37**: 130–137. doi:10.1139/f80-017

Vazquez, E., V. Acuña, J. Artigas, and others. 2013. Fourteen years of hydro-biogeochemical monitoring in a Mediterranean catchment. Bodenkultur **64**: 13–20.

Vázquez, E., S. Amalfitano, S. Fazi, and A. Butturini. 2011. Dissolved organic matter

composition in a fragmented Mediterranean fluvial system under severe drought conditions. Biogeochemistry **102**: 59–72. doi:10.1007/s10533-010-9421-x

Vázquez, E., E. Ejarque, I. Ylla, A. M. Romaní, and A. Butturini. 2015. Impact of drying/rewetting cycles on the bioavailability of dissolved organic matter molecular-weight fractions in a Mediterranean stream. Freshw. Sci. **34**: 263–275. doi:10.1086/679616

Vázquez, E., A. M. Romaní, F. Sabater, and A. Butturini. 2007. Effects of the Dry–Wet Hydrological Shift on Dissolved Organic Carbon Dynamics and Fate Across Stream–Riparian Interface in a Mediterranean Catchment. Ecosystems **10**: 239–251. doi:10.1007/s10021-007-9016-0

Velasco, J., A. Millan, M. R. Vidal-Abarca, M. L. Suarez, C. Guerrero, and M. Ortega. 2003. Macrophytic, epipelic and epilithic primary production in a semiarid Mediterranean stream. Freshw. Biol. **48**: 1408–1420. doi:10.1046/j.1365-2427.2003.01099.x

Vervier, P., M. Dobson, and G. Pinay. 1993. Role of interaction zones between surface and ground waters in DOC transport and processing: considerations for river restoration. Freshw. Biol. **29**: 275–284. doi:10.1111/j.1365-2427.1993.tb00763.x

Villanueva, V. D., J. Font, T. Schwartz, and A. M. Romaní. 2011. Biofilm formation at warming temperature: acceleration of microbial colonization and microbial interactive effects. Biofouling **27**: 59–71. doi:10.1080/08927014.2010.538841

Viviroli, D., D. R. Archer, W. Buytaert, and others. 2011. Climate change and mountain water resources: overview and recommendations for research, management and policy. Hydrol. Earth Syst. Sci **15**: 471–504. doi:10.5194/hess-15-471-2011

Viviroli, D., H. H. Dürr, B. Messerli, M. Meybeck, and R. Weingartner. 2007. Mountains of the world, water towers for humanity: Typology, mapping, and global significance. Water Resour. Res. **43**. doi:10.1029/2006WR005653

Volk, C. J., C. B. Volk, and L. A. Kaplan. 1997. Chemical composition of biodegradable dissolved organic matter in streamwater. Limnol. Oceanogr. **42**: 39–44. doi:10.4319/lo.1997.42.1.0039

Vörösmarty, C. J., P. B. McIntyre, M. O. Gessner, and others. 2010. Global threats to human water security and river biodiversity. Nature **467**: 555–561. doi:10.1038/nature09440

Wagner, K., M. M. Bengtsson, K. Besemer, A. Sieczko, N. R. Burns, E. R. Herberg, and T. J. Battin. 2014. Functional and structural responses of hyporheic biofilms to varying sources of dissolved organic matter. Appl. Environ. Microbiol. **80**: 6004–12. doi:10.1128/AEM.01128-14

Wagner, K., M. M. Bengtsson, R. H. Findlay, T. J. Battin, and A. J. Ulseth. 2017. High

light intensity mediates a shift from allochthonous to autochthonous carbon use in phototrophic stream biofilms. J. Geophys. Res. Biogeosciences **122**: 1806–1820. doi:10.1002/2016JG003727

Wallace, J. B., and S. L. Eggert. 2015. Terrestrial and Longitudinal Linkages of Headwater Streams. Southeast. Nat. **14**: 65–86. doi:10.1656/058.014.sp709

Ward, J. V, and J. A. Stanford. 1982. Thermal Responses in the Evolutionary Ecology of Aquatic Insects. Annu. Rev. Entomol. **27**: 97–117. doi:10.1146/annurev.en.27.010182.000525

Webster, J. R., and J. L. Meyer. 1997. Organic Matter Budgets for Streams: A Synthesis. J. North Am. Benthol. Soc. **16**: 141–161. doi:10.2307/1468247

Weishaar, J. L., G. R. Aiken, B. A. Bergamaschi, M. S. Fram, R. Fujii, and K. Mopper. 2003. Evaluation of Specific Ultraviolet Absorbance as an Indicator of the Chemical Composition and Reactivity of Dissolved Organic Carbon. Environ. Sci. Technol. **37**: 4702–4708. doi:10.1021/es030360x

Weiß, M., M. Flörke, L. Menzel, and J. Alcamo. 2007. Model-based scenarios of Mediterranean droughts. Adv. Geosci **12**: 145–151.

Wetzel, R. G. 1984. Detrial dissolved and particulate organic carbon functions in aquatic ecosystems. **35**: 503–509.

Wiegner, T. N., R. L. Tubal, and R. A. MacKenzie. 2009. Bioavailability and export of dissolved organic matter from a tropical river during base- and stormflow conditions. Limnol. Oceanogr. **54**: 1233–1242. doi:10.4319/lo.2009.54.4.1233

Williams, D. D. 2007. The Biology of Temporary Waters,.

Wilson, H. F., and M. A. Xenopoulos. 2009. Effects of agricultural land use on the composition of fluvial dissolved organic matter. Nat. Geosci. **2**: 37–41. doi:Doi 10.1038/Ngeo391

Wohl, E., K. Dwire, N. Sutfin, L. Polvi, and R. Bazan. 2012. Mechanisms of carbon storage in mountainous headwater rivers. Nat. Commun. **3**. doi:10.1038/ncomms2274

Wohl, E., R. O. Hall, K. B. Lininger, N. A. Sutfin, and D. M. Walters. 2017. Carbon dynamics of river corridors and the effects of human alterations. Ecol. Monogr. **87**: 379–409. doi:10.1002/ecm.1261

Wolfaardt, G. M., J. R. Lawrence, R. D. Robarts, and D. E. Caldwell. 1994. The role of interactions, sessile growth, and nutrient amendments on the degradative efficiency of a microbial consortium. Can. J. Microbiol. **40**: 331–340. doi:10.1139/m94-055

Wondzell, S. M., and M. N. Gooseff. 2013. Geomorphic Controls on Hyporheic

Exchange Across Scales: Watersheds to Particles, p. 203–218. *In* Treatise on Geomorphology.

Wu, J., C. Miao, X. Zhang, T. Yang, and Q. Duan. 2017. Detecting the quantitative hydrological response to changes in climate and human activities. Sci. Total Environ. **586**: 328–337. doi:10.1016/J.SCITOTENV.2017.02.010

Ylla, I., I. Sanpera-Calbet, I. Muñoz, A. M. Romaní, and S. Sabater. 2011. Organic matter characteristics in a Mediterranean stream through amino acid composition: Changes driven by intermittency. Aquat. Sci. **73**: 523–535. doi:10.1007/s00027-011-0211-x

Ylla, I., I. Sanpera-Calbet, E. Vázquez, A. M. Romaní, I. Muñoz, A. Butturini, and S. Sabater. 2010. Organic matter availability during pre- and post-drought periods in a Mediterranean stream. Hydrobiologia **657**: 217–232. doi:10.1007/s10750-010-0193-z

Young, R. G., and A. D. Huryn. 1996. Interannual variation in discharge controls ecosystem metabolism along a grassland river continuum. Can. J. Fish. Aquat. Sci. **53**: 2199–2211. doi:10.1139/f96-186

Yvon-Durocher, G., J. M. Caffrey, A. Cescatti, and others. 2012. Reconciling the temperature dependence of respiration across timescales and ecosystem types. Nature **487**: 472–476. doi:10.1038/nature11205

Zarnetske, J. P., M. N. Gooseff, T. R. Brosten, J. H. Bradford, J. P. McNamara, and W. B. Bowden. 2007. Transient storage as a function of geomorphology, discharge, and permafrost active layer conditions in Arctic tundra streams. Water Resour. Res. **43**. doi:10.1029/2005WR004816

Zarnetske, J. P., R. Haggerty, S. M. Wondzell, and M. A. Baker. 2011a. Dynamics of nitrate production and removal as a function of residence time in the hyporheic zone. J. Geophys. Res. **116**: G01025. doi:10.1029/2010JG001356

Zarnetske, J. P., R. Haggerty, S. M. Wondzell, and M. A. Baker. 2011b. Labile dissolved organic carbon supply limits hyporheic denitrification. J. Geophys. Res. **116**: G04036. doi:10.1029/2011JG001730

Zhu, T., and M. Dittrich. 2016. Carbonate Precipitation through Microbial Activities in Natural Environment, and Their Potential in Biotechnology: A Review. Front. Bioeng. Biotechnol. **4**: 4. doi:10.3389/fbioe.2016.00004

Zoppini, A., S. Amalfitano, S. Fazi, and A. Puddu. 2010. Dynamics of a benthic microbial community in a riverine environment subject to hydrological fluctuations (Mulargia River, Italy). Hydrobiologia **657**: 37–51. doi:10.1007/s10750-010-0199-6

Zoppini, A., and J. Marxsen. 2010. Importance of Extracellular Enzymes for

Biogeochemical Processes in Temporary River Sediments during Fluctuating Dry–Wet Conditions, p. 103–117. *In* Springer, Berlin, Heidelberg.

Annex

11 Annex

11.1 Supplementary Information Chapter 1

Table SI 1: Fluorescence maxima of the four PARAFAC components

Component 1	
Ex	
296	0.1259
Em	
379	0.0774
403	0.1045
405	0.1054
409	0.1063
411	0.1063
417	0.1076
420	0.1078
422	0.1076
425	0.1068
432	0.1043
Component 2	
Ex	
251	0.084
349	0.1748
Em	
313	0.0007
317	0.0007
443	0.1218
447	0.1223
451	0.1224
457	0.1216
460	0.1201
Component 3	
Ex	
263	0.1088
383	0.1494
Em	
344	0.0027
346	0.0027
474	0.1594
476	0.1593
479	0.159
Component 4	
Ex	
274	0.1982
276	0.1988
Em	
322	0.1671
394	0.0145
406	0.025
420	0.0151

Table SI 2: Average and SD of chemical parameters of HZ_{up}, pool and HZ_{dw} for the different hydrological phases. Discharge ranges between pool and HZ_{dw} for the different hydrological phases and punctual measurements of water stable isotopes

Location	Hydrology	n	T (ºC)	EC (μS cm^{-1})	pH	DO (mg L^{-1})	ln([O_2^-]/[N–NH_4^+])	DOC (mg L^{-1})	Q (L s^{-1})	δD ‰	$\delta^{18}O$ ‰
HZ_{up}	Pre-drought	4	19 ± 3.3	236.8 ± 11.5	6.9 ± 0.1	2.9 ± 1.9	4.4 ± 1.3	3.7 ± 0.1	ranges	*n*=1	*n*=1
HZ_{up}	Contraction	5	19.8 ± 0.8	251 ± 15.1	7 ± 0.2	0.9 ± 0.6	2.2 ± 0.7	3.4 ± 1.3		-4.55	-28.4
HZ_{up}	Frag-mentation	4	20.8 ± 0.6	324.3 ± 19.9	7 ± 0.3	0.8 ± 0.5	2.2 ± 0.6	2.7 ± 0.5		-4.73	-27.2
HZ_{up}	Dry	4	21.4 ± 0.4	368.5 ± 17.9	7 ± 0.2	1.1 ± 0.2	2.4 ± 0.5	2.1 ± 0.2		-4.87	-28.9
HZ_{up}	Rewetting	2	18.6 ± 0.2	221.5 ± 0.7	7.1 ± 0.1	3.8 ± 0.1	4.8 ± 0.3	5.6 ± 0.5			
Pool	Pre-drought	4	19.6 ± 4.7	230.3 ± 6.7	7 ± 0.2	7.7 ± 2.2	5.5 ± 0.4	2.6 ± 0.3	6-3.5		
Pool	Contraction	5	21.7 ± 2.1	255 ± 8.6	7 ± 0.2	7 ± 1	5.6 ± 0.4	2.5 ± 0.2	1-0.5	-3.96	-25.8
Pool	Frag-mentation	4	20 ± 1.4	284.8 ± 10.6	6.9 ± 0	4.5 ± 0.5	4.8 ± 0.4	3.1 ± 0.4	0.07-0.04	-4.91	-29.6
Pool	Dry	4	22.9 ± 1	330 ± 16	6.9 ± 0.1	4.7 ± 1.2	5 ± 0.3	4.1 ± 0.3	0.007-0	-4.31	-25.8
Pool	Rewetting	2	17.6 ± 0.1	227.5 ± 0.7	7.5 ± 0.1	9.9 ± 0	6.3 ± 0.1	5.9 ± 1	40-20		
HZ_{dw}	Pre-drought	4	18.4 ± 0	235.5 ± 8.7	6.9 ± 0.2	1.5 ± 0.3	4.5 ± 0.5	2.9 ± 0.7			
HZ_{dw}	Contraction	5	20.5 ± 0	254 ± 8.9	6.9 ± 0.1	1.1 ± 0.7	3.2 ± 2.3	2.4 ± 0.4		-3.85	-25.9
HZ_{dw}	Frag-mentation	4	20.1 ± 0.6	284 ± 8.9	7.1 ± 0.3	0.4 ± 0.2	2.8 ± 0.6	2.7 ± 0.5		-4.51	-27.8
HZ_{dw}	Dry	4	21 ± 0.4	325.3 ± 21.9	6.7 ± 0	0.5 ± 0.3	2 ± 0.5	3.1 ± 0.2		-4.54	-27.3
HZ_{dw}	Rewetting	2	18.1 ± 0.4	222 ± 2.8	7.1 ± 0	4.2 ± 0.2	5.3 ± 0.3	5.2 ± 0.7			

Table SI 3: Original input to PCA

Location	Date	Hydrology	FI	HIX	BIX	SR	$SUVA_{254}$	$E_2:E_3$	C1 (%)	C2 (%)	C3 (%)	C4 (%)
Pool	5/6/2014	pre-drought	1.50	0.82	0.53	0.86	2.63	5.82	30.80	32.28	26.77	10.15
SWdw	5/6/2014	pre-drought	1.50	0.83	0.52	0.89	2.35	6.20	30.55	33.39	26.40	9.66
SWup	5/6/2014	pre-drought	1.50	0.82	0.55	0.86	2.33	5.82	32.06	30.65	25.05	12.24
HZdw	5/6/2014	pre-drought	1.60	0.65	0.51	1.03	2.20	5.55	31.36	26.41	20.02	22.21
HZup	5/6/2014	pre-drought	1.50	0.75	0.54	0.91	1.74	6.45	34.82	25.97	22.15	17.05
Lateral	5/6/2014	pre-drought	1.55	0.84	0.55	0.83	2.25	7.30	32.23	32.83	25.78	9.16
Pool	11/6/2014	pre-drought	1.48	0.85	0.55	0.93	2.30	6.44	30.31	32.76	28.19	8.74
HZdw	11/6/2014	pre-drought	1.48	0.80	0.54	1.39	2.17	7.42	30.70	30.69	26.53	12.08
HZup	11/6/2014	pre-drought	1.49	0.78	0.55	0.76	1.70	7.22	32.05	28.30	25.18	14.48
Lateral	11/6/2014	pre-drought	1.54	0.80	0.61	1.02	1.50	9.71	30.86	30.41	25.19	13.55
Pool	19/6/2014	pre-drought	1.50	0.87	0.57	0.67	2.27	6.64	31.21	33.25	27.93	7.60
HZdw	19/6/2014	pre-drought	1.60	0.88	0.58	0.69	2.18	7.88	28.94	34.25	30.24	6.58
HZup	19/6/2014	pre-drought	1.51	0.85	0.55	0.87	1.84	7.20	31.30	32.25	26.91	9.55
Pool	23/6/2014	pre-drought	1.38	0.83	0.50	1.17	2.26	4.77	34.28	33.83	23.00	8.90
SWdw	23/6/2014	pre-drought	1.40	0.83	0.52	1.07	2.25	4.77	33.02	34.85	23.46	8.67
SWup	23/6/2014	pre-drought	1.34	0.80	0.50	1.04	2.40	5.33	33.82	32.73	22.87	10.58
HZdw	23/6/2014	pre-drought	1.36	0.80	0.52	1.07	2.34	5.18	34.74	33.21	22.59	9.46
HZup	23/6/2014	pre-drought	1.38	0.73	0.52	1.00	1.83	6.36	32.33	29.93	21.14	16.60
Lateral	23/6/2014	pre-drought	1.42	0.81	0.54	1.02	1.84	5.42	34.33	33.50	21.52	10.65
Pool	3/7/2014	contraction	1.49	0.87	0.56	1.09	2.40	5.64	29.96	33.52	28.67	7.85
HZdw	3/7/2014	contraction	1.51	0.88	0.58	1.01	2.47	5.60	30.31	33.81	29.87	6.00
HZup	3/7/2014	contraction	1.49	0.85	0.56	0.81	1.96	7.11	28.45	33.21	28.79	9.55
Lateral	3/7/2014	contraction	1.57	0.87	0.58	1.10	2.16	6.44	28.53	34.84	29.03	7.60
Pool	10/7/2014	contraction	1.37	0.84	0.50	0.92	2.33	4.85	33.56	35.72	23.03	7.69
SWdw	10/7/2014	contraction	1.34	0.86	0.49	1.07	2.14	6.33	36.00	34.97	22.70	6.32
SWup	10/7/2014	contraction	1.34	0.86	0.50	0.85	2.33	4.92	33.92	36.15	23.53	6.39
HZdw	10/7/2014	contraction	1.35	0.84	0.53	1.08	2.44	4.75	33.85	35.37	22.89	7.89
HZup	10/7/2014	contraction	1.38	0.79	0.51	0.89	2.11	6.20	32.38	34.48	22.32	10.83
Lateral	10/7/2014	contraction	1.41	0.80	0.53	2.50	1.86	12.20	33.62	33.37	20.70	12.31
Pool	17/7/2014	contraction	1.50	0.93	0.52	1.18	1.96	5.18	30.67	37.89	31.44	0.00
HZdw	17/7/2014	contraction	1.53	0.87	0.58	1.56	1.87	5.64	30.52	34.69	29.52	5.26
HZup	17/7/2014	contraction	1.54	0.92	0.55	1.05	0.90	6.88	34.50	34.19	31.32	0.00
Lateral	17/7/2014	contraction	1.61	0.93	0.58	0.96	0.25	6.67	31.26	37.89	29.30	1.56
Pool	23/7/2014	fragment	1.52	0.87	0.55	0.98	2.52	4.86	30.27	34.28	28.10	7.35
SWdw	23/7/2014	fragment	1.51	0.85	0.58	1.09	2.66	5.08	28.25	33.76	29.80	8.20
HZdw	23/7/2014	fragment	1.51	0.84	0.57	0.92	2.65	6.00	28.21	32.02	28.74	11.02

Annex

Location	Date	Hydrology	FI	HIX	BIX	SR	$SUVA_{254}$	$E_2:E_3$	C1 (%)	C2 (%)	C3 (%)	C4 (%)
HZup	23/7/2014	fragment	1.53	0.83	0.59	0.91	2.33	6.78	29.12	32.56	27.67	10.65
Lateral	23/7/2014	fragment	1.56	0.88	0.58	1.06	2.47	6.20	30.20	34.29	28.81	6.70
Pool	28/7/2014	fragment	1.51	0.94	0.52	0.98	2.50	5.13	31.58	37.34	30.35	0.72
HZdw	28/7/2014	fragment	1.50	0.93	0.56	1.13	2.47	6.40	31.98	36.78	31.12	0.12
HZup	28/7/2014	fragment	1.53	0.85	0.61	1.40	2.41	5.70	32.27	34.23	24.86	8.63
Lateral	28/7/2014	fragment	1.51	0.93	0.55	1.03	2.74	6.67	30.82	37.02	29.88	2.28
Pool	4/8/2014	fragment	1.53	0.87	0.55	0.89	2.70	5.56	31.23	33.59	27.25	7.93
SWdw	4/8/2014	fragment	1.56	0.83	0.57	1.10	2.67	4.95	31.00	31.18	27.58	10.24
HZdw	4/8/2014	fragment	1.53	0.85	0.59	1.18	2.63	5.46	29.68	33.28	28.76	8.28
HZup	4/8/2014	fragment	1.57	0.81	0.61	1.05	1.90	6.00	28.69	32.55	26.41	12.35
Lateral	4/8/2014	fragment	1.54	0.85	0.57	1.34	1.94	6.30	31.12	33.13	26.44	9.30
Pool	12/8/2014	dry	1.54	0.88	0.55	0.96	2.66	5.10	31.20	34.51	27.81	6.48
HZdw	12/8/2014	dry	1.52	0.85	0.55	1.09	2.52	6.17	31.23	33.74	26.52	8.51
HZup	12/8/2014	dry	1.57	0.84	0.58	0.95	1.91	6.71	28.81	32.85	27.97	10.37
Lateral	12/8/2014	dry	1.55	0.83	0.56	0.95	2.26	6.55	31.42	33.76	27.87	6.95
Pool	19/8/2014	dry	1.53	0.88	0.55	1.09	2.66	5.18	30.57	33.94	26.93	8.56
HZdw	19/8/2014	dry	1.53	0.86	0.57	1.00	2.51	6.15	30.22	32.58	26.20	11.01
HZup	19/8/2014	dry	1.56	0.81	0.62	1.04	1.87	5.71	30.84	33.47	27.29	8.40
Pool	26/8/2014	dry	1.57	0.90	0.58	0.95	2.55	5.48	29.84	35.52	28.64	6.00
HZdw	26/8/2014	dry	1.55	0.89	0.58	0.98	2.40	6.08	29.09	35.54	29.29	6.08
HZup	26/8/2014	dry	1.59	0.81	0.67	1.15	1.95	5.88	29.25	33.06	26.04	11.64
Lateral	26/8/2014	dry	1.61	0.88	0.60	1.12	2.10	6.08	29.54	34.86	27.91	7.68
Pool	3/9/2014	dry	1.53	0.89	0.55	0.98	2.56	6.05	32.76	34.69	26.29	6.27
HZdw	3/9/2014	dry	1.54	0.88	0.58	0.90	2.26	8.10	32.84	35.10	25.26	6.79
HZup	3/9/2014	dry	1.55	0.89	0.58	0.91	2.22	7.17	29.13	35.63	29.48	5.77
Lateral	3/9/2014	dry	1.60	0.89	0.59	0.86	2.09	7.80	30.90	34.91	27.35	6.83
Pool	2/10/2014	rewetting	1.52	0.88	0.53	0.87	2.95	5.37	28.44	34.23	31.23	6.10
HZdw	2/10/2014	rewetting	1.50	0.89	0.53	0.90	3.02	5.48	28.77	34.83	31.58	4.82
HZup	2/10/2014	rewetting	1.50	0.89	0.54	0.81	2.95	5.94	28.74	34.57	31.12	5.57
Lateral	9/10/2014	rewetting	1.53	0.86	0.57	0.94	2.74	5.44	30.74	32.68	28.09	8.50
Pool	9/10/2014	rewetting	1.53	0.91	0.55	0.91	2.87	5.68	28.53	35.42	31.82	4.23
HZdw	9/10/2014	rewetting	1.50	0.90	0.56	0.94	2.69	5.78	29.05	35.09	31.12	4.74
HZup	9/10/2014	rewetting	1.49	0.91	0.55	0.93	2.52	6.00	28.95	35.00	32.07	3.98
Lateral	9/10/2014	rewetting	1.53	0.89	0.57	0.96	2.42	6.50	29.51	33.62	29.37	7.50

Table SI 4: Days with precipitation during sampling period. Data are mean values from the two closest weather stations operated and provided by METEOCAT (Servei Meteorològic de Catalunya).

Date	Precip.
26/6/2014	7.65
29/6/2014	2.4
7/7/2014	11.5
28/7/2014	15
29/7/2014	1
22/8/2014	50
23/8/2014	8
5/9/2014	31.1
14/9/2014	4.8
16/9/2014	3.6
17/9/2014	12.8
22/9/2014	5.8
23/9/2014	1.4
28/9/2014	40.3
29/9/2014	4.2
5/10/2014	5.7

11.2 Supplementary Information Chapter 2

Table SI 5: Days with precipitation during monitoring period. Data are taken from the meteorological station "Dos rius- Montnegre Corredor", operated and provided by METEOCAT (Servei Meteorològic de Catalunya).

Date	Precip.
22/7/2015	21
24/7/2015	2.3
25/7/2015	1.5
31/7/2015	12.4
1/8/2015	20.1
13/8/2015	16.5
14/8/2015	10.5
15/8/2015	22.0
18/8/2015	8.7
22/8/2015	4.2

Figure SI 1: Relationship between DOC concentration of grab samples and fluorescence measured by both fluorescence sensors taken together measured at approximately the same time.

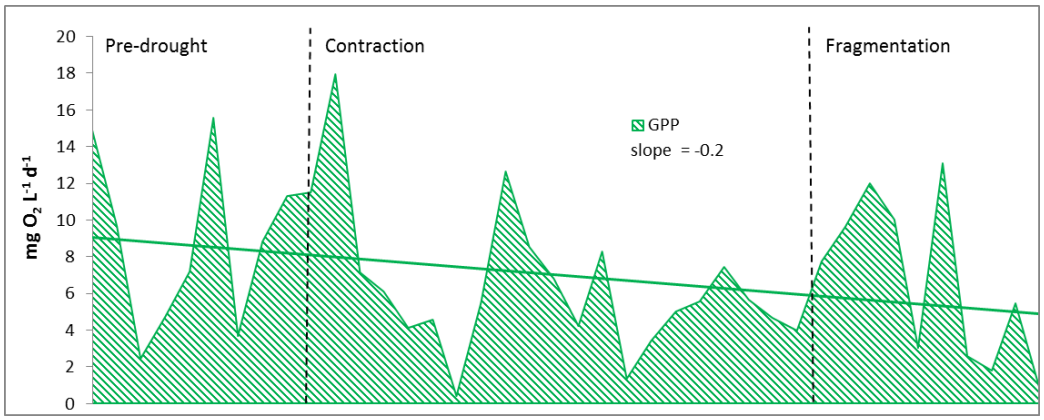

Figure SI 2: GPP during June and July 2014. On the top the hydrological phases are indicated separated by dashed lines. The green line shows the decline of GPP as drought persists.

Table SI 6: Mean ± SD of reaeration coefficient, water temperature, GPP, NEP and ER during summer drought of 2014 and 2015 in the Fuirosos pool.

	k (min^{-1})	Water Temperature (ºC)	GPP ($mgO_2\ L^{-1}\ d^{-1}$)	NEP ($mgO_2\ L^{-1}\ d^{-1}$)	ER ($mgO_2\ L^{-1}\ d^{-1}$)
2014					
pre-drought	0.008 ± 0.004	20 ± 1	10 ± 5	-20 ± 13	-30 ± 18
contraction	0.005 ± 0.003	21 ± 1	6 ± 3	-21 ± 14	-26 ± 14
fragmentation	0.007 ± 0.003	21 ± 1	7 ± 4	-43 ± 19	-49 ± 22
dry	0.004 ± 0.003	20 ± 1	4 ± 2	-27 ± 19	-32 ± 18
2015					
fragmentation	0.009	24	10	-67	-76
dry	0.015 ± 0.010	24 ± 0	24 ± 10	-95 ± 69	-119 ± 75
rewetting1	0.010 ± 0.009	24 ± 1	19 ± 8	-72 ± 85	-91 ± 85
rewetting2	0.006 ± 0.004	23 ± 1	19 ± 10	-23 ± 29	-42 ± 26
rewetting3	0.017 ± 0.011	21 ± 1	31 ± 20	-73 ± 56	-104 ± 59

Table SI 7: Aikakes information criterion (AIC) for the different GLS-models with the lowest value in bold.

Autocorrelation *p*	AIC (Pool-model)	AIC (HZ-model)
1	3155	3982
2	**3153**	3983
3	3156	3985
4	3158	3984
5	3159	**3980**
6	3161	3981

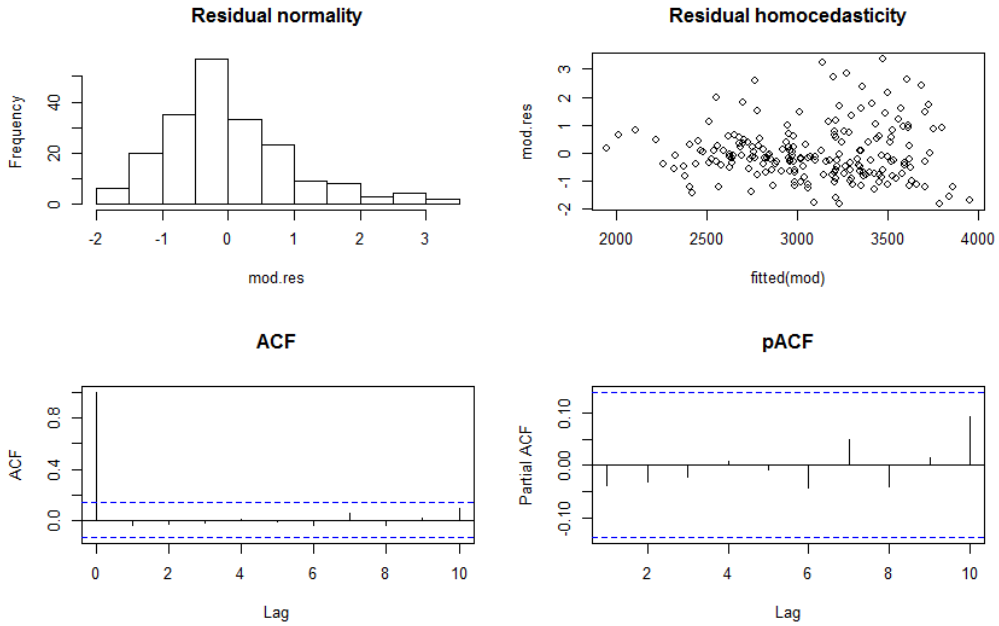

Figure SI 3: Residuals from the GLS model for the pool data set and autocorrelation analysis.

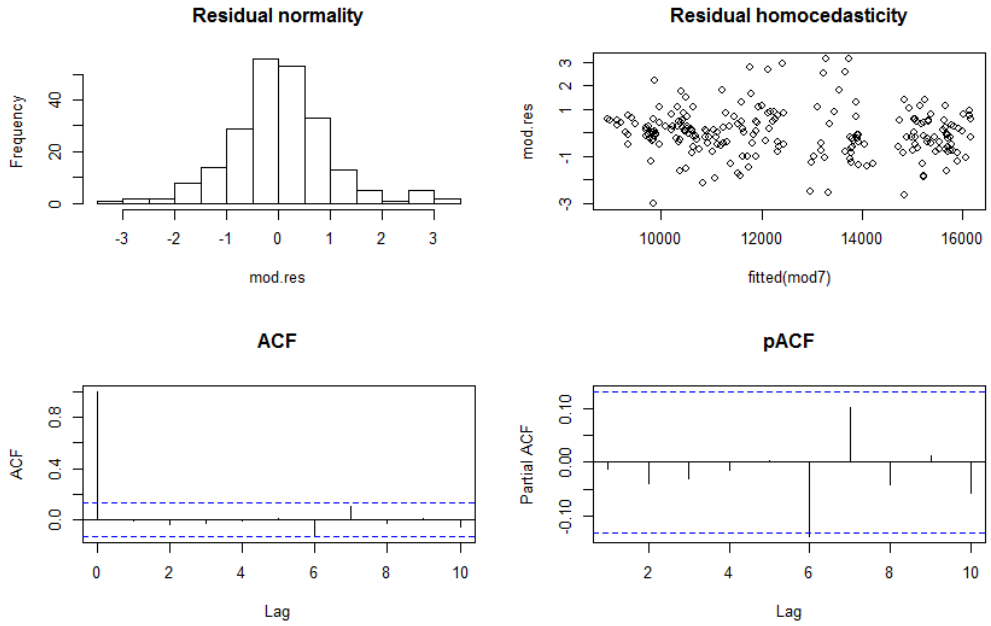

Figure SI 4: Residuals from the GLS model for the HZ data set and autocorrelation analysis.

11.3 Supplementary Information Chapter 3

Table SI 8: Data from Chapter 3

Location	Campaign	Bact*	LD	glu*	phos*	cbh*	leu*	pH	DOC*	O_2*
Pool	Pre-drought	5.26	0.16	0.015	0.158	0.007	0.450	7.23	3.08	9.01
Stream	Pre-drought	6.17	0.18	0.022	0.217	0.003	0.536	7.00	2.77	9.21
Stream	Pre-drought	4.09	0.07	0.041	0.116	0.047	0.523	6.94	2.99	8.93
HZ_{inf}	Pre-drought	11.2	1.18	0.019	0.204	0.000	0.664	7.12	2.84	7.09
HZ_{dw}	Pre-drought	9.99	1.14	0.045	0.769	0.000	0.270	7.05	2.71	1.44
HZ_{up}	Pre-drought	34.4	0.18	0.005	1.594	0.000	0.725	7.01	3.74	1.69
L1	Pre-drought	13.8	0.23	0.033	0.057	0.000	0.067	6.46	4.31	0.44
L2	Pre-drought	10.4	0.23	0.000	0.070	0.001	0.272	6.93	2.89	3.82
Pool	Contraction	6.21	0.05	0.122	0.278	0.000	0.468	6.91	2.46	7.11
Stream	Contraction	4.85	0.09	0.102	0.311	0.000	0.500	6.87	3.18	7.11
Stream	Contraction	5.44	0.04	0.109	0.216	0.000	0.323	7.02	2.33	7.11
HZ_{inf}	Contraction	1.81	0.81	0.000	0.134	0.000	0.033	6.82	2.26	4.88
HZdw	Contraction	6.36	0.83	0.098	0.488	0.000	0.098	6.94	2.15	1.81
HZup	Contraction	15.2	0.24	0.013	0.377	0.000	0.226	7.10	3.11	1.30
L1	Contraction	12.2	0.16	0.053	0.132	0.000	0.020	6.52	5.13	1.48
L2	Contraction	11.9	0.20	0.000	0.216	0.000	0.130	6.73	2.55	0.89
Pool	Transition	8.96	0.02	0.096	0.121	0.000	1.814	6.88	2.81	5.66
Stream	Transition	7.25	0.03	0.083	0.091	0.000	1.982	7.10	2.96	2.00
Stream	Transition	4.43	0.12	0.087	0.023	0.049	0.927	7.11	1.97	7.37
HZ_{inf}	Transition	0.987	0.37	0.028	0.019	0.004	0.121	6.99	4.96	1.48
HZ_{dw}	Transition	23.3	0.79	0.091	0.264	0.000	0.839	7.05	3.15	0.31
HZ_{up}	Transition	8.57	0.90	0.005	0.070	0.010	0.033	6.75	5.75	0.50
L1	Transition	13.8	0.42	0.006	0.022	0.000	0.015	6.72	7.80	1.20
L2	Transition	4.63	0.15	0.014	0.015	0.010	0.279	6.65	2.40	3.10
Pool	Fragmentation	57	0.01	0.109	0.532	0.003	1.010	6.91	3.16	4.72
Stream	Fragmentation	6.45	0.09	0.111	0.089	0.000	0.550	6.87	2.55	1.91
HZ_{inf}	Fragmentation	1.58	0.40	0.003	0.027	0.000	0.211	6.93	2.26	3.33
HZ_{dw}	Fragmentation	5.98	0.86	0.002	0.040	0.000	0.159	6.85	2.47	0.69
HZ_{up}	Fragmentation	17.4	0.38	0.008	0.035	0.000	0.096	7.19	2.24	1.52
L1	Fragmentation	7.54	0.21	0.002	0.001	0.000	0.041	6.54	4.61	1.41
L2	Fragmentation	6.99	0.30	0.019	0.036	0.003	0.275	6.80	2.08	1.14
Pool	Dry	60.7	0.05	0.037	0.074	0.000	0.345	6.95	4.33	5.14
HZ_{dw}	Dry	11.1	0.06	0.000	0.000	0.000	0.000	6.70	3.40	0.31
HZ_{up}	Dry	218	0.35	0.000	0.000	0.000	0.046	7.04	1.85	1.24
L1	Dry	9.01	0.08	0.000	0.000	0.000	0.000	6.50	3.92	0.62
L2	Dry	29.4	0.09	0.017	0.000	0.000	0.000	6.63	3.58	3.48

Location	Campaign	NO_3*	SRP*	NH_4*	FI	HIX	BIX	SR	$SUVA_{254}$	E_2:E_3
Pool	Pre-drought	0.06	0.03	0.03	1.50	0.87	0.61	0.67	2.27	6.64
Stream	Pre-drought	0.06	0.02	0.03	1.36	0.86	0.59	0.72	2.48	6.58
Stream	Pre-drought	0.09	0.02	0.03	1.45	0.93	0.56	0.94	2.56	6.17
HZinf	Pre-drought	0.37	0.03	0.03	1.51	0.89	0.58	0.70	2.40	7.20
HZ_{dw}	Pre-drought	0.22	0.03	0.04	1.60	0.88	0.61	0.69	2.18	7.88
HZup	Pre-drought	0.22	0.03	0.05	1.51	0.85	0.55	0.87	1.84	7.20
L1	Pre-drought	0.06	0.02	0.19	1.52	0.93	0.59	0.78	1.62	8.45
L2	Pre-drought	0.09	0.02	0.09	1.41	0.91	0.60	0.78	2.18	8.50
Pool	Contraction	0.12	0.02	0.05	1.49	0.87	0.59	1.09	2.40	5.64
Stream	Contraction	0.12	0.02	0.04	1.49	0.89	0.64	1.02	1.92	5.82
Stream	Contraction	0.12	0.02	0.03	1.53	0.92	0.59	1.06	2.36	5.80
HZ_{inf}	Contraction	0.71	0.03	0.02	1.50	0.89	0.60	1.07	2.30	5.50
HZ_{dw}	Contraction	0.40	0.02	0.03	1.51	0.88	0.59	1.01	2.47	5.60
HZ_{up}	Contraction	0.09	0.02	0.08	1.49	0.85	0.59	0.81	1.96	7.11
L1	Contraction	0.06	0.02	0.28	1.59	0.94	0.57	0.83	2.38	7.11
L2	Contraction	0.06	0.02	0.10	1.57	0.87	0.60	1.10	2.16	6.44
Pool	Transition	0.22	0.03	0.03	1.50	0.93	0.57	1.18	1.96	5.18
Stream	Transition	0.31	0.02	0.03	1.52	0.91	0.59	1.13	1.76	5.50
Stream	Transition	0.22	0.02	0.03	1.61	0.93	0.64	0.67	2.69	7.00
HZ_{inf}	Transition	0.67	0.04	0.03	1.49	0.94	0.59	1.46	0.97	5.67
HZ_{dw}	Transition	0.35	0.03	0.23	1.53	0.87	0.63	1.56	1.87	5.64
HZ_{up}	Transition	0.13	0.01	0.09	1.54	0.92	0.59	1.05	0.90	6.88
L1	Transition	0.17	0.02	0.33	1.62	0.94	0.59	0.96	1.76	6.41
L2	Transition	0.13	0.01	0.14	1.61	0.93	0.59	0.96	2.51	6.67
Pool	Fragmentation	0.26	0.01	0.07	1.51	0.94	0.56	0.98	2.50	5.13
Stream	Fragmentation	0.16	0.03	0.05	1.53	0.92	0.58	1.01	2.47	5.50
HZ_{inf}	Fragmentation	1.10	0.03	0.03	1.48	0.95	0.59	1.06	2.57	5.55
HZ_{dw}	Fragmentation	0.16	0.02	0.04	1.50	0.93	0.58	1.13	2.47	6.40
HZ_{up}	Fragmentation	0.07	0.02	0.12	1.53	0.85	0.60	1.40	2.41	5.70
L1	Fragmentation	0.12	0.02	0.42	1.58	0.94	0.58	0.86	2.54	6.10
L2	Fragmentation	0.16	0.01	0.15	1.51	0.93	0.60	1.03	2.74	6.67
Pool	Dry	0.06	0.03	0.04	1.53	0.89	0.57	0.98	2.56	6.05
HZ_{dw}	Dry	0.04	0.02	0.10	1.54	0.88	0.59	0.90	2.26	8.10
HZ_{up}	Dry	0.06	0.01	0.09	1.55	0.89	0.58	0.91	2.22	7.17
L1	Dry	0.04	0.02	0.43	1.58	0.99	0.59	0.90	1.97	8.10
L2	Dry	0.02	0.01	0.15	1.60	0.89	0.58	0.86	2.09	7.80

* *Bact=10^6 cells mL^{-1}, activities=nmol mL^{-1} h^{-1} , concentrations=mg L^{-1}*

Table SI 9: Extracellular enzyme activities (nmol mL^{-1} h^{-1}) from October samples, when Q<20 L s^{-1}.

Location	glu	phos	cbh	leu
HZdw	0.000	0.000	0.000	0.024
Hzinf	0.000	0.000	0.000	0.153
Hzup	0.000	0.000	0.000	0.156
L1	0.000	0.000	0.000	0.000
L2	0.000	0.000	0.000	0.000
Pool	0.033	0.037	0.000	0.811
Stream	0.036	0.054	0.000	0.866
Stream	0.027	0.000	0.000	0.425
Stream	0.039	0.012	0.000	0.563

11.5 Supplementary Information Chapter 4

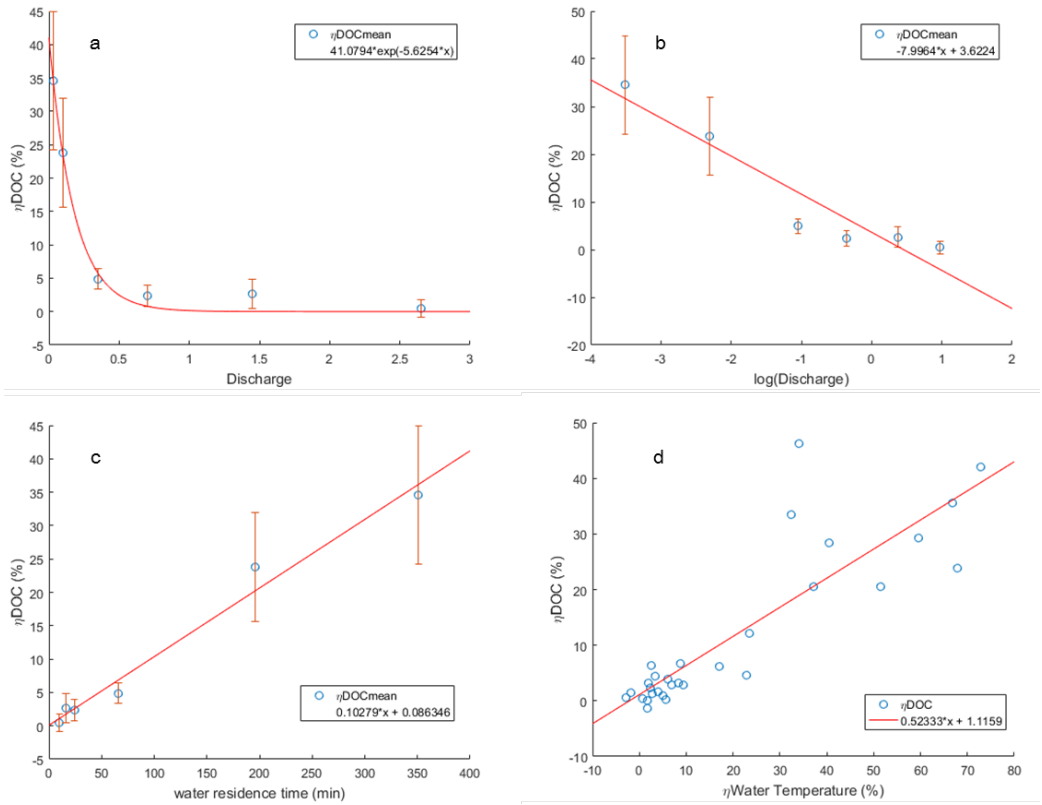

Figure SI 5: a) Exponential fit between average ηDOC and discharge. Linear models of average *η*DOC (*n* = 6) with the predictor variables b) log(Discharge) and c) water residence time. The error bars represent the standard deviation over the whole sampling period (*n* = 6 x 5). d) Linear model of *η*DOC (n = 30) with *η*water residence time.

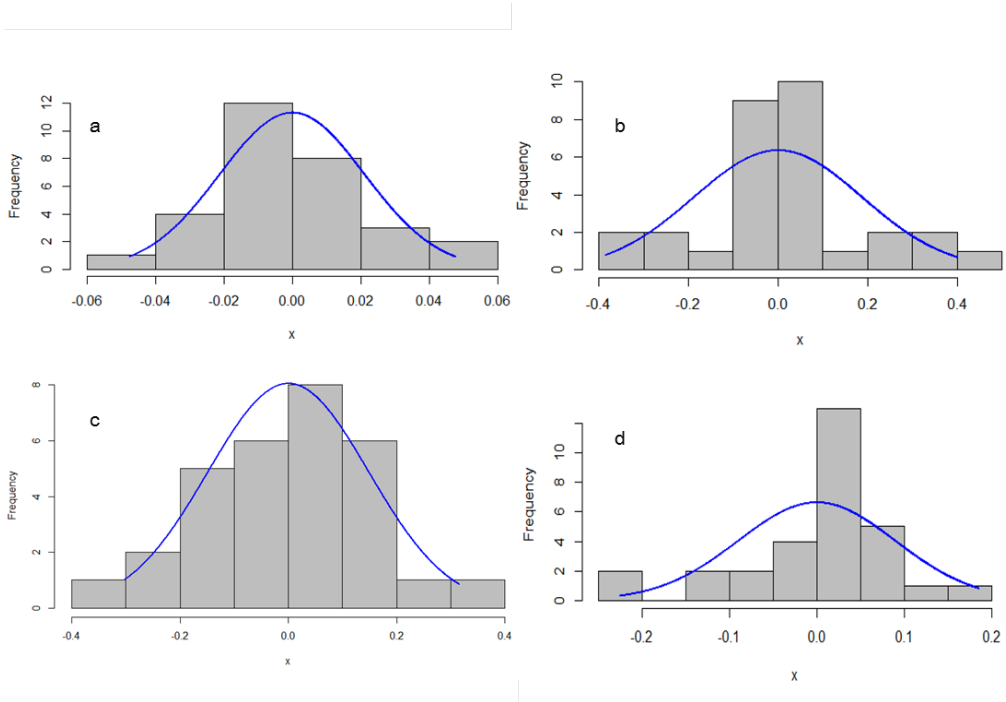

Figure SI 6: Histograms of model residuals after normalization. a) *η*DOC (Shapiro-Wilk test *p* = 0.766) without any transformation, b) ηNO_3 (*p* = 0.074) transformed by the power of 2, c) *η*C3 (*p* = 0.074) and d) $\eta SUVA_{254}$ (*p* = 0.016) both transformed by the power of -2.

Table SI 10: Daily temperature ranges (ºC), mean light values (µmol m^{-2} s^{-1}), NEP (mg O_2 L^{-1} d^{-1}) and GPP (mg O_2 L^{-1} d^{-1}) data during treatment. The day chosen for the carbon mass balance is in bold letters.*

	F1 k = .0019 min^{-1}				F2 k = .0032 min^{-1}				F3 k = .0088 min^{-1}				F4 k = .0114 min^{-1}			
Day	T	Light	NEP	GPP	T	Light	NEP	GPP	T	Light	NEP	GPP	T	Light	NEP	GPP
4		211	2.5	15.0		112	4.0	15.3		114	-0.6	19.0		111	-1.9	14.8
5	14.5 - 10.1	40	7.1	14.3	11.2 - 9.0	37	5.2	15.2	9.9 - 8.4	31	0.0	19.0	9.7 - 8.4	28	-1.4	14.8
6	10.6 - 8.8	68	13.5	17.8	10.5 - 8.1	49	11.7	19.6	9.5 - 7.9	54	4.2	22.6	9.2 - 8.0	47	5.4	20.3
7	10.9 - 7.4	93	11.6	16.1	11.0 - 7.3	46	11.8	20.8	9.7 - 7.6	66	5.4	26.1	9.3 - 7.8	68	7.0	23.8
8	14.4 - 9.0	150	12.0	17.3	13.8 - 8.5	112	14.6	25.3	10.4 - 7.6	98	9.8	31.6	9.5 - 7.8	117	10.9	28.1
9	11.5 -7.5	114	9.8	14.7	11.5 - 6.8	70	11.0	20.6	9.7 - 7.2	62	3.9	25.5	9.3 - 7.5	61	6.3	23.4
10	12.4 - 8.3	93	8.1	13.9	12.2 - 7.9	18	13.1	24.1	9.8 - 7.6	52	2.5	26.1	9.4 - 7.7	53	5.7	23.9
11	14.9 - 7.2	147	6.3	13.5	14.7 - 7.0	70	11.3	23.4	11.0 - 7.4	90	1.6	30.1	10.4 - 7.7	83	9.0	27.9
12	17.4 - 7.8	204	0.5	9.6	16.9 - 7.4	85	5.4	19.4		146	-6.4	22.2	10.8 - 7.9	92	6.1	24.6
13	18.1 - 8.1	210	-1.0	10.4	17.6 - 7.4	81	5.4	21.9		148	0.5	31.0	11.4 - 7.9	91	7.9	28.5
14	16.0 - 12.0	95	-5.1	8.3	15.3 - 11.1	86	-4.4	18.6	12.1 - 9.2	75	-8.1	28.1	11.2 - 9.1	56	0.4	22.9
15	14.8 - 10.4	113	-2.3	9.1	14.4 - 9.7	105	1.8	21.4	11.0 - 8.7	90	1.9	36.1	10.4 - 8.8	51	9.6	27.8
16	18.2 - 10.6	130	-4.4	8.3	17.7 - 9.9	112	-1.6	21.1	12.4 - 8.8	91	-0.9	33.8	11.5 - 8.8	72	7.5	28.4
17	**19.9 - 11.3**	**161**	**-7.2**	**9.3**	**19.4 - 10.6**	**68**	**-2.0**	**23.7**	**13.4 - 9.2**	**92**	**1.8**	**39.0**	**12.4 - 9.2**	**69**	**6.3**	**29.0**
18	18.0 - 11.3	115	-9.0	6.1	17.7 - 10.5	56	-9.5	17.0	12.8 - 9.0	95	-4.7	31.9	11.9 - 9.1	42	2.4	22.4
19	15.1 - 11.9	99	-11.2	1.9	14.4 - 10.9	103	-18.7	5.9	11.2 - 9.4	95	-21.7	11.3	10.6 - 9.3	47	-7.4	10.2
20	13.7 - 11.3	94	-10.9	1.0	13.2 - 10.7	98	-17.4	2.6	10.7 - 9.0	86	-29.7	0.6	10.2 - 9.0	54	-17.1	0.7
21	15.5 - 7.6	121	-7.7	0.1	15.6 - 7.3	123	-14.9	1.0		117	-25.3	1.4	11.2 - 7.9	50	-11.0	1.8

* *Days refer to the start of the treatment.*

Table SI 11: All *η*-values as %: Loc (Outlets of Flumes F1-F6) and discharge (Q L s^{-1}) of each flume and *η*water temperature (WT).

Date	Location	Q	ηWT	ηO_2	ηDOC	ηNH4	ηNO2	ηNO3	ηPO4	ηE2E3	$\eta SUVA_{254}$	ηSR	ηFI	ηHIX	ηBIX	ηC1	ηC2	ηC3	ηC4
18/8/15	F1	2.65	0.3	-0.6	0.7	-47.9	100.0	-1.5	0.0	1.0	-0.4	-0.5	-2.0	-4.2	3.6	-4.1	-4.0	-14.7	213.6
18/8/15	F2	2.65	0.3	-0.1	0.0	-70.8	0.0	-1.7	0.0	0.5	-0.7	0.9	5.4	-0.2	4.0	-0.5	0.5	17.7	-20.6
18/8/15	F3	2.65	0.3	0.2	0.5	-65.6	-33.3	-3.9	0.0	1.0	-0.7	-0.8	0.2	-4.0	0.2	-3.8	-4.4	4.9	186.9
18/8/15	F4	2.65	0.3	0.4	0.0	-66.7	-66.7	-2.6	0.0	-1.0	0.8	1.9	-1.4	-5.0	4.0	-4.5	-5.0	14.3	208.5
18/8/15	F5	2.65	0.3	0.2	0.0	-82.3	-33.3	-4.5	0.0	-1.5	0.8	-0.1	5.5	-4.0	3.3	-3.6	-4.7	11.3	179.4
18/8/15	F6	2.65	0.3	0.1	2.9	-75.0	66.7	-3.2	0.0	-3.0	-1.1	3.7	-0.5	-4.4	3.4	-4.0	-5.6	22.9	190.5
21/8/15	F1	2.65	0.0		-0.2	-61.1	-66.7	-0.2	0.0	2.4	-0.5	-2.4	1.4	2.5	-4.6	5.8	-0.6	-7.8	-44.7
21/8/15	F2	2.65	0.0		-0.5	-94.4	-66.7	-0.6	0.0	0.5	0.9	-0.6	-1.9	-0.8	-5.0	2.2	-3.3	49.0	-19.0
21/8/15	F3	2.65	0.0		0.1	-50.0	-33.3	0.5	0.0	2.4	-1.5	-1.8	-6.3	3.3	-4.1	7.2	-0.6	-0.4	-60.6
21/8/15	F4	2.65	0.0		-0.5	44.4	-66.7	0.3	0.0	2.4	-0.3	-2.1	-6.9	1.7	-2.8	6.5	-2.9	0.0	-38.9
21/8/15	F5	2.65	0.0		0.4	0.0	-66.7	-0.1	0.0	2.4	-1.7	-0.5	-3.5	1.0	0.3	5.7	-2.4	19.8	-43.5
21/8/15	F6	2.65	0.0		-0.5	-5.6	-66.7	-0.2	0.0	3.0	0.3	0.4	-2.4	1.1	-0.9	5.0	-2.8	-0.4	-25.7
24/8/15	F1	2.65	5.9		-0.4	-89.5	7.1	-2.2	0.0	-4.5	-3.2	4.2	-0.3	-0.8	2.4	-3.1	0.9	-6.7	37.9
24/8/15	F2	2.65	4.9		-0.4	-86.8	-35.7	-3.0	0.0	1.5	-5.1	-2.8	1.2	-1.1	1.5	-1.9	-0.4	4.5	25.3
24/8/15	F3	2.65	4.9		-0.4	-98.7	-14.3	-2.1	0.0	-2.0	-5.1	-3.6	-0.7	-0.1	-3.7	-1.9	0.9	-1.7	17.4
24/8/15	F4	2.65	4.9		-0.4	-98.7	-14.3	-2.7	0.0	-2.6	-5.1	-1.3	4.0	-0.7	0.6	-1.7	-0.1	-0.6	25.1
24/8/15	F5	2.65	3.9		-0.4	-98.7	7.1	-2.5	0.0	-37.6	47.1	12.4	3.1	-0.8	-1.9	-1.6	-0.7	1.7	27.4
24/8/15	F6	2.65	3.9		3.3	-98.7	28.6	-2.9	0.0	1.5	-9.0	-5.0	5.8	-0.7	-5.3	-1.6	-0.5	-8.1	34.0
27/8/15	F1	2.65	8.2	0.7	0.5	-38.1	20.0	-1.3	0.0	4.8	-3.4	-1.1	-6.6	1.1	-4.7	13.6	4.5	-61.3	-46.2
27/8/15	F2	2.65	8.2	2.1	0.2	-30.6	-70.0	-0.1	0.0	1.1	-3.1	9.9	-6.7	-2.7	-1.2	9.8	0.1	-40.7	-23.5
27/8/15	F3	2.65	7.2	2.2	0.3	-56.2	20.0	0.3	0.0	0.4	-3.9	1.3	-4.3	0.6	0.0	13.8	3.8	-57.9	-46.5
27/8/15	F4	2.65	5.2	1.9	0.5	-54.1	50.0	0.3	0.0	0.4	-4.1	-2.1	-2.3	0.2	-8.7	12.3	3.3	-62.5	-36.0
27/8/15	F5	2.65	3.1	2.1	0.8	-59.4	20.0	-0.4	0.0	4.8	-4.3	-1.1	1.1	0.3	-2.9	13.7	3.8	-68.3	-40.9
27/8/15	F6	2.65	2.1	1.3	1.5	-55.2	20.0	0.1	0.0	-2.2	-2.9	0.7	-1.4	0.0	-2.1	12.9	3.0	-67.1	-35.3
31/8/15	F1	2.65	2.6	1.1	-2.8	0.0	-16.7	-0.1	-82.4	-0.8	2.7	-0.2	-1.4	-3.7	-2.9	-5.3	-2.6	209.3	-3.3
31/8/15	F2	2.65	2.5	2.3	-3.4	0.0	-16.7	-0.8	-64.7	-0.8	3.2	0.7	-5.4	0.4	-0.6	-0.4	0.9	-20.7	4.0
31/8/15	F3	2.65	2.6	0.4	-4.9	0.0	-33.3	-1.1	-82.4	-2.2	8.2	3.0	-4.4	-5.3	0.4	-4.7	-3.4	3.6	55.0
31/8/15	F4	2.65	2.8	2.5	-3.9	0.0	-33.3	-0.6	-47.1	0.0	4.6	1.0	3.5	-0.7	-1.8	-1.8	-0.2	-36.3	25.0
31/8/15	F5	2.65	2.4	-1.1	-4.2	0.0	-33.3	-1.4	5.9	-5.5	7.4	4.8	-5.3	-0.6	-0.8	-1.6	0.4	-33.2	19.5
31/8/15	F6	2.65	2.8	2.0	-5.0	0.0	16.7	-2.2	-47.1	-0.8	4.9	0.0	0.3	-1.1	-3.2	-2.1	-0.3	-1.6	18.9

Continuation SI11

Date	Location	Q	ηWT	ηO_2	ηDOC	ηNH4	ηNO2	ηNO3	ηPO4	ηE2E3	$\eta SUVA_{254}$	ηSR	ηFI	ηHIX	ηBIX	ηC1	ηC2	ηC3	ηC4
3/9/15	F1	0.03	51.5	34.5	20.6	-69.8	380.0	-25.2	0.0	-3.8	-12.8	2.9	2.3	0.6	4.4	-0.7	-0.4	26.8	-9.0
3/9/15	F2	0.10	23.4	4.6	12.1	-39.6	110.0	-13.6	0.0	-0.7	-8.4	1.6	-1.5	-0.7	1.4	-2.9	0.4	-14.9	38.4
3/9/15	F3	0.35	6.0	0.1	3.8	-51.7	50.0	-5.2	0.0	0.3	-5.0	-0.7	2.9	2.8	0.4	2.3	2.9	-31.3	-24.7
3/9/15	F4	0.73	5.6	0.1	0.2	-9.4	-40.0	-2.9	0.0	4.0	-3.2	-3.4	-1.3	2.9	5.6	2.3	3.2	-25.1	-31.2
3/9/15	F5	1.45	2.5	-0.3	6.3	-41.6	-10.0	-1.2	0.0	2.3	-9.5	-2.1	-2.8	2.2	-3.8	0.9	3.7	-40.0	-10.4
3/9/15	F6	2.65	1.6	-0.9	-1.3	-25.5	-10.0	0.7	0.0	2.3	-2.5	-2.9	-7.7	1.8	8.6	1.3	2.6	-5.4	-31.0
7/9/15	F1	0.03	56.3	26.1	-13.3	17.9	252.2	-18.3	-89.7	-4.4	-10.9	23.5	12.5	-5.5	4.8	-9.7	-1.5	221.8	12.4
7/9/15	F2	0.10	49.3	40.3	8.8	111.0	200.0	-5.3	-89.7	-5.7	-4.2	11.2	7.5	0.6	-1.3	-0.1	0.3	60.9	-100.0
7/9/15	F3	0.35	20.9	14.8	4.6	613.8	69.6	-0.9	-89.7	-3.4	0.3	5.8	3.6	2.2	-1.8	1.2	1.0	22.6	-100.0
7/9/15	F4	0.73	12.3	9.0	3.0	485.5	43.5	-0.4	-37.9	-1.4	-0.2	5.6	2.1	1.2	-0.6	-0.1	-0.3	69.9	-100.0
7/9/15	F5	1.45	4.9	5.6	-0.7	349.0	4.3	-0.4	-37.9	-2.3	2.8	4.1	2.6	2.9	-2.5	1.3	1.6	13.5	-100.0
7/9/15	F6	2.65	2.6	3.8	1.4	222.8	-21.7	-0.2	-79.3	-1.4	-0.4	3.0	5.8	2.4	0.7	1.5	1.3	11.7	-100.0
10/9/15	F1	0.03	40.4	38.3	28.3	288.0	307.1	-9.8	-25.0	-12.4	-11.1	12.2	-3.7	-2.7	1.6	-2.3	-5.1	105.8	71.7
10/9/15	F2	0.10	37.1	40.1	20.5	212.0	392.9	-12.9	-25.0	-8.4	-9.3	8.9	-1.9	-3.4	5.4	-4.0	-4.4	150.3	62.0
10/9/15	F3	0.35	8.3	6.3	3.1	-20.0	28.6	-4.1	-25.0	-3.4	-0.9	4.3	0.1	-3.4	2.6	-3.4	-3.3	129.6	41.7
10/9/15	F4	0.73	4.0	3.9	1.6	-80.0	7.1	-2.1	-25.0	-1.2	-0.5	2.8	-1.9	-0.5	2.5	-0.4	-0.7	-0.5	26.2
10/9/15	F5	1.45	1.9	2.5	3.1	-36.0	-35.7	-1.8	-25.0	-13.0	3.8	11.8	6.9	-1.0	1.4	-0.8	-1.6	8.5	48.7
10/9/15	F6	2.65	2.3	1.5	2.4	-80.0	135.7	-1.7	-25.0	-18.8	11.5	20.3	1.9	-3.6	4.3	-3.8	-4.1	155.6	45.5
13/9/15	F1	0.03	66.8	19.9	35.5	128.5	384.6	-7.5	0.0	-8.0	-15.4	8.0	-0.3	-2.0	-4.6	1.0	-5.6	272.1	-16.9
13/9/15	F2	0.10	67.9	18.6	23.8	81.4	361.5	-8.4	0.0	-8.5	-10.8	9.5	-0.6	-1.2	-3.1	2.1	-4.9	270.2	-30.9
13/9/15	F3	0.35	17.0	-3.3	6.2	-49.4	61.5	-3.7	0.0	-2.9	-3.4	3.3	3.5	-0.7	1.5	3.3	-2.9	137.5	-31.8
13/9/15	F4	0.73	6.9	6.8	2.9	191.3	38.5	-0.7	0.0	-0.5	-0.9	1.7	-1.7	1.1	-3.5	4.2	-2.3	141.3	-44.6
13/9/15	F5	1.45	2.8	3.4	1.2	-98.3	130.8	-1.4	0.0	1.4	-1.0	0.0	1.2	2.2	-0.8	6.1	-1.2	67.3	-55.5
13/9/15	F6	2.65	0.6	3.0	0.4	-98.3	84.6	-0.6	0.0	0.8	-0.8	-0.2	-1.7	1.5	-0.5	5.3	-1.9	73.1	-45.3
16/9/15	F1	0.03	72.9	3.8	42.0	222.1	550.0	-8.6	-81.3	-17.6	-7.4	9.3	1.8	-5.4	-4.5	-5.0	-10.7	92.8	65.0
16/9/15	F2	0.10	59.7	18.9	29.2	241.9	600.0	-10.1	-81.3	-17.0	-2.8	10.6	-0.2	-3.9	-3.6	-0.4	-10.8	115.3	15.2
16/9/15	F3	0.35	22.9	12.2	4.7	45.6	83.3	-3.2	31.3	-1.5	2.0	4.8	-3.0	-3.2	-1.4	-0.5	-6.0	36.5	24.7
16/9/15	F4	0.73	9.3	8.8	2.8	1.5	50.0	-2.5	-81.3	-3.2	-1.3	0.7	-0.3	0.1	-3.2	-0.8	0.2	-26.1	18.3
16/9/15	F5	1.45	5.0	4.6	1.0	-18.4	50.0	-0.9	-100.0	3.3	-0.1	-2.6	0.3	-0.7	0.3	-4.0	1.8	-46.3	46.8
16/9/15	F6	2.65	1.8	2.5	0.1	27.9	33.3	-0.6	-100.0	3.3	0.1	0.1	-1.0	0.6	-1.1	0.6	0.9	5.5	-13.8
21/9/15	F1	0.03	34.1	-7.4	46.3	38.0	212.0	-6.1	0.0	-13.6	-14.0	14.5	1.5	-8.5	-6.9	-7.9	-12.5	241.9	86.6
21/9/15	F2	0.10	32.3	-1.5	33.4	54.6	296.0	-1.9	0.0	-12.7	-13.1	10.4	-1.5	-8.3	0.2	-10.1	-9.6	234.3	88.9
21/9/15	F3	0.35	8.7	4.5	6.7	15.7	44.0	-2.2	0.0	-3.0	-2.5	5.7	1.0	-0.8	-5.4	0.5	-3.0	86.6	-10.5
21/9/15	F4	0.73	3.5	6.4	4.4	15.7	44.0	-2.3	0.0	-4.2	-1.1	4.7	-3.9	-0.9	-1.8	-1.1	-2.2	50.0	10.3
21/9/15	F5	1.45	-1.8	3.4	1.5	18.5	8.0	-1.6	0.0	-1.5	0.4	4.4	1.2	-0.5	-1.5	1.6	-2.6	86.0	-22.5
21/9/15	F6	2.65	-2.9	3.0	0.5	26.9	32.0	-0.8	0.0	-2.2	0.6	4.1	-6.3	0.0	-5.1	2.0	-2.3	73.3	-24.0

Continuation SI11

Date	Location	Q	ηWT	ηO_2	ηDOC	ηNH4	ηNO2	ηNO3	ηPO4	ηE2E3	$\eta SUVA_{254}$	ηSR	ηFI	ηHIX	ηBIX	ηC1	ηC2	ηC3	ηC4
22/9/15	F1	2.65	4.1	-1.9	1.4	0.0	40.0	-0.4	-25.0	-5.9	0.3	13.7	-0.6	0.3	2.9	1.6	-2.0	36.8	-13.0
22/9/15	F2	2.65	4.2	0.0	0.8	0.0	80.0	0.3	50.0	-5.9	0.9	15.6	5.2	0.5	-3.2	1.0	-1.4	20.6	-6.0
22/9/15	F3	2.65	2.5	0.2	0.8	0.0	80.0	0.1	-25.0	-9.0	1.7	15.6	2.0	-2.0	-3.1	-0.4	-4.5	43.9	15.2
22/9/15	F4	2.65	2.1	0.6	0.8	400.0	120.0	0.3	-25.0	-9.0	0.9	19.3	-5.2	0.9	0.6	2.0	-0.8	15.2	-15.3
22/9/15	F5	2.65	1.9	-1.2	1.4	0.0	60.0	1.3	125.0	-9.7	0.3	16.9	3.3	0.2	3.4	1.4	-1.5	36.8	-13.7
22/9/15	F6	2.65	1.8	1.5	0.8	0.0	140.0	0.5	50.0	-9.7	0.9	12.9	0.9	1.2	0.2	2.0	-0.7	18.4	-17.1
23/9/15	F1	2.65	0.1	6.1	1.8	9.7	-16.7	-0.8	-57.1	-1.9	-0.6	0.0	6.8	-0.5	-6.3	0.2	-1.4	-7.7	10.5
23/9/15	F2	2.65	0.1	1.8	0.8	-30.6	0.0	-0.7	-57.1	-1.9	0.4	2.2	7.5	-0.3	-3.6	0.3	-1.6	8.0	4.5
23/9/15	F3	2.65	0.1	2.2	0.8	-8.1	-16.7	-0.5	200.0	-1.9	-0.3	0.9	3.0	-0.3	-1.2	0.4	-0.9	-6.5	5.2
23/9/15	F4	2.65	0.1	8.0	0.8	-33.9	33.3	-0.8	157.1	2.4	0.4	0.7	2.8	-0.6	-2.8	-0.5	-1.6	-2.7	16.0
23/9/15	F5	2.65	0.1	3.1	1.8	35.5	-16.7	-0.8	157.1	-1.9	-0.6	2.1	3.9	-4.2	-0.5	-3.5	-5.0	46.0	44.7
23/9/15	F6	2.65	0.1	7.9	0.8	6.5	133.3	0.5	-14.3	-1.9	0.4	0.5	9.2	-0.7	1.0	0.2	-0.7	4.6	0.9
24/9/15	F1	2.65	2.6	1.0	0.5	3.4	-6.3	-1.2	-25.0	0.6	0.4	0.1	-4.2	-1.8	5.0	-2.2	-0.6	7.3	61.7
24/9/15	F2	2.65	2.4	0.7	0.5	86.2	12.5	-1.6	-25.0	0.3	-0.3	-1.6	1.9	-0.1	0.9	-0.1	-0.3	14.1	-4.1
24/9/15	F3	2.65	2.3	0.9	-0.1	19.0	31.3	-0.8	-25.0	-2.2	-0.1	3.2	-1.8	-1.5	0.9	-1.2	-1.2	47.1	10.4
24/9/15	F4	2.65	2.3	0.8	0.5	81.0	-6.3	-1.9	-25.0	-2.6	-0.7	5.6	-1.2	-0.8	0.7	-0.4	-0.2	6.8	8.1
24/9/15	F5	2.65	2.3	1.4	-0.1	29.3	-25.0	-2.3	-25.0	-0.9	-0.5	2.2	1.3	0.2	-0.9	0.2	-0.3	9.4	-9.5
24/9/15	F6	2.65	2.4	1.4	-0.8	-63.8	31.3	-2.2	-25.0	-2.2	0.5	4.0	0.1	-0.3	-0.1	0.1	-0.8	11.0	0.0

Table SI 12: Absolute data of Chapter 4: Loc (Outflow of Flumes F1-F6 and Inflow T) and discharge in L s^{-1} (Q) of each flume and water temperature (WT ºC). O_2 in mg L^{-1} and all other concentrations in µg L^{-1}. Fluorescence indices are dimensionless and PARAFAC components C1-C4 in %.

Date	Loc	Q	WT	O_2	DOC	$N\text{-}NH_4$	$N\text{-}NO_2$	$N\text{-}NO_3$	$P\text{-}PO_4$	$E_2{:}E_3$	$SUVA_{254}$	SR	FI	HIX	BIX	C1	C2	C3	C4
18/8/15	F1	2.65	10.0	8.23	1370	5.0	0.6	1047	0.1	6.3	2.9	0.80	1.67	0.88	0.68	53.8	37.7	2.3	6.2
18/8/15	F2	2.65	10.2	8.27	1360	2.8	0.3	1044	0.1	6.3	2.9	0.81	1.79	0.91	0.68	55.9	39.4	3.1	1.6
18/8/15	F3	2.65	10.8	8.3	1367	3.3	0.2	1020	0.1	6.3	2.9	0.80	1.71	0.88	0.66	54.0	37.5	2.8	5.7
18/8/15	F4	2.65	10.5	8.31	1360	3.2	0.1	1035	0.1	6.2	3.0	0.82	1.68	0.87	0.68	53.6	37.3	3.0	6.1
18/8/15	F5	2.65	12.9	8.3	1360	1.7	0.2	1014	0.1	6.2	3.0	0.81	1.80	0.88	0.68	54.1	37.4	3.0	5.6
18/8/15	F6	2.65	15.7	8.29	1400	2.4	0.5	1028	0.1	6.1	2.9	0.84	1.69	0.87	0.68	53.9	37.0	3.3	5.8
18/8/15	T		13.7	8.28	1360	9.6	0.3	1062	0.1	6.3	2.9	0.81	1.70	0.91	0.66	56.1	39.2	2.7	2.0
21/8/15	F1	2.65	12.7		1193	0.7	0.1	1017	0.1	6.4	2.9	0.81	1.80	0.90	0.67	55.2	39.2	2.4	3.2
21/8/15	F2	2.65	15.6		1190	0.1	0.1	1013	0.1	6.3	2.9	0.83	1.74	0.88	0.66	53.3	38.1	3.8	4.7
21/8/15	F3	2.65	17.5		1197	0.9	0.2	1024	0.1	6.4	2.9	0.82	1.67	0.91	0.67	55.9	39.2	2.6	2.3
21/8/15	F4	2.65	13.2		1190	2.6	0.1	1022	0.1	6.4	2.9	0.81	1.66	0.90	0.68	55.5	38.3	2.6	3.6
21/8/15	F5	2.65	10.0		1200	1.8	0.1	1018	0.1	6.4	2.9	0.83	1.72	0.89	0.70	55.1	38.5	3.1	3.3
21/8/15	F6	2.65	9.1	8.05	1190	1.7	0.1	1017	0.1	6.5	2.9	0.83	1.73	0.89	0.69	54.8	38.3	2.6	4.3
21/8/15	T		8.0		1196	1.8	0.3	1019	0.1	6.3	2.9	0.83	1.78	0.88	0.70	52.1	39.5	2.6	5.8
24/8/15	F1	2.65	10.0		1090	0.8	0.5	952	0.1	6.2	2.8	0.94	1.68	0.88	0.73	50.7	40.6	3.3	5.4
24/8/15	F2	2.65	10.2		1090	1.0	0.3	945	0.1	6.6	2.8	0.88	1.70	0.88	0.72	51.4	40.0	3.7	4.9
24/8/15	F3	2.65	10.7		1090	0.1	0.4	953	0.1	6.4	2.8	0.87	1.67	0.89	0.68	51.4	40.5	3.5	4.6
24/8/15	F4	2.65	10.5		1090	0.1	0.4	947	0.1	6.3	2.8	0.89	1.75	0.88	0.71	51.4	40.1	3.6	4.9
24/8/15	F5	2.65	12.9		1090	0.1	0.5	949	0.1	4.1	4.3	1.01	1.73	0.88	0.70	51.5	39.9	3.6	5.0
24/8/15	F6	2.65	12.8		1130	0.1	0.6	945	0.1	6.6	2.7	0.86	1.78	0.88	0.67	51.5	40.0	3.3	5.2
24/8/15	T		13.1		1094	7.6	0.5	974	0.1	6.5	2.9	0.90	1.68	0.89	0.71	52.3	40.2	3.6	3.9
27/8/15	F1	2.65	12.4	10.37	981	5.8	0.4	998	0.1	6.2	2.8	0.93	1.62	0.90	0.68	52.3	40.1	1.9	5.7
27/8/15	F2	2.65	15.7	10.52	978	6.5	0.1	1010	0.1	6.0	2.8	1.03	1.62	0.87	0.71	50.5	38.4	3.0	8.2
27/8/15	F3	2.65	16.1	10.53	979	4.1	0.4	1014	0.1	5.9	2.8	0.95	1.66	0.90	0.72	52.4	39.8	2.1	5.7
27/8/15	F4	2.65	13.0	10.5	981	4.3	0.5	1014	0.1	5.9	2.8	0.92	1.70	0.89	0.65	51.7	39.6	1.9	6.8
27/8/15	F5	2.65	10.0	10.52	983	3.8	0.4	1008	0.1	6.2	2.7	0.93	1.76	0.89	0.70	52.3	39.8	1.6	6.3
27/8/15	F6	2.65	9.1	10.43	990	4.2	0.4	1012	0.1	5.8	2.8	0.94	1.71	0.89	0.70	52.0	39.5	1.6	6.9
27/8/15	T		8.0	10.3	976	9.4	0.3	1011	0.1	5.9	2.9	0.94	1.74	0.89	0.72	46.0	38.3	5.0	10.6
31/8/15	F1	2.65	10.0	10.35	966	0.1	0.5	985	0.1	5.9	2.6	0.94	1.68	0.85	0.69	49.4	38.1	6.0	6.5
31/8/15	F2	2.65	10.2	10.48	961	0.1	0.5	978	0.2	5.9	2.6	0.95	1.61	0.89	0.71	52.0	39.5	1.5	7.0
31/8/15	F3	2.65	10.7	10.28	946	0.1	0.4	975	0.1	5.8	2.7	0.97	1.63	0.84	0.71	49.7	37.8	2.0	10.5
31/8/15	F4	2.65	10.4	10.5	956	0.1	0.4	980	0.3	6.0	2.6	0.95	1.77	0.88	0.70	51.2	39.1	1.2	8.5
31/8/15	F5	2.65	12.9	10.13	953	0.1	0.4	971	0.6	5.6	2.7	0.99	1.62	0.88	0.71	51.3	39.3	1.3	8.1
31/8/15	F6	2.65	11.0	10.44	945	0.1	0.7	964	0.3	5.9	2.6	0.94	1.71	0.88	0.69	51.0	39.0	1.9	8.0
31/8/15	T		10.6	10.24	994	0.1	0.6	986	0.6	6.0	2.5	0.94	1.71	0.89	0.71	52.2	39.2	1.9	6.8

Continuation SI 12:

Date	Loc	Q	WT	O_2	DOC	$N\text{-}NH_4$	$N\text{-}NO_2$	$N\text{-}NO_3$	$P\text{-}PO_4$	$E_2{:}E_3$	$SUVA_{254}$	S_R	FI	HIX	BIX	C1	C2	C3	
3/9/15	F1	0.03	9.8	12.91	1130	1.5	1.6	728	0.1	6.2	2.3	0.89	1.75	0.89	0.72	52.4	38.6	4.5	4.5
3/9/15	F2	0.10	11.0	10.04	1050	3.0	0.7	841	0.1	6.4	2.4	0.88	1.68	0.88	0.69	51.3	38.9	3.0	6.8
3/9/15	F3	0.35	12.4	9.61	973	2.4	0.5	923	0.1	6.5	2.5	0.86	1.76	0.91	0.69	54.0	39.9	2.4	3.7
3/9/15	F4	0.73	10.7	9.61	939	4.5	0.2	945	0.1	6.7	2.6	0.84	1.68	0.91	0.72	54.0	40.0	2.7	3.4
3/9/15	F5	1.45	9.8	9.57	996	2.9	0.3	962	0.1	6.6	2.4	0.85	1.66	0.90	0.66	53.3	40.2	2.1	4.4
3/9/15	F6	2.65	9.1	9.51	925	3.7	0.3	981	0.1	6.6	2.6	0.84	1.58	0.90	0.74	53.5	39.8	3.4	3.4
3/9/15	T		8.0	9.6	937	5.0	0.3	974	0.1	6.4	2.6	0.87	1.71	0.88	0.69	52.8	38.7	3.5	4.9
7/9/15	F1	0.03	10.0	13.85	1650	5.7	2.7	825	0.1	5.7	2.7	0.97	1.85	0.86	0.69	51.8	37.7	8.6	1.9
7/9/15	F2	0.10	10.2	15.4	2070	10.2	2.3	957	0.1	5.6	2.9	0.87	1.76	0.92	0.65	57.4	38.4	4.3	0.0
7/9/15	F3	0.35	10.7	12.61	1990	34.5	1.3	1000	0.1	5.8	3.1	0.83	1.70	0.93	0.65	58.1	38.7	3.3	0.0
7/9/15	F4	0.73	10.2	11.97	1960	28.3	1.1	1006	0.6	5.9	3.0	0.83	1.68	0.92	0.66	57.3	38.1	4.5	0.0
7/9/15	F5	1.45	12.9	11.6	1890	21.7	0.8	1006	0.6	5.8	3.1	0.82	1.68	0.94	0.64	58.1	38.9	3.0	0.0
7/9/15	F6	2.65	11.0	11.4	1930	15.6	0.6	1008	0.2	5.9	3.0	0.81	1.74	0.94	0.67	58.3	38.8	3.0	0.0
7/9/15	T		9.9	10.98	1903	4.8	0.8	1010	1.0	6.0	3.0	0.78	1.64	0.91	0.66	57.4	38.3	2.7	1.7
10/9/15	F1	0.03	9.4	14.88	1630	9.7	1.9	977	0.1	5.8	2.6	0.89	1.67	0.90	0.68	55.2	37.7	3.9	3.2
10/9/15	F2	0.10	10.0	15.08	1530	7.8	2.3	943	0.1	6.0	2.6	0.86	1.71	0.89	0.70	54.2	38.0	4.7	3.0
10/9/15	F3	0.35	11.0	11.44	1310	2.0	0.6	1039	0.1	6.4	2.9	0.82	1.74	0.89	0.69	54.5	38.5	4.3	2.6
10/9/15	F4	0.73	10.2	11.18	1290	0.5	0.5	1060	0.1	6.5	2.9	0.81	1.71	0.92	0.68	56.3	39.5	1.9	2.4
10/9/15	F5	1.45	9.8	11.03	1310	1.6	0.3	1064	0.1	5.7	3.0	0.88	1.86	0.91	0.68	56.0	39.1	2.0	2.8
10/9/15	F6	2.65	9.1	10.92	1300	0.5	1.1	1065	0.1	5.3	3.2	0.95	1.77	0.89	0.70	54.3	38.1	4.8	2.7
10/9/15	T		8.0	10.76	1270	2.5	0.5	1084	0.1	6.6	2.9	0.79	1.74	0.92	0.67	56.5	39.8	1.9	1.9
13/9/15	F1	0.03	10.0	12.58	1620	13.1	2.1	923	0.1	5.9	2.4	0.89	1.72	0.88	0.67	52.9	38.1	3.9	5.1
13/9/15	F2	0.10	10.2	12.44	1480	10.4	2.0	914	0.1	5.8	2.5	0.90	1.71	0.89	0.69	53.5	38.4	3.8	4.2
13/9/15	F3	0.35	10.6	10.14	1270	2.9	0.7	962	0.1	6.2	2.7	0.85	1.78	0.89	0.72	54.1	39.2	2.5	4.2
13/9/15	F4	0.73	10.0	11.2	1230	16.7	0.6	991	0.1	6.4	2.8	0.84	1.69	0.91	0.68	54.6	39.5	2.5	3.4
13/9/15	F5	1.45	12.9	10.85	1210	0.1	1.0	985	0.1	6.5	2.8	0.83	1.74	0.92	0.70	55.6	39.9	1.7	2.7
13/9/15	F6	2.65	10.6	10.8	1200	0.1	0.8	992	0.1	6.4	2.8	0.82	1.70	0.91	0.70	55.2	39.7	1.8	3.4
13/9/15	T		9.2	10.49	1196	5.7	0.4	998	0.1	6.4	2.8	0.83	1.72	0.90	0.71	52.4	40.4	1.0	6.1
16/9/15	F1	0.03	9.2	11.4	1560	14.6	3.9	939	0.1	5.2	2.6	0.97	1.74	0.84	0.67	49.1	35.1	5.9	9.9
16/9/15	F2	0.10	9.6	13.06	1420	15.5	4.2	924	0.1	5.2	2.7	0.98	1.70	0.85	0.68	51.4	35.1	6.6	6.9
16/9/15	F3	0.35	10.6	12.32	1150	6.6	1.1	995	0.7	6.2	2.9	0.93	1.66	0.85	0.70	51.4	37.0	4.2	7.5
16/9/15	F4	0.73	9.7	11.95	1130	4.6	0.9	1002	0.1	6.1	2.8	0.89	1.70	0.88	0.68	51.2	39.4	2.3	7.1
16/9/15	F5	1.45	9.8	11.48	1110	3.7	0.9	1018	0.0	6.5	2.8	0.86	1.71	0.88	0.71	49.5	40.0	1.7	8.8
16/9/15	F6	2.65	9.1	11.25	1100	5.8	0.8	1021	0.0	6.5	2.8	0.89	1.69	0.89	0.70	51.9	39.7	3.2	5.2
16/9/15	T		8.0	10.98	1099	4.5	0.6	1027	0.5	6.3	2.8	0.88	1.71	0.88	0.71	51.6	39.3	3.1	6.0
21/9/15	F1	0.03	10.0	9.8	1513	14.9	2.6	960	0.1	5.6	2.4	0.92	1.75	0.82	0.65	48.7	34.8	5.9	10.7
21/9/15	F2	0.10	10.2	10.42	1380	16.7	3.3	1002	0.1	5.6	2.4	0.89	1.70	0.82	0.70	47.5	35.9	5.7	10.8
21/9/15	F3	0.35	10.6	11.06	1103	12.5	1.2	999	0.1	6.2	2.7	0.85	1.75	0.89	0.66	53.1	38.5	3.2	5.1
21/9/15	F4	0.73	9.9	11.26	1080	12.5	1.2	997	0.1	6.2	2.7	0.84	1.66	0.89	0.69	52.3	38.8	2.6	6.3
21/9/15	F5	1.45	12.9	10.94	1050	12.8	0.9	1005	0.1	6.3	2.8	0.84	1.75	0.89	0.69	53.7	38.7	3.2	4.4
21/9/15	F6	2.65	10.5	10.9	1040	13.7	1.1	1013	0.1	6.3	2.8	0.84	1.62	0.90	0.67	53.9	38.8	3.0	4.4
21/9/15	T		9.0	10.58	1034	10.8	0.8	1021	0.1	6.4	2.8	0.80	1.73	0.90	0.70	52.8	39.7	1.7	5.7

Continuation SI 12:

Date	Loc	Q	WT	O_2	DOC	$N\text{-}NH_4$	$N\text{-}NO_2$	$N\text{-}NO_3$	$P\text{-}PO_4$	$E_2{:}E_3$	$SUVA_{254}$	SR	FI	HIX	BIX	C1	C2	C3	C4
22/9/15	F1	2.65	9.2	10.38	1017	0.1	0.7	1041	0.1	6.1	2.7	0.97	1.66	0.88	0.72	52.4	38.6	3.1	5.9
22/9/15	F2	2.65	9.4	10.58	1010	0.1	0.9	1049	0.2	6.1	2.8	0.98	1.76	0.88	0.67	52.1	38.8	2.7	6.4
22/9/15	F3	2.65	10.3	10.6	1010	0.1	0.9	1047	0.1	5.9	2.8	0.98	1.70	0.86	0.67	51.4	37.6	3.2	7.8
22/9/15	F4	2.65	9.6	10.64	1010	0.5	1.1	1049	0.1	5.9	2.8	1.02	1.58	0.89	0.70	52.6	39.1	2.6	5.7
22/9/15	F5	2.65	9.8	10.45	1017	0.1	0.8	1059	0.3	5.8	2.7	1.00	1.73	0.88	0.72	52.3	38.8	3.0	5.9
22/9/15	F6	2.65	9.1	10.74	1010	0.1	1.2	1051	0.2	5.8	2.8	0.96	1.69	0.89	0.70	52.6	39.1	2.6	5.6
22/9/15	T		8.0	10.58	1002	0.1	0.5	1046	0.1	6.5	2.7	0.85	1.67	0.88	0.70	51.6	39.4	2.2	6.8
23/9/15	F1	2.65	10.0	10.4	1020	6.8	0.5	1122	0.1	6.0	2.7	0.91	1.81	0.88	0.65	52.0	39.2	2.4	6.4
23/9/15	F2	2.65	10.2	9.98	1010	4.3	0.6	1124	0.1	6.0	2.7	0.93	1.82	0.88	0.67	52.0	39.1	2.8	6.1
23/9/15	F3	2.65	10.2	10.02	1010	5.7	0.5	1126	0.7	6.0	2.7	0.92	1.74	0.88	0.69	52.1	39.3	2.4	6.1
23/9/15	F4	2.65	9.7	10.58	1010	4.1	0.8	1123	0.6	6.3	2.7	0.91	1.74	0.88	0.68	51.6	39.1	2.5	6.7
23/9/15	F5	2.65	12.6	10.1	1020	8.4	0.5	1123	0.6	6.0	2.7	0.93	1.76	0.85	0.69	50.0	37.7	3.8	8.4
23/9/15	F6	2.65	10.4	10.57	1010	6.6	1.4	1137	0.2	6.0	2.7	0.91	1.85	0.88	0.71	52.0	39.4	2.7	5.9
23/9/15	T		8.8	9.8	1002	6.2	0.6	1132	0.2	6.2	2.7	0.91	1.69	0.89	0.70	51.9	39.7	2.6	5.8
24/9/15	F1	2.65	9.0	10.41	1630	2.0	0.5	1159	0.1	5.7	3.1	0.79	1.64	0.90	0.67	56.6	37.7	2.1	3.6
24/9/15	F2	2.65	9.4	10.38	1630	3.6	0.6	1155	0.1	5.7	3.1	0.77	1.75	0.92	0.65	57.8	37.8	2.2	2.1
24/9/15	F3	2.65	10.1	10.4	1620	2.3	0.7	1164	0.1	5.5	3.1	0.81	1.68	0.91	0.65	57.2	37.5	2.8	2.4
24/9/15	F4	2.65	9.8	10.39	1630	3.5	0.5	1152	0.1	5.5	3.1	0.83	1.69	0.91	0.65	57.7	37.9	2.0	2.4
24/9/15	F5	2.65	9.6	10.45	1620	2.5	0.4	1147	0.1	5.6	3.1	0.80	1.74	0.92	0.64	58.0	37.9	2.1	2.0
24/9/15	F6	2.65	9.1	10.45	1610	0.7	0.7	1148	0.1	5.5	3.1	0.82	1.72	0.92	0.64	58.0	37.7	2.1	2.2
24/9/15	T		7.8	10.31	1622	1.9	0.5	1173	0.1	5.6	3.1	0.79	1.71	0.92	0.64	57.9	38.0	1.9	2.2

11.6 Supplementary Information General Discussion

Table SI 13: Metadata of the literature review to plot figure 8.5.

Study	Location	Region	Category	Status	MinGPP	MaxGPP	MinER	MaxER
Acuña et al. 2004	Fuirosos	Spain	MedDesert	Pristine	0.1	1.9	0.4	32.0
Acuña et al. 2011	Pampa stream	Argentina	LowLand	Nutrient	3.0	22.9	17.0	30.0
Acuña et al. 2015	Flumes	Fuirosos	Flume	Pristine	10.0	50.0	6.0	9.5
Argerich et al. 2016	Forested headwater	Oregon	Forest	Pristine	0.1	1.2	0.4	5.3
Beaulieu et al. 2013	Shephard Creek	Ohio	MedDesert	Nutrient	0.0	12.5	0.4	12.9
Bernot et al. 2010	9 Streams	USA	Forest	Pristine	0.1	3.9	0.4	23.1
Bernot et al. 2010	9 Streams	USA	LowLand	Nutrient	0.1	16.2	0.9	15.7
Bernot et al. 2010	9 Streams	USA	LowLand	Nutrient	0.1	11.9	0.5	17.9
Boulêtreau et al. 2010	Flumes	France	Flume	Pristine	3.8	9.6	0.6	2.2
Bunn et al. 2003	Arid stream	Australia	MedDesert	Pristine	2.7	4.8	1.7	2.1
Busch and Fisher 1981	Sycamore stream	Arizona	MedDesert	Pristine	4.4	12.5	5.5	
Dodds et al. 1996	Prairie stream	Kansas	LowLand	Pristine	0.6	1.3	NA	NA
Dodds et al. 1996	Forest stream	Kansas	Forest	Pristine	0.0	0.6	NA	NA
Fellows et al. 2001	Rio Calveras	New Mexico	Forest	Pristine	0.2	1.7	6.7	14.7
Fellows et al. 2001	Gallina creek	New Mexico	Forest	Pristine	0.5	0.6	2.3	2.9
Fellows et al. 2006	Streams	Australia	Forest	Nutrient	0.0	3.0	0.0	2.3
Fuß et al. 2017	Streams	Austria	LowLand	Nutrient	0.0	3.3	1.9	11.7
Gawne et al. 2007	Murray river	Australia	LargeRiver	Nutrient	1.6	2.8	2.4	2.9
Graeber et al. 2018	Revitalized reach	Denmark	LowLand	Nutrient	3.6	4.8	4.4	4.5
Chapter 2	Fuirosos	Spain	MedDesert	Pristine	0.0	4.0	1.9	22.6
Chapter 4	F1	Austria	Flume	Pristine	0.0	2.0	0.5	1.8
Chapter 4	F2	Austria	Flume	Pristine	0.1	2.8	0.9	2.9
Chapter 4	F3	Austria	Flume	Pristine	0.1	4.3	2.1	4.1
Chapter 4	F4	Austria	Flume	Pristine	0.1	3.2	1.4	2.5
Chapter 2	Fuirosos	Spain	MedDesert	Pristine	0.0	14.4	2.2	58.2
Jones Jr et al. 1996	Desert stream	Arizona	MedDesert	Pristine	2.7	12.3	3.6	6.5

Study	Location	Region	Category	Status	MinGPP	MaxGPP	MinER	MaxER
Kurz et al. 2017	Flumes	England	Flume	Pristine	3.5	7.0	2.0	5.5
Lupon et al. 2016	Font de Regas	Spain	Forest	Pristine	0.1	0.6	5.5	10.0
Mulholland et al. 2001	Several streams	USA	Forest	Pristine	0.1	3.0	2.4	29.0
Preiner et al. 2008	Danube	Austria	LargeRiver	Nutrient	1.3	3.8	0.5	1.3
Proia et al. 2016	Fluvia Lentic	Spain	MedDesert	Pristine	0.0	0.4	1.3	2.4
Proia et al. 2016	Fluvia Lotic	Spain	MedDesert	Pristine	1.3	1.8	0.4	0.5
Proia et al. 2016	Fluvia Lentic	Spain	MedDesert	Nutrient	0.5	20.3	1.5	7.4
Proia et al. 2016	Fluvia Lotic	Spain	MedDesert	Nutrient	2.0	4.6	0.8	1.6
Roberts et al. 2007	Walker Branch	Tennessee	Forest	Pristine	0.0	10.8	1.0	16.0
Smith and Kaushal 2015	Urban streams	USA	LowLand	Nutrient	0.0	8.0	0.0	16.0
Uehlinger and Naegeli 1998	Necker	Germany	LargeRiver	Nutrient	2.5	2.5	3.5	3.5
Ulseth et al. 2017	Ybbs	Austria	Forest	Pristine	0.0	29.1	0.0	54.2
Vautier et al in prep.	Stream	Bretagne	Forest	Pristine	0.4	0.5	17.2	26.5
Vautier et al in prep.	Stream	Bretagne	LowLand	Nutrient	0.1	1.6	3.1	26.3
Velasco et al. 2003	Stream	Spain	MedDesert	Nutrient	5.2	26.4	2.7	10.2
Young and Huryn 1996	Grassland river	NewZealand	LargeRiver	Pristine	0.3	9.6	0.7	9.8